Pseudomonas aeruginosa PQS mediated virulence regulation and interference

Eduard Vico Oton, MSc.

Thesis submitted to the University of Nottingham for the degree of Doctor of Philosophy

September 2018

Declaration

The work presented here is my own unless clearly acknowledged. No part has been used for submission of another degree at the University of Nottingham or elsewhere.

Eduard Vico Oton, September 2018.

Abstract

Pseudomonas aeruginosa is a ubiquitous bacterium that can be found in most mesophilic aquatic and terrestrial habitats. Furthermore, *P. aeruginosa* (PA) is an important opportunistic pathogen that can infect humans, animals, insects and plants. *P. aeruginosa* has three hierarchically organised quorum sensing (QS) systems named *las*, *rhl* and *pqs*. The *las* and *rhl* are classic QS systems that use an *N*-acylhomoserine lactone as autoinducers. The *las* system is the major QS system of the cell and controls the other two and there is partial redundancy with the *rhl* system regarding the genes and functions controlled by the system. Activated functions are related to motility, virulence and biofilm formation. The *pqs* system is a QS system based in alkyl-4(1*H*)-quinolones (AQs) molecules, specifically the 2-heptyl-3,4-dihydroxyquinoline called **p**seudomonas **q**uinolone **f**actor (PQS). The *pqs* system is under control of *las* and *rhl* and can in turn influence the expression of *rhl*. The *pqs* system controls virulence, iron acquisition, biofilm maturation and the oxidative stress response.

The PqsR is the main regulator of the *pqs* system upon activation with PQS. The inhibition of QS and in particular the *pqs* system is an approach to decrease the virulence of *P. aeruginosa in vivo* to improve the outcome of antibiotic treatments and decrease the *P. aeruginosa* associated morbidity. The SENBIOTAR project (sensitising *Pseudomonas aeruginosa* biofilms to antibiotics and reducing virulence through novel target inhibition, MRC project MR/N501852/1) aims at developing PqsR antagonists that inhibit the *pqs* system. A series of potential inhibitors were tested for activity in a *pqsA*-lux transcriptional reporter in Chapter 3. Two compounds, SEN016 and SEN066 were found to actively inhibit expression and SEN016 was used for further *in silico* optimisation, developing a series of compounds that were tested for IC50 and **i**sothermal **t**itration **c**alorimetry (ITC). The lead compound SEN089 showed a $K_{(D)}$ (dissociation constant) of 2.66 nM and IC50 of 67 nM while compounds SEN022 and SEN066 did not bind to $PqsR_{LBD}$ even if they inhibited *pqs*. The compounds were tested in a variety of phenotypes and strains. Results from Chapter 4 show that compounds effectively inhibit phenotypes under *pqs* regulation but not others

controlled by different regulatory systems. The data evidenced significant differences on the efficacy of compounds when tested in other strains. Notably, SEN089 remained the overall best compound. Moreover, data provided evidence that *P. aeruginosa* has at least two autolytic mechanisms, one is activated by *pqs* whereas the other is repressed by PQS. A novel hypothesis for the role of PQS in the CF lung is also discussed there. In Chapter 3, some compounds were tested in biofilm models to assess the relevance of *pqs* inhibition. There was a significant increased bioactivity between the compounds and antibiotics tested as well as between the compounds and shearing forces. Several guidelines are provided for optimal confocal imaging aimed at quantitation. Furthermore, another novel hypothesis is presented regarding the role of *pqs* in the biofilm of the CF lung describing it as a response mechanism rather than an active system.

In summary, a series of PqsR antagonists were developed and analysed for binding affinity to PqsR, secondary unspecific activity, *pqs* inhibition, biofilm impact and an additive effect on antibiotic treatment in different strains of *P. aeruginosa*. The compounds successfully inhibit *pqs* and had a significant impact in virulence modulation as well as sensitivity towards tobramycin or ciprofloxacin. This work explores the inhibition of *pqs* as an effective therapeutic target and suggests multiple novel mechanisms through which *pqs* regulates the physiology of the cell.

Acknowledgements

A PhD thesis is akin to a path into the unknown with only general directions given. Everyone realises sooner or later that the path has no end, there is always a new corner, a new crossroads, a funny looking thing in the distance… Stopping is thus as important as starting. We are fortunate enough to not walk it alone and a whole bunch of people walks along, offering support in a myriad ways. This is a small collection of those who helped me greatly along this personal trip.

First and foremost, I would love to thank my supervisors, Miguel, Stephan and Fadi, whose work and guidance has been outstanding.

Second only to them, Laura. Easily the other single most contributing person for this thesis' completion. Her bright light has kept me from crashing time and time again and her importance can't be put in words alone. Fortunately, she knows.

To my family, who have been an untiring shoulder, always keeping me on my feet. Gràcies papes, Albert, Isa i sobretot, Teresa i Josep!

Equally important, I want to thank my family of choice, those friends new and old, far and close. All these people have defined who I am and I hope I have been able to be as helpful to them as they are to me.

To the people in the lab: Most importantly my mentor and role model Diana. But also to Manu, Ioanna, Natalia, Elena, Josh, Matt… the list could go on. To the rest of my amazing friends: Lorenzo (obviously) and Sophie, Marco and Christian and Rupert (a killer combo). Collectively they have made Nottingham the best place, even with its lack of proper mountain ranges.

Some paths are not only walked, and this particular one had a significant amount of climbing too. For that I want to thank the whole climbing squad. If you somehow read this, consider yourself included!

Finally, my friends from back home, my oldest and best friends, the kind of people that makes you consider coming back and settling down even when the perspectives for jobs are as bad as fishing for food in a two-day muddy puddle.

Table of contents

List of figures

List of tables

Abbreviations

°C	Degrees Celsius
2-AA	2-aminoacetophenone
2-ABA	2-amynobenzoylacetate
2-ABA-CoA	2-aminobenzoylacetyl-CoA
AA	anthranilic acid
aa	amino acid
Ap	Ampicillin
AQ	2-Alkyl-4-Quinoline
AUC	Area under the curve
BB	Benzamide-benzamidazole
bp	base pair
CAA	Casamino acids media
Cb	Carbenicillin
CBDI	Co-inducer binding domain I
CBDII	Co-inducer binding domain II
CDM	Chemically defined media
CF	Cystic fibrosis
CFTR	Cystic fibrosis transmembrane conductance regulator
ChIP	Chromatin immunoprecipitation
CLSM	Confocal laser scanning microscopy
CV	Crystal Violet
DHQ	Dihydroxyquinoline
DMSO	Dimethyl sulfoxide
eDNA	Extracellular DNA

eGfp	Enhanced green fluorescence protein
Etho	Ethidium homodimer
EPS	Extracellular polymeric substances
Gfp	Green fluorescence protein
Gm	Gentamycin
h	hours
HCl	Hydrochloric acid
HCN	Hydrogen Cyanide
HHQ	2-Heptyl-3,4-dyhydroxyquinoline
HQNO	4-hydroxy-2-heptylquinoline-N-oxide
HTH	Helix-turn-helix domain
IC_{50}	Inhibitory concentration 50%
IPTG	Isopropyl β-D-1-thiogalactopyranoside
ITC	Isothermal titration calorimetry
Km	Kanamycin
$K_{(D)}$	Dissociation constant
kDa	kilo Daltons
L	Litre
LB	Lysogeny broth media
LBD	Ligand binding domain
Lttr	LysR-type transcriptional regulator
M	Molar
min	minutes
ml	Millilitres
mM	Millimolar concentration

mm	Millimetre
nM	Nanomolar concentration
OD	Optical density
ON	Overnight culture
OMV	Outer membrane vesicle
PA	*Pseudomonas aeruginosa*
PAINS	Pan assay interference compounds
PI	Propidium iodide
PIA	*Pseudomonas* isolation agar
PQS	*Pseudomonas* quinolone signal, 4-hydroxy-2-heptylquinoline
PQS QS	*Pseudomonas* quinolone signal quorum sensing
QS	Quorum sensing
QZN	Quinazolinone
rcf	Relative centrifugal force
RLU	Relative light unit
RPM	Revolutions per minutes
RPMI	Roswell park memorial institute media
S17	*Escherichia coli* S17
SN	Supernatant
SPR	Surface plasmon resonance
T#SS	Type # secretion system
T4P	Type IV pili
TCS	Two component systems
Tet	Tetracycline
UV	Ultraviolet light

VS	Virtual Screening
µg	Microgram
µL	Microliter
µM	Micromolar concentration
µm	Micrometre

1. Introduction

Pseudomonas aeruginosa is a Gram-negative rod-shaped bacterium well known and studied for its diverse and adaptable metabolism that allows it to colonise many different environments, ranging from coastal waters to animal skin (Bhattacharya *et al.* 2000; Römling *et al.* 2005; Rehm 2008; Ansari *et al.* 2015). *P. aeruginosa* is classified within the γ-proteobacterium class, which in turn is part of the Proteobacteria phylum. The adaptability of *P. aeruginosa* allows it to grow in a wide range of conditions, in temperatures ranging from 5.5 to 45 °C (with the optimal range being 25-41 °C) and tolerate pH between 4 and 9, allowing it to grow in both acid and basic environments (Trunk *et al.* 2010). *P. aeruginosa* can also proliferate extensively within hosts if tissue barriers are broken or the immune system is compromised, making it an important opportunistic pathogen for a broad range of hosts, from plants to humans (Van Delden and Iglewski 1998; He *et al.* 2004; Moradali, Ghods and Rehm 2017). Especially relevant for humans are the infections caused in people suffering from cystic fibrosis (CF) (Girard and Bloemberg 2008; Folkesson *et al.* 2012; Bjarnsholt 2013). However, the pathogenicity of *P. aeruginosa* should not be the defining characteristic of this microorganism as it is present in many different environments and some strains are found as beneficial plant symbionts (Sulochana *et al.* 2014).

P. aeruginosa achieves this ecological versatility through an extensive metabolic network, very finely regulated by a hierarchical system of regulators responding to internal and external signalling that is still not fully understood (Schuster and Greenberg 2006; Lee and Zhang 2014). All of this is encased in large genomes (~5-7 Mbp) and with so many systems, it is not surprising that *P. aeruginosa* contains some of the largest amount of regulatory genes described in bacteria, comprising ~8% of the total genome (Stover *et al.* 2000; Goodman *et al.* 2009; Moradali, Ghods and Rehm 2017). The *P. aeruginosa* pangenome has a core of 4000 conserved genes supported by an accessory genome of 10000 genes and >3000 rare genes, present only in few strains (Hilker *et al.* 2015).

It has been observed that the size of the core genome of *P. aeruginosa* is much larger than what would be expected, with clinical isolates sharing many genes with isolates from the environment (Grosso-Becerra *et al.* 2014). This means that theoretically, strains found naturally in the environment could easily become pathogens and that pathogenic strains can also survive and persist in natural environments.

The size of the genome sits in disarray with the genome reduction often observed in many pathogenic strains and other studies that indicate high levels of homologous recombination in pathogenic strains and a widespread presence of genomic islands (GIs) (Moran 2002; van Mansfeld *et al.* 2010; Morales-Espinosa *et al.* 2012; Merhej, Georgiades and Raoult 2013; Grosso-Becerra *et al.* 2014). It is unclear why there is such level of conservation but it is probably the reason behind the size and complexity of *P. aeruginosa* regulatory network.

1.1. *P. aeruginosa* relevance, prevalence and pathogenicity

1.1.1. *P. aeruginosa* in industry

The metabolic versatility of *P. aeruginosa* gives it a huge potential for bioremediation purposes and as such it has been successfully used to clean xenobiotics from different environments and in laboratory conditions. These include: long chain hydrocarbons (Sakthipriya, Doble and Sangwai 2016; Ebadi *et al.* 2017), aromatic molecules (Kotresha and Vidyasagar 2008; Mukherjee and Bordoloi 2012; Safdari *et al.* 2017), recalcitrant insecticides (Kulkarni and Kaliwal 2015) and Cr, Cu, Fe, Mn and Zn heavy metals (Pérez-Silva *et al.* 2009; Awasthi *et al.* 2015; Kang *et al.* 2015).

This very same versatility can also be directed in biosynthetic processes that generate molecules of interest. A few products natively produced by *P. aeruginosa* have industrial use, one of the most widely used are polyhydroxyalkanoates (PHA), which can be used to make biodegradable plastics or as drug delivery vectors. *P. aeruginosa* can accumulate very high amounts of PHAs which can add up to 75% of the total dry weight (Fernández *et al.* 2005; Singh and Mallick 2009). Rhamnolipids are another relevant product, these biosurfactants can be used in bioremediation but

also in a range of products, including bio-detergents and oils from the pharmaceutical and food industry and provide a biodegradable alternative to synthetic recalcitrant biosurfactants (Soberón-Chávez, Lépine and Déziel 2005; Nitschke and Costa 2007; Fakruddin 2012). The simultaneous production of rhamnolipids and PHA accumulation make *P. aeruginosa* an interesting organism for optimised industrial processes which could collect the secreted rhamnolipids and the intracellularly accumulated PHAs (Costa *et al.* 2009). There are other secreted products that could be used in industrial processes, *P. aeruginosa* can produce alginate in very high quantities and the pathway is well-known, facilitating bioengineering that could provide a substitute to seaweed alginate (Maleki *et al.* 2016). The metabolic versatility of *P. aeruginosa* makes it a good candidate to recycle waste products in order to generate secreted enzymes such as lipases and proteases that are useful in a variety of industries (Sharon *et al.* 1998; Ganesh Kumar *et al.* 2008; Mahanta, Gupta and Khare 2008).

However, the ubiquity of *P. aeruginosa* also has a negative impact in many situations, the development of thick biofilms can have serious biofouling effects that may render systems contaminated and unusable. In the food industry, Pseudomonas can contaminate foods from many sources mostly through biofilm development (Meliani and Bensoltane 2015), *P. aeruginosa* in particular can spoil milk and be found in drinking water (Raposo *et al.* 2017). Pseudomonas biofouling is also relevant in other industries, the same characteristics that makes it good for bioremediation makes it a fouling agent of fossil fuels (Bojanowski, Crookes-Goodson and Robinson 2016) and can significantly damage the surfaces where it grows (Barnes *et al.* 2014).

1.1.2. *P. aeruginosa* as bio-stimulant and biocontrol agent

P. aeruginosa has been found to establish facultative mutualistic relationships with a variety of plants (Sulochana *et al.* 2014). The bacteria can grow in the rhizosphere sustained by the plant secretions, meanwhile, the presence of *P. aeruginosa* can enhance the development of the plant through the release of phytohormones such as indole acetic acid

(Bhakthavatchalu, Shivakumar and Sullia 2013; Sulochana *et al.* 2014; Radhapriya *et al.* 2015). Moreover, the presence of *P. aeruginosa* in the rhizosphere has been observed to act as biocontrol agent against phytopathogens by secreting strong siderophores that chelate iron. *P. aeruginosa* has a competitive advantage under low iron conditions and restricts the development of phytopathogens (Sasirekha and Srividya 2016). Production of other factors such as hydrogen cyanide (HCN) and chitinases are directly harmful for phytopathogens and the presence of *P. aeruginosa* can stimulate the plant's own defence mechanisms (Audenaert *et al.* 2002; Minaxi and Saxena 2010; Sulochana *et al.* 2014). All these factors make the presence of *P. aeruginosa* a desirable factor for a healthy rhizosphere.

1.1.3. *P. aeruginosa* as an opportunistic pathogen

Pseudomonas spp. can be naturally found as a commensal microorganism of plants and animals (Paulsen *et al.* 2005; Cogen, Nizet and Gallo 2008). *P. aeruginosa* is a common member of the human skin microbiota, however it can easily become pathogenic if the skin barrier is broken or the person is immunocompromised (Cogen, Nizet and Gallo 2008). *P. aeruginosa* can infect many other hosts but most of the studies on non-human infections have focused on plants because of its economic impact, although domestic animals and fish can also be infected posing a significant economic burden, particularly in aquaculture (Tripathy *et al.* 2007; Thomas *et al.* 2014; Haenni *et al.* 2015).

P. aeruginosa acute infections are maintained through the production of a wide range of virulence factors, however, thanks to its complex regulatory network, virulence can be finely tuned and *P. aeruginosa* can establish into chronic infections that are highly resistant to antibiotics (Mah *et al.* 2003; Lewis 2007). *P. aeruginosa* presents significant changes in the phenotypes displayed between acute and chronic infections (Table 1.1). Moreover, dispersed cells can also be considered distinct from biofilm or planktonic, adding an often overlooked third lifestyle (Chua *et al.* 2014).

Table 1.1. Acute and chronic *P. aeruginosa* infection characteristics.

	Acute infection	Chronic infection	References
Lifestyle	Planktonic, motile	Biofilms, sessile and dispersed	(Chua *et al.* 2014)
Infection characteristics	Invasive, exotoxins and proteases, motility, very pro-inflammatory	Localised, extracellular matrix, lower virulence, resistance to treatment, release of virulent dispersed cells	(Ma *et al.* 2009; Chua *et al.* 2014; Moradali, Ghods and Rehm 2017)
Iron uptake systems	Pyochelin, pyoverdine,	Heme groups, soluble Fe^{2+}	(Minandri *et al.* 2016)
Secretion systems	T1SS, T2SS, T3SS and T5SS	T2SS (LasB), T6SS	(Bleves *et al.* 2010; Zhang *et al.* 2017)
Virulence factors	Proteases, phospholipases, chitinases, lectins, phenazines, MVs, LPS, flagella, pilli	Exopolysaccharides, alginate, eDNA, proteases, lectins, LPS, dispersed cells	(Fuxman Bass *et al.* 2010; Jensen *et al.* 2010; Burrows 2012; Chua *et al.* 2014; Maura *et al.* 2016)
Regulator networks	QS, RsmA, Vfr, sRNA	QS, cyclic di-GMP, RsmY, RsmZ, GacA/GacS, other TCS, sRNA	(Goodman *et al.* 2004; Jimenez *et al.* 2012; Moradali, Ghods and Rehm 2017)

Abbreviations: T#SS, type # secretion system; MV, membrane vesicles; LPS, lipopolysaccharide; QS, quorum sensing; TCS, two component system.

Once a chronic infection by *P. aeruginosa* has established, it is extremely difficult to eradicate. Antibiotic concentrations required to kill bacteria in biofilms are much higher than those required to achieve the same effect in their planktonic counterparts. Moreover, the development of biofilms favours the development of persister cells and antibiotic resistance and the immune response is unable to clear them (Ciofu *et al.* 2017). The establishment of a biofilm in the infection creates a persisting inflammatory response in the area which damages the tissue. Bacteria change their

phenotype to become less immunogenic, by secreting less virulence factors and being metabolically less active. However, some components of the biofilm are intrinsically immunogenic such as the exopolysaccharides or eDNA (Flemming, Neu and Wozniak 2007; Fuxman Bass *et al.* 2010). The innate immune response against biofilms will assemble specific inflammasomes which in turn will direct the adaptive immune response. The tissue damage also generates a positive feedback loop that recruits polymorphonuclear leukocytes or macrophages which contribute in the maintenance of the ineffective inflammation and collateral damage (Jensen *et al.* 2010; Høiby *et al.* 2015).

1.1.3.1. *P. aeruginosa* in cystic fibrosis

Most of the work done in infections by *P. aeruginosa* biofilms has focused on cystic fibrosis (CF) models. Cystic fibrosis is an autosomal recessive disease caused by mutations in the cystic fibrosis transmembrane conductance regulator (CFTR). This gene encodes a chlorine channel regulator mainly expressed in the epithelium of multiple tissues and blood cells. Its inactivation results in impaired electrolyte and water transport which will significantly impact the quality of fluids and mucus, particularly affecting the lungs and gastrointestinal system (O'Sullivan and Freedman 2009). Several hypothesis exist for the infection predisposition that the CF patients show (O'Sullivan and Freedman 2009).

The mucociliary layer of CF patients is deficient in its function and this allows *P. aeruginosa* to remain in the lungs and colonise them. Furthermore, the CF patients present an unbalanced immune response which favours chronic inflammation and damages the tissue (Voynow, Fischer and Zheng 2008; Williams, Dehnbostel and Blackwell 2010). These factors strongly favour the chronic establishment of *P. aeruginosa* and other pathogens which then become very hard to treat with conventional antibiotics. *P. aeruginosa* develops biofilms anaerobically all over the lung lumen, and these biofilms are surrounded by neutrophils which maintain the inflammation but are incapable of clearing out the bacteria (Bjarnsholt *et al.* 2009; Jensen *et al.* 2010). Ultimately, it is the sustained inflammation that causes irreversible damage to the lung, eventually leading to respiratory failure and death (Cantin *et al.* 2015).

1.2. *P. aeruginosa* virulence and colonisation factors

P. aeruginosa has evolved to either coexist, control or outcompete other microorganisms found in a similar environment, becoming really efficient at surface colonisation and nutrient scavenging (Botzenhart and Döring 1993; Rohmer, Hocquet and Miller 2011). Meanwhile, its tools for long term survival are limited to the standard DNA repair mechanisms and an enhanced oxidative stress response (Ochsner *et al.* 2000). Many virulence factors are used by *P. aeruginosa* regardless of the colonised environment, however there is a significant fraction of virulence factors specifically adapted for certain environments, thus, the secretome of *P. aeruginosa* will be different when colonising a water pipe than when growing in the CF lung. These changes are probably guided by surface recognition and attachment mechanisms (Scott *et al.* 2013; Nguyen *et al.* 2018).

1.2.1. Motility mechanisms

P. aeruginosa is capable of swimming, swarming, twitching and sliding thanks to the production of flagella, type IV pili (T4P), biosurfactants and other motility-related elements (Murray and Kazmierczak 2008; Yeung *et al.* 2009; Chow *et al.* 2011). Flagella and type IV pili are also key components for the irreversible attachment of *P. aeruginosa* onto surfaces and biofilm development (Barken *et al.* 2008; Chow *et al.* 2011), maturation into mushroom-capped biofilms involves T4P and flagella mediated migrations of subpopulations to form the cap (Shrout *et al.* 2006; Barken *et al.* 2008). Nevertheless, it is worth pointing out that the relevance of this biofilm structure in nature is debatable, the architecture of the biofilm in nature depends on the environmental factors and it is highly possible that the classic mushroom-capped structure or even the composition of the matrix are significantly different between natural and experimental biofilms (Joo and Otto 2012; Ghanbari *et al.* 2016).

Generally, *P. aeruginosa* has a single, unsheathed polar flagellum, this is necessary for swimming and swarming motility but the flagellum itself is also recognised as a virulence factor. The flagellum *per se* is formed by a chain of flagellin proteins classically divided in serotypes a and b (Campodónico *et al.* 2010). Flagella are metabolically expensive to build

and move, and the structure is highly immunogenic and pro-inflammatory (Feuillet *et al.* 2006).The whole flagellar system is formed by more than 20 proteins, most of them involved in a complex yet elegant flagellar motor (Figure 1.1). The flagellum can hence be divided into three parts, the base body embedded in the cell membranes and containing the motor, a short curved part that emerges from the outer membrane, and a long external filament which flexibility allows it to move at high speeds without breaking (Dasgupta, Arora and Ramphal 2004). The flagellum plays an important role in attachment, biofilm establishment and transition from motile to sessile cells (Sauer *et al.* 2002). This transition appears to be divided in two stages, a first and fast inhibition at the phenotypic level which halts the flagellar function and a slower inhibition of the expression of the flagellar genes (Guttenplan and Kearns 2013). On the other hand, the absence of flagellar motility is important to develop mature biofilm structures (Klausen *et al.* 2003a; Shrout *et al.* 2006). In mature biofilms, motile bacteria develop at the empty centres of microcolonies, from which they will disperse and swim away (Sauer *et al.* 2002). Thus, flagella are important in establishment, development and dispersal of biofilms. The flagellum system is tightly regulated by multiple regulators, some of the known ones include FleQ, FleS/R and the intracellular signal c-di-GMP, while chemotaxis is regulated by FliA and CheY (Dasgupta, Arora and Ramphal 2004; Kato *et al.* 2008; Guttenplan and Kearns 2013). Finally, any potential flagellar regulation by quorum sensing (QS) systems is believed to be through the control of expression of the master regulator RpoN (Venturi 2006).

Type IV pili mediate the other main motility mechanism by PA. T4P are proteinaceous fibres protruding from the bacteria in all directions. These fibres are assembled and disassembled at the base, which in general terms is what allows twitching to occur as the tip of the pili acts as a hook. In *P. aeruginosa* and other Gram-negatives, T4P are built by an assembly mechanism in the inner membrane (PilB, C, D, T and U) that collects membrane-bound pre-pilin, cleaves the signal peptide and polymerises the now called major pilin (PilA) in the pilus itself, which will be secreted by a secretin embedded in the outer membrane (PilQ) (Figure 1.1) (Melville and

Craig 2013). T4P are involved in adherence, twitching motility, competence for DNA uptake, biofilm formation and pathogenesis (Persat *et al.* 2015). Twitching is a motility that occurs in high humidity and low viscosity surfaces where cells align and move together like in a raft (Burrows 2012). Moreover, T4P have also been involved in alternative motility mechanisms and systems useful to detach from surfaces (Gibiansky *et al.* 2010). T4P and twitching motility are important for host pathogenicity (Burrows 2012), T4P establish the first contact with the host and are important during acute infections while chronic infections are often characterised by a lack of T4P (Mahenthiralingam, Campbell and Speert 1994). For biofilms, the presence of T4P is important as an initial attachment tool, very much like the flagellum. T4P also plays an important role in the correct development of microcolonies (Klausen *et al.* 2003a; Barken *et al.* 2008). T4P and twitching are also tightly regulated, chemotactic signalling systems can influence twitching motility, the RpoN super regulator controls the expression of *pilA*, also controlled by a two component system; PilR/S. AlgR/FimS is another TCS that controls expression, interestingly, the expression of lectin LecB is required for PilJ involved in pilus synthesis (Sonawane, Jyot and Ramphal 2006). T4P is also regulated by general regulators such as Vfr and c-di-GMP. Pili-mediated surface sensing is independent of QS systems, but it is hypothesised that pili-related surface sensing can increase sensitivity to the *las* system (Persat *et al.* 2015). Furthermore, there is some evidence linking the presence of working *las* and *rhl* systems with successful twitching motility (Glessner *et al.* 1999).

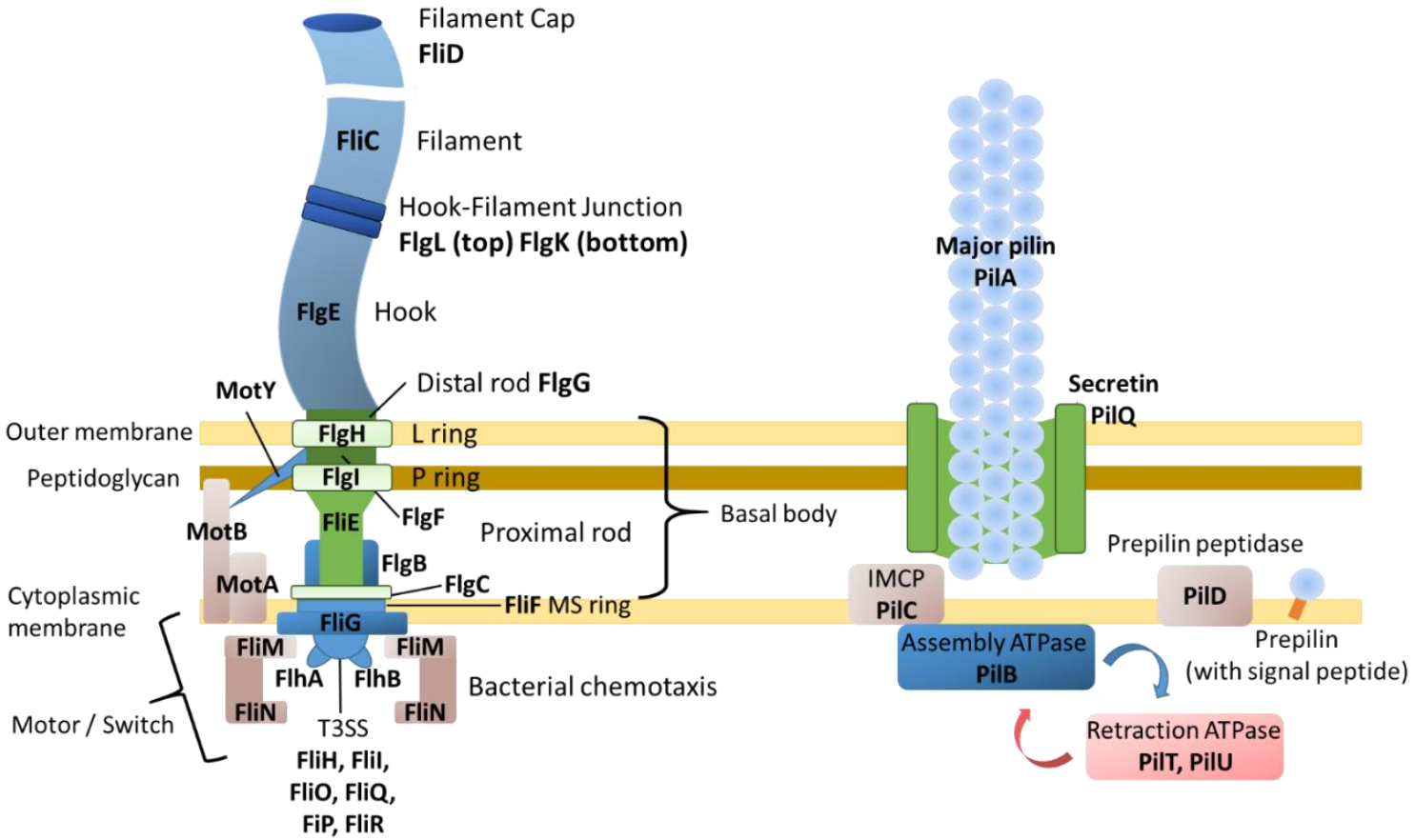

Figure 1.1. Structures of the flagellum and type 4 pili (T4P) in *P. aeruginosa*. The flagellum **(left)** is a representation drawn from information available in KEGG database (Kanehisa *et al.* 2017) and the T4P **(right)** is an adaptation of the figure available in a publication by Melville & Craig, 2013. The flagellum is subdivided in different parts; the filament, the hook, the basal body and the motor. The T4P representation is a summarised scheme including the major components of the system. IMCP stands for inner membrane core protein, accessory proteins to PilC are not shown for the sake of simplification. The flagella, T4P, membranes and peptidoglycan layer are not drawn to scale. An in-depth review of both systems and their mechanism of action has been published by Van Gerven *et al.*, (2011).

Rhamnolipids are another very important element for *P. aeruginosa* motility and biofilm formation. Rhamnolipids are glycolipidic surface-active molecules produced by many bacterial species, that act as an important surfactant for twitching motility and biofilm formation, earning a central role in the physiology of *P. aeruginosa* (Soberón-Chávez, Lépine and Déziel 2005). The rhamnolipids from *P. aeruginosa* have been the most extensively studied due to the clinical and industrial relevance of this bacteria. Surfactants are useful for the industry as they greatly reduce the interphase tension between a liquid and another surface, reducing the energy loss which makes whatever process more efficient and less abrasive. As discussed above on the application of rhamnolipids in industry, *P. aeruginosa* is the main organism used in biosurfactant production (Dobler *et al.* 2017). Mono-rhamnolipids are synthesised by the enzymes encoded by the *rhlAB* operon, and further modified in di-rhamnolipids by the enzyme encoded by the *rhlC* gene (Rahim *et al.* 2001). Besides its role in biofilms and motility, rhamnolipids themselves can induce death of polymorphonuclear leukocytes *in vitro*, disrupt the natural function of epithelial cells to facilitate the colonisation of tight junctions by *P. aeruginosa*, and inhibit ciliary beating (Read *et al.* 1992; Zulianello *et al.* 2006; Van Gennip *et al.* 2009). In motility, the production of rhamnolipids is an important element for effective migration through swarming, with different rhamnolipids controlling the swarming patterns and bacteria distribution *in vitro*, which suggests they have an important biological role guiding bacterial expansion (Déziel *et al.* 2003; Tremblay *et al.* 2007). In biofilms, rhamnolipids play a critical role for the structural integrity of the general architecture (Davey, Caiazza and O'Toole 2003), notably, the presence of rhamnolipids on surfaces can create an anti-adherent layer that prevents attachment of other cells to that surface, providing a competitive advantage over potential posterior colonisers (Nickzad and Déziel 2014). Rhamnolipids are also actively involved in biofilm dispersal mechanisms, intra- and inter-species (Schooling *et al.* 2004; Boles, Thoendel and Singh 2005; Bhattacharjee, Nusca and Hochbaum 2016). The production of rhamnolipids is regulated by the super regulators RpoN, RpoS and the QS systems *las* and *rhl* (Dobler *et al.* 2016). Interestingly, it is suggested that rhamnolipids have a close relationship with the *pqs* system, as the signal

molecules from this system are highly hydrophobic and the presence of rhamnolipids significantly increases their solubilities and hence bioactivities (Calfee *et al.* 2005).

1.2.2. Siderophores

Iron is used as cofactor for a wealth of enzymatic functions, as an electron donor or an acceptor in photosynthesis, in respiration and in nitrogen fixation processes. In many environments, the bioavailability of iron is often the main limiting factor for the development of many organisms. Within complex animals, the chelation of iron is a defence mechanism on its own right, usually achieved by lactoferrin, ferritin and transferrins, with iron also being immobilised in heme group proteins. The limited bioavailability of this micronutrient has driven evolutionary processes that resulted in highly efficient iron acquisition mechanisms especially in microorganisms (Mielczarek, E. V.; McGrayne 2000; Skaar 2010). Siderophores are small molecules with high affinity for iron and other metals. One of the characteristics used to catalogue siderophores is a small peptide chain that serves as the core and provides the characteristic blue-green colour (Albrecht-Gary *et al.* 1994).

P. aeruginosa produces two siderophores with great affinity for iron, pyoverdine and pyochelin. Pyochelin has a lower affinity than pyoverdine (Albrecht-Gary *et al.* 1994; Brandel *et al.* 2012). Due to its affinity, pyoverdine is the most relevant siderophore in the host environment, where it has been calculated that the ferric iron (Fe^{3+}) concentration is 10^{-18} M (Wandersman and Delepelaire 2004). The structure of pyoverdine is highly variable and strain-specific, possibly related to better adaptations of the siderophore to each environment where the strain grows (Hoegy, Mislin and Schalk 2014). Three different pyoverdines have been identified in *P. aeruginosa* depending on the peptide chain length of the molecule (Meyer *et al.* 1997). Moreover, *P. aeruginosa* can also use xenosiderophores from other bacteria, uptake heme groups and use phenazines (like pyocyanin) coupled with the iron uptake system Feo to reduce Fe^{3+} to ferrous iron (Fe^{2+}) (Dean and Poole 1993; Cornelis and Dingemans 2013).

Expectedly, pyoverdine is extremely important in *P. aeruginosa* virulence. During the colonisation of the CF lung the synthesis of pyoverdine allows *P. aeruginosa* to successfully scavenge the necessary iron, moreover, the levels of intracellular iron control biofilm development through the iron-dependent transcriptional regulator Fur (Banin, Vasil and Greenberg 2005). Available data suggests that pyoverdine is one of the key factors in the initial establishment of infection, however the importance of the siderophore decreases in chronic infections as pyoverdine-negative and QS-negative mutants (which activate pyoverdine) can often be found in chronic CF lungs, where most iron acquisition is performed by heme groups (Stintzi *et al.* 1998; Nguyen *et al.* 2014; Minandri *et al.* 2016). Furthermore, pyoverdine is actually necessary for pathogenesis in *Caenorhabditis elegans* models and mammalian infection models, acting by directly removing ferric iron (Fe^{3+}) from the host, damaging the mitochondria (Kang *et al.* 2018).

The synthesis of pyoverdine activates the production of other virulence factors, while the expression of its biosynthesis genes is regulated by several factors. Some of these, like polysaccharides Pel and Psl, cell aggregation or intracellular c-di-GMP levels are also key factors for the biofilm development, in accordance to the stages when pyoverdine availability is most important (Llamas *et al.* 2014; Chen *et al.* 2015b; Visaggio *et al.* 2015). QS is also involved in pyoverdine regulation, and some molecules like the Pseudomonas quinolone signal (PQS) can, in addition to act as signalling molecules, also chelate iron (Bredenbruch *et al.* 2006). Out of all the regulators, Fur (ferric uptake regulator) is probably the most important for iron-related genes. The relevance of this regulator is such that under certain growth conditions *fur* is a housekeeping gene for *P. aeruginosa* (Pasqua *et al.* 2017). Fur is a potent transcriptional regulator that binds to a *fur*-box in the promoter of target genes, ultimately balancing the intracellular iron homeostasis. When the concentrations of Fe^{2+} are too high, Fur inhibits the expression of iron acquisition and virulence-related genes, including pyoverdine and pyochelin, at the same time Fur activates the transcription of genes involved in iron storage and oxidative stress to protect against iron toxicity (Troxell and Hassan 2013).

1.2.3. Proteases

The wide range of proteases secreted by *P. aeruginosa* are also one of the characteristics that make this bacterium so successful in many environments by degrading complex macromolecules into usable nutrients and / or acting as a defence-attack mechanism. In the host environment, these proteases can damage the tissue, degrading elements like collagen or laminin, but also efficiently degrade molecules from the immune system such as cytokines, making them an important virulence factor. Several proteases can be detected in the CF lungs, including elastase B (LasB), alkaline protease, protease IV and PasP (Hoge *et al.* 2010). The expression of proteases is necessary to ensure the survival of the population in a highly hostile and / or competitive environment. Biofilms have also been found to produce high levels of proteases, maintaining their secretion even under treatment with antibiotics that target active metabolism (Ołdak and Trafny 2005).

Proteases are often divided into 6 different types depending on the active residues involved in the cleaving: Aspartic-proteases, cysteine-proteases, glutamic-proteases, metalloproteases, serine-proteases and threonine-proteases. To put into perspective the importance of proteases in *P. aeruginosa*, 2.8% of the genes in the PAO1 genome correspond to this class of proteins, with most of those (54%) being serine-proteases, followed by metalloproteases (29%) (Hoge *et al.* 2010).

The metalloprotease LasB is an elastase that works in tandem with LasA to cleave elastin, a protein that plays a structural support role in tissues. LasB can also degrade other proteinaceous substrates of relevance such as collagen (structural support) or IgG and other elements of the immune system (Hoge *et al.* 2010). This strong activity of LasB makes it a highly immunogenic component that triggers an inflammatory response and the recruitment of polymorphonuclear leukocytes such as neutrophils, making it an important virulence factor in acute infections under strong regulation (Kon *et al.* 1999). The most important regulation of LasB is probably QS. LasB is under strong regulation by the *las* and, secondarily, the *rhl* QS systems in acute infections and the early stages of chronicity (Pearson, Pesci and Iglewski 1997). The *pqs* system also has an impact over *lasB*

expression, albeit indirectly, through the activation of the *rhl* system (McKnight, Iglewski and Pesci 2000).

The alkaline protease AprA or aeruginolysin is a metallo-endoprotease that uses zinc as co-factor (Häse and Finkelstein 1993). AprA cleaves a number of substrates, including laminin and important components of the immune system like IFN-γ, TNF-α and IL-6, effectively impairing the immune system response to *P. aeruginosa* invasion (Hoge *et al.* 2010). AprA is secreted by the type 1 secretion system (T1SS) (Wagner *et al.* 2016) and it can act in tandem with other virulence factors. It has been shown that its activity provides the necessary building blocks to promote pyocyanin biosynthesis (Iiyama *et al.* 2017) and it can work along with elastase to degrade exogenous flagellin, limiting the immune recognition of this subunit without compromising bacterial motility (Casilag *et al.* 2016). Similarly to *lasB*, the expression of *aprA* is under strong regulation by the *las* system, however, unlike *lasB*, the presence of *rhl* alone is not sufficient to express *aprA*, suggesting that *las* is the main QS system regulating AprA (Casilag *et al.* 2016). Finally, the production of AprA is also iron-regulated, tuning the expression of the gene encoding this protease with the conditions often found within the host (Shigematsu *et al.* 2001).

The protease IV is a serine-endoprotease that cleaves the carboxyl-side of lysine amino acids (Elliott and Cohen 1986). This protease cleaves fibrinogen, an important element for blood coagulation that is recruited in the inflammatory response. Other targets of protease IV also include important elements of the immune system like elements of the complement (innate response) or IgG (adaptive response) (Engel *et al.* 1998). Protease IV is under indirect iron regulation through the control of PvdS which is regulated by Fur meaning that its expression is inhibited in higher iron concentrations (Hoge *et al.* 2010). Notably, protease IV has a negative feedback loop of sorts through substrate degradation. Protease IV can degrade lactoferrin and transferrin (Wilderman *et al.* 2001), the degradation of these proteins releasing chelated iron and increasing its bioavailability, which in turn will activate the Fur system and inhibit expression of Protease IV to prevent toxic intracellular iron accumulation.

P. aeruginosa small protease (PasP) is a relatively novel secreted protease from *P. aeruginosa* that was identified from corneal epithelial erosions but detected in every *Pseudomonas* strain tested (Marquart *et al.* 2005; Tang *et al.* 2009). PasP can degrade structural proteins such as collagen and fibrinogen and immune-related proteins, like C3 (part of the complement, innate response) or C1q although PasP does not degrade immunoglobulins. As a matter of fact, PasP is highly immunogenic, however rabbit antibodies are ineffective at inactivating the protein (Tang *et al.* 2009). Most research on PasP has focused on its role in keratitis even if it has also been detected in CF lungs (Hoge *et al.* 2010). PasP plays an important role in the degradation of structural barriers sensitive to collagenases and the inhibition of the innate response however its regulation has not yet been fully elucidated (Tang *et al.* 2013).

The main proteases described here from *P. aeruginosa* all play similar roles, effectively degrading structural components that cause cell and tissue damage at the same time as they degrade immune-system components that help the bacteria to evade an effective response. All these proteases are under regulation of systems closely related to the acute stage of infections such as iron-mediated responses or QS. Their presence is therefore tightly tied to the establishment of acute infections but their relevance decreases in chronic infections.

1.2.4. Other colonisation factors

Besides motility components, iron scavenging mechanisms or peptidases, *P. aeruginosa* also presents other important factors that significantly help in colonisation and competition. One of the most important and studied factors is pyocyanin. Pyocyanin is a type of phenazine, a redox secondary metabolite with a bright blue hue under neutral or alkaline conditions produced by many *P. aeruginosa* strains (Lau *et al.* 2004). Pyocyanin redox activity causes cellular and tissue damage but it can also directly inhibit catalase expression, induce neutrophil apoptosis or kill competitors (in presence of oxygen or nitric oxide) (Lau *et al.* 2004). Pyocyanin synthesis is strongly regulated by the *pqs* system but also by *las* and *rhl*. Other regulators controlling pyocyanin production include the GacA / GacS two-component regulatory system (TCS) and the virulence regulator Vfr

(Fuqua, Parsek and Greenberg 2001). Hydrogen cyanide (HCN) is another significant poison produced by *Pseudomonas* (Blumer and Haas 2000). HCN toxicity comes from the inhibition of the cytochrome c oxidase and other metalloenzymes, inducing the blocking of respiration and cellular death. It is believed that the function of HCN is to outcompete other organisms in the environment while *P. aeruginosa* avoids self-poisoning through active detoxification mechanisms and respiration using a cyanide-insensitive terminal oxidase (Lenney and Gilchrist 2011). The molecular mechanisms of HCN regulation are still not clear but it has been observed that its production is tightly regulated by oxygen and only induced in microaerobiosis conditions, while it is not produced in anaerobiosis or aerobiosis (Lenney and Gilchrist 2011). *P. aeruginosa* also secretes other proteins than proteases which have a significant impact over colonisation success. One of these components is the exotoxin A (ToxA), an enzyme that can effectively inhibit protein synthesis and actively induce cell apoptosis (Michalska and Wolf 2015). *P. aeruginosa* also synthetises haemolytic phospholipases (PLCH) and non-haemolytic phospholipase (PLCN) which have different substrate affinities to degrade multiple tissue components (Ostroff, Vasil and Vasil 1990).

1.2.5. Secretion systems

P. aeruginosa has multiple secretion machineries to transport all these elements to the extracellular environment. Five out of the six (T1SS-T6SS, excepted T4SS which is not found in this species) secretion systems are found in *P. aeruginosa* and sometimes in multiple copies, highlighting the relevance of these systems (Bleves *et al.* 2010). These systems are very important for the correct secretion of their specific substrates and virulence as without the secretion systems *P. aeruginosa* is unable to establish any infection. The T1SS is a basic mechanism with three components, a protein in each membrane and an adapter in the periplasm (Delepelaire 2004). This system recognises its substrates through a non-cleavable C-terminal signal peptide and transports them unfolded, an example of which is the alkaline proteases AprA (Bleves *et al.* 2010). The T2SS has evolved to translocate large proteins and complexes, its conformation includes many more proteins than the T1SS but they are arranged in three main

components: An inner membrane platform, a large channel and a fimbrilar structure. This is similar to the T4P hence the occasional reference as pseudopilus (Filloux 2004). T2SS secretes some of the major proteases such as LasB, LasA, protease IV and ToxA (Bleves *et al.* 2010). The T3SS works as a syringe mechanism, directly injecting its substrates into the cytosol of the target, often eukaryotic cells. As the T2SS is similar to the type 4 pili base structure, the T3SS is similar to the flagellum assembly machinery. The T3SS is often formed by an extracellular syringe or needle, attached to a transmembrane cylindrical mechanism that anchors the needle and translocates the substrate (Cornelis 2006). The substrates, which are recognised by a non-cleavable N-terminal signal and transported unassembled through a 7 nm wide channel, are four proteins called effectors (ExoS, ExoT, ExoU and ExoY). *P. aeruginosa* strains are divided in *cytotoxic* or *invasive* isolates depending on the effectors they harbour, ExoU, ExoT and sometimes ExoY correspond to the cytotoxic isolates which cause rapid cell death whereas ExoS, ExoT and often ExoY correspond to invasive isolates, which cause a slower cellular death similar to apoptosis after the bacteria is often internalised. The genes *exoU* and *exoY* are never found together in the same strain, the reason though is yet unknown (Bleves *et al.* 2010). The expression of T3SS genes is regulated by ExsA, which induces the genes under calcium restriction but also depending on global regulators like cAMP and the Gac-Rsm system. QS systems usually inhibit T3SS gene expression, suggesting that it is not important for the acute infection but may be relevant for the chronic establishment of the pathogen (Bleves *et al.* 2010). The T5SS is the simplest system as the substrates move through the inner membrane thanks to a translocating system and then leave the outer membrane through a β-barrel protein. The substrates can remain attached to the outer membrane after secretion or be released after signal cleavage (Bleves *et al.* 2010). In *P. aeruginosa* the T5SS secretes an esterase which hydrolyses fatty acids and is involved in rhamnolipid synthesis. Other elements secreted by the T5SS include proteases of which some can activate NF-κB mediated inflammation (innate response) (Bleves *et al.* 2010). The last secretion system present in *P. aeruginosa* is the T6SS, similarly to the T3SS, works as an injection system with an extracellular component that penetrates membranes of Bacteria

and Eukarya alike (T6SS is structurally similar to the tail of phage λ). T6SS secretes a range of effectors that can kill bacteria or eukaryotic cells, provide a fitness advantage to *P. aeruginosa* and even play a role in biofilm development. The regulation of T6SS is a complex multi-layered system involving different mechanisms (including QS) (Chen *et al.* 2015a).

1.3. *P. aeruginosa* Biofilms

The formation of biofilms is the most successful strategy for bacterial colonisation and persistence, and the predominant way of life of these microorganisms (Geesey *et al.* 1977; Costerton *et al.* 1995). During biofilm growth, bacteria aggregate and multiply within a matrix mostly formed by extracellular polymeric substances (EPS) with a high water content. EPS are the critical support in which bacteria proliferate and contain many organic polymers, including polysaccharides, proteins, extracellular DNA (eDNA) and membrane vesicles (MVs) (Schooling and Beveridge 2006; Flemming, Neu and Wozniak 2007). Bacterial communities embedded within biofilms exhibit a very distinct transcriptome and proteome from their planktonic counterparts and are usually considered to be metabolically less active, although significant differences exist within the subpopulations of the biofilm (Rollet, Gal and Guzzo 2009; Williamson *et al.* 2012). Moreover, cells dispersing from mature biofilms constitute a third physiological state, different from planktonic and biofilm stages (Chua *et al.* 2014).

Biofilm formation is such a successful strategy to achieve bacterial colonisation that these can be grown virtually everywhere, with most natural biofilms developing as mixed species communities with co-existing populations, establishing complex ecological relationships between the populations encased in the matrix and with the matrix and the environment itself (Tyson *et al.* 2004; Aruni *et al.* 2015). The matrix that surrounds the communities and their physiological characteristics make them extremely resilient to the action of antibiotics and other treatments. This causes very serious problems and economic losses in industry through biofouling, the accumulation of organisms and organic matter that can lead to surface damaging, pipe clogging and contamination (Fitridge *et al.* 2012). Moreover, pathogens capable of forming biofilms pose very serious health

problems and are etiological agents of chronic infections such as those in wounds, prosthetic devices, catheters, etc. (Mihai *et al.* 2015).

As an opportunistic human pathogen, *P. aeruginosa* can colonise with ease the respiratory airways of cystic fibrosis patients, developing encroaching infections that can become untreatable (Govan and Deretic 1996; James *et al.* 2008). The development of biofilms by *P. aeruginosa* follows the classical four steps: (1) primary and reversible attachment; (2) secondary and irreversible attachment (microcolony formation); (3) biofilm formation (macrocolony formation) and (4) dispersal (Stoodley *et al.* 2002; Ma *et al.* 2009; Monds and O'Toole 2009) (Figure 1.2). In a classic *P. aeruginosa* mono-species biofilm model, biofilm formation is initiated upon surface sensing and recognition. As previously mentioned, motility elements such as flagella, T4P and rhamnolipids play an important role on initial attachment (O'Toole and Kolter 1998a; Pamp and Tolker-Nielsen 2007) but other factors such as QS or the presence of bacterial surface-bound lectins are also very important at this stage (De Kievit *et al.* 2001; Tielker *et al.* 2005). This recognition and attachment triggers a series of signalling cascades that switch the lifestyle towards biofilm growth. Microcolony formation starts right after the attachment and loss of motility (Klausen *et al.* 2003a). During this stage, the biofilm matures and subpopulations are created, with a basal layer of non-motile, mostly dormant cells, and upper layers of more metabolically active cells from which dispersing cells will develop (Klausen *et al.* 2003a; Chiang *et al.* 2012). Macrocolonies are large structures formed under certain conditions by mature biofilms. These structures often encase motile cells ready for dispersal in empty cavities found in the upper middle part of the structure (Pamp and Tolker-Nielsen 2007; Barken *et al.* 2008). All the components of the extracellular matrix are extremely relevant at this stage to maintain the natural biofilm homeostasis. The biofilm dispersal is a very complex process triggered by a wealth of internal and external signals and cues, including but not limited to motility, rhamnolipids, quorum-sensing, autolysis and environmental factors (Kim and Lee 2016). It must be noted that the development of mushroom-shaped biofilms is not necessarily an indicator of mature biofilms and there are many cases particularly in the natural environment

where mature biofilms present completely different architectures, developing in microbial mats or other formations (Bengtsson *et al.* 2018).

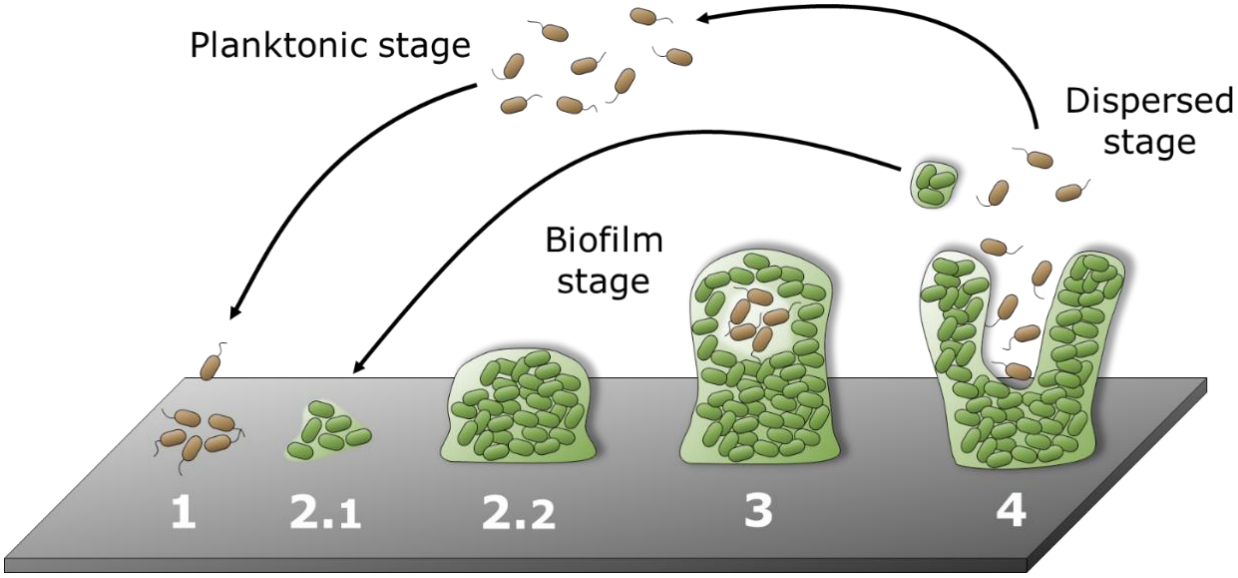

Figure 1.2. *P. aeruginosa* biofilm cycle with planktonic and dispersed stages. 1: Primary and reversible attachment by motile cells upon surface recognition. **2.1:** Secondary and irreversible attachment, surface recognition triggers loss of motility and switch to biofilm physiology, the matrix starts building up. **2.2:** Microcolony development, young microcolonies start developing the biofilm structure as the matrix matures and cell-to-cell adhesion takes place. Biofilm subpopulations start originating here. **3:** Macrocolony formation, a mature biofilm grows fully developed macrocolonies, with centres empty of matrix and full with dispersal cells originated from the active subpopulation. Biofilm structure is maintained. **4:** Dispersal, different signals trigger the dispersal of mature colonies, opening the cap and releasing the motile cells in dispersal physiology (Chua *et al.* 2014). Chunks of biofilm are also sheared and can re-attach somewhere else to start the cycle all over again. Adapted from the classic figure by Stoodley *et al.*, 2002; Dirckx & Davies, 2003.

1.3.1. The bacteria within the biofilm

The bacteria that develop within the biofilm grow embedded and anchored in the biofilm matrix, which provides a protective microenvironment that concentrates nutrients and ensures the persistence of the population or community. Bacteria growing within the biofilm divide into functionally and physiologically distinct subpopulations which also are spatially separated, further underlying the inherent complexity of this lifestyle. In *P. aeruginosa*, the differentiation of these subpopulations will have a direct impact over the development of the biofilm structure and several important factors such as the carbon source can influence this (Klausen *et al.* 2003a; Meylan *et al.* 2017). Partly controlled by QS, motile bacterial subpopulations separate through migration involving T4P and flagella climbing to the upper layers of the microcolonies aided by eDNA. In growth models that develop mushroom-like structures, the non-motile fraction

remains in the stalk (Klausen *et al.* 2003a; Okshevsky and Meyer 2015). However, the system that triggers the differentiation of motile and non-motile subpopulations is currently unknown.

The differentiation of subpopulations generates a physiological stratification within the biofilm, with most of the metabolic activity concentrated on the outer layers. The subpopulation found there is therefore referred to as *active* while the subpopulations from the inner parts of the biofilms with low metabolic activity are considered *inactive* or *dormant* (Walters *et al.* 2003; Werner *et al.* 2004). One of the current hypotheses about these differences in activity is related to how much more limited nutrient and oxygen availability in the inner layers of the biofilm will be, which incidentally renders the dormant subpopulation highly resistant to any antibiotics that target metabolically active cells (Ciofu *et al.* 2017). Moreover, the dormant cells contain a small fraction of persister cells, a group of cells highly resilient to the treatment with antibiotics (Lewis 2007; Wood, Knabel and Kwan 2013).

In mature microcolonies, a matrix-free cavity is formed which houses motile bacteria that are ready to be released for dispersal (Mann and Wozniak 2012). This subpopulation matures from the active subpopulation and differentiates itself by expressing genes useful for a free-living stage as dispersed cells, releasing from defined points in the microcolony upon different signals (Purevdorj-Gage, Costerton and Stoodley 2005; McDougald *et al.* 2012; Chua *et al.* 2014). The active subpopulation of *P. aeruginosa* biofilms is also capable of adapting to membrane-targeting antibiotics by expressing a series of resistance genes. However, the dormant population does not present a dynamic response flexible and active enough to counteract these antibiotics, therefore is sensitive to them (Chiang *et al.* 2012). It is important to note that the dormant subpopulation does not remain inactive *per se* and also plays a key role in the continued maintenance of the biofilm. It has been observed that most of the autolytic processes thought to be relevant for membrane vesicle (MV) and eDNA release happen in the stalk and inner layers of the biofilm, from this subpopulation (Werner *et al.* 2004; Allesen-Holm *et al.* 2006). Most of the studies related to this subpopulation have focused on its role in

antimicrobial resistance (Bjarnsholt 2013). The dormant or inactive population has a decreased metabolism with overrepresentation of expressed overlapping genes involved in stress and stringent responses (Stewart *et al.* 2015). Moreover, there is evidence that this subpopulation is the driver for antibiotic resistance development. The process would happen through an increased mutation rate, particularly in the DNA oxidative damage repair systems that allows the community to increase their genotypic heterogeneity and develop resistance mechanisms (Conibear, Collins and Webb 2009; Mandsberg *et al.* 2009).

1.3.2. The biofilm matrix

The composition of the biofilm matrix is highly variable depending on the producing strains and the environment where the biofilm is growing. In CF lungs, hyper-mucoid strains have high colonisation success and are often found dominating the infections. These strains are usually alginate overproducers (Govan and Deretic 1996). Production of alginate favours the establishment of chronic inflammation, protects against the immune system and antimicrobials and enhances attachment in the lung environment (Govan and Deretic 1996; Leid *et al.* 2005). On the other hand, biofilms from water treatment plants have a very large matrix, rich in protein and especially in eDNA (Frølund *et al.* 1996). This matrix was found to contain high quantities of carbohydrates, humic and uronic acids. These are all common products expected from the degradation of organic matter, suggesting that in this environment, the matrix also plays a very important role at immobilising and concentrating the available nutrients from the media to the biofilm. All components of the matrix are interconnected, and each plays a significant role in the interactions with the environment and itself.

1.3.2.1. Alginate

Alginate is a high molecular weight, acetylated polysaccharide with non-repetitive monomers of glucoronic and mannuronic acids and a net negative charge (Evans and Linker 1973). Alginate has been observed to be mainly produced by *P. aeruginosa* clinical isolates from the lungs of CF patients, where it confers a mucoid phenotype (Govan and Deretic 1996).

Alginate plays an important role in water and nutrient retention (Sutherland 2001), other advantages provided by alginate overproduction in this environment have been discussed above. Notably, it has been found that alginate is not required for biofilm formation *in vitro*, and such biofilms are aptly named non-mucoid biofilms (Wozniak *et al.* 2003; Wozniak, Sprinkle and Baynham 2003). Synthesis of alginate is carried out by the *alg* operon, regulated by AlgU, which is itself under control of the proteins encoded by the *mucABCD* operon. Most hyper-mucoid strains have been observed to harbour mutations in the repressor MucA, while other regulators of alginate include the membrane associated MucR, the TCS KinB/AlgB and FimS/AlgR, DNA-binding proteins AmrZ, AlgP and AlgQ and the super regulator RpoN as well as the intracellular signalling molecule c-di-GMP and the *las* QS system (Quiñones, Dulla and Lindow 2005; Hay, Remminghorst and Rehm 2009; Hay *et al.* 2014).

1.3.2.2. Pel polysaccharide

The structure of the Pel polysaccharide was described recently by Jennings *et al.*, 2015. Pel is a polymer of 1-4 linked and partially acetylated galactosamine and glucosamine sugars positively charged at neutral and slightly acidic pH. During biofilm formation, Pel can be found in a cell-bound form and a secreted, much lighter form (80 kDa vs 0.5 kDa) which may play different roles. Moreover, there is evidence that Pel localisation in the biofilm is strain-dependent. In PA14, Pel was found in the periphery of microcolonies and stalk whereas in PAO1 it concentrated in the stalk and basal layers (Jennings *et al.*, 2015). Interestingly, the periphery of PAO1 microcolonies was rich in Psl polysaccharide. Meanwhile, a Psl negative mutant of PAO1 was found to have Pel in the periphery, suggesting that Psl is dominant in that area, but Pel can substitute it in its absence. The positive charge of Pel makes it closely interact with the eDNA fraction of the matrix, with both elements co-localised in the stalk where they are found cross-linked in the typical pH found in biofilms (Jennings *et al.* 2015). Taking this all together, current data available from Pel implies that this polysaccharide mostly provides structural support and a protective layer against aminoglycoside antibiotics (Colvin *et al.* 2011; Jennings *et al.* 2015).

1.3.2.3. Psl polysaccharide

The Psl polysaccharide is based on a distinct pentasaccharide repeat containing D-mannose, D-glucose and L-rhamnose (Byrd *et al.* 2009). Psl synthesis is carried by the *psl* locus containing 15 co-transcribed genes with homology to carbohydrate biosynthesis genes (Friedman and Kolter 2004; Jackson *et al.* 2004; Matsukawa and Greenberg 2004). Like Pel (above), Psl also plays an important role in biofilm formation in *P. aeruginosa* (Yang *et al.* 2011) but unlike Pel, Psl does not have any net charge at neutral or slightly acidic pH and is not found cross-linked with eDNA. Available data indicates that Pel is the main provider of biofilm structural support, it can be found in the periphery of the microcolonies and increases adherence as well as cell-to-cell interactions since it is anchored to the surface of the bacterial cells too (Ma *et al.* 2006, 2009, Byrd *et al.* 2009, 2010). The presence of Psl also plays a role in several mechanisms of antibiotic resistance and survival of *P. aeruginosa in vivo* by limiting complement-mediated opsonisation and neutrophil killing (Mishra *et al.* 2012; Wei and Ma 2013). Nevertheless, it has also been shown to have proinflammatory activity through indirect stimulation of NF-κB (Byrd *et al.* 2010) which could be important for the maintenance of an inflammatory response in chronic infections.

Both Pel and Psl polysaccharides are required for initial microcolony formation (Schurr 2013) during which, c-di-GMP, iron signalling and *las* and *rhl* QS systems are upregulated, favouring the release of eDNA and other EPS. This helps the migration of a motile subpopulation to the upper layers of the microcolonies through flagellum-mediated chemotaxis (Barken *et al.* 2008). This subpopulation will then bind to the eDNA through type IV pili and remain anchored through Psl, leading to the formation of mushroom-shaped colonies and maturation of the biofilm (Figure 1.3) (Yang *et al.* 2011). Notably, it has been observed that PA14 does not produce Psl, which could explain the previously mentioned differences in Pel distribution (Zegans *et al.* 2012).

1.3.2.4. Extracellular DNA (eDNA)

Extracellular DNA has possibly been one of the most exhaustively studied components of the biofilm matrix because of its critical relevance within the biofilm, as the presence of eDNA is critical from the onset of biofilm development (Whitchurch *et al.* 2002). The release of eDNA is a poorly understood process that seems to involve the release of membrane vesicles through different mechanisms, sometimes under *las* and *pqs* system regulation (Spoering and Gilmore 2006; Wei and Ma 2013; Thomann *et al.* 2016; Turnbull *et al.* 2016). A fraction of these vesicles seem to involve the autolysis of the stalk subpopulation, further accentuating the differences between stalk and cap subpopulations (Parsek and Tolker-Nielsen 2008). The released eDNA appears to be from random fragments of the chromosome (Ma *et al.* 2009). eDNA serves as a cell-to-cell interconnecting element that can be found in particularly high concentrations in the stalk of mushroom-like microcolonies (Allesen-Holm *et al.* 2006). However, the presence of eDNA extends through the whole matrix, developing along the Pel and Psl fractions suggesting that it also plays a role in the biofilm structure (Figure 1.3) (Mann and Wozniak 2012; Jennings *et al.* 2015). eDNA maintains the acidic homeostasis of the biofilm which favours the establishment of bonds with other elements of the matrix and protects against antibiotics (Ma *et al.* 2009; Wilton *et al.* 2015). Thanks to the characteristics of dsDNA, eDNA creates a large number of hydrogen bonds that serves to strongly attach to many surfaces and molecules in an unspecific manner (Tseng *et al.* 2018). To further highlight the relevance of eDNA, the cells can use it as a carbon source, to coordinate biofilm migration and for the correct development of mushroom-like microcolonies (Finkel and Kolter 2001; Parsek and Tolker-Nielsen 2008; Mulcahy, Charron-Mazenod and Lewenza 2010; Gloag *et al.* 2013).

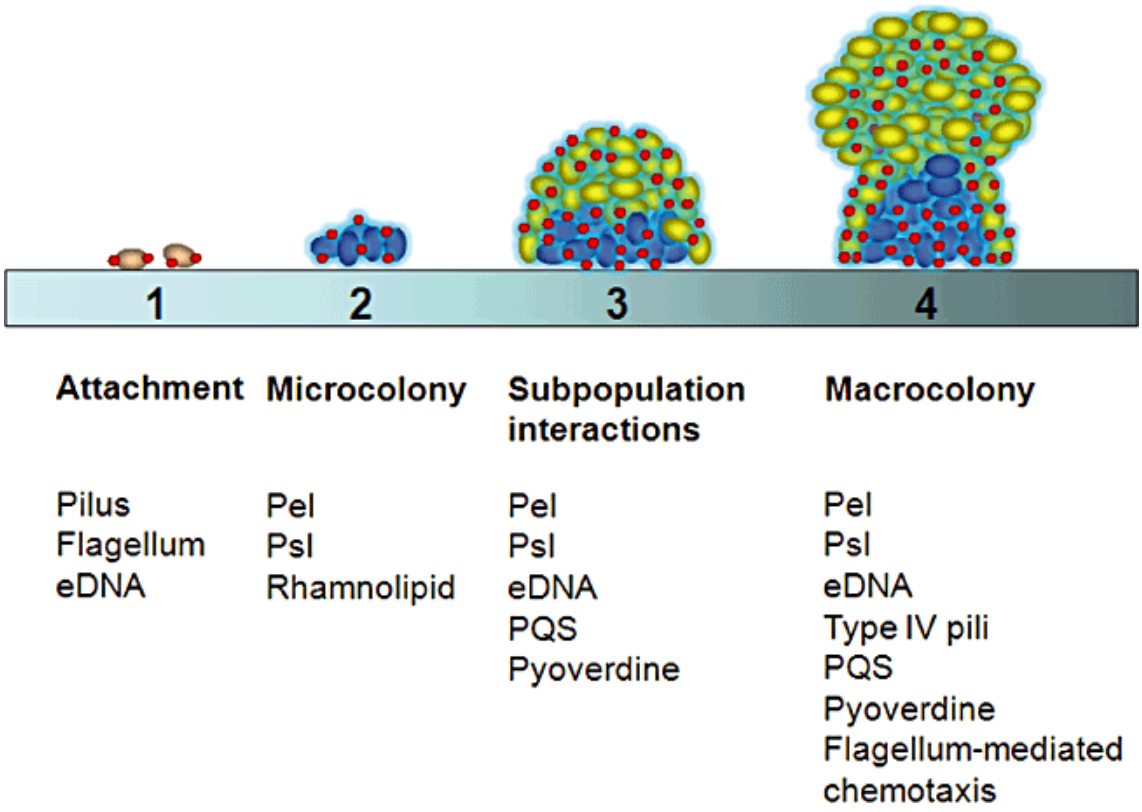

Figure 1.3. Extracted from Yang *et al.*, 2011. Proposed model for *P. aeruginosa* biofilm development. 1: individual planktonic cells attach to the surface. **2:** attached cells form microcolonies. **3:** subpopulations interact with each other during biofilm structure development. **4:** macrocolonies are formed in mature biofilms. **Red dots** represent eDNA; **blue** and **yellow** ovals represent cells of non-motile and motile biofilm subpopulations, respectively; **cyan** represents Pel and Psl polysaccharides. Some of the main phenotypes are listed below each stage.

1.3.2.5. Proteins, MVs and other accessory elements

The matrix also contains a wealth of other components with auxiliary functions, including cyclic β glucans, LPS, membrane vesicles (MVs) and motility appendages such as T4P, flagella and fimbriae. Most of these factors play auxiliary adhesion roles, provide structural support and are under regulation of c-di-GMP (Mann and Wozniak 2012; Wei and Ma 2013). Most of the proteins found in the matrix are either secreted, come from cell debris after autolysis or are found associated with MVs (the most common fraction). Proteinases are the most common type of proteins and many of these are considered virulence factors like LasA, LasB or protease IV (Toyofuku *et al.* 2012). Other notable functions from the matrix proteasome are oxidative stress response proteins, DNA-binding and iron acquisition proteins (Toyofuku *et al.* 2012). MVs are a major component of the matrix with key roles for its function within and without the biofilm. Since MVs are formed by the outer membrane, they contain

lipopolysaccharides (LPS) but they also house the previously mentioned proteins and DNA. MVs play important roles as virulence factors and delivery mechanisms, cell-to-cell communication, nutrient acquisition, horizontal gene transfer, antibiotic resistance and even competition with other organisms (Schooling and Beveridge 2006; Kulp and Kuehn 2010). Following the previously mentioned differences in the extracellular matrix of PA14, it has also been observed that their MV production and regulation is significantly different from PAO1 (Florez *et al.* 2017).

1.4. *P. aeruginosa* quorum sensing systems

Quorum sensing (QS) is a cell-to-cell communication system that coordinates the physiology of the population once the signal molecules reach a concentration threshold. These signals are constantly produced and self-induce the expression of their biosynthesis genes, therefore they are often named autoinducers. The full activation of the system depends on reaching a critical population density at which point the signal molecules accumulate over a threshold concentration, the autoinducing positive feedback loop is highly enhanced and the regulation of all the phenotypes under the system's control will supersede any other regulation. Hence the name, initially used by Fuqua *et al.*, 1994, as bacteria will only undertake certain behaviours upon reaching (or sensing) a certain quorum (minimum number of members required to perform or approve a certain action). QS systems are a widespread regulation tool found in Bacteria, Archaea and Eukarya domains (Charlesworth *et al.* 2017), and it is not uncommon that a certain species have multiple systems (Lee and Zhang 2014). All QS systems are based on the production of diffusible small signal molecules (autoinducers) that bind and activate a regulatory protein which will trigger the expression of a wide range of genes. Some of the most studied QS systems regulate virulence and biofilm formation (Whitehead *et al.* 2001; Deng *et al.* 2011).

The first QS system was elucidated after studies of bioluminescence in *Vibrio fischeri* and the *luxI*-*luxR* system (Nealson, Platt and Hastings 1970) in which *luxI* encodes the synthase for the autoinducer *N*-(3-oxohexanoyl)-L-homoserine lactone (OHHL) that regulates the population-density bioluminescence of this bacterium (Stewart and Williams 1992; Williams *et*

al. 1992). This is when the first family of QS signal molecules, the *N*-acylhomoserine lactones (AHLs) were discovered. From then on, paralogues of this system have been sought after in many other bacteria, making the AHL-based QS systems the most widely studied to date.

Many molecules used as autoinducers fall within chemically distinct families. The previously mentioned AHLs are found in Gram-negative bacteria and fall within the category of the classic system where the autoinducer binds to the regulator to control gene expression. Different species produce different acyl chain lengths and can have substitutions in the third carbon position. Other QS families found in Gram-negatives include autoinducer-2 (AI-2), alkyl-4(1*H*)-quinolones, indole, pyrones, fatty acids (diffusible signal factors or DFS) and dialkylresorcynols (Defoirdt 2018). On the other hand, most Gram-positive base their QS systems on different mechanisms, the most common ones relying on processed oligo-peptides called autoinducing peptides (although signalling peptides are widely found in Gram-negatives too). Another family of autoinducers are the γ-butyrolactones (Polkade *et al.* 2016).

As a model organism, the QS systems of *P. aeruginosa* have been thoroughly studied, with at least three accepted systems that are hierarchically connected: *las*, *rhl*, and *pqs* (Lee and Zhang 2014). This fine regulation is what allows *P. aeruginosa* a great level of adaptability and survival in many environments.

1.4.1. LasI / LasR system

One *luxI*-*luxR* paralogue found in *P. aeruginosa* is the *las* system, the first and most dominant QS system described in *P. aeruginosa* (Figure 1.4). The *lasI* gene encodes an enzyme that synthetises an AHL described as *N*-(3-oxododecanoyl)-L-homoserine lactone (3-oxo-C12-HSL). The substrate of LasI is a 3-oxo-C12-acyl group attached to an acyl carrier protein (ACP) and *S*-adenosyl-*L*-methionine (Pearson *et al.* 1994; Gould, Schweizer and Churchill 2004). 3-oxo-C12-HSL binds to LasR, allowing it to form an active dimeric structure that can bind to dsDNA and control gene expression (Kiratisin, Tucker and Passador 2002). The *las* system is the dominant QS regulatory network of *P. aeruginosa* and controls a myriad of phenotypes

including the other systems *rhl* and *pqs* (Figure 1.4). LasR was originally identified as a *luxR* homologue regulator for the elastase gene *lasB* and other virulence factors, and was soon related to LasI and the rest of the system (Jones *et al.* 1993). Very extensive research has been performed on the *las* system ever since. Conserved recognition sequences called *las-rhl* boxes have been identified in promoter regions of genes under regulation of either QS system, roughly 10% of the genes of *P. aeruginosa* have this box near their promoters, showing the extensive regulation carried over by *las* and *rhl* (Schuster and Greenberg 2006). Out of the many genes under LasR regulation, it is interesting to point out the induction of *rsaL*. This protein is a transcriptional repressor of *lasI*, binding in the *rsaL-lasI* bidirectional promoter to inhibit *lasI* expression, generating a strong negative feedback loop that supersedes the positive one from LasR (hence the name). RsaL is also an inhibitor of transcription of other genes activated by the *las* system, balancing its activity to avoid overexpression (Rampioni *et al.* 2007). Other important super-regulators control the expression of *lasR*, a good summary of them can be found elsewhere (Lee and Zhang 2014).

It is worth noting that about a third of the clinical isolates from chronic CF lung infections harbour *las* loss of function mutations mainly in *lasR* (LaFayette *et al.* 2015). These isolates are also correlated to worse medical outcomes. The loss of *las* regulation does not seem to impact the maintenance of biofilms suggesting that its role is more limited to the initial establishment and architectural maintenance. Furthermore, CF-adapted, *las* negative isolates, present significantly impaired acute virulence mechanisms and can still grow in biofilm form, albeit without structure (LaFayette *et al.* 2015). This suggests that the main role of the *las* system is played during the initial stages of the infection. The worsening conditions correlate to an increased collateral tissue damage from the inflammatory response. A significant virulence factor activated by *las* are a set of proteases that degrade cytokines, so the absence of these proteases will cause the establishment of an hyper-inflammatory response (LaFayette *et al.* 2015).

1.4.2. RhlI / RhlR system

The second autoinducer to be discovered in *P. aeruginosa* was *N*-butyryl-L-homoserine lactone (C4-HSL) (Pearson *et al.* 1995), synthesised by RhlI and binding to the transcriptional regulator RhlR and self-inducing, in a classic positive feedback loop system, its own expression (Figure 1.4). The *rhl* system is an important quorum sensing mechanism under control of the *las* and to a certain extent, the *pqs* systems (Figure 1.4) (Lee and Zhang 2014). The *rhl* system also binds to the *las-rhl* box found in many promoters of PA. The C4-HSL (traditionally called BHL), binds to RhlR to create the RhlR-C4-HSL complex that will induce the expression of multiple genes involved in virulence and colonisation (Schuster and Greenberg 2006). Some of the genes under strongest *rhl* regulation are *rhlAB*, directly controlling the synthesis of rhamnolipids (see 1.2.1), which is not under the control of the *las* system. The *rhl* system is closely related to *las*, both play their more significant roles during the early stages of exponential growth, when the cells are more metabolically active (Choi *et al.* 2011). Additionally, *rhl* and *las* have some uniquely regulated genes, but most of them are overlapped. This redundancy might be useful for the bacteria to ensure a robust regulation that will only be lost upon loss-of-function mutations in both systems (Lee and Zhang 2014).

The *rhl* system has been observed to react to the presence of IFN-γ through an IFN-γ-OprF complex. Once this important molecule for the immune system activates *rhl*, *P. aeruginosa* increases the synthesis of many virulence-related genes under *rhl* control, reacting to the innate, inflammatory response by increasing its virulence through secretion of factors such as the lectin LecA or pyocyanin. Finally, the absence of *rhl* does not inhibit biofilm formation, although the biofilms developed are

significantly thinner and flat (Moradali, Ghods and Rehm 2017).

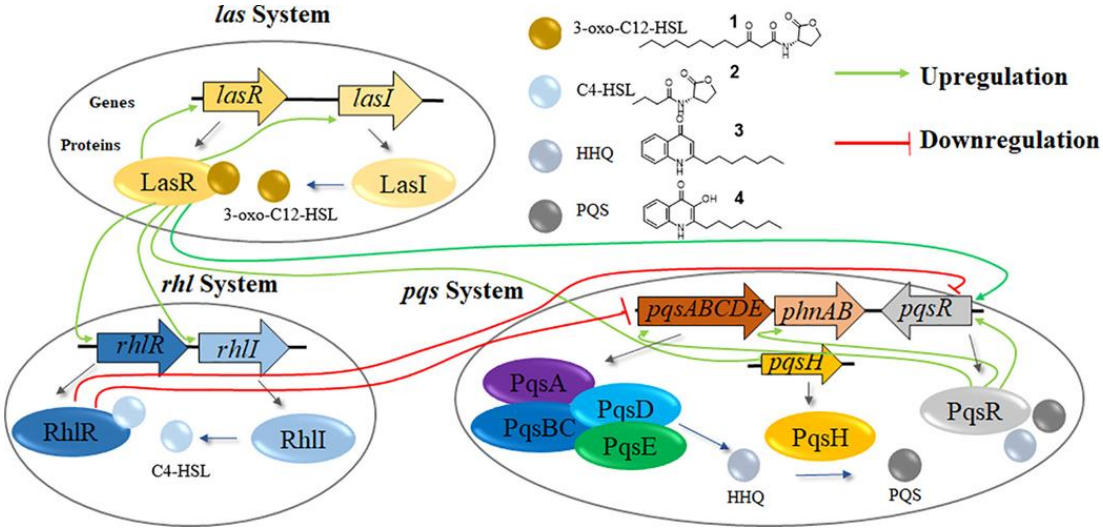

Figure 1.4. Extracted from Soukarieh *et al.* (2018b). Diagram of the interconnected *las*, *rhl*, and *pqs* QS systems in *P. aeruginosa.* Green arrows and red blocked lines indicate up- or down-regulation, respectively. Oval shapes represent various proteins, colour coded circle shapes represent quorum sensing signal molecules (QSSMs) and large coloured arrows represent genes. Thin grey arrows represent protein expression, and thin blue arrows indicate QSSMs biosynthesis.

1.4.3. The *pqs* system

A third autoinducer was identified as 2-heptyl-3,4-dihydroxyquinoline (PQS) (Pesci *et al.* 1999). Quinolone autoinducers are a different family of molecules (alkyl-4(1*H*)-quinolones vs AHLs), and with interesting properties on their own, e.g. some can act as antibiotics, or in the case of PQS, chelate iron (Bredenbruch *et al.* 2006; Heeb *et al.* 2011). The precursor of PQS, 4-hydroxy-2-heptylquinoline (HHQ) and PQS both can bind to PqsR and therefore act as coinducers (Figure 1.4). However, as a gene transcription inducer PQS is much more active than HHQ (Xiao *et al.* 2006). PQS and HHQ regulate their own production through a standard positive feedback loop (Cao *et al.* 2001). The *pqs* system in *P. aeruginosa* is very important for the control of a wide range of genes with a role in virulence and biofilm formation and physiology, but its expression is under the control of the other systems *las* and *rhl* as the *pqsR* (historically called *mvfR*) promoter has a *las/rhl* box (Figure 1.4) (Camilli and Bassler 2006). The *pqs* is a more complex system than its AHL-based counterparts, as PQS works through at least three different signalling pathways: (i) PQS can act in a classic positive feedback loop binding to PqsR and activating the *pqsA* promoter, (ii) a system where PQS-PqsR requires the activity of PqsE regulator to control gene expression and (iii) a siderophore activation

mechanism through iron chelation, simulating a low iron environment for *P. aeruginosa* (Diggle *et al.* 2007). Moreover, PQS also binds to other proteins, like the efflux pump protein MexG (Hodgkinson *et al.* 2016).

The synthesis of PQS is a branching metabolic pathway that can generate several byproducts of biological interest (Figure 1.5). The first step is carried out by PqsA which converts anthranilic acid (AA) into AA-CoA. This is further transformed to 2-aminobenzoylacetyl-CoA (2-ABA-CoA) by PqsD. The thioesterase PqsE breaks 2-ABA-CoA into 2-aminobenzoylacetate (2-ABA) (Dulcey *et al.* 2013; Drees and Fetzner 2015). 2-ABA is an important molecule in the pathway because it can be used by PqsBC to produce HHQ (Dulcey *et al.* 2013), by PqsL to change it to its hydroxylamine form, or converted into non-AQ byproducts dihydroxyquinoline (DHQ) or 2-aminoacetophenone (2-AA). HHQ can be converted into PQS by PqsH in an oxygen dependent reaction controlled by *las* (Schertzer, Brown and Whiteley 2010). The byproducts DHQ and 2-AA are important for other biological functions (Kesarwani *et al.* 2011; Gruber *et al.* 2016). Finally, the product of PqsL can be converted into 4-hydroxy-2-heptylquinoline-N-oxide (HQNO), this is done by PqsBC (Dulcey *et al.* 2013). HQNO is a very effective *Staphylococcus aureus* bacteriostatic compound thanks to which most *P. aeruginosa* strains out-compete *S. aureus* in many environments. HQNO can inhibit the activity of many bacterial cytochromes, significantly decreasing oxidative respiration and growth (Hotterbeekx *et al.* 2017). HQNO is synthesised by PqsL using the same substrate that PqsBC uses for HHQ production (Figure 1.5). This direct competition makes *pqsL* mutants overproduce HHQ and PQS as they have more available substrate. Interestingly, the accumulation of very high concentrations of PQS (but not of HHQ) in high cell density areas induces a prophage that creates lytic plaques, suggesting that *pqs* controls autolysis to a certain extent (D'Argenio *et al.* 2002).

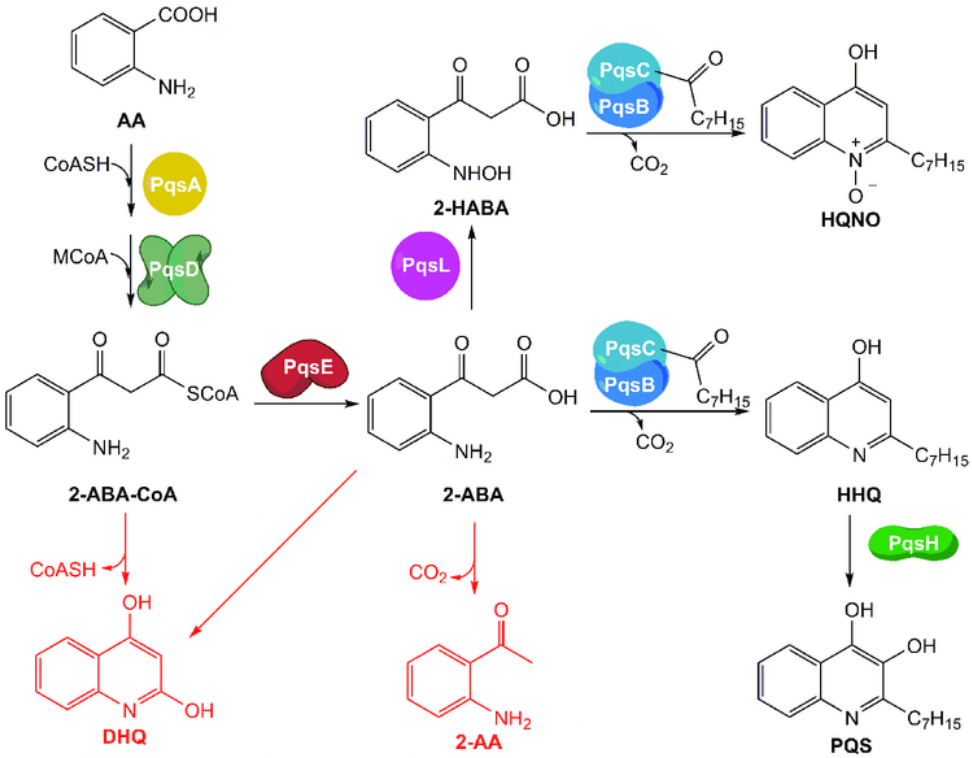

Figure 1.5 Current model for the PQS biosynthesis pathway. Modified from Allegretta *et al.* (2017). AA, anthranilic acid; CoASH, Coenzyme A; MCoA, malonyl-CoA; 2-ABA-CoA, 2-aminobenzoylacetyl-CoA; 2-ABA, 2-aminobenzoylacetate; DHQ, dihydroxyquinoline; 2-AA, 2-aminoacetophenone; 2-HABA, 2-hydroxylaminobenzoylacetate; HHQ, 4-hydroxy-2-heptylquinoline; HQNO, 4-hydroxy-2-heptylquinoline-N-oxide; PQS, *Pseudomonas* Quinolone Signal, 2-heptyl-3,4-dihydroxyquinoline. Non-AQ by-products are shown in red.

The data available for the *pqs* system shows that this system is more specialised than its *las* and *rhl* counterparts, tightly regulating many genes involved in virulence and biofilm development (Heeb *et al.* 2011). Although there is good overlapping between systems, the genes under *pqs* control can often be related to a specific type of virulence. The virulence factors involved in the colonisation stages and those that would be considered as "attacking" or "aggressive" such as proteases or motility are often under strong *las* and *rhl* regulation (Whitehead *et al.* 2001; Balasubramanian *et al.* 2013). In contrast, *pqs* has a much more limited control over such genes, instead *pqs* regulates genes with functions generally more related to scavenging and survival, regulation of the production of HQNO, pyocyanin or eDNA are examples of this (D'Argenio *et al.* 2002; Lau *et al.* 2004; Allesen-Holm *et al.* 2006; Bredenbruch *et al.* 2006; Häussler and Becker 2008). Important exceptions would be pyocyanin, HCN and some T3SS substrates, upregulated by *pqs* (Rampioni *et al.* 2016). Moreover, virulence controlled by *las* and *rhl* is the most immunogenic but at the same

time includes many immune evasion facilitators (Lee and Zhang 2014) whereas *pqs* plays a significant role in the appearance of persisters (Starkey *et al.* 2014; Allegretta *et al.* 2017). The *las, rhl* and *pqs* systems are interconnected in a complex regulatory network with an apparent hierarchy with the *las* system on top, regulating the other two, while *rhl* and *pqs* can influence the expression of one another (Balasubramanian *et al.* 2013; Lee and Zhang 2014).

The *pqs* system has been closely tied to the production of eDNA, a major component of the biofilm matrix (see 1.3.2.4) (D'Argenio *et al.* 2002; Allesen-Holm *et al.* 2006; Thomann *et al.* 2016). The exact molecular mechanism has not yet been described but it is generally accepted that *pqs* controls autolysis and MV release events that would secrete eDNA (Mashburn-Warren *et al.* 2008). However, there are many reported instances where these mechanisms occur independently of *pqs* (Turnbull *et al.* 2016), suggesting that this control is conditional or redundant with other mechanisms. It is worth highlighting that the conversion of HHQ to PQS by PqsH is an oxygen-dependent reaction whereas *pqsH* is expressed regardless of oxygen availability (Schertzer, Brown and Whiteley 2010). This creates an interesting paradigm for the function of *pqs* in biofilm formation and development. As early biofilms are thinner and therefore have less oxygen stratification, *pqs* can be active and regulate eDNA production, whereas mature biofilms are highly stratified and have low oxygen areas (Borriello *et al.* 2004), and in this case *pqs* will not be active but PqsH will accumulate. Once dispersal events occur, oxygen availability is highly likely to increase through the remaining biofilm, activating the previously inactive *pqs* that will positively regulate the secretion of eDNA *de novo*, making *pqs* play an important role in biofilm formation and maintenance. The disruption of *pqs* breaks this cycle, sensitising and dispersing biofilms (Maura and Rahme 2017).

PqsE is a notable component of the *pqs* system. This effector is not required for the production of PQS, but controls a subset of genes that are not covered by PqsR and has a very significant impact in virulence in several infection models as well as biofilm formation (Rampioni *et al.* 2010). Important advances have been made to unravel the transcriptome under

regulation of PqsE and have provided very significant data that highlights the importance of PqsE within and outside the *pqs* system (Rampioni *et al.* 2016; Zender *et al.* 2016). The stringent response also plays a role in controlling the *pqs* system through the signal molecule (p)ppGpp (Schafhauser *et al.* 2014). The presence of the alarmone (p)ppGpp actively represses the transcription of *pqsR* and *pqsA*, strongly inhibiting the whole *pqs* system while it induces the *las* and *rhl* systems, further highlighting the different roles between QS systems. The stringent response is one of the most important survival mechanisms and it is activated when carbon sources are switched or as a response to starvation. The stringent response halts bacterial growth and actively increases antibiotic resistance (Nguyen *et al.* 2011). This response is only active under considerably detrimental conditions as a fast reaction against an immediate threat for the population. Under these circumstances the *pqs* system is switched off, cellular growth is arrested and the *las* and *rhl* systems are enhanced, polarising the population towards a physiology that favours motility and colonisation. Interestingly, PQS can act as a pro-oxidant yet activate the oxidative stress response, conditions that might become useful upon contact with a high volume of reactive oxygen species (ROS) from polymorphonuclear leukocytes for example (Häussler and Becker 2008).

Recent findings have shown that PQS also binds to MexG (Hodgkinson *et al.* 2016), MexG is part of an efflux pump system involved in the transport of substrates from the cytoplasm to the extracellular milleau, including but not limited to, antibiotics. This system also plays other functional roles, including growth and virulence regulation (Aedekerk *et al.* 2005). Although this does not seem to be part of the *pqs* system *per se*, it provides evidence that this autoinducer has secondary targets, potentially regulating other phenotypes through a PqsR-independent manner, as described by Rampioni *et al.* 2010.

1.5. Quorum sensing inhibition as population control mechanism

Quorum sensing coordinates bacterial virulence, life cycles, biofilm development, antibiotic resistances, etc. (Ng and Bassler 2009). As the

bacteria quickly adapted to the unrestricted use of antibiotics and the production pipeline has run almost dry, the scientific community quickly focused its attention at alternative targets, with QS being one of the most prominent because of the extent of its regulation, notably on virulence. An extensive review on the topic of QS inhibition and its current state was very recently done by Defoirdt (2018). The interference with QS can be done at many levels: targeting transduction through signal degradation, targeting the signal biosynthesis itself, targeting the effector proteins, blocking their regulatory function or even with antibodies that induce the immune response upon contact with signal molecules (Defoirdt 2018). Interestingly, some instances are known where QS systems are desirable and therefore the molecules targeting it are agonists (Ng and Bassler 2009).

Generally, the inhibition of QS is not paired with a bactericidal effect. QS-inhibiting compounds are being developed in a post-antibiotic resistance mind-frame, meaning that the emergence of strains resistant to the inhibitors is an issue as paramount as the activity of the compound itself. It is generally accepted that the development of resistances against inhibitors is more unlikely than against antibiotics, however, the inhibition of QS systems could carry over changes in the fitness of the population (Defoirdt, Boon and Bossier 2010). A study about the fitness of a *P. aeruginosa rhl* mutant in mice lungs was performed showing that the mutant had lower cell counts and dissemination, which could translate to decreased fitness if it were to compete with the wild type (Imamura *et al.* 2005). Nevertheless, an interesting counterargument can be postulated if data from experiments with QS "cheaters" is included into the equation. Cheaters are considered bacteria harbouring mutations that prevent them from responding to QS. These bacteria will not concur on the cost of metabolising all the secretome controlled by QS, but they will make use of the public goods (secretome) available thanks to the secretion from co-operators (the subpopulation that responds to QS). In an environment where QS is a significant factor for survival and fitness, the frequency of cheaters increases as they exploit the co-operators (Ghoul *et al.* 2014). Under these conditions, the cheater has higher fitness than the co-operator, but only because of the public goods actively produced by the

latter, the presence of high levels of cheaters is a burden to the overall population and could collapse it back to levels that are sustainable for the co-operators so the total population will be lower than in a pure co-operator population (Sandoz, Mitzimberg and Schuster 2007). In the host environment, QS is important for fitness but not *essential*, the widespread inhibition of QS makes the population behave as cheaters and could pose a selective pressure towards inhibitor insensitive strains, but the burden of a cheating majority is likely to be too much for the newly emerging co-operators which won't be able to reach a high enough population to sustain the cheaters unless they have a significant increase in fitness under those particular conditions. However, there are already documented instances of resistance development to QS inhibitors (Maeda *et al.* 2012) and QS has also been shown to control an important range of private (intracellular) goods that could help only the co-operator, such as oxidative stress or motility in *P. aeruginosa* (Defoirdt 2018).

The development of an ideal antagonist must include a wide range of characteristics. The compound must be specific to the target, with very good affinity (low IC_{50}, lower than the co-inducer), metabolically stable and not cytotoxic. Specificity is often tied to affinity so a very active compound will probably be also specific for its target, however, the compound stability in mammalian models can prove to be very tricky and so can the cytotoxicity. Despite the very significant advances in QS inhibitors, the compounds have to be proven safe and effective, with those and other hurdles that have to be overcome to reach therapeutic use, no compound has seen clinical use yet, for neither *Pseudomonas* spp. nor others (Rampioni, Leoni and Williams 2014; Defoirdt 2018; Soukarieh *et al.* 2018b). Drug repurposing is currently the major shortcut being investigated towards clinical use of QS inhibitors, testing already available drugs for their QS inhibiting properties (Rampioni, Leoni and Williams 2014; Defoirdt 2018)

As a conclusion, QS interference is a promising therapeutic approach that could effectively improve the outcome of infections. However, the full extent of the regulatory networks is often unknown or poorly understood and the bacteria can develop resistance to this interference, especially in

environments where QS provides an important boost in fitness such as in acute infections. It is therefore important to have a deep understanding of the control that the targeted QS mechanism exerts over the population as well as its role in the host environment. Moreover the interference of QS should be coupled with other synergistic therapies like antibiotic treatment to decrease the chances of multi-resistant strains.

1.6. SENBIOTAR project, *pqs* antagonist development and use in therapy

The inhibition of *pqs* in *P. aeruginosa* has received increasing attention in recent years (Calfee, Coleman and Pesci 2001; Ji *et al.* 2016; Thomann *et al.* 2016; Maura and Rahme 2017; Kitao *et al.* 2018; Soukarieh *et al.* 2018a). The characteristics of the *pqs* system make it a desirable target as its virulence is closely related to the maintenance of the infection and chronicity of the biofilm, and there is available data showing that *pqs* mutants show attenuated virulence (see 1.4.3). Moreover, the hierarchical structure of QS in *P. aeruginosa* puts *pqs* below or at the same level of *rhl* (Figure 1.4), while still controlling significant genes very important for virulence, the regulation of *pqs* is not as extensive as that of *las* and is triggered at later stages of the life cycle of the population, this could mean that the development of QS inhibitor resistances is more unlikely, although to the knowledge of the author, there is no published bibliography on this or the effect of long term inhibition of *pqs*. The specific targeting of *pqs* and PqsR is commented in detail in the introduction of Chapter 3: PqsR gene regulator purification and antagonist binding kinetics.

The SENBIOTAR (sensitising *Pseudomonas aeruginosa* biofilms to antibiotics and reducing virulence through novel target inhibition, MRC project MR/N501852/1) research program is a multidisciplinary consortium aimed at taking an integral approach towards *pqs* inhibition research in order to generate effective antagonists that would be safe for humans and work synergistically with antibiotics. The members of the consortium are from groups based in four different universities: The team from the University of Uppsala was in charge of the formulation of the compounds and performs the corresponding cytotoxicity and half-life *in vivo* assays.

The team from the University of Copenhagen have been working on the development of antisense peptide nucleic acids (PNAs) that aim to block the translation of the *pqsABCDE* operon by targeting the ribosome binding site area of *pqsA* to establish two layers of inhibition (transcriptional with the PqsR antagonists and translational with the PNAs), further decreasing the chances of resistance development and increasing the overall activity. The team in the University of Laval have been performing all the mice model work and kindly provided the clinical isolates as well as the sequences of their genomes. Finally, the team in the University of Nottingham has been working on the screening, chemical synthesis and optimisation of the PqsR antagonists and the evaluation of their activity on *P. aeruginosa*. By tackling the project in a coordinated manner, the partners of this consortium have focused on their corresponding areas of expertise simultaneously, speeding up the research process.

1.7. Project overview and objectives

The work performed in this thesis mainly focuses on the microbiology part of SENBIOTAR and aims at screening and validating the impact of PqsR antagonists on the biology of *P. aeruginosa* from a clinical context.

In the first results chapter the work presented focuses on the biochemical part of the research, showing some of the activity assays performed to originally select active compounds that would get optimised later on *in silico*. The IC_{50} of the optimised compounds were determined and the most active were selected for later phenotypic assays. A special emphasis in studying the binding between the compounds and the PqsR ligand binding domain ($PqsR_{LBD}$) is given in the chapter.

The second results chapter explores the impact of many different active compounds over the production of PQS, HHQ and HQNO as well as other phenotypes. Some of the phenotypes tested are under strong direct regulation by *pqs* such as pyocyanin production, whereas others like the production of elastases, are not. The inclusion of these phenotypes was aimed at studying the full extent of *pqs* inhibition and to confirm that the compounds did not present secondary activities that could potentially be undesirable. The autolysis phenotype is included in this chapter, although

its mechanisms are not yet fully known. This was an important phenotype to assess as published data can appear contradicting regarding the role of *pqs* in autolysis. The results showed that the inhibition of *pqs* caused a reduction of autolysis in one experiment but not in another, suggesting that this phenotype is mediated by multiple mechanisms, which being unknown, are not controllable.

The third and last results chapter summarises all the work performed in different biofilm models. The chapter itself is subdivided by biofilm models and quantitation approaches. This distribution was chosen to show the work in a technically comprehensive manner. The fact that the compounds have a significant impact in all biofilm models and show increased antibiotic activity indicate that the *pqs* system is relevant in all the conditions tested. Besides all the biological data obtained from the results, this last chapter also includes technical descriptions of the optimisation processes undertaken as well as a thorough discussion of the advantages and shortcomings of the approach taken, aimed at any readers who could benefit from this knowledge for their own experiments.

In summary, this study aims to tackle the development of PqsR antagonists and study the extent of *pqs* inhibition of certain physiology and biofilm formation by different strains of *P. aeruginosa in vitro*. The work presented here establishes the bases for future research, especially on the analysis of biofilm formation under different growth conditions.

Specifically, the aims for this work were to:

- Characterise and validate antagonists of PqsR activity.
- Study the impact of the antagonists over different phenotypes of multiple *P. aeruginosa* strains, including phenotypes not under *pqs* regulation.
- Establish a number of biofilm models and determine the impact of PqsR antagonists on them.

2. Materials and Methods

2.1. Bacterial strains and growth conditions

2.1.1. Main media and antibiotic concentrations

Lysogeny broth (LB) media was used for general growth (Sambrook and Russell 2001). Antibiotics were added at the following concentrations whenever needed: For culturing of *E. coli*, ampicillin (Ap), 100 µg/ml; carbenicillin (Cb), 100 µg/ml; gentamicin (Gm), 20 µg/ml; kanamycin (Km) 25 µg/ml; streptomycin (Sm) 100 µg/ml; tetracycline (Tet), 25 µg/ml. For the culture of *P. aeruginosa*, Cb, 400 µg/ml; Gm, 20 µg/ml; Km, 300 µg/ml; Sm, 1000 µg/ml; Tet, 125 µg/ml. For the counter-selection of *sacB* recombinants, sucrose was used at 12 % (w/v) on a modified LB medium that contained no NaCl to avoid cell lysis by osmosis.

2.1.1.1. *Pseudomonas* isolation agar

Pseudomonas isolation agar (PIA) was purchased from Sigma-Aldrich and used to grow *Pseudomonas* in order to separate them from *E. coli* donor strains in conjugations as well as ensuring selective growth. This medium was prepared following the manufacturer's instructions and contains 20 g/l enzymatic digest of gelatin (peptone), 1.4 g/l $MgCl_2$, 10 g/l K_2SO_4, 0.025 g/l 5-chloro-2-(2,4-dichlorophenoxy)phenol (irgasan™) and 13.6 g/l agar. Irgasan™ is a wide spectrum antimicrobial effective against *E. coli*.

2.1.1.2. Casamino acids

Casamino acids medium (CAA) was used for pyoverdine quantification assays. The media contains 0.5 % casamino acids, 3.3 mM K_2HPO_4 and 3 mM $MgSO_4$. D-glucose was used as carbon source; a 20 % (w/v) solution was filter-sterilised (0.22 µm) and added to 0.5 % final concentration after autoclaving the rest of the media.

2.1.1.3. Chemically defined medium

Chemically defined medium (CDM) was used in some 2-alkyl-4-quinolone extractions because the bacteria growing in it produce a reduced amount of them compared to that from LB and there is less background signal from the undefined composition of the yeast extract. The media contains 3 mM KCl, 3 mM NaCl, 12mM $(NH_4)_2SO_4$, 3.2 mM $MgSO_4 \cdot 7H_2O$, 0.02 mM $FeSO_4$

· $7H_2O$, 1.2 mM K_2HPO_4 and 50 mM 3-(N-morpholino)propane-sulfonic acid (MOPS) at pH 7.8. 20 mM D-glucose was used as carbon source.

2.1.1.4. M9 minimal medium

M9 minimal medium was used in some biofilm assays. This medium contains 240.7 mg/l $MgSO_4$, 11.098 mg/l $CaCl_2$ and D-glucose as carbon source at 0.4 %. M9 salts were prepared as a 5x stock solution, their final concentration is: 1 g/l NH_4Cl, 6.78 g/l Na_2HPO_4, 3 g/l KH_2PO_4 and 0.5 g/l NaCl. These salts are commercially available from Sigma-Aldrich.

2.1.1.5. M63 minimal medium

M63 minimal medium was used in crystal violet and other biofilm assays. This medium contains 1 mM $MgSO_4$ and D-glucose as carbon source at 0.2 %. M63 salts were prepared at 5x, their final concentration is 2 g/l $(NH_4)_2SO_4$, 13.6 g/l KH_2PO_4 and 0.5 mg/l $FeSO_4 \cdot 7H_2O$, adjusted to pH 7.0 with KOH.

2.1.1.6. RPMI 1640 media

Roswell park memorial institute medium 1640 (RPMI) was used for biofilm assays. RPMI was used without L-Glutamine nor phenol red with 20 mM D-Glucose and 2 µM $FeCl_3$.

2.1.1.7. Congo-red agar

Congo-red agar plates were used to test the cell lysis phenotype in colony morphology biofilms. The medium was prepared with 10 g/l Triptone, 15 g/l Bacto Agar, 40 mg/l Congo Red, 10 mg/l Comassie Brilliant Blue R-250. 25 ml were poured in each plate, with either 0, 0.5, 1 or 2 µM inhibitor added from DMSO stock solutions.

2.1.2. Long term storage

Bacterial stocks were prepared for long term storage at -80 °C by mixing 750 µL of overnight culture with 750 µL of autoclaved 50% glycerol (w/v) to a 25% final concentration.

2.1.3. General chemicals

All chemicals were purchased from Sigma-Aldrich unless stated otherwise.

2.1.4. Bacterial strains, plasmids and primer list

All bacterial strains used in this study are listed in Table 2.1.

Table 2.1. Strains used in this project.

Name	Genotype	Reference
E. coli		
DH5α	F⁻ Φ80*lac*ZΔM15 Δ(*lac*ZYA-*arg*F) U169 *rec*A1 *end*A1 *hsd*R17 (rK⁻, mK⁺) *pho*A *sup*E44 λ⁻ *thi*⁻ 1*gyr*A96 *rel*A1	(Grant *et al.* 1990)
S17-1	RP4 2-Tc::Mu-Km::Tn7, *recA, thi, pro*, *hsdR*⁻, *hsd*M⁺	(Simon, Priefer and Pühler 1983)
BL21	F- *hsdS gal*	(Studier and Moffatt 1986)
P. aeruginosa		
PAO1-L	PAO1 Lausanne subline, wild type	B. Holloway, *via* D. Haas
PAO1-N	PAO1 Nottingham subline, wild type	**, from Holloway's isolate (Holloway 1955)
PAO1-W	PAO1 Washington subline, wild type	(Stover *et al.*, 2000)
Δ*pqsA*	PAO1-L, Δ*pqsA*	(Yi-Chia 2014)
Δ*pqsR*	PAO1-L, Δ*pqsR*	*
PAO1-N Δ*pqsR*	PAO1-N, Δ*pqsR*	(Rampioni *et al.* 2016)
Δ*pqsL*	PAO1-N, Δ*pqsL*	Rampioni G., *et al.* Unpublished
Δ*pvdB*	PAO1-N, Δ*pvdB*	**
Δ*lasR*	PAO1-N, Δ*lasR*	**
PA14	PA14, wild type	(Mathee 2018)
PAO1 279	CF clinical isolate from Québec, ID 1451, ≥95 % PAO1 homology	Université Laval collection
PA14 AL191	CF clinical isolate from München, ID 1350, ≥95 % PA14 homology	Université Laval collection
PALESB58	CF clinical isolate from Liverpool, ID LES B58	Université Laval collection
PAK 6085	CF clinical isolate from Québec, ID 1331, ≥95 % PAK homology	Université Laval collection
PA7 48	CF clinical isolate from Montréal, ID 197S020911BSL_PA3, ≥95 % PA7 homology	Université Laval collection

CF stands for Cystic fibrosis. *, Created during this study. **, Laboratory collection.

All vectors used through this thesis are listed in Table 2.2.

Table 2.2. Plasmids used in this thesis

Name	Genotype	Reference
$PqsR_{LBD}$	pET28a::*pqsR*$^{94-309}$ Km^R Cm^R	(Ilangovan *et al.* 2013)
Suicide pEX18	pEX18 *oriT*$^+$ *sacB*$^+$ pUC18 MCS	(Hoang *et al.* 1998)
Empty mCTX	mCTX-*lux* Gm^R promoterless	**
P*pqsA*-lux	mCTX::P*pqsA*-lux Gm^R	**
P*km*-lux	mCTX::P*km*-lux Gm^R	**
P*lecA*-lux	mCTX::P*lecA*-lux Gm^R	*
P*hol*-lux	mCTX::P*hol*-lux Gm^R (PA0614)	*
P*lys*-lux	mCTX::P*lys*-lux Gm^R (PA0629)	*
mTn7::*gfp*	mTn7::*gfp* Gm^R	(Koch, Jensen and Nybroe 2001)

*, Created during this study. **, Laboratory collection.

The primers used in this thesis are listed in Table 2.3.

Table 2.3. Primers used in this thesis.

Primer name	Sequence 5' -> 3'	Reference
MiniCTXLuxSeqFw	ATAACACAAAAATATAAGAAGCAAG	(Hoang *et al.* 1998)
MiniCTXLuxSeqRv	GAGAGTCATTCAATATTGGCAGGTA	(Hoang *et al.* 1998)
SeqPqsR.Fw	CGGCATGCCAGCGTTAATACTT	*
SeqPqsR.Rv	CATCCCGAGTCGATTCTCACCA	*
FWpqsRUp Ilangovan 2013	ATAAAGCTTTCTTAGAACCGTTCCTGG	(Ilangovan *et al.* 2013)
RVpqsRDown Ilangovan 2013	ATATCTAGAAGTTCTGCCTGCTCGGCG	(Ilangovan *et al.* 2013)
RVpqsRUp Ilangovan 2013	ATAGGATCCAGGTTATGAATAGGCATC	(Ilangovan *et al.* 2013)
FWpqsRDown Ilangovan 2013	ATAGGATCCAGAGTAGAGCGTTCTCCA	(Ilangovan *et al.* 2013)
PA0614_HindIII.Fw	ATAAAGCTTTGGAGCACTATCTCAATCGCGA	*
PA0614_BamHI.Rv	ATAGGATCCGGGGACGCACCTTTACAAGAAT	*
PA0629_HindIII.Fw	ATAAAGCTTCGACAGAGCGGGCAGAGCGCCA	*
PA0629_BamHI.Rv	ATAGGATCCCACTCCGATGGGTTTCAGGCGT	*

Restriction sites are underlined, Fw, forward primer; Rv, reverse primer *, Created in this study.

2.2. Bacterial cloning

2.2.1. Lux based reporter construction

Lux-based transcriptional reporters were built using the vector mCTX-lux as backbone (Becher and Schweizer 2000). A list of the reporter vectors created can be found in Table 2.2. Briefly, the desired promoter region would be amplified by PCR with primers which introduced the appropriate flanking restriction sites that matched those of the vector in the right direction. Both insert and vector would then be digested and purified with a clean-up kit or by gel extraction respectively. The fragments were ligated (16°C for 2 h and 4°C ON) together and electroporated (ideal electroporation time 5.00 ms) to a an electrocompetent strain, usually S17-1.

The recipient S17-1 strains can be conjugated with any *P. aeruginosa* to create a *lux*-based reporter strain with the mini-CTX construct stably inserted in the chromosome. Reporters build in this fashion are extremely useful to monitor gene expression and regulation through the emission of light which was detected using a TECAN™ infinite F200 PRO plate reader.

Constitutive reporter control strains were also built. This was done using the mCTX::P*km*-lux Tet^R vector which expresses lux constitutively thanks to the kanamycin promoter. This is helpful to detect and subtract potential undesired bias by unspecific interactions with the *lux* operon or with the bioluminescence metabolism.

2.2.2. *pqsR* knock-out

The PAO1-L Δ*pqsR* mutant was a necessary negative control for AQ quantification data. An in frame deletion mutant was available in PAO1-N. The truncated gene was amplified and cloned into the suicide vector pEX18 Gm^R. The resulting pEX18::Δ*pqsR* Gm^R was electroporated into S17-1 to obtain a Δ*pqsR* allele exchange strain.

A conjugation with PAO1-L WT was performed and the mutant was later selected following sucrose selection with 12 % sucrose during all vector curating stages. The resulting colonies were screened for double recombination leading to allelic exchange and the desired constructs were

screened by PCR amplification and sequencing. A final selection round was done by performing a pyocyanin assay and discarding the clones with higher amounts of pyocyanin produced. The resulting *pqsR* mutants did not have any resistance marker as the resistance was embedded to the suicide vector, lost after the second recombination.

2.2.3. mTn7 transposon based resistance tagging

Some strains were tagged with a mTn7 transposon carrying either a Gm^R or Tet^R cassette in order to select them during fitness assays. Mini-Tn7 delivery strains *E. coli* S17-1 / pUCP18::mTn7-Gm^R Ap^R and *E. coli* S17-1 / pUCP18::mTn7-Tet^R Ap^R were conjugated with wild types and Δ*pqsA* mutants of strains PAO1-L and PA14. The tagged strains were selected by plating the matings on PIA media with the right antibiotics. Each strain was tagged separately with each antibiotic in order to avoid potential biases in the assay caused by the expression of one of the cassettes.

2.2.4. mTn7 based fluorescence tagging

Fluorescent strains were created using a mTn7 transposon with an unstable, enhanced *gfp* protein next to a constitutive promoter with high expression levels (Lanzer and Bujard 1988; Andersen *et al.* 1998; Koch, Jensen and Nybroe 2001). The tag was inserted into *P. aeruginosa* through triparental conjugation. The donor (with the mTn7 tag), two helpers (one with the mobilisation machinery and the other with the transposase) and receiver strains were added in a 1:1:1:1 ratio. The conjugation was plated in PIA plates with gentamicin as antibiotic marker.

2.3. *In silico* analysis of *pqsR* and *pqsA*

The promoter regions and gene sequences *pqsA* (PA0996) and *pqsR* (PA1003) from laboratory strains PAO1-L and PA14 were analysed and compared with the five selected clinical isolates PAO1 279, PA14 AL191, PALESB58, PAK 6085 and PA7 48. The comparison was performed to identify potential significant differences that could have an impact on the expression and amino acid sequence of PqsA and PqsR. Clinical isolate genomic sequences were requested form the Laval University library.

The genomes (or scaffolds if the complete, assembled genome was not available) of each strain were compared with BLAST, using the sequences from PAO1-L as the query. The BLAST was performed using the in-house available genome library based in Sequence server (Priyam *et al.* 2015). Results were used to download the aligning fragments which were further analysed in depth using the web-based toolkit for molecular biology Benchling. The fragments analysed for *pqsR* included the whole 999-nucleotide open reading frame and 747 nucleotides upstream containing the predicted promoter and a *las*/*rhl* binding box for a total of 1746 nucleotides. The *pqsA* analysis included the whole 1554-nucleotide open reading frame and 500 nucleotides upstream for a total of 2054.

2.4. Phenotypic assays

2.4.1. Lux based reporters

Bioluminescent reporter activity was performed in 96 well microtiter plates within TECAN™ infinite F200 PRO plate readers. Briefly, the reporter strains were grown overnight. The OD_{600} was then adjusted to 0.05 or 0.01 in LB with the compound to be tested at the desired concentration. 200 µL were added to sterile plates (black walls, clear, flat bottom) in triplicates. Outer wells were filled with 150 µL of water to minimise evaporation during the assay. Plates were incubated with a lid for 24 hours at 37°C static inside the TECAN™. Growth (OD_{600}) and light (relative light units, RLU) were read every 30 minutes from time 0.

2.4.1.1. Activity assays and IC_{50}

A threshold of 10 µM was arbitrarily set to select which inhibitory compounds would classify as being active; a threshold of 50% average signal repression at this concentration was required to consider a compound as active. An IC_{50} assay was then performed, with the most active compounds being analysed first. The PAO1-L mCTX::P*pqsA*-lux reporter strain was used for this assay, and the PAO1-L mCTX::P*km*-lux was used as a control in parallel to rule out any effect over the bioluminescence unrelated to the target, PqsR. Reporters were also integrated in the chromosome of other strains to measure their strain-specific IC_{50} values.

For the IC_{50}, candidate inhibitory compounds were tested at eight fixed decreasing concentrations set to accommodate a logarithmic scale: 10, 3.1, 1, 0.31, 0.1, 0.031, 0.01 and 0.0031 µM. For the analysis, only the maximum value was taken for each concentration over time. The maximums are then averaged between biological replicates and this value was used to calculate the IC_{50} and its standard deviation.

2.4.1.2. Transcriptional regulation

To monitor gene expression and regulation a series of bioluminescence-based reporters were created using the *luxCDABE* operon from the mCTX-*lux* vector (either Gm^R or Tet^R). TECAN™ infinite F200 PRO plate readers were used to grow strains and measure growth (OD_{600}) as well as bioluminescence (RLU) produced by the reporter strains. The assays were always done using biological triplicates for the reporter and the P*km*-lux control.

2.4.2. Pyocyanin assays

Pyocyanin production was quantified as an indirect measure of the PQS QS system inhibition using a simplified acid-base extraction method based on previous work (Essar *et al.* 1990). The strain of interest was grown in 10 ml of LB in 100 ml conical glass flasks with 3x IC_{50} or an equivalent volume of DMSO as control (considered 100% pyocyanin production later on). The flasks were incubated overnight for 16 hours at 37°C 200 rpm, the samples were then centrifuged and 7.5 ml of supernatant (SN) was filtered (0.45 µm) into a 15 ml falcon tube. 4.5 ml of Chloroform was added and the mixture was vortexed twice for optimal mixing. The mixture was centrifuged again at 10000 rcf for 10 minutes and the top layer and protein, white interphase were removed to recover 3 ml of the chloroform organic phase. 1.5 ml of 0.2 M HCl was added to the separated fraction and vortexed twice again. Finally, the upper, acidic layer was recovered (900 µL) and read in a spectrophotometer at OD_{520}. Pyocyanin concentration (µg/ml) was calculated by multiplying the OD_{520} value by 17.072 (mass extinction coefficient) and 1.5 (to extrapolate total amount of pyocyanin, since 3 ml out of a total 4.5 ml had been used). All experiments were performed using biological triplicates.

2.4.3. Pyoverdine assays

Pyoverdine production was quantified to establish if the tested PqsR antagonists had any secondary impact over a phenotype that is not under strong PQS regulation. For this assay, the strains were initially grown in LB before adjusting the OD_{600} to 0.05 in 10 ml of CAA medium (the low iron content promotes pyoverdine production) with the desired concentration of compound (or the equivalent volume of DMSO). Cultures were grown in 100 ml flasks at 37°C shaking at 200 rpm for 16 hours. After the incubation period, the OD_{600} was read, the cultures were centrifuged at 10000 rcf and the supernatant was filtered (0.45 µm). The filtered supernatant was measured at OD_{450} to obtain a rough estimate of pyoverdine production. The assays were averaged from biological triplicates and the results were presented as OD_{450} / OD_{600} ratios.

2.4.4. Elastase assay, LasB activity

Elastase activity was also quantified to determine the extent of phenotypic inhibition by the utilised compounds. Cultures were standardised to OD_{600} 0.01 in 10 ml in LB with the wanted compound concentration or an equivalent DMSO volume for the control. The samples were grown overnight for 16 hours, the OD_{600} was measured and then samples were centrifuged to filter sterilise the supernatant (0.22 µm). 100 µL of filtered SN were mixed with 900 µL of 20 mg/ml elastin-Congo red in ECR buffer (12.1 g/l Tris base, 194.7 mg/l $CaCl_2$, autoclave and adjust to pH 7.5 with HCl). Special care was taken to ensure that there was an even distribution of elastin-Congo red among the samples as it is insoluble in ECR. The mixture was incubated at 37°C shaking at 200 rpm for 4 hours to allow the secreted elastase to break down the elastin-Congo red. After the incubation, the samples were centrifuged and 800 µL of supernatant was carefully recovered to read the OD_{495}. Each condition was performed with biological triplicates, results were presented as OD_{494} / OD_{600} ratio.

2.4.5. Azocasein assay, general protease activity

In order to test if the antagonists had any impact in other proteases, an azocasein assay was performed. As before, an overnight was adjusted to OD_{600} 0.01 in 10 ml of fresh LB media with the compounds at 3x IC_{50} or an

equivalent volume of DMSO. Samples were incubated in triplicates in 100 ml flasks at 37°C and 200 rpm for 16 hours. Samples were centrifuged (1000 rcf) and the supernatant was filter sterilised (0.45 µm). 100 µL of filtered SN was added to 900 µL of 5 mg/ml azocasein solution in ECR (12.1 g/l Tris base, 194.7 mg/l $CaCl_2$, autoclave and adjust to pH 7.5 with HCl). The azocasein is soluble in ECR but the solution must be prepared gently to avoid the generation of foam. Samples were then incubated at 37°C shaking at 200 rpm for 15 minutes. After the incubation, 500 µL of 10% trichloroacetic acid was added to precipitate the proteins and stop the reaction. Samples were centrifuged at maximum speed for 3 minutes and 900 µL was collected to measure OD_{400}. Results were plotted as 1:10 OD_{400} (sample signal had to be diluted).

2.4.6. Autolysis and eDNA production

2.4.6.1. Extracellular DNA in liquid cultures

To examine autolysis in liquid media, extracellular DNA (eDNA) release was assessed. Cultures were standardised at OD_{600} 0.01 in 5 ml of LB with 3x IC_{50} or an equivalent volume of DMSO. Samples were incubated in triplicates in 50 ml falcon tubes at 37°C and 200 rpm for 18 hours. Cell density was measured reading the OD_{600}. 1 ml of each sample was then centrifuged and the supernatant filtered (0.22 µm). 450 µL of the filtered supernatant was mixed with 50 µL of 3 M sodium acetate ($C_2H_3NaO_2$) pH 5.2 with 1 ml ice cold 100% ethanol and stored at -20°C for 30 minutes to precipitate any DNA found in the sample. After the incubation period the samples were centrifuged at maximum speed for 30 minutes at 4°C and the pellet (sometimes not visible) was washed with 70% ethanol. After the wash, the ethanol was carefully removed and the samples were air dried before resuspension in molecular grade water. eDNA concentration was measured using a NanoDrop™ spectrophotometer. The assay was performed using biological triplicates for each condition.

2.4.6.2. Ethidium homodimer dye in microtiter plates

Ethidium homodimer (etho) is a membrane-impermeable, fluorescent DNA intercalating dye with excitation/emission wavelengths of 528/617 nm. This dye is useful to detect eDNA and dead cells thanks to its high

brightness. Etho was used to detect eDNA from biofilms growing in 96-well polystyrene plates. PAO1-L WT was grown in 200 µL/well of 95:5 M63:LB media, starting from an OD_{600} of 0.05 and incubating for 24 hours static at 37°C inside the TECAN™ infinite F200 PRO. The PqsR antagonists were added from time 0 at 3x IC_{50} or 1 µM. OD_{600} and fluorescence readings were taken every 30 minutes. Fluorescence was set at bottom reading, the gain setting was calculated from a blank well (sterile media with etho) at 100% and the Z position was set to be adjusted from a DMSO only well. All experiments were performed in biological triplicates.

2.5. 2-alkyl-4-quinolone extractions

2-alkyl-4-quinolones (AQs) quantification is the most critical assay to test PqsR antagonists as they are the direct product of the *pqs* system. Biological triplicates were used for this experiment. Cultures were standardised at OD_{600} 0.05 in 5 ml of LB with 3x IC_{50} of the desired compounds or an equivalent volume of DMSO for the control. After 16 hours growth at 37°C and 200 rpm the cultures were centrifuged at 10000 rcf for five minutes and the supernatants were filtered (0.45 µm). 100 µL of SN was added to 400 µL fresh LB, supplemented with the internal standard 7Cl-7CPQS at a final concentration of 20 nM (other internal standards can be used to test different by-products). 500 µL of acidified ethyl acetate (0.1% acetic acid) were added to the Eppendorf tubes and they were well mixed for 2-3 minutes, after which they were left standing to allow total layer separation and the upper, organic layer was recovered into a new Eppendorf. The ethyl acetate extraction step was repeated twice and transferred to the same Eppendorf. Samples were then stored at -20°C until they were analysed with mass spectrometry.

2.5.1. LC-MS/MS quantification

The extracted supernatants were dried using a vacuum Speedvac concentrator and resuspended in 100 µL methanol (MetOH). 2 µL of each sample was run through the liquid chromatography phase (column Phenomenex Gemini C18, 3.0 µm, 100 x 3.0 mm) at 450 µL/min, 40°C with mobile phases: A) 0.1% (v/v) formic acid (CH_2O_2) in water with 2 mM 2-picolinic acid; B) 0.1% (v/v) CH_2O_2 in MetOH. A linear gradient was used

from 30% to 99% B over 5 minutes. The gradient stayed at 99% B for 3 more minutes before going down to 30% in a minute and staying at 30% B for further 4 minutes to allow column equilibration. An Applied Biosystems Qtrap 4000 hybrid triple-quadrupole linear iron trap mass spectrometer (Foster City, CA, USA) was used as MS platform with an electrospray ionisation interface. The system was controlled with Analyst software (Foster City, CA, USA). The screening of the LC eluent was performed using positive electrospray (+ES) with multiple reaction monitorin (MRM). Quantitation was performed by calculating peak area and dividing the analyte peak are by the internal standard peak area.

2.6. Cell lysis phenotype

The expression of a PQS-mediated autolytic phenotype was analysed by growing colony biofilms on Congo red plates. The strain used was PAO1-N Δ*pqsL* and the negative controls were PAO1-L WT and PAO1-L Δ*pqsR*. Briefly, 10 µL drops of overnight cultures were inoculated on Congo red plates (10 g/l Triptone, 15 g/l Bacto Agar, 40 mg/l Congo Red, 10 mg/l Comassie Brilliant Blue R-250) with either 0, 0.5, 1 or 2 µM inhibitor added from DMSO stock solutions. Plates were incubated for 24 hours at 37°C static, after which pictures of the colonies were taken. PAO1-N Δ*pqsL* presents lytic plates under control (DMSO) conditions due overproduction of HHQ and PQS, negative controls should be unaffected. Each condition was carried out in triplicates.

2.7. *P. aeruginosa* biofilms

2.7.1. Chamber slide static biofilms

One of the models to grow biofilms used the Nunc™ Lab-Tek II 8-well glass slides. PAO1-L mTn7::*gfp* Gm^R or PAO1-W mTn7::*gfp* Gm^R, and propidium iodide (1 µM) were used. Briefly, an overnight was adjusted to OD_{600} 0.05 in the desired media and 500 µL were added to each well with the corresponding experimental condition (3x IC_{50} or 10 µM and DMSO for the controls). The microchambers were incubated static at 37°C for 6, 16 or 18 hours. The media was then carefully removed to allow visualisation. Alternatively, microscopy was performed without removing the supernatant.

2.7.2. Microfluidics biofilms - Bioflux™

Biofilms were grown in a microfluidics model using the Bioflux™ system (Conant, Schwartz and Ionescu-Zanetti 2010). The Bioflux 200 system was used either with 48- or 24-well plate configurations. The advantage of the system is that it allows to constantly feed the sample with fresh media flowing with defined shear force while the microcolonies grow within a viewing channel optimised for microscopy thanks to the thin bottom layer of the plate. The *gfp*-tagged strain was grown overnight and later adjusted to OD_{600} in 10% LB (media containing 3x IC_{50} or an equivalent volume of DMSO). Before adding the bacterial suspension, the wells and channels were primed with fresh media by adding 100 µL 10% LB in the inlet and setting a manual flow of 11 dyn/cm^2 for few seconds, until a drop could be observed in all outlets. The plates were then disconnected and 70 µL of bacterial suspension were added in the outlet, then the inlet was filled with fresh media. The system was set up again and an automatic program was loaded. The general program would be as follows: 2 seconds 2 dyn/cm^2 from outlet to inlet (bacteria seeding into viewing channel), 40 minutes 0 dyn/cm^2 from inlet, 20 seconds 2 dyn/cm^2, 16 hours 0.45 dyn/cm^2 and 2 hours 0.1 dyn/cm^2 (in case the system could not be attended in time). Antibiotic treatment was performed by removing the remaining media in the inlet and waste from the outlet and adding fresh media with the desired conditions in the inlet before continuing a manual run at 0.5 dyn/cm^2. Once the whole run was done it was disconnected and the biofilm was analysed by confocal laser scanning microscopy (CLSM).

2.7.3. Biofilms on borosilicate glass coverslips

For this biofilm assay, a *gfp*-tagged PAO1-W subline was used in parallel to the main PAO1-L *gfp* strain because it presents enhanced biofilm formation. The surface chosen for this model was coverslips of borosilicate glass (22x22 mm thickness n°1). Cultures were grown overnight at 37°C in 5 ml RPMI 1640 supplemented with 20 mM D-glucose and 2 µM $FeCl_3$. The next day, cultures were restarted with fresh medium until they reached an OD_{600} around 0.5, samples were then adjusted to OD_{600} 0.01 in 25 ml of fresh RPMI (with the same supplements). This was added to UV-sterilised petri dishes containing glass coverslips. Cultures were left static at 37°C for 1.5

to 2 hours to allow for irreversible attachment. After seeding time, the compounds of interest were added at 3x IC_{50} (or an equivalent volume of DMSO) and the plates were moved to incubate at 37°C 60 rpm for 16 hours to develop a mature biofilm. After this incubation time, the media was replaced with 25 ml of fresh RPMI (with or without compound) with tobramycin and propidium iodide (PI), at concentrations of 100 µg/ml and 2 µM respectively, and further incubated for 4 hours at 37°C 60 rpm. Coverslips were removed and viewed by CLSM.

2.7.4. Confocal laser scanning microscopy (CLSM)

Microscopy imaging of biofilms was performed using the LSM 700 from ZEISS. The microscope was supported with the ZEN 2009 software platform (ZEISS), and was controlled using the software and supported by the microscope's own touchscreen display. Within the Acquisition tab in Zen 2009, smart setup was chosen. The eGFP and PI settings were chosen to be loaded selecting Fastest mode. Z stack was selected for scan mode. Afterwards, within light path, the contrast phase option was ticked in (therein called T-PMT). In the Acquisition Mode tab, the bit depth was always selected to be 16 bit. The speed was lowered to 6 or 7 when time allowed it. Reducing the speed increases the pixel dwelling time which has a direct impact on the smoothness of the picture taken (longer pixel dwell means more excitation light collected and therefore better signal-to-noise ratio), an alternative approach is to increase the averaging of the picture. The frame size was generally kept at 512x512, most of the options within acquisition mode have a very direct impact over image and signal quality, however the acquisition time would also increase accordingly and due time constrains, the options were always selected to find the best compromise between acquisition time and signal quality. The gain and laser intensity options could be found within the Channels tab, only the lasers to be used were selected (488 and 555) so the lifespan of the unused lasers would be unaffected. The laser intensity was generally selected to be constant for each experiment and within the 2 – 15% range (optimal at 5%). The pinhole was always set at 1 air units (AU) and the gain (master) was never set above 800 and always below 750 if possible because a significant amount of background noise is detected above those gain levels. This

settings were also left unmodified through the experiments (unless a certain gain turned to be too high for an experimental condition in which case it would be changed just enough to get proper signal distribution). The gain and laser intensity settings were fine-tuned while being live. Once the image was presented under the desired intensity (that which allows maximum separation between signal and background noise and has minimal oversaturation), a Z-stack was established. Using the Z-stack tab, the first slice was set in the very base of the sample, but not below it, the last slice was set at the end of the upper end of the channel (for bioflux) or above the tallest microcolonies in other models. The slice interval was kept constant over the experiment, checking that there was at least a small section overlapping (although the optimal is 50% section overlap). At least three images were taken of each well for each condition in order to be analysed later, usually with Comstat2 (Vorregaard 2008).

In some cases the signal can be hard to observe directly (even if it is present). Changing the gain or laser intensity settings will have a strong impact over signal and signal-to-noise ratio so it is not desirable if the images are to be quantified. For this reason in this situations it is always better to adjust the display presentation. Changing to min/max or best fit as well as 0.45 gamma will change the brightness and contrast shown in the display, allowing the user to observe the image under better circumstances without having any impact on the signal itself. The range indicator palette can be selected for each channel under the Channels option within the display section or in the Light Path tab, this is a very useful tool to establish the relative pixel intensity distribution. This allows to observe signal even if it cannot be seen with the usual green and red colours and determine if it has good separation from the background (which should be blue) and if it is too saturated (red). An ideal relative pixel intensity distribution will show sharp contrasts, with bacterial signal coming up in black/gray against a blue background (no signal) and red (oversaturated) parts within the densest microcolonies.

2.7.5. Flow cytometry

Total cell counts were performed using flow cytometry (MoFlo® Astrios™ Cell Sorter, Beckman Coulter). Samples were collected from the effluent in

the outlet of bioflux systems and from a portion of the biofilm that could be detached after washing at the highest pressure (20 dyn/cm^2) for 5 minutes. 100 µL were taken from each sample and mixed with 20 µL of beads (CountBright™ Absolute Counting Beads, ThermoFisher Scientific). The flow cytometer was configured to detect the size range of *P. aeruginosa* with an unlabelled, wild type sample. Gfp and PI were measured and plotted to get the required cell counts. Kaluza Analysis software (Becman Coulter) was used as data analysis tool.

2.7.6. Data analysis and quantification with Comstat2

The plugin Comstat2 of Image J was used to analyse and quantify biofilm microscopy pictures (Heydorn *et al.* 2000; Vorregaard 2008). Comstat2 was loaded by opening ImageJ and going to Plugins>Comstat2. The directory with all the raw data files was loaded into "Observed directories". Comstat2 opens then a new window with all the recognised files from the selected observed directory. Each image will have one channel for each laser / white light used during the CLSM and they were left ticked or unticked depending on the needs of the analysis (channel corresponding to contrast phase was always left unmarked). Connected volume filtration was unselected for the analysis. Biomass and Surface were the parameters often selected for quantification. Results are produced in a .csv file that was analysed using Microsoft Excel.

2.7.7. High throughput assays

2.7.7.1. Crystal violet assay for total biomass

Crystal violet (CV) assays were performed in order to measure total biomass of the biofilm samples. The procedure was done following the protocol described by Frei *et al.* Briefly, media was removed from the samples and they were washed once with PBS, letting them dry before adding CV 0.1 % in water with 5% ethanol. The stain was removed after 15 minutes and samples were washed thrice with PBS. Each sample was let dry and afterwards re-solubilised with 30% acetic acid. Signal was measured by reading OD_{595}.

2.7.7.2. 96-well plates. ATP measurement for active biomass

The total amount of ATP was measured as a direct quantification of metabolically active biomass. ATP measurements were done using the BacTiter-Glo™ Microbial cell viability assay from Promega. The assay was performed growing PAO1-L WT in 96-well polystyrene plates using 200 µL of M63/LB (95:5) media per well. Biofilms were grown at 37°C static for 48 hours. Replacing the media after the initial 24 hours. Tobramycin was added along with the fresh media. After the incubation, the supernatants were removed and a vigorous wash was performed with PBS. 100 µL PBS were added together with 100 µL of the luciferase mix (fast to prevent bias between samples but without creating bubbles) and the plate was left shaking at 150 rpm for 3 minutes. A single luminescence measure was taken immediately afterwards with a TECAN™ infinite F200 PRO. All conditions were tested with three or more biological replicates.

2.8. Hit compounds docking

The available compound libraries were docked *in silico* against the PqsR active site. The "Extra Precision" (XP) mode of Glide docking was used for docking calculations based on OPLS-AA 2005 force field. The van der Waals radius used had a 1.0 scale factor and was applied to atoms of protein with absolute partial charges ≤ 0.25. Each ligand was analysed in five positions after energy minimisation. The best dockings were selected visually and using the XP Glide Score (XP Gscore) (Friesner *et al.* 2006).

2.9. PqsR purification and kinetics

2.9.1. PqsR expression

The PqsR ligand binding domain ($PqsR_{LBD}$) was expressed in *E. coli* BL21 pET28a::*pqsR*$^{94-309}$. The strain was grown at 37°C 200 rpm in 500ml LB to OD_{600} 0.8 (using 2 L flasks). After the OD_{600} was reached, PqsR was overexpressed by adding IPTG at 1 mM and incubating at 20°C for 16 hours. Cell pellets were collected by centrifugation and resuspended in 15 ml Tris-HCl (this can be stored at -80°C). Bacteria was sonicated (Fisherbrand sonic dismembrator model 705 with sound enclosure) using the macrotip and 12 µm amplitude, 12 minutes, 15 seconds power/rest

intervals. The lysate was centrifuged at 13000 rcf for 10 minutes (pellet was re-sonicated if it was too large). Lysates and centrifuge temperature were kept at 4°C to minimise protein degradation.

2.9.2. His-Trap Nickel column

Cell lysate was filtered (0.22 µm) and moved to a fresh 50 ml falcon tube. A histrap column (HisTrap™ HP 5 ml purification column, GE healthcare) was equilibrated at room temperature and washed with 10 ml miliQ water at 2 ml/min. Binding buffer (20 mM imidazole, 20 mM Tris-HCl and 300 mM NaCl) was pumped at 2 ml/min until 10 ml ran through. During this stage, NaCl and imidazole was added to the lysate in order to match the buffer concentrations. After that, the sample was loaded to the column with a 1 ml/min flow rate and the flow through was collected and kept on ice (in case it would be required later). Finally the column was rinsed again with 10 ml of binding buffer to elute non-specific proteins and contaminants, flow rate was lowered to 1 ml/min by the end of the wash and the column was closed. Good care was taken to ensure the column matrix did not take any air during the whole process.

2.9.3. AKTA prime fragmentation

The AKTA prime inlets A & B were initially washed with milliQ water using a flow rate of 4 ml/min with a 0.5 MPa pressure limit, 10 minutes at 0% B and 10 minutes at 100% B. The AKTA was paused after this to change the inlets into low (A) and high (B) imidazole buffer, a new run was then started with 4 ml/min flow rate, 0.5 MPa and 100% B for 10 minutes and 0% B for 10 more minutes. The Nickel column was then connected to start fragmentation. 5 ml fractions were prepared after setting up a gradient with 100% B target in a total volume of 60 ml at 1 ml/min flow rate. PqsR is expected to present a sharp peak in the UV spectra at 35 ml.

After gradient completion, 25 µL of sample was collected from the fractions with PqsR for Nanodrop™ and SDS-PAGE analysis. A final wash was performed to both inlets running 20 ml of miliQ water and finally replaced with 20 ml 20% ethanol. Fractions were flash frozen with liquid nitrogen for further analysis.

2.9.4. Nickel column regeneration

After every purification process, the HisTrap™ column had to be equilibrated again so it could be reused. To do so, 10 ml of 8M Urea (pH 8.0) was run through the column first. Afterwards, 10 ml 100 mM EDTA were run to strip the used nickel, the column should turn totally white here. 10 ml of miliQ water ran through afterwards to wash the column, finally, the column nickel was re-established by running 10 ml of 50 mM $NiSO_4$ at 1 ml/min (column should go back to original colour again). To store the column, 15 ml of 20% ethanol were run as a final wash after the nickel and before storage at 4°C.

2.9.5. SDS-PAGE

Sodium dodecyl sulfate polyacrylamide gel electrophoresis (SDS-PAGE) was performed to test the protein fractions obtained from the protein purification work. The gel was divided into the stacking (3% acrylamide) and separating (16% acrylamide) gels. To prepare two gels, the stacking gel was done with 2 ml of stacking buffer (0.5 M Tris 6.8 pH, 0.4 % SDS), 400 µL acrylamide, 1.45 ml distilled H_2O, 50 µL APS and 5 µL TEMED. The separating gels were done with 2.5 ml of separating buffer (1.5 M Tris pH 8.8 and 0.4 % SDS), 2.4 ml acrylamide, 5.05 ml distilled H_2O, 50 µL APS and 5 µL TEMED. The glass casettes were prepared and tested for leaks with isopropanol before making the gels. TEMED and APS were added immediately before use to avoid premature polymerisation. The separating gel was poured first, once it was settled, the TEMED and APS were added to the stacking gel, the lane comb was carefully added before polymerisation with special care to avoid bubbles. The running apparatus was loaded with running buffer (25 mM Tris pH 6.8, 192 mM glycine, 0.1% SDS) to the mark. Samples were loaded mixed with loading buffer (50 mM Tris pH 6.8, 100 mM DTT, 2% SDS, 0.1% bromophenol blue and 10% glycerol). The machine ran first at 16 mA through the stacking gel and then at 40 mA through the separating gel until the marker front reached the bottom of the gel.

2.9.6. Isothermal titration calorimetry (ITC)

Isothermal titration calorimetry (ITC) was used to detect direct binding between PqsR antagonists and the $PqsR_{LBD}$. The MicroCal PEAQ-ITC from Malvern was used to run the assays. Firstly, $PqsR_{LBD}$ protein pellets were thawed to room temperature and the concentration was measured using NanoDrop™. Using Malvern's software, ITC was washed before each assay and deep washed afterwards, a wash or rinse was performed between runs. Each run was done at 25°C with 19 injections and 90 second spacing (the first injection had a 150 second spacing), each injected 2 µL volume in 4 seconds, differential power (DP) was set at 5.0 with high feedback. The sample cell was loaded with 10 µM $PqsR_{LBD}$ in SEC buffer (20 mM Tris Base and 150 mM NaCl) and 4% DMSO. The syringe was loaded with 100 µM of compound in SEC buffer with 4% DMSO.

3. Chapter 3: PqsR gene regulator purification and antagonist binding kinetics

3.1. Introduction

This chapter focuses on the screening and initial validation of the PqsR inhibitors as part of the SENBIOTAR drug discovery programme. Dr. Fadi Soukarieh performed all the chemical synthesis for the optimisation of the compounds identified and, for this reason, work discussed in the following pages does not include the synthesis steps. Instead it focuses on the screening, determination of *pqsA* transcription inhibition and whether the compounds were able to directly bind to the purified target regulator PqsR. Due to intellectual property reasons, we are unable to disclose some of the structures of the compounds used in this thesis.

3.1.1. Inhibition of the *pqs* biosynthetic enzymes

The inhibition of the synthesis of AQs through the inactivation of one of the biosynthetic enzymes has been pursued as a potential path for the attenuation of virulence (Allegretta *et al.* 2017; Soukarieh *et al.* 2018b). The biosynthesis operon *pqsABCDE* includes all genes required for 4-hydroxy-2-heptylquinoline (HHQ) production whereas *pqsH* which catalyses the step from HHQ to 2-heptyl-3,4-dihydroxyquinoline (PQS) is found elsewhere (Gallagher *et al.* 2002).

The first enzyme PqsA is a CoA-ligase. The inhibition of *pqsA* blocks the *pqs* system and decreases biofilm formation (Allesen-Holm *et al.* 2006; Rampioni *et al.* 2010; Kim, Park and Lee 2015). Some *pqsA* inhibitors have been developed with partial success (Lesic *et al.* 2007; Coleman *et al.* 2008; Ji *et al.* 2016). The recent elucidation of the crystal structure of the PqsA ligand binding domain (LBD) is a big step forward towards the further development of better PqsA inhibitors (Witzgall, Ewert and Blankenfeldt 2017).

The second and third genes in the operon form the dimer PqsBC which catalyses the formation of HHQ from 2-amynobenzoylacetate (2-ABA) and octanoyl CoA (Drees *et al.* 2016). Several PqsBC inhibitors have been reported (Kesarwani *et al.* 2011; Allegretta *et al.* 2017; Maura and Rahme

2017). Nevertheless, inhibition of PqsBC leads to accumulation of by-products DHQ and 2-AA which are linked to an increase in persistence and chronicity, contesting the clinical relevance of PqsBC inhibition (Kesarwani *et al.* 2011; Gruber *et al.* 2016; Allegretta *et al.* 2017).

PqsD is the second enzyme in the biosynthesis pathway after PqsA and produces 2-ABA-CoA (Dulcey *et al.* 2013). Extensive research has been performed, resulting in many inhibitors from different origins and methodologies: From a structural homologue (Klein *et al.* 2012), to a ligand-based approach (Storz *et al.* 2012), urea based (Sahner *et al.* 2013) or as dual PqsD/PqsR inhibitors (Thomann *et al.* 2016). A common issue with PqsD inhibitors has been their poor selectivity which could lead to potential issues (Storz *et al.* 2012; Sahner *et al.* 2013).

The last but possibly most interesting gene of the operon is *pqsE*, a thioesterase that can also act as a gene regulator independently of PqsR (Farrow *et al.* 2008; Rampioni *et al.* 2010; Drees and Fetzner 2015). PqsE removes the CoA group from 2-ABA-CoA to form 2-ABA, precursor of HHQ. The complexity of the PqsE role and the relatively small volume of knowledge has left it mostly untargeted for inhibition. There has been one attempt through fragment based drug discovery which developed compounds that inhibit the thiosterase activity but did not impact pyocyanin production (Zender *et al.* 2016). Important advances regarding PqsE have been done and they will provide very useful insights for the development of specific inhibitors against this very interesting target (Rampioni *et al.* 2016).

3.1.2. Targeting PqsR

The *pqs* system was first described by Pesci *et al.*, 1999. This was the third QS system described in *Pseudomonas* after *las* and *rhl*, systems based in acyl-homoserine lactones as signals. The *pqs* auto-inducing signals are alkyl-quinolones, chemically very different molecules that are well known for their antibiotic properties (Figure 3.1). The *pqs* system regulates a wide range of virulence factors through the activation of PqsR (Maura *et al.* 2016), furthermore, mutations in *pqsR* create attenuated virulence strains as demonstrated in murine infection models (Cao *et al.* 2001; Diggle *et al.*

2003). Interestingly, transcriptomic data suggested that PqsR only regulated the *pqsABCDE* operon (Rampioni *et al.* 2016), however, chromatin immunoprecipitation (ChIP) data suggested other binding sites, most of which were not in promoter regions, rather fully or partially inside genes, and should be validated (Maura *et al.* 2016).

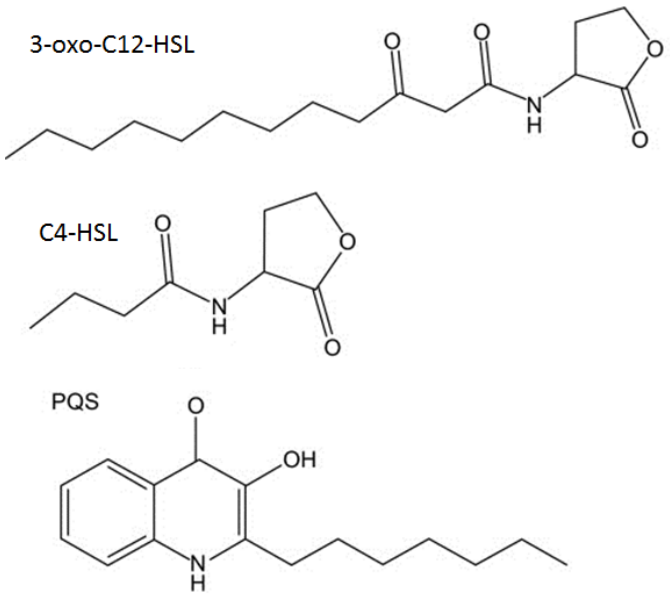

Figure 3.1. Extracted and modified from Lee & Zhang (2014). Structures of *P. aeruginosa* quorum sensing (QS) signals. Top to bottom, first, *N*-(3-oxododecanoyl)-homoserine lactone (3-oxo-C12-HSL) signal molecule of the *las* system; *N*-butyrylhomoserine lactone (C4-HSL) of the *rhl* system and 2-heptyl-3-hydroxy-4-quinolone (*Pseudomonas* Quinolone Signal, PQS) of the *pqs* system. 3-oxo-C12-HSL and C4-HSL are homoserine lactones with different carbon chain lengths from the amino group whereas the "head" of PQS is a 3-hydroxy-4 quinolone.

3.1.2.1. PqsR protein structure and ligand binding domain

PqsR, originally known as MvfR (*m*ultiple *v*irulence *f*actor *Regulator*), was originally identified as a LysR-like transcription regulator mostly related to the control of virulence factors but that also happened to regulate PQS biosynthesis (Cao *et al.* 2001).

LysR transcriptional regulators (lttr) are a conserved family found in many bacteria and with orthologues in the Archaea and Eukarya. Lttr protein members are related by the DNA binding domain which is a classic helix-turn-helix (HTH) of the winged-helix variety, formed by three helices with a β-pleated sheet between the second and third. The first and second

helices interact with DNA while the third embeds in the major DNA groove. Moreover, these regulators often require co-inducers that are related to the regulated genes and vary depending on the LTTR they control (Figure 3.2). A detailed review on Lttrs was done by Maddocks & Oyston, 2008 with further updates from Housseini B Issa, Phan and Broutin 2018.

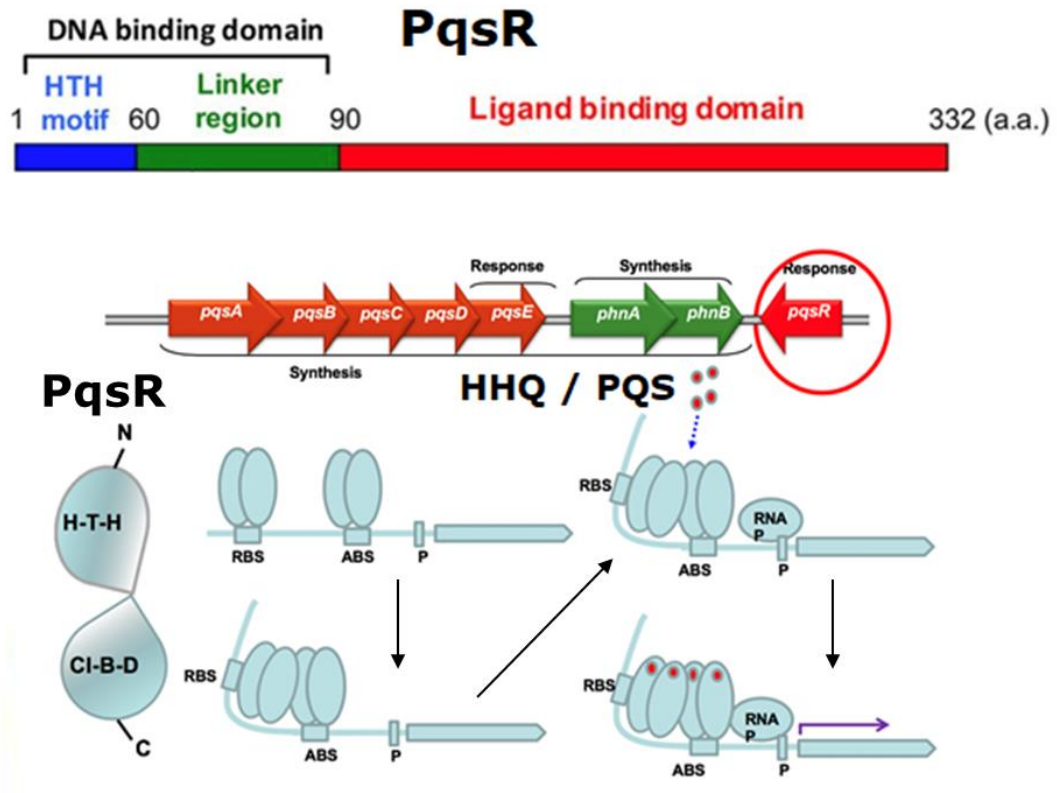

Figure 3.2. Linear and functional diagram of PqsR. The PqsR protein is represented linearly showing the DNA binding domain with the helix-turn-helix and linker regions and the ligand binding domain. Its relative position in the genome is also shown, finally, a graphic representation showing the double dimer structure binding to the DNA, bending the promoter and activating when the auto-inducers HHQ or PQS bind to PqsR. Information has been extracted from Maddocks and Oyston (2008) and Ilangovan *et al.* (2013).

PqsR was originally identified as a membrane bound protein and suggested to be cleaved during stationary phase by an as yet unknown process (Cao *et al.* 2001). Later, HHQ and PQS were described as co-inducers required for its activation (Xiao *et al.* 2006). The ligand binding domain ($PqsR_{LBD}$) structure has been elucidated, enabling the design of an optimal platform to develop antagonists (Kefala *et al.* 2012; Xu *et al.* 2012; Ilangovan *et al.* 2013). The PqsR protein has a size of 38 KDa. The $PqsR_{LBD}$ found in the C-terminal has been purified in the absence of the N-terminal HTH domain as the presence of the latter caused problems with solubility during purification (Ilangovan *et al.* 2013). Crystallography data showed that the

ligand binding domain had two sub-domains, CBDI and CBDII (called *c*o-inducer *b*inding *d*omain) separated by a hinge region, the CBDII has two A / B pockets, the A pocket interacts with the alkyl chain whereas the B pocket accommodates the quinolone ring of the ligands (Figure 3.3). The length of the alkyl chain determines the affinity of the co-inducer (Fletcher *et al.* 2007; Ilangovan *et al.* 2013).

The paper by Ilangovan *et al.*, 2013, described in much more depth the unique characteristics of the $PqsR_{LBD}$. The alkyl chain of the AQs binds into the A pocket through hydrophobic interactions and the quinazolinone head is buried in the B pocket. A small sub pocket is found in the B pocket although neither HHQ nor PQS interact with it.

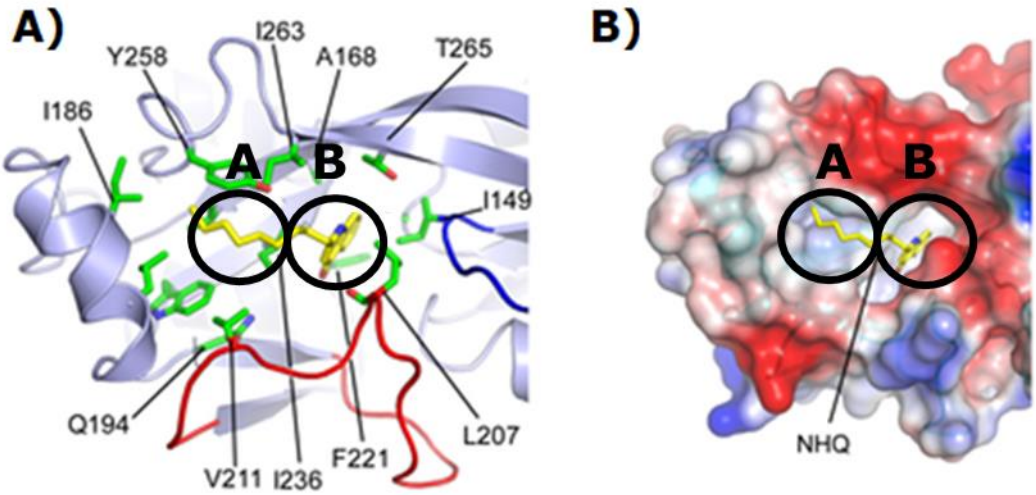

Figure 3.3. $PqsR_{LBD}$ A and B pockets from CBDII. Modified from Ilangovan *et al.* 2013. 2-nonyl-4-hydroxyquinoline, NHQ in: **A)** Stereo diagram of the topology of the $PqsR_{CBD}$-NHQ complex showing the ligand as a yellow stick and relevant amino acids are highlighted in green. **B)** Charge surface representation of the $PqsR_{CBD}$ showing the hydrophobic pocket occupied by NHQ, red represents acidic and blue are basic residues. The quinolone ring is buried within the **B pocket** and the alkyl chain bound to the more accessible **A pocket**.

3.1.3. PqsR as target for antagonists

The characteristics of the $PqsR_{LBD}$ make it an interesting target to develop specific antagonists that would block the active site and render PqsR inactive (Ilangovan *et al.* 2013; Soukarieh *et al.* 2018a).

Work in this project has focused in the development and study of PqsR antagonists in a laboratory environment, putting affinity and specificity in the spotlight. The information regarding the effectiveness of PqsR

antagonists in animal models is currently limited, however one of the patented inhibitors by Spero Therapeutics presented a 50% decrease in AQ levels in acute thigh infection models in mice from oral administration of 4 doses of 200 mg/Kg (Zahler 2016). A very recent review by Soukarieh *et al.* 2018b collects the current advancements in PqsR antagonists (Figure 3.4) (as well as other components of the *pqs*, *las* and *rhl* systems) and their therapeutic prospects.

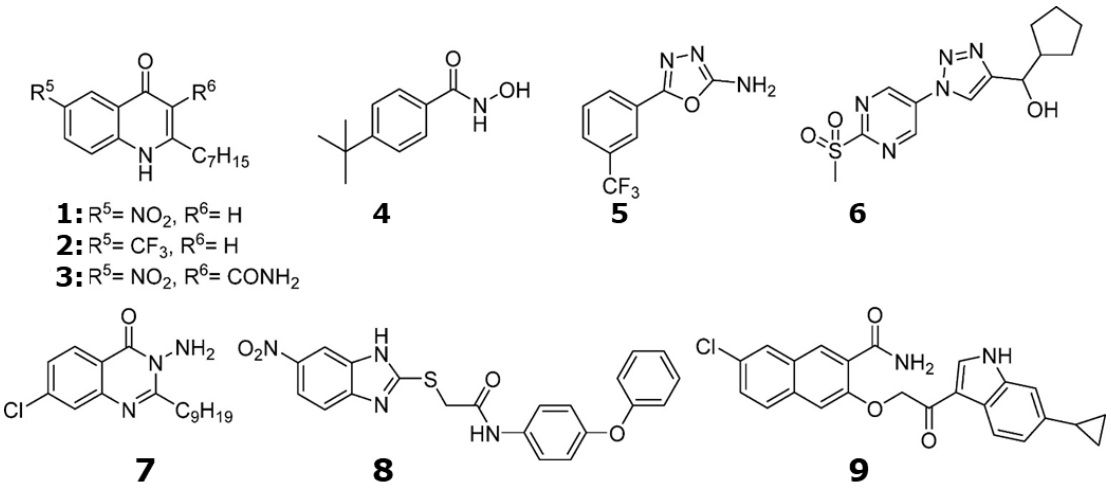

Figure 3.4. Some published structures of PqsR antagonists Modified from Soukarieh *et al.* (2018b). Compounds **1** and **2** turned to be strong agonists upon further research (Lu *et al.* 2012). Compound **3** is from Lu *et al.* (2014), compound **4** is from Lu *et al.* (2014b), compound **5** and **6** are from Zender *et al.* (2013), compound **7** is from Ilangovan *et al.* (2013), compound **8** is from Starkey *et al.* (2014) and compound **9** is from Zahler (2016).

The compounds used in this project were derived from the quinazolinone (QZN) inhibitor (Ilangovan *et al.* 2013). Moreover, the library was developed following the same strategy. It is interesting to note that the substitution with a halogen (Cl or F) in the C-7 position highly enhanced the activity of the QZNs tested regardless of whether they were agonists or antagonists and thus it was considered as a key element for the development of the compounds. The parent compound, 3-NH_2-7Cl-C9-QZN (IC_{50} = 4.3 μM) competes with HHQ and PQS to bind in the active site in similar fashion to the native AQs (above). It is worth pointing out that the halogenated group binds to the threonine 265 in the sub pocket natively unused by the AQs. This interaction was explored in depth during the development of the library of PqsR antagonists. Additionally, the amino substituent in the 3rd position creates a hydrogen bond with leucine 207. The resulting interaction between the active site and the QZN inhibitor was

found to be similar to that of HQNO but with the QZN presenting more interactions. This coupled with the observed biological effect of the inhibitor was the reason behind the choice of 3-NH_2-7Cl-C9-QZN as parent compound for the library.

The PqsR antagonists included a quinolone part that would bind to the B pocket, with an aromatic tail interacting with the hydrophobic regions in the A pocket. Previous studies had shown that the affinity of a ligand to the A pocket was dependent on the chain length, the native molecules HHQ and PQS present a C7 alkyl tail but C9 tails have also shown very low EC_{50} values (Fletcher *et al.* 2007), however, the alkyl tail is not required for specific binding to this hydrophobic pocket. In a recent publication by Kitao *et al.* (2018), the crystal structure of $PqsR_{LBD}$ bound to a non-ligand, benzamine-benzimidazole (M64) antagonist showed that the compound induced a conformational change in an adjacent region to the $PqsR_{LBD}$ domain that was not observed in the native form or bound to a congener. The authors of the paper hypothesise that their compound could trigger a conformational change in the DNA binding domain, unfortunately, to date, no full PqsR protein has been purified, due to the solubility issues mentioned, and hence this hypothesis remains to be tested (Kitao *et al.* 2018). With this flexibility in mind, the development and optimisation of antagonists performed by Dr. Fadi Soukarieh presented changes in both parts of the antagonists, these changes allowed the development of a group of compounds in structurally distinct families.

3.1.3.1. Common workflow for lead-like drug discovery

The development of new compounds with specific targets often follows the same workflow regardless of the target's nature. Virtual screening (VS) is usually the first step in drug discovery (Zhu *et al.* 2013) although the method is also useful for other applications (Sommer *et al.* 2017). VS is complemented with more classic high throughput assays to confirm the activity of the best scoring compounds. A classic approach is the development of *lux*-based bioreporters that monitor the expression of the target. Another important element is the confirmation of direct binding, for which isothermal titration calorimetry is the gold standard (Velázquez-Campoy *et al.* 2004 and below). The compounds are further tested in

secondary assays to confirm a biological effect and more importantly, target selectivity (Zhu *et al.* 2013). These steps are particularly important to prevent PAINS in the assay (Dahlin *et al.* 2015). Pan assay interference compounds (PAINS) are promiscuous substructures that lack selectivity or have a widespread biological impact resulting in hits reporting false positives that must be filtered out (Baell and Holloway 2010; Dahlin *et al.* 2015). A recent publication noted that more than 450 substructures are currently classified as PAINS, of which some are found in commonly investigated compounds and can still plague researchers even with current filters (Jasial, Hu and Bajorath 2017).

PAINS are a very significant issue, however the raising trend of avoiding them at all costs should be re-evaluated as highlighted by two independent groups that published on the topic (Capuzzi, Muratov and Tropsha 2017; Jasial, Hu and Bajorath 2017). Notably, both papers show that while PAINS are an issue, there are many instances in which a defined PAINS substructure is found in both active and inactive hits, thus the association of PAINS with overly reactive hits is incorrect, and while neither Capuzzi *et al.,* nor Jasial *et al.,* offer a practical solution towards this, they provide strong evidence that the current approach to PAINS should be reevaluated.

With the advent of 'big data' analysis, data mining has become an alternative approach towards drug discovery studies (Sang *et al.* 2018). By looking into the wealth of literature available, seemingly unrelated papers can be linked together to determine potential relationships (much akin to separate pieces of the same puzzle). This approach facilitates the development of strong hypothesis that could significantly speed up the discovery process (Smalheiser 2012)

Finally, once confirmed as hits, the relevant compounds will be studied in detail for the ability to repress any phenotypes. The best can then be tested in *in vivo* studies using appropriate infection models for the attenuation of virulence as well as for the determination of pharmacokinetic and pharmacodynamic properties.

3.2. Aims of the chapter

This chapter aimed to validate the activity of PqsR antagonists identified from a compound library and further optimised by Dr. Fadi Soukarieh using medicinal chemistry-based approaches. These compounds were developed as part of the SENBIOTAR programme. More specifically, the main objectives of this chapter are:

- To perform the initial identification of PqsR antagonists from a compound library using a *P. aeruginosa* mCTX::P*pqsA*-lux bioreporter strain and a relatively high concentration of compounds (10 µM).
- To determine the IC_{50} values of the best candidates from different families and shortlist the best hits for further optimisation.
- To provide evidence of binding of the selected compounds to the PqsR ligand binding domain.

3.3. Results

3.3.1. *In silico* docking and activity assays for the compound library

A library composed of around 83000 drug-like diverse compounds was virtually screened by Dr. Soukarieh using the Schrödinger Suite to identify structures that may likely bind in the ligand binding domain of PqsR (Friesner *et al.* 2006). The *in silico* docking for these compounds was performed based on previous crystallography data of PqsR and antagonists (Ilangovan *et al.* 2013). The top scored compounds were obtained and screened at 10 uM using the *lux* bioreporter (Figure 3.5). This concentration was chosen as an arbitrary, maximum acceptable for a compound to be deemed active. Only compounds showing at least 50% inhibition of the *lux* signal in the reporter when compared to the control were selected for further analysis.

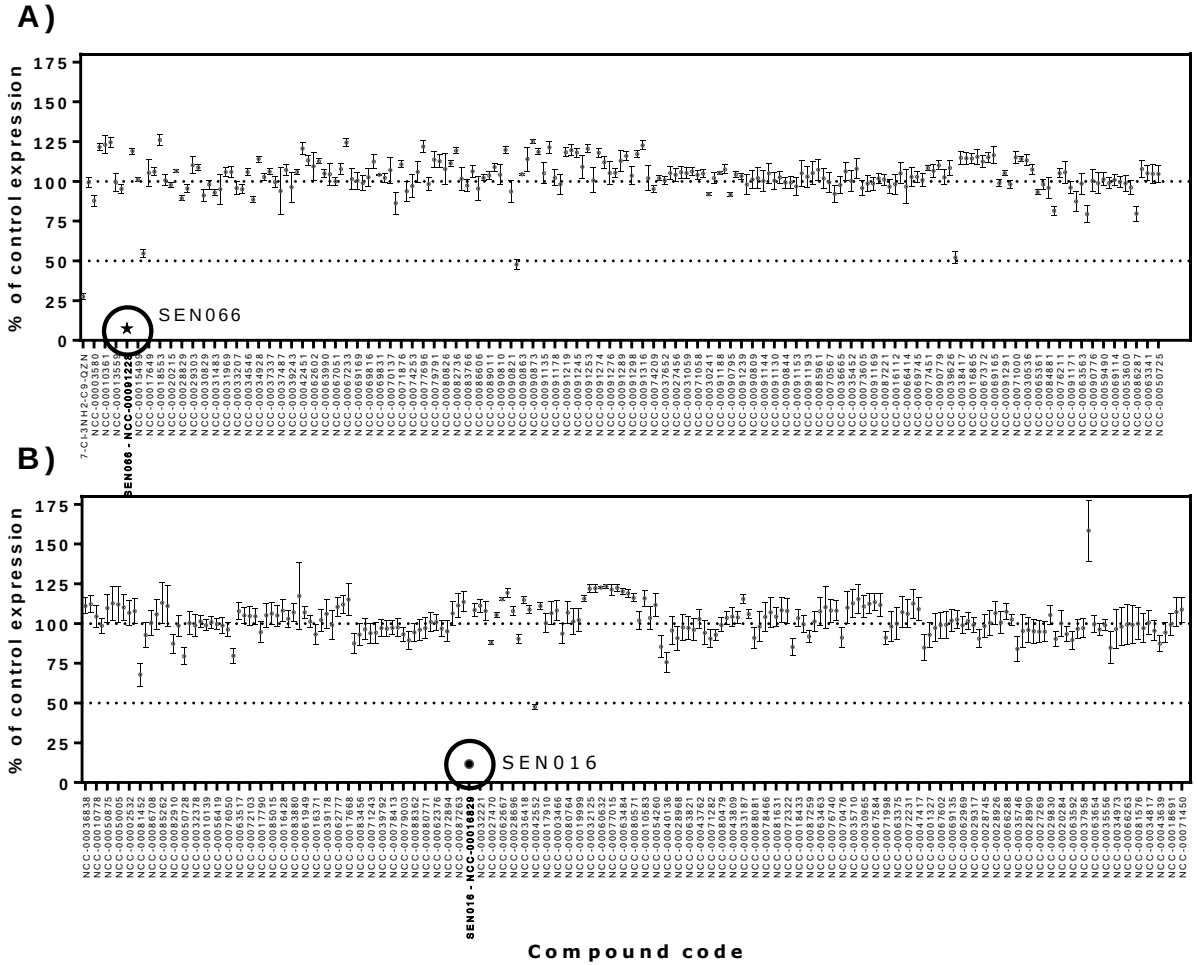

Figure 3.5. Activity assays at 10 µM. 397 compounds are shown including active compounds **A) SEN066** (★) which had 92.59 % inhibition and **B) SEN016** (●) with 88.32% inhibition. The assays were performed by measuring the total light inhibition of PAO1-L WT mCTX::P*pqsA*-lux Gm^{R} reporters with 10 µM of compound compared to the light expression of a control containing no compounds and with the same volume of solvent (DMSO). Error bars represent the standard deviation of biological triplicates. Active compounds were considered as those with higher than 50% inhibition.

SEN016 and SEN066 were the two active compounds found. SEN016 was used as benchmark for further chemical synthesis optimisation developed by Dr Fadi Soukarieh. Out of this process, a batch of compounds with refined potency was obtained, including: SEN089, SEN088, SEN086, SEN071, SEN019 and SEN032. SEN022, SEN050 and SEN020 were also obtained albeit with much lower activity. The optimisation process for SEN066 was not explored due to time and resource constraints. The structure of some compounds is hereby presented to illustrate the structural variability between some of the main families (Table 3.1).

Table 3.1. Some families of PqsR inhibitors.

1st Generation, SEN019 family	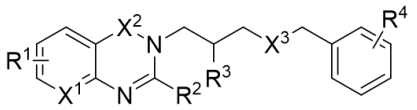
2nd Generation, SEN032	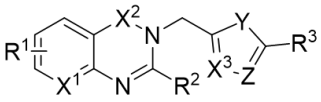
3rd Generation SEN066 family	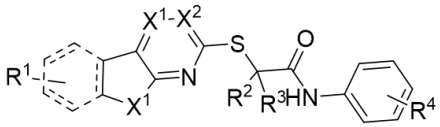
4th generation SEN089 family	**IP PROTECTED**

SEN016 was selected as the main candidate for further chemical optimisation.

3.3.2. Determination of the IC_{50} for the more active hit compounds

The compounds with the highest activity at 10 µM were further analysed to determine their IC_{50} values using the *P. aeruginosa* mCTX::P*pqsA*-lux bioreporter strain. The assay was performed static in 200 µl of LB for 24 hours at 37° C and both planktonic growth as OD_{600} and relative light units (RLUs) were measured in a TECAN™ plate reader. Several concentrations of compound were tested in triplicate with logarithmic increases, the highest value of all time points was averaged between replicates and used

for each concentration to plot the required values for IC_{50} which was calculated in Graphpad Prism7.

The first compounds tested were the original SEN016 and SEN066 as well as SEN019 (developed from SEN016) and SEN032. All these compounds presented a good IC_{50} in PAO1-L, well below the 10 μM activity threshold (Figure 3.7). As time progressed, other compounds were optimised from the synthesis progress, SEN089 presented the lowest IC_{50} value and had really good activity in phenotypic assays (Figure 3.7 and Figure 3.6).

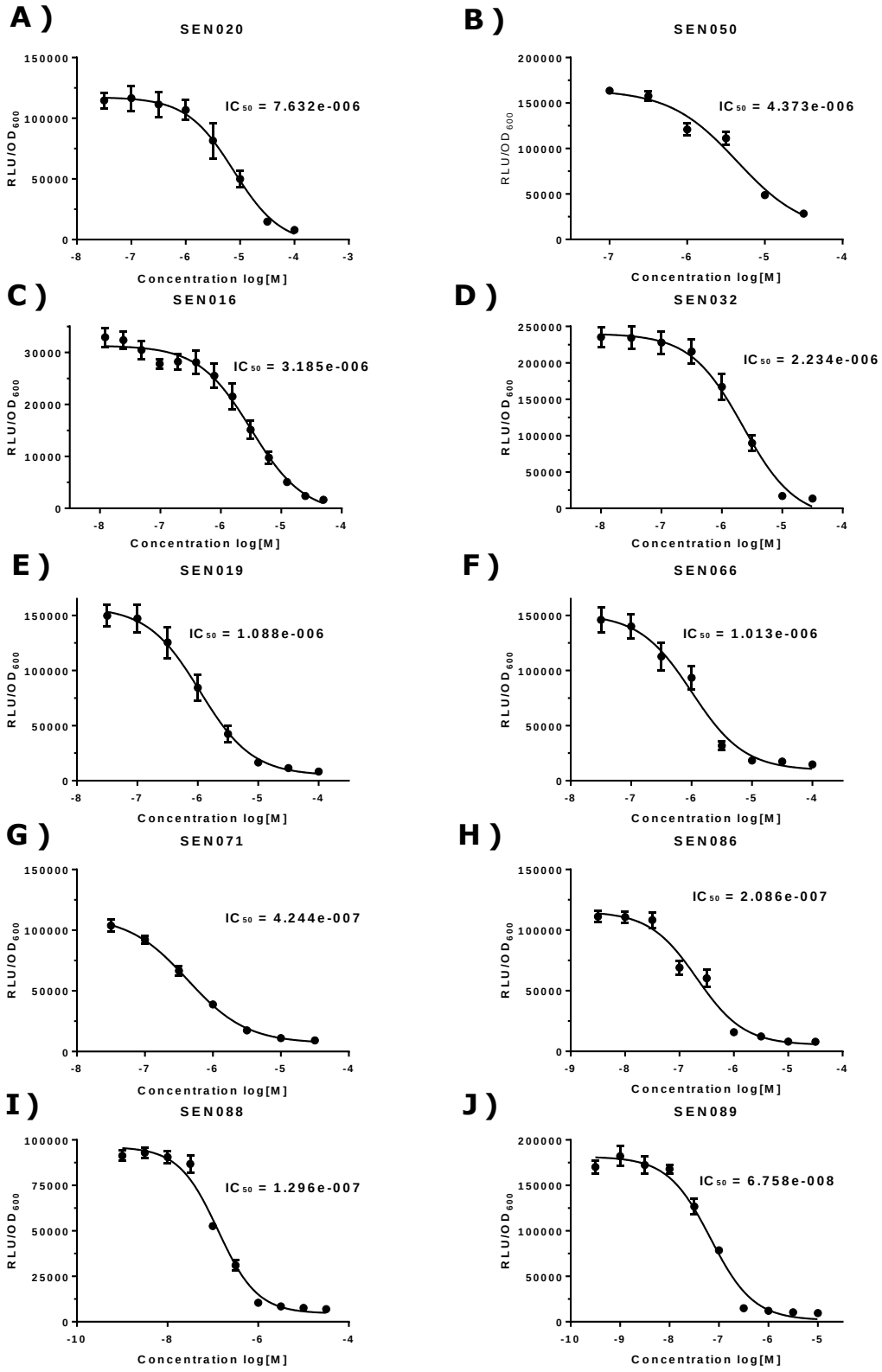

Figure 3.6. IC_{50} graphs for SENBIOTAR compounds. IC_{50} values were obtained from assays in 96 well microtiter plates where PAO1-L mCTX::P*pqsA*-lux Gm^R was grown in 200 µL LB for 24 hours static at 37°C, measurements of OD_{600} and relative light units RLUs were obtained every half an hour and used to calculate the IC_{50} value. +/- Error bars were calculated from biological triplicates, in some instances they are shorter than the radius of the dot and thus are not shown. **A)** SEN020, **B)** SEN050, **C)** SEN016, **D)** SEN032, **E)** SEN019, **F)** SEN066, **G)** SEN071, **H)** SEN086, **I)** SEN088, **J)** SEN089.

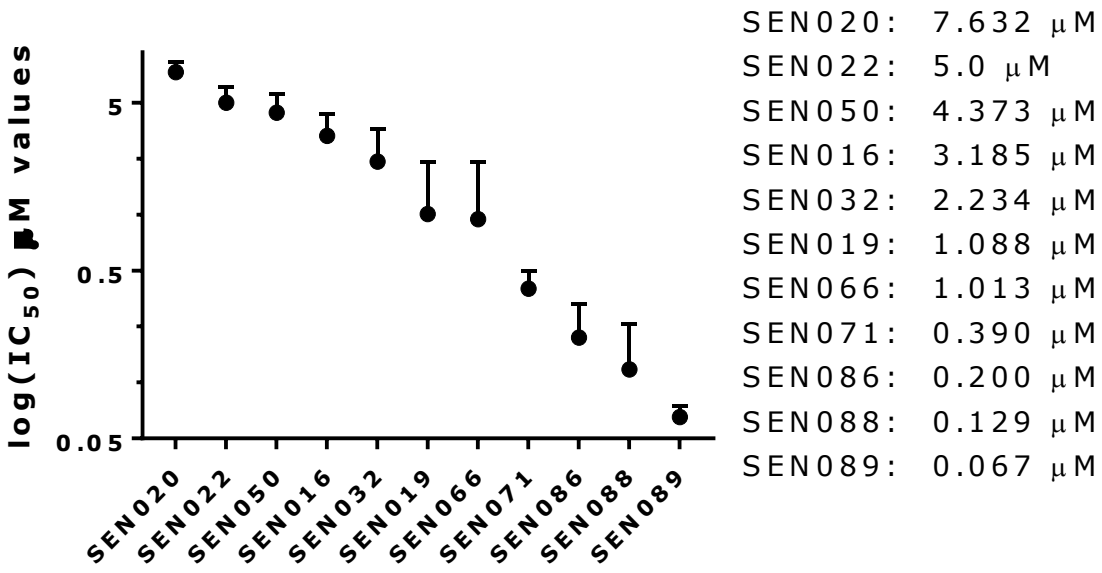

Figure 3.7. IC_{50} values for SENBIOTAR active compounds in PAO1-L WT. IC_{50} values were obtained from assays in 96 well microtiter plates where PAO1-L mCTX::P*pqsA*-lux Gm^R was grown in 200 µL LB for 24 hours static at 37°C, measurements of OD_{600} and relative light units RLUs were obtained every half an hour and used to calculate the IC_{50} value.

3.3.3. PqsR protein purification

PqsR is a key transcriptional regulator, particularly for the *pqs* system (Xiao *et al.* 2006). PqsR activates upon binding with either HHQ or PQS. Studying the binding of antagonists to PqsR can provide very useful information for further development of antagonist compounds and understanding the mechanisms of action.

For this reason, the co-inducer binding domain of PqsR ($PqsR^{94-309}$) was expressed in *E. coli* BL21(DE3) expression strain. A HisTrap™ HP column was used to immobilise the protein which was later released in an imidazole gradient elution of 0 to 500 mM imidazole, collected in 5 ml fractions.

During the imidazole gradient elution using an AKTA™ prime, several parameters were measured, the UV absorbance was used to monitor the elution of the bound protein. Results show that the protein eluted in two close peaks, which could imply a certain degree of aggregation. Nevertheless the absorbance intensity was good, with the second peak slightly above 950 mAu (Figure 3.8). Fractions 11 to 16 were collected and snap frozen for later use. The small peak in the area with low levels of imidazole could correspond to an unspecific co-extracted fraction.

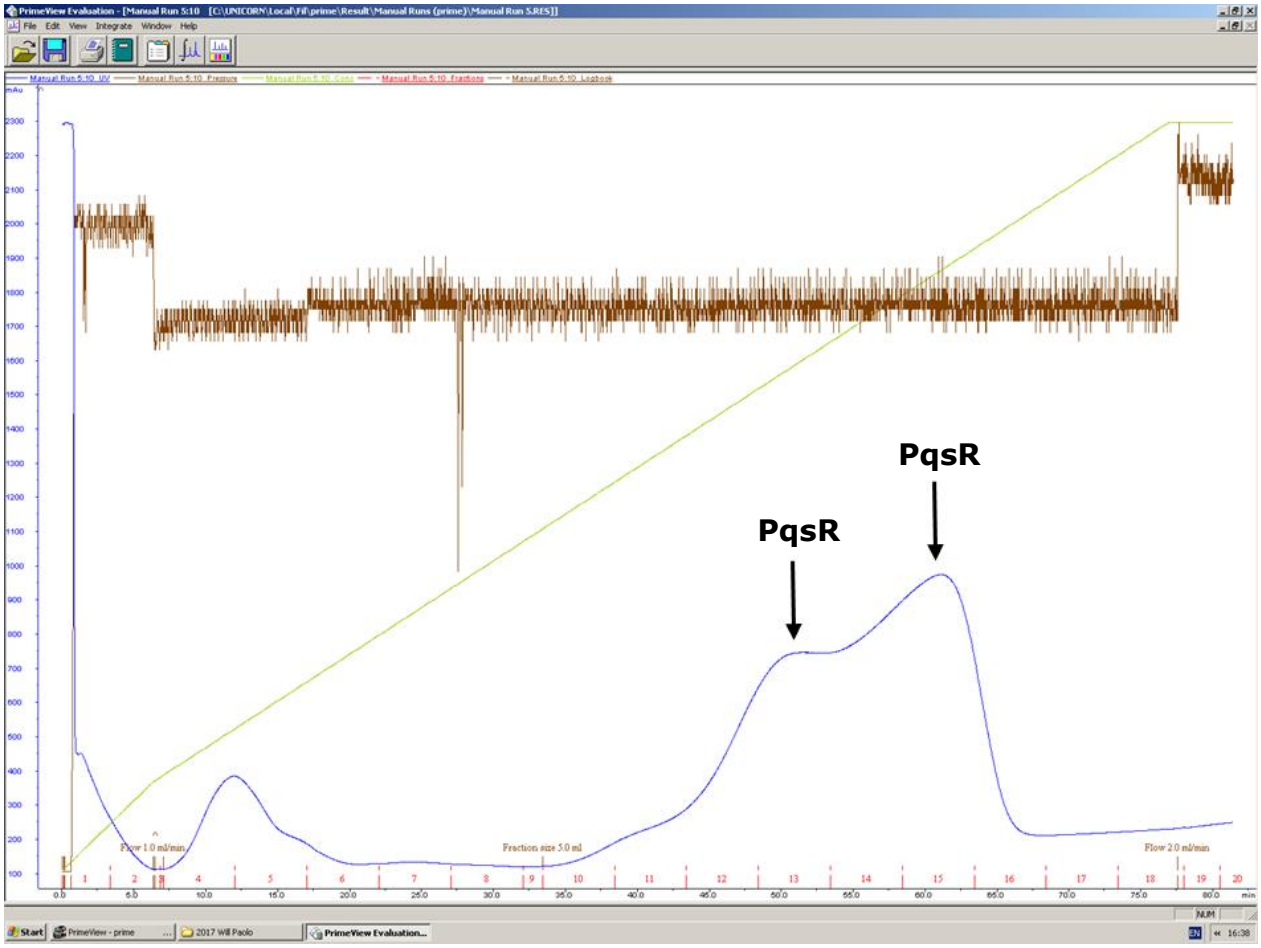

Figure 3.8. PqsR protein elution profile. $PqsR^{94-309}$ had been immobilised in a His-trap column and eluted with 0-500 mM imidazole gradient solution using an AKTA machine. Fractions 11 to 16 were collected for further purification. In **blue**, UV absorbance directly correlating to protein presence and concentration in the elution. In **brown**, system pressure. In **green**, imidazole gradient formation. Black arrows point at the PqsR peaks, the first bump is caused by a small degree of aggregation.

Several samples were collected at different stages of the purification process to run in an SDS-PAGE gel. Before and after sonication samples were collected as well as small samples of AKTA fraction 11, 12, 13, 14, 15 and 16. Results show that there was a significant smear in the samples before and after sonication caused by an overload of the lanes. However, all fractions from the AKTA presented a very large quantity of protein corresponding to the $PqsR_{LBD}$ purified protein (Figure 3.9).

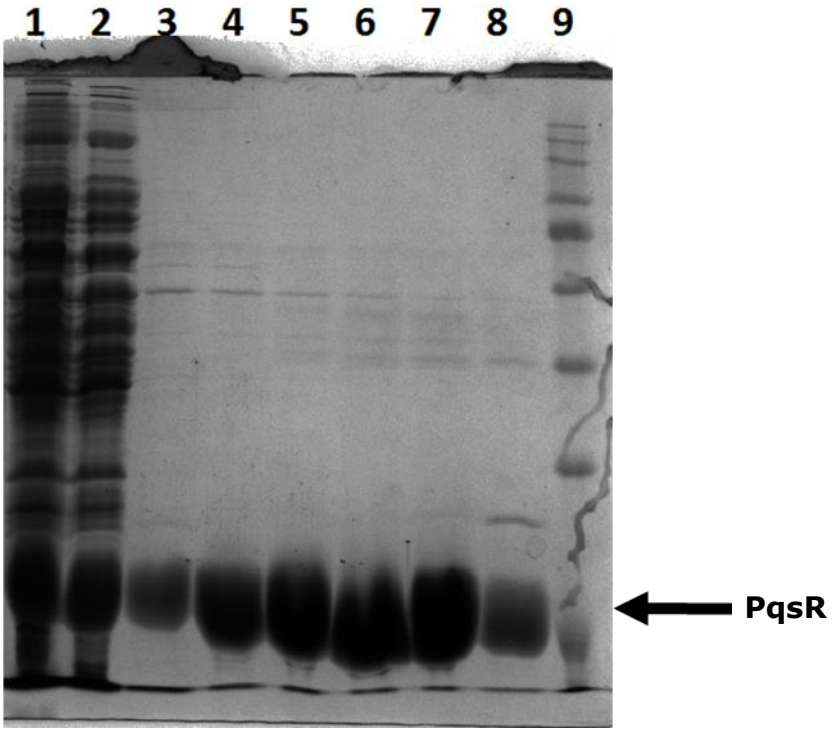

Figure 3.9. SDS-PAGE protein gel for multiple steps of PqsR purification. 16% Acrylamide SDS-PAGE, 5 µl of sample were mixed with 5 µl of loading buffer. **(1)** Before sonication. **(2)** After sonication. **(3)** AKTA fraction 11. **(4)** AKTA fraction 12. **(5)** AKTA fraction 13. **(6)** AKTA fraction 14. **(7)** AKTA fraction 15. **(8)** AKTA fraction 16. **(9)** Molecular weight marker. The black arrow points at the protein band. The smeared look is caused by a very high concentration of protein.

The fractions were prepared in aliquots and frozen at -80°C. Each aliquot would be defrosted and measured in a NanoDrop™ before being used the very same day. The protein could not be stored at 4°C as it precipitated at that temperature.

3.3.4. Isothermal titration calorimetry (ITC) of PqsR with PQS and antagonists

The antagonist compounds were selected and optimised for their P*pqsA*-lux inhibiting properties. Activity assays and IC_{50} showed that the addition of compounds directly inhibited the expression of the *pqsABCDE* operon, however, it did not provide evidence of direct binding to PqsR, specifically its ligand binding domain (LBD).

For this reason, a series of ITC assays was performed using the purified $PqsR_{LBD}$ and SEN compounds. ITC is a highly sensitive, quantitative methodology to monitor the kinetics of molecular interactions. The technique bases its readings in changes of free energy within a cell in equilibrium. This allows for great precision and forgoes the use of any

chromophore, fluorophore or enzyme that could bias the measurements by altering the stoichiometry (Freire, Mayorga and Straume 1990; Velázquez-Campoy *et al.* 2004). Nevertheless, this means that the buffers must be especially balanced to avoid background noise. The protein and compounds used the same SEC buffer and DMSO (at 4%) to keep the equilibrium.

In total, compounds SEN020, SEN050, SEN022, SEN066, SEN032, SEN019, SEN071, SEN086, SEN088 and SEN089 were tested with the ITC. The obtained $K_{(D)}$ values showed strong correlation to previously calculated IC_{50} values, albeit at much lower concentrations since this was performed in a completely clean, purified environment (Figure 3.10). SEN020, the L-isomer of SEN019, also bound to $PqsR_{LBD}$, even if it had originally been deemed not active because of above-threshold inhibition at 10 µM (23%), it showed low affinity that correlated with the low activity. The ITC graphs for the compounds tested can be found in Figure 3.11.

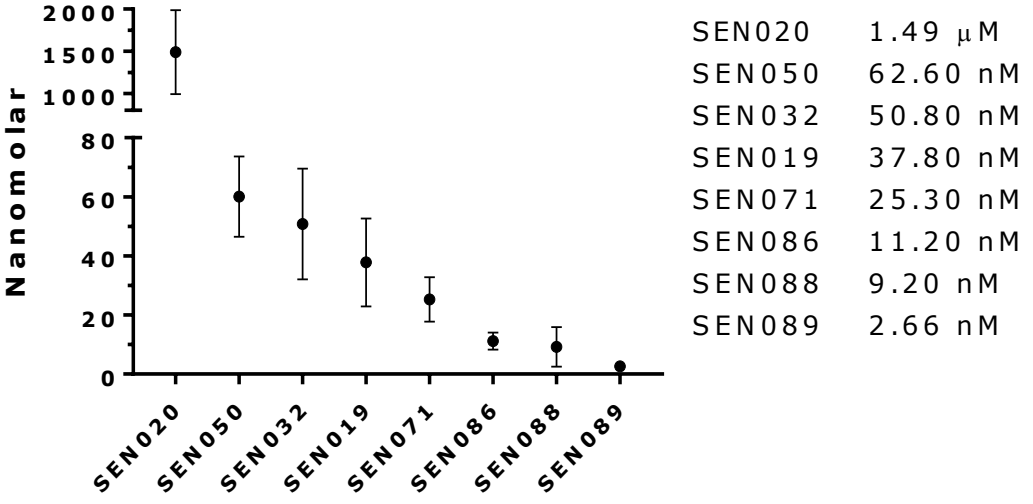

Figure 3.10. Isothermal Titration Calorimetry (ITC) $K_{(D)}$ values of different SEN compounds with $PqsR_{LBD}$. Results show the $K_{(D)}$ values of different SENBIOTAR PqsR antagonists tested on $PqsR_{LBD}$ and the standard deviation. The assay was performed using 10 µM of $PqsR_{LBD}$ in SEC buffer with 4% DMSO and 100 µM of compound in the same SEC buffer with 4% DMSO. +/- Error bars represent the standard deviation of runs in triplicate.

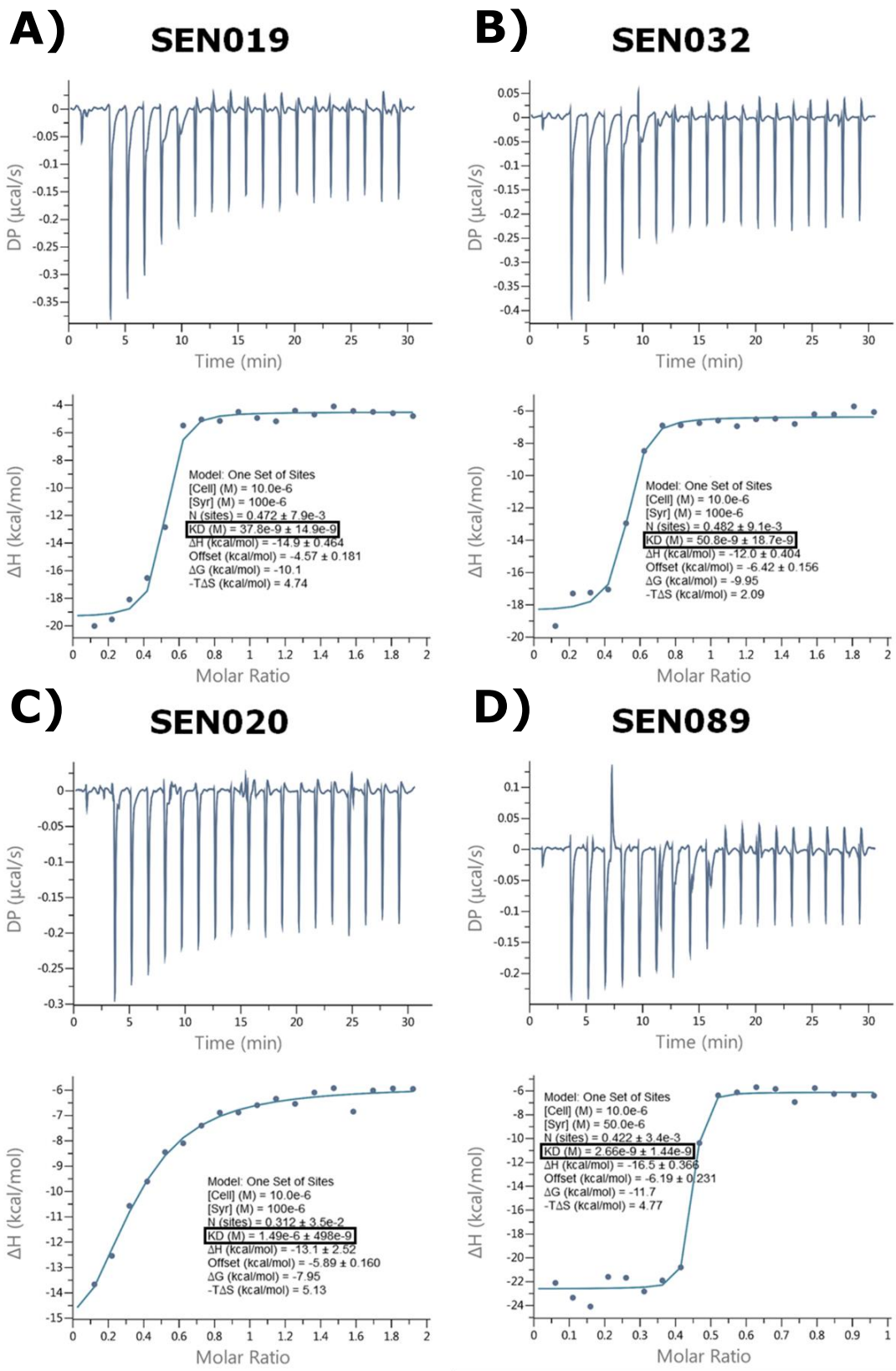
A)
SEN019
DP (µcal/s)
Time (min)
ΔH (kcal/mol)
Molar Ratio
Model: One Set of Sites
[Cell] (M) = 10.0e-6
[Syr] (M) = 100e-6
N (sites) = 0.472 ± 7.9e-3
KD (M) = 37.8e-9 ± 14.9e-9
ΔH (kcal/mol) = -14.9 ± 0.464
Offset (kcal/mol) = -4.57 ± 0.181
ΔG (kcal/mol) = -10.1
-TΔS (kcal/mol) = 4.74
B)
SEN032
DP (µcal/s)
Time (min)
ΔH (kcal/mol)
Molar Ratio
Model: One Set of Sites
[Cell] (M) = 10.0e-6
[Syr] (M) = 100e-6
N (sites) = 0.482 ± 9.1e-3
KD (M) = 50.8e-9 ± 18.7e-9
ΔH (kcal/mol) = -12.0 ± 0.404
Offset (kcal/mol) = -6.42 ± 0.156
ΔG (kcal/mol) = -9.95
-TΔS (kcal/mol) = 2.09
C)
SEN020
DP (µcal/s)
Time (min)
ΔH (kcal/mol)
Molar Ratio
Model: One Set of Sites
[Cell] (M) = 10.0e-6
[Syr] (M) = 100e-6
N (sites) = 0.312 ± 3.5e-2
KD (M) = 1.49e-6 ± 498e-9
ΔH (kcal/mol) = -13.1 ± 2.52
Offset (kcal/mol) = -5.89 ± 0.160
ΔG (kcal/mol) = -7.95
-TΔS (kcal/mol) = 5.13
D)
SEN089
DP (µcal/s)
Time (min)
ΔH (kcal/mol)
Molar Ratio
Model: One Set of Sites
[Cell] (M) = 10.0e-6
[Syr] (M) = 50.0e-6
N (sites) = 0.422 ± 3.4e-3
KD (M) = 2.66e-9 ± 1.44e-9
ΔH (kcal/mol) = -16.5 ± 0.366
Offset (kcal/mol) = -6.19 ± 0.231
ΔG (kcal/mol) = -11.7
-TΔS (kcal/mol) = 4.77

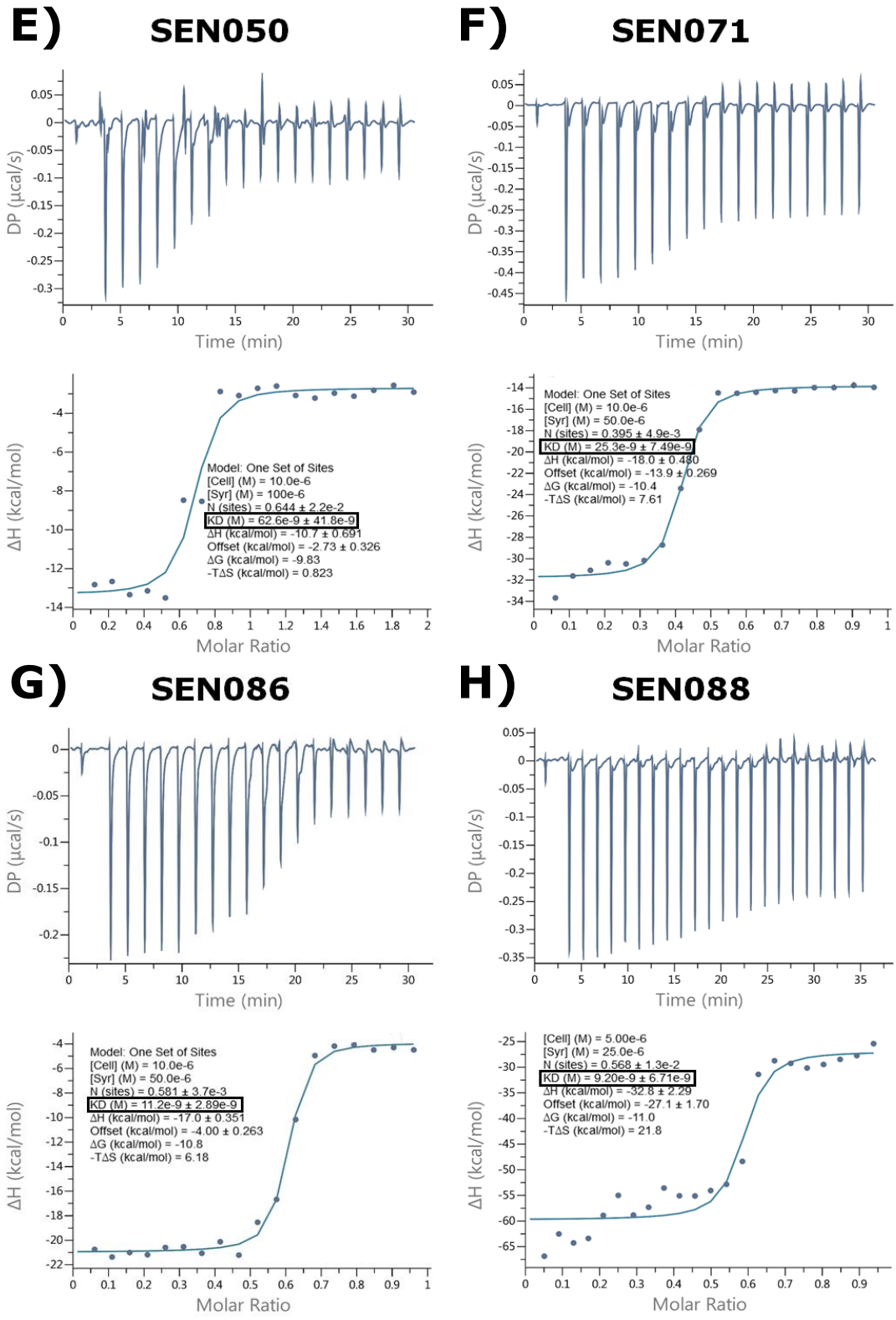

Figure 3.11. ITC binding data of 100 µM A) SEN019, B) SEN032, C) SEN020, D) SEN089, E) SEN050, F) SEN071, G) SEN086 and H) SEN088 into 10 µM $PqsR_{LBD}$. The experiment was performed in triplicates, at a reference power of 5.00 over 19 injections with 2 µL per injection during 4 seconds and a spacing of 90 seconds between injections except for the first one which had 150 seconds of spacing. A black square has been drawn around the $K_{(D)}$ value.

Interestingly, compounds SEN022 and SEN066 showed no binding with $PqsR_{LBD}$ (n=3) (Figure 3.12) although there seems to be a correlation with SEN20, this could be the product of temperature differences between the sample and the ligand. The lack of a clear sigmoidal curve provides evidence of no binding.

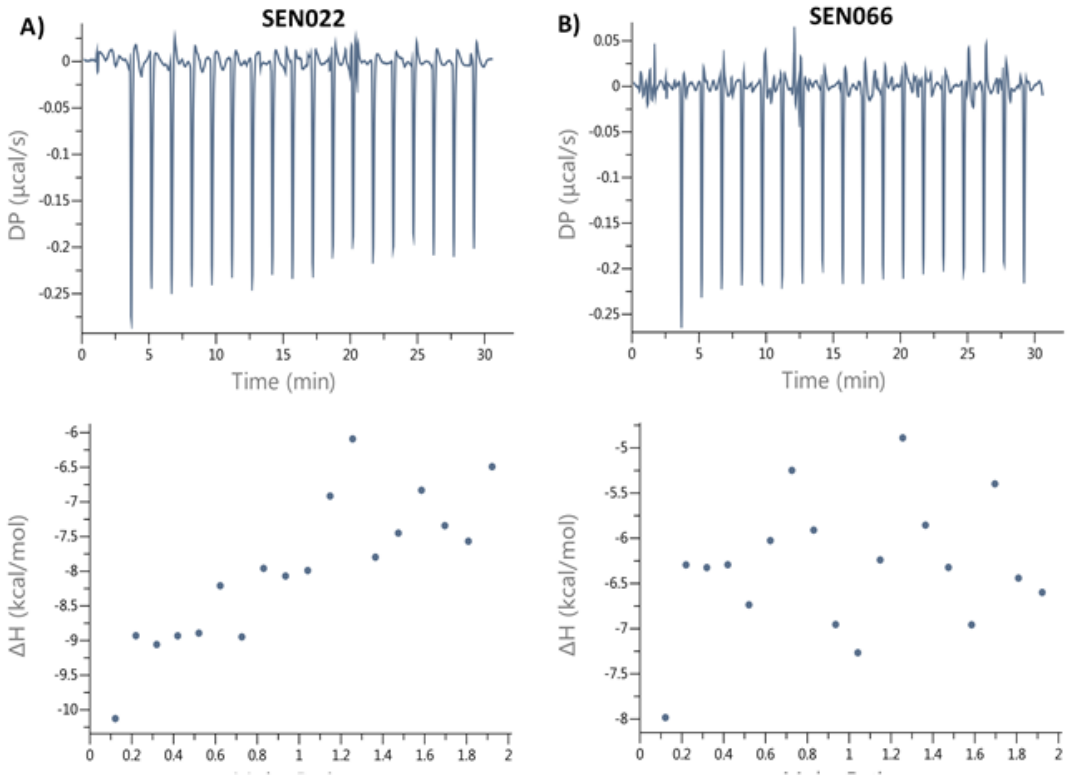

Figure 3.12. ITC binding data of 100 µM A) SEN022 and B) SEN066 into 10 µM $PqsR_{LBD}$. The experiment was performed in triplicates, at a reference power of 5.00 over 19 injections with 2 µL per injection during 4 seconds and a spacing of 90 seconds between injections except for the first one which had 150 seconds of spacing. Data shows no binding.

A blank run was performed with SEN088 and buffer as a control to test that the binding signal was not coming from unspecific interaction. Results showed that there was no binding when there was no protein, providing evidence that the compounds were not interacting with the buffer used (Figure 3.13).

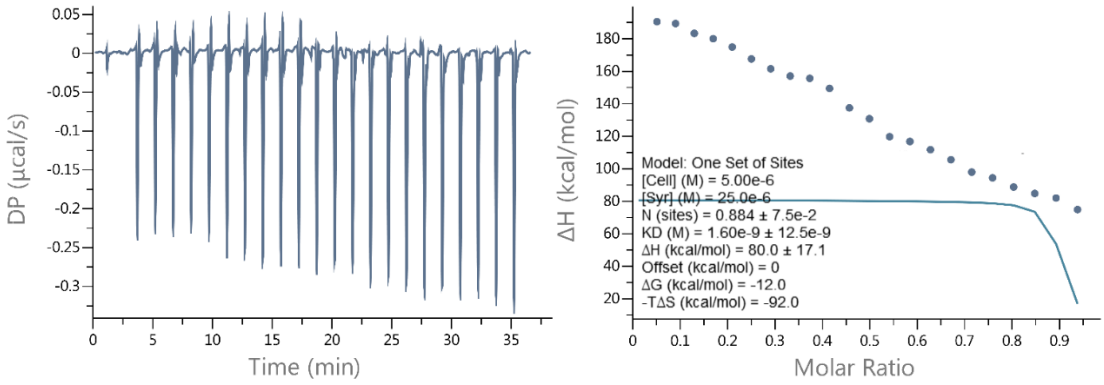

Figure 3.13. ITC negative binding data of a blank, buffer sample with SEN089 added. The experiment was performed in triplicates, at a reference power of 6.00 over 23 injections with 1.6 µL per injection during 4 seconds and a spacing of 90 seconds between injections. Data shows no binding.

3.4. Discussion

Work performed in this chapter was aimed at testing multiple compounds kindly provided by Dr. Fadi Soukarieh.

3.4.1. Selection of active hit compounds

A virtual screening was performed on a library of 83000 compounds, the best scored compounds were then subjected to P*pqsA*-lux bioreporter activity assays that screened a wide range of compounds, 397 of those are shown here, out of which only two, SEN016 and SEN066, were significantly active. Another two compounds were close to the 50% threshold and one of them was further optimised and SEN032 was produced (Figure 3.5). SEN016 was selected for further chemical optimisation and that process generated a good yield of active compounds. SEN016 was chosen over SEN066 because its structure was more novel than SEN066 and therefore represented a new venue to explore (Figure 3.4.8). Nevertheless, the screening of the available library and chemical optimisation of SEN066 continued as a side-project. The activity assays show that most of the compounds from the library had little to no impact over the inhibition, with light signal moving around 100% in most cases, notably, some compounds enhanced the production of light, particularly the library hit NCC-00034813 that had an increment of 58.44% from the control so it could be considered as an active enhancer (Figure 3.5). The reasons why this compound might increase P*pqsA*-lux expression are currently unknown and this venue was

not further pursued, moving on to test the active compounds for IC_{50} instead.

3.4.2. IC_{50} values in PAO1-L WT

The compounds that proved active at 10 μM as well as those found from chemical optimisation of SEN016 were analysed to test the IC_{50} in the model, wild type strain PAO1-L. The assay showed that all compounds tested had very good IC_{50} values, with only the highest around 5 μM and the most active at 67 nM (Figure 3.7). This range is within what has been very recently published by this and other groups, where PqsR antagonists between 5 and 1 μM IC_{50} have been described (Maura and Rahme 2017; Soukarieh *et al.* 2018a), this is notable when compared to the IC_{50} values obtained by Ilangovan *et al.*, 2013 (the best being 4.3 μM). The improvement of the affinity of antagonists in the last five years demonstrates the rapid evolution of these compounds and the range of optimisation that the $PqsR_{LBD}$ target offers. The compounds with IC_{50} values within nanomolar range are very interesting candidates for further stability studies in mammalian backgrounds and retention times in clinically relevant models (Soukarieh *et al.* 2018b).

The IC_{50} values found in Figure 3.7 were used to calculate the working concentration for most phenotypic assays and some biofilm assays performed. The working concentration was established as 3 times the IC_{50} value to ensure that a significant biological response could be observed.

3.4.3. $PqsR_{LBD}$ binding assays

The purification process of the $PqsR_{LBD}$ domain had been previously optimised, the purified fragment was the $PqsR^{94\text{-}309}$, a variation of the published $PqsR^{94\text{-}309}$ but without the 23 amino acid C-terminal tail (Ilangovan *et al.* 2013). The purification conditions do not differ greatly from those of proteins with good solubility and the fact that expression can be performed in standard LB media make it a protein easy to purify and obtain in high quantities.

Purification of the ligand binding domain was highly relevant to this research as it could be used in ITC assays to test if the compounds directly bind to the domain and their affinity (Figure 3.10). The compounds bound

to the ligand with an affinity that strongly correlated with the IC_{50} values (Figure 3.7). This correlation is important to increase the confidence in the IC_{50} data even when obtained from *lux* reporters in planktonic cultures grown in rich media. Nevertheless, the most notable result was the lack of binding by SEN022 and SEN066 (Figure 3.12). These compounds are not among the most active, with IC_{50} values of 5 and 2.6 μM respectively, however, they are from different families than the others, setting them apart from the $PqsR_{LBD}$ binding antagonists. SEN066 presents a structure that is similar to previously published compounds by Starkey *et al.* (2014), interestingly their lead compound M64 binds to the $PqsR_{LBD}$ as shown in their ITC experiments. It is not currently known what the cause of this significant difference is, and if this is due to specificity or size. However, SEN022 and SEN066 can still inhibit P*pqsA*-lux expression. It is hypothesised that this activity could be due to secondary binding to a different site in the PqsR protein. Another possibility is that these compounds bound the PqsE regulator instead of PqsR, which would lower AQ production without completely supressing it (Rampioni *et al.* 2010; Drees and Fetzner 2015). This hypothesis remains untested as the project moved forward with the $PqsR_{LBD}$ binding compounds.

3.4.4. Conclusions and future directions

Initially, two compounds were observed to be active (≥50% inhibition) below 10 μM in the bioreporter activity assays. One of them, SEN016, was further optimised with chemical synthesis to obtain a batch of active compounds with small but significant structural variations. The most active of these compounds were selected to elucidate their IC_{50}. The objective was to obtain a wide range of different compounds that could be tested for further optimisation methods that could carry a significant decrease in the IC_{50} values. Out of all the compounds tested, SEN089 had the lowest IC_{50} and $K_{(D)}$ values by far, with a 47.5 fold decrease compared to the original SEN016, and the other members of its family, SEN088 and SEN086, were the lowest scoring too (Figure 3.7 and Figure 3.10).

The ITC data provided very interesting information, especially regarding SEN022 and SEN066 as they were the only two active compounds that did not bind to the $PqsR_{LBD}$ (Figure 3.12). It would be useful to determine if

these compounds are binding to another part of PqsR or inhibit *pqsA* through PqsE or another unknown mechanism. If they bound to PqsE, the other *pqs* regulator (Déziel *et al.* 2005; Farrow *et al.* 2008; Rampioni *et al.* 2010, 2016), they would be the first PqsE antagonists described to the author's knowledge. The inhibition of PqsE would hinder the production of virulence factors such as pyocyanin, swarming and correct biofilm development, affecting the capability to adapt to the host (Farrow *et al.* 2008; Rampioni *et al.* 2010, 2016). Other mechanisms could include the inhibition of the *las* system (Schertzer, Boulette and Whiteley 2009) or other more general secondary effects that would result in strong *pqsA* inhibition.

The work presented here corresponds to the first results of a large body of research and aims to provide direction and purpose to future experiments regarding these compounds. Furthermore, constant development and optimisation performed by fellow colleagues generates a steady stream of new compounds to test for activity and IC_{50} data.

4. Chapter 4: 4-hydroxy-2-alkylquinoline phenotype regulation and antagonist mediated interference

4.1. Introduction

4.1.1. The *pqs* QS System

The *pqs* operon is the main body of genes responsible for the biosynthesis of 2-alkyl-4-quinolines and the correct functioning of the *pqs* system. The operon consists of genes *pqsABCDE,* supported by *pqsH* and *pqs*L located elsewhere in the chromosome (Figure 4.1). The *pqs* operon is under the transcriptional regulation of PqsR (MvfR). The main signal molecules of the system are 2-heptyl-3,4-dihydroxyquinoline (PQS) and its precursor 4-hydroxy-2-heptylquinoline (HHQ) which has a 100-fold lower potency than PQS (Xiao *et al.* 2006). The operon contains all the necessary genes to produce HHQ, while PqsH catalyses the conversion of HHQ to PQS in an oxygen-dependent manner (Schertzer, Brown and Whiteley 2010). PqsL on the other hand synthetises 4-hydroxy-2-heptylquinoline *N*-oxide (HQNO) which is an inhibitor of quinone-reactive cytochrome b enzymes in various organisms and therefore a potent biocide but with apparently no signalling functions. Metabolically, PqsL directly competes with PqsBC for substrate (2-amynobenzoylacetate, 2-ABA). The mechanisms by which *P. aeruginosa* avoids self-poisoning with HQNO are currently unknown (Voggu *et al.* 2006; Heeb *et al.* 2011).

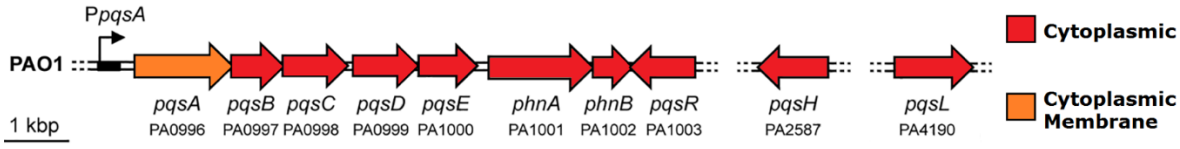

Figure 4.1. Gene organisation of the *pqs* genes in *P. aeruginosa* PAO1. The core of the *pqs* QS biosynthetic system is found in the *pqsABCDE* operon. These genes are required to complete the pathway up to HHQ signal molecule, *pqsH* is required to produce the PQS signal molecule whereas PqsL competes with PqsBC for substrates to produce HQNO instead of HHQ (and PQS). All these genes and the *phnAB* cluster (contributing to anthranilate production) are under direct regulation by PqsR. Modified from (Rampioni *et al.* 2016).

4.1.2. PQS regulation and other phenotypes

PQS and HHQ both can independently bind to PqsR and act as inducers of this transcriptional regulator. These molecules can be considered as autoinducers due to the upregulation of *pqsABCDE* by PqsR. The global (direct and indirect) PqsR regulon includes a wide range of important genes, most of those useful to survive in an environment as hostile as the human host (Maura *et al.* 2016).

Some genes under PQS regulation are strongly related to iron acquisition and oxidative stress and, although they might not be directly harmful to a host they are equally essential for fitness and survival. Additionally, PQS on its own can chelate iron and promote the expression of the iron starvation response *via* PqsR-independent manner (Bredenbruch *et al.* 2006; Diggle *et al.* 2007). The iron-chelation, paired with increased siderophore production, could be a mechanism through which *P. aeruginosa* limits iron availability for potential competitors while making it readily available to membrane bound siderophores (Diggle *et al.* 2007). Recent findings have unravelled the role of PA2374 (TseF) in this process. This protein is secreted by a T6SS and bound to membrane vesicles (MVs) where it interacts with PQS to deliver membrane-bound iron to intracellular siderophore receptors, notably, TseF does not interact with Fe^{2+}/Fe^{3+} directly but exclusively through PQS, making it a *pqs*-dependent pathway (Lin *et al.* 2017).

Furthermore, PQS can have anti- or pro-oxidant properties (Häussler and Becker 2008). Häussler & Becker showed that *pqsL* mutants which overproduce PQS had increased sensitivity towards oxidative stresses deriving from H_2O_2 and ciprofloxacin exposure and therefore increased oxidative damage upon DNA. However, they also observed anti-oxidant activity. Although their tests were performed at relatively high concentrations of PQS that would rarely be found in nature, it evidenced that PQS (in a PqsR-independent manner) leads to a differentation of two subpopulations, one promoting autolysis and the other inducing a physiological change towards a less metabolically active cell type (D'Argenio *et al.* 2002; Häussler and Becker 2008). In addition, PqsR has recently been shown to directly promote the expression of oxidative stress

response genes (Maura *et al.* 2016). It is important to note that the hydrophobicity of PQS ensures that the molecule is embedded in cell membranes and MVs (Mashburn and Whiteley 2005).

4.1.2.1. Pyocyanin

Pyocyanin is a pigmented phenazine and a virulence factor produced in large quantities in hyper-virulent strains. *Pseudomonas* produces pyocyanin to generate reactive oxygen species (ROS) which cause widespread cellular damage in multiple hosts (Lau *et al.* 2004). The synthesis of pyocyanin involves two almost identical operons termed *phzA$_1$B$_1$C$_1$D$_1$E$_1$F$_1$G$_1$* (*phz1*) and *phzA$_2$B$_2$C$_2$D$_2$E$_2$F$_2$G$_2$* (*phz2*), which drive the production of phenazine-1-carboxylic acid (PCA) which is further converted to pyocyanin by two modifying enzymes, PhzM and PhzS, in addition to PhnAB (Mavrodi *et al.* 2001). The expression of these genes is strongly regulated by the *pqs* system, especially *phnAB* which is found immediately after the *pqsABCDE* operon (Cao *et al.* 2001; Lau *et al.* 2004). The *phnAB* operon has been associated with PQS synthesis and its expression pattern follows that of *pqsR* (Cao *et al.* 2001; Gallagher *et al.* 2002).

4.1.2.2. Pyoverdine

Pyoverdine is a key component for iron acquisition in *P. aeruginosa* (Meyer and Abdallah 1978; Poole and McKay 2003). The synthesis of pyoverdine involves many steps often by genes labelled *pvd*- or *pvc*- (Tsuda, Miyazaki and Nakazawa 1995; Stintzi *et al.* 1996, 1999). The expression of pyoverdine biosynthesis genes is modulated by the iron availability in the medium, being highly expressed under low iron conditions. The *las* and *rhl* QS systems have been involved at least partially in pyoverdine biosynthesis gene regulation (Stintzi *et al.* 1998) although more recent findings showed that *lasR* or *rhlR* mutants did not produce significantly different levels of pyoverdine (Feinbaum *et al.* 2012). Another research paper suggested that PqsR can promote pyoverdine production at late stationary phase by directly binding to the *pvd* operon (Maura *et al.* 2016).

Feinbaum *et al.,* observed that a mutation in PA0745 significantly inhibited pyoverdine biosynthesis gene expression and virulence. PA0745 is a putative enoyl-CoA hydratase isomerase that has been linked to synthesis

of *cis*-2-decenoic acid (CDA). CDA is structurally related to the signal molecule known as diffusible signal factor (DSF) and could play an active role in biofilm dispersal and related phenotypes (Feinbaum *et al.* 2012; Amari, Marques and Davies 2013; Rahmani-Badi *et al.* 2015).

4.1.2.3. Elastase

Elastases are one of the main extracellular proteases secreted by *P. aeruginosa.* Encoded by *lasB* (PA3724), this virulence factor has a wide range of substrates and besides causing tissue damage it can also present immune-modulating properties (Casilag *et al.* 2016). This important virulence factor is under regulation of the three known QS systems, mainly by the *las* and *rhl* systems but also *pqs* (McKnight, Iglewski and Pesci 2000; Calfee, Coleman and Pesci 2001), although some evidence suggests that *pqs* regulation is mediated by PqsE in a PQS-independent, *rhlR*-dependent manner (Farrow *et al.* 2008).

4.1.2.4. Lectins

Lectins are also very important virulence factors for *P. aeruginosa* (Bajolet-Laudinat *et al.* 1994). These proteins play a role in surface recognition and attachment but their cytotoxic activity also makes them highly immunogenic (Chemani *et al.* 2009). The *lecA* (PA2570) and *lecB* (PA3361) genes code the two lectins found in the PAO1 genome. LecA binds to galactose and LecB to fucose, their expression is under partial QS regulation by the *las* and/or *rhl* systems (Diggle *et al.* 2003; Schuster and Greenberg 2007) and also by PqsE in a PQS-independent manner (Rampioni *et al.* 2010).

4.1.3. PQS in the biofilm

P. aeruginosa grown in biofilms tend to develop hypermutable phenotypes with mutation frequencies increased ≈100-fold compared to planktonic cells. Increased mutation rates are significantly driven by oxidative stress and accumulation of mutations against genes involved in oxidative damage protection is commonplace, which in turn allows the rapid emergence of highly resistant strains (Driffield *et al.* 2008; Conibear, Collins and Webb 2009; Mandsberg *et al.* 2009). PQS has been linked to the stress response (Bredenbruch *et al.* 2006; Häussler and Becker 2008; Nguyen *et al.* 2011).

However, this relationship is not yet fully understood. An example is the relationship between AQs production and ppGpp levels, studies have been published where ppGpp promotes AQs in some instances (Xu *et al.* 2016) or downregulates them in others (Nguyen *et al.* 2011; Schafhauser *et al.* 2014) although there were significant differences in the experimental design between these studies.

Another important phenotype somewhat under PQS control is autolysis (D'Argenio *et al.* 2002). Regulation of autolysis has a significant impact in biofilm development. Autolysis is necessary for microcolony formation and correct biofilm dispersal (Ma *et al.* 2009). This is at least partially achieved by the release of extracellular DNA (eDNA) in the matrix, which is essential component for the biofilm structure development (Whitchurch *et al.* 2002; Allesen-Holm *et al.* 2006). eDNA provides cell-to-cell links, has been observed to play a role in biofilm migration and creates a cation-poor environment that increases resistance to cationic antimicrobial peptides and amynoglicosides (such as tobramycin) (Allesen-Holm *et al.* 2006; Mulcahy, Charron-Mazenod and Lewenza 2008; Gloag *et al.* 2013; Okshevsky and Meyer 2015).

Another significant mechanism of eDNA release that also has been to some extent related to the *pqs* system are the MVs. *P. aeruginosa* MVs have been known for a long time (Weng, Bayer and London 1975), and these bi-layered vesicles contain a wealth of molecules, including virulence factors, DNA and up to 86% of produced PQS (Weng, Bayer and London 1975; Kadurugamuwa and Beveridge 1995; Mashburn and Whiteley 2005). MVs are produced naturally and under stress conditions in planktonic and especially, biofilm lyfestyles (Kadurugamuwa and Beveridge 1995; Schooling and Beveridge 2006; Turnbull *et al.* 2016). The production of MVs has been thoroughly studied and current evidence suggests that it is closely tied to pyocin synthesis (Toyofuku *et al.* 2014; Turnbull *et al.* 2016). The synthesis of MVs has been sometimes reported to be under PQS regulation (Mashburn-Warren *et al.* 2008) whereas other publications indicate the contrary (Turnbull *et al.* 2016). This apparently contradictory data can be understood if MV production is viewed as a general cell function which is used by the *pqs* system to release signal molecules. The PQS signal

regulates its own packaging and delivery, but there are other MVs not under *pqs* regulation, effectively creating at least two distinct types of MVs which may have different biological functions.

It should however be noted that PQS and the *pqs* system are not the only autolysis-inducing system and independent mechanisms also regulate this poorly understood phenotype (Heurlier *et al.* 2005; Turnbull *et al.* 2016).

4.2. Aims of the chapter

The main objective of this chapter is to analyse in depth the effect that the PqsR antagonists have over *P. aeruginosa* at a phenotypic level through regulation of the 4-hydroxy-2-alkylquinoline production by the *pqs* QS system. At a more specific level, the aims are to:

- Establish the conservation of the *pqs* system in clinical isolates to further support its role as an anti-virulence target.
- Determine the effect of SENBIOTAR compounds in different *P. aeruginosa* strains including clinical isolates.
- Study potential unspecific effects of the compounds not strongly regulated by the *pqs* system.
- Determine the effect that PqsR inhibition has on *P. aeruginosa* physiology.

The coverage of phenotypes and isolates tested varies between compounds because some of them only became readily available at later stages of the project and some assays could not be repeated due to time constraints. An example is SEN089 which was initially hard to synthesise in large quantities hence some assays were performed with the second best antagonist, SEN088. Furthermore, the author would like to acknowledge the collaboration of MSc students Fred Athanasius Dratibi, Jack Finch, Hannah Parrot, Ann Chong, Benjamin Kennedy and Janyce Gomes who worked hard in obtaining the IC_{50}, pyocyanin and AQ assays for clinical isolates with different compounds.

4.3. Results

4.3.1. *P. aeruginosa* clinical isolates, strain characterisation and selection

Due the nature of the SENBIOTAR research programme, the importance of testing the generated PqsR compounds in clinical isolates was paramount to ensure they work beyond standard lab strains. For this reason, a representative clinical isolate from each main *P. aeruginosa* group and subgroups was selected and kindly provided by Prof. Roger Levesque at the University of Laval, Canada.

The chosen strains were selected because they were all cystic fibrosis isolates with high 4-hydroxy-2-alkylquinolines (AQs) production which were coupled with a high pyocyanin output, except for the PAK 1331 strain (Table 4.1). These strains were chosen with a view to see a clearer effect of the impact of the SENBIOTAR PqsR inhibitors on different clinical isolates.

Table 4.1. *Pseudomonas aeruginosa* clinical isolates profile. Strain group shows under which group each isolate falls with a 95% homology (genus threshold). Original and isolate IDs show the first identification code given and the particular one for that single isolate. An overview of the production of *pqs*, *rhl* and *las* quorum sensing molecules is given as well as pyocyanin production calculated from growth in 10 ml of LB. QS autoinducer values are represented in Mean peak area / Internal Standard ratio.

Strain group	Original ID	Isolate ID	Origin	City	HHQ	HQNO	PQS	C4-AHL	OxoC 12-AHL	Pyocyanin production µg/ml
PAO1 95%	279	1451	CF	Quebec	4.71E+07	1.56E+07	1.84E+07	1.39E+05	2.21E+03	14.46
PA14 95%	AL191	1350	CF	Munich	1.52E+07	1.84E+07	3.09E+07	1.11E+06	1.63E+04	8.72
LESB58 95%	LES	LES	CF	Liverpool	5.83E+07	1.72E+07	1.95E+07	3.37E+05	2.79E+04	10.8
PAK 95%	6085	1331	CF	Quebec	1.90E+07	5.78E+06	5.74E+06	2.94E+05	5.61E+03	6.59
PA7 95%	197S020911BSL_PA3	48	CF	Montreal	6.50E+06	2.61E+07	3.90E+07	8.95E+05	7.91E+03	16.84

Further reference to the clinical isolates is done by using the strain group and original ID with the exception of the PA7 isolate which is referred by its isolate ID for simplicity.

4.3.1.1. IC_{50} values for clinical isolates

The P*pqsA*-lux and P*km*-lux bioreporters were built in the clinical isolates to determine the IC_{50} values of several compounds. The assays were

performed in a 96-well polysterene plate grown static with 200 µl of LB for 24 hours at 37° C. Growth was monitored as OD_{600} and light as relative light units (RLUs). The experiments were performed using a TECAN™ plate reader. Several compound concentrations were tested in triplicate with logarithmic concentration increases.

Results show important differences between the tested strains although all IC_{50} values were below the 10 µM activity threshold set for this project and thus all compounds are considered active in all strains (Table 4.2). Unfortunately, data could not be completed because of time constraints as some of these bioreporters were obtained late in the project.

Table 4.2. IC_{50} values for different compounds in clinical isolates.

	***P. aeruginosa* strains**						
PqsR antagonists	**PAO1-L WT**	**PA14 WT**	**PAO1 279**	**PA14 AL191**	**PALESB58 LES**	**PAK 6085**	**PA7 48**
SEN019	1.088	8.246	2.341	1.089	0.846	1.113	1.141
SEN032	2.234	-	1.539	0.711	0.645	2.703	1.13
SEN086	0.2	0.437	0.184	0.544	0.171	0.333	0.312
SEN088	0.129	-	0.147	-	-	-	0.107

4.3.1.2. Genetic conservation of *pqsA* and *pqsR* in clinical isolates

Although all clinical isolates fall under the *P. aeruginosa* species, they present significant differences in the production of their AQs and pyocyanin (Table 4.1). Furthermore, the differences are also very significant when discerning the IC_{50} values for each strain (Table 4.2). For this reason, the sequences of *pqsR* and *pqsA* as well as that of their promoter regions were analysed and compared in order to look for any dissimilarities that could be behind the phenotypic differences.

The genomes (or scaffolds if the fully assembled genome was not available) of the strains used were kindly provided by Prof. Roger Levesque at the University of Laval, Canada. They were searched with BLAST, using sequences from the PAO1-L WT genome as query. The BLAST was performed using the in-house available genome library based in Sequenceserver (Priyam *et al.* 2015). Results were used to download the

aligning fragments which were further analysed in depth using the tools available in Benchling (web-based toolkit for molecular biology).

The fragment analysed for *pqsR* included the whole open reading frame and 747 nucleotides upstream containing the predicted promoter and a LasR/RhlR binding box for a total of 1746 nucleotides. Sequences were organized by decreasing bit score (Table 4.3) and analysed for missense mutations or other significant modifications.

Table 4.3. BLAST query for *pqsR* and 757 bp upstream. Sequenceserver (BLAST 2.2.31+) was used to search against the database of the group of *P. aeruginosa* genomes. 251 hits were found but only those with a significant e-value are shown in the table. The table is modified from the original summary that the server provides.

Strain name	% identity	alignment length	mismatches	gaps	seq. start	seq. end	e-value	bit score
PAO1-L WT	100	1746	0	0	1086097	1087842	0	3149
PAO1 279	99.89	1746	2	0	218107	216362	0	3140
PALESB58 LES	99.77	1747	3	1	4761264	4759518	0	3130
PAK 6085	99.6	1747	6	1	161321	159575	0	3115
PA7 48	99.2	1748	12	2	475860	474113	0	3083
PA14 AL191	98.97	1748	16	2	163938	162191	0	3065

Most of the mismatches or insertions were found beyond the *las*/*rhl* box, between the box and the promoter. Few of them are in the coding region, all but one as silent mutations. PA14 AL191 has the only missense mutation of the alignment (C>T) which changes A288V.

The analysis of the *pqsA* gene along with the 500 nucleotides upstream of the starting codon provided more mismatches within the 2054 nucleotides aligned (Table 4.4).

Table 4.4 BLAST query for *pqsA* and 500 bp upstream. Sequenceserver (BLAST 2.2.31+) was used to blast against the database of the group of *P. aeruginosa* genomes. Six hits were found after limiting the search to show only significant e-value results. Table is modified from the original summary that the server provides.

Strain name	% identity	alignment length	mismatches	gaps	seq. start	seq. end	e-value	bit score
PAO1 WT	100	2054	0	0	1077962	1080015	0	3705
PALESB58 LES	99.81	2054	4	0	4769398	4767345	0	3687
PAK 6085	99.81	2054	4	0	169456	167403	0	3687

PAO1 279	99.76	2054	5	0	226242	224189	0	3681
PA14 AL191	99.17	2054	17	0	172072	170019	0	3627
PA7 48	98.59	2054	29	0	483994	481941	0	3573

The alignment presented more mismatches within the *pqsA* sequence than *pqsR*, albeit most of them were silent. All clinical isolates present a substitution in one of the bases inside the predicted *las*/*rhl* box. In the PAO1-L reference genome the box sequence is 5' CTGTGAGAT**T**TGGGAG 3' while all the clinical isolates present it as 5' CTGTGAGAT**C**TGGGAG 3'.

Some strains present missense mutations. In particular, PALESB58 LES, PA14 AL191 and PA7 48. PALESB58 LES is the closest to the reference sequence with only four mismatches so it is significant that one of those is an amino acid substitution. The mismatch is in the codon 354 changing an R to a C. Arginine (R) is a positively charged amino acid while cysteine (C) is a polar, uncharged amino acid which can create disulphide bonds.

PA14 AL191 and PA7 48 strains are the lowest scoring in the alignment due to a high number of mismatches with the reference sequence. Most occur around the upstream area or are silent mutations, but they also have two substitutions in the PqsA amino acid chain. Both strains share a mutation not found in the others, PA14 AL191 and PA7 48 also have a unique mutation each.

In *pqsA*, the unique substitution in PA14 AL191 is a G285S (G>A). Glycine (G) is the smallest and simplest amino acid, it is non-polar and aliphatic whereas serine (S) is polar (also uncharged). The significant difference in polarity between these two amino acids could have a potential impact on the structure of that region of the protein as well as bonding affinity since this amino acid is located within the predicted AMP-binding synthesis / ligase domain (Winsor *et al.* 2016). According to the NCBI Conserved Domain Database, this position is six aa after two amino acids predicted to be in the active site of PqsA, so if the substitution has an impact on the protein structure, it could be directly affecting its substrate binding affinity.

The unique substitution in PA7 48 *pqsA* comes from one mismatch found in the 345 codon, a G>A substitution that creates A345T. A second mutation is found in this codon but the change (G>T) is in the third nucleotide and silent. Alanine (A) is a simple non-polar aliphatic amino acid while threonine (T) is a polar, uncharged amino acid with hydrophilic properties.

Finally, the shared substitution in *pqsA* between PA14 AL191 and PA7 48 changes R347Q, following a G>A transition. In this position, arginine (R) is substituted by glutamine (Q) which is a polar, uncharged amino acid. The change in the charge of the aa in this position could affect the protein structure at best since the aa position is not particularly close to any binding or active sites.

4.3.2. Impact of PqsR antagonists on *pqsA* expression in *P. aeruginosa*

The use of *lux*-based reporters is a useful tool to measure gene expression. Because of the short half-life of the light signal, transcriptional regulation can be monitored over time by adding the desired promoter region in front of the *lux* operon. The pminiCTX-*lux* vector as backbone (Becher and Schweizer 2000) allows the reporter vector to stably insert as a single copy within a tRNA gene of the genome of *P. aeruginosa* chromosome with little or no physiological consequences. This highly improves the stability of the reporter constructs but also has the added benefit to more closely emulate the expression and regulation of genes within the chromosome.

The *pqsA* gene is the first gene in the *pqs* operon under direct regulation of PqsR (Déziel *et al.* 2004). The promoter area found before this gene (and therefore the main operon promoter) was hence chosen to report any inhibitory activity of PqsR antagonists over the regulator (the cloned region spanned from the -493 to the +21 base pairs). Thus, the pminiCTX::P*pqsA*-lux reporter was inserted in each laboratory strain and clinical isolates.

The first compounds tested from the SEN compound library were SEN019 and SEN032 at 3 µM. Results from the area under the curve of the bioluminescence measured per cell over time show that both compounds had a significant inhibitory effect over the activity of the *pqsA* promoter,

however the strength of the inhibition varied significantly between strains tested (Figure 4.2).

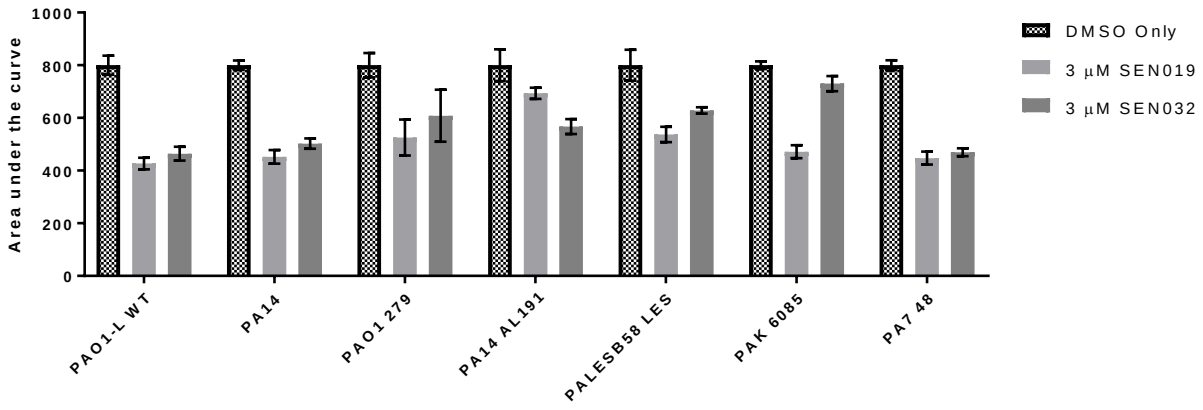

Figure 4.2. Activity of a P*pqsA-lux* transcriptional reporter in different *P. aeruginosa* strains with 3 μM SEN019 or SEN032 PqsR antagonists. Reporters were based on mCTX::P*pqsA*-lux Tet^R construct. Data was compared to the expression of "DMSO Only" group with mCTX::P*pqsA*-lux Tet^R. Constitutive expression was monitored with strains which had the mCTX::Pkm-lux Tet^R construct to ensure there were no biases caused by an effect on the *lux* operon or on bioluminescence per se. The area under the curve was calculated from the curve of all data points up to 8 h. +/- Error bars represent the standard deviation between biological triplicates.

4.3.3. Impact of PqsR antagonists on pyocyanin production in *P. aeruginosa* strains

Pyocyanin is a virulence factor that has been studied in depth due its importance in pseudomonas pathogenicity (Lau *et al.* 2004). As a phenazine, pyocyanin is a pigmented secondary metabolite that generates high quantities of ROS, and PqsR has been shown to have a strong impact on the production of this metabolite (Cao *et al.* 2001).

A comparison between pyocyanin production in the PAO1-L WT strain and the corresponding Δ*pqsA* and Δ*pqsR* isogenic mutants was established as the baseline. Whilst the type strain shows high levels of pyocyanin production this was almost abolished in both mutants (Figure 4.3). This further supports the analysis of pyocyanin production as a way to test the impact of PqsR antagonists in the inhibition of virulence.

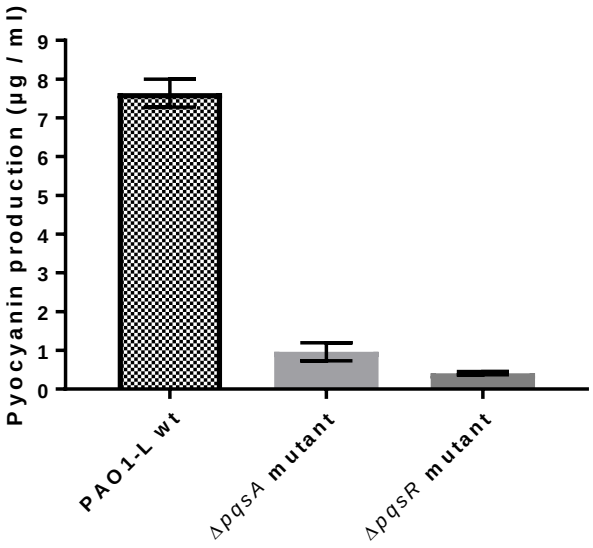

Figure 4.3. Pyocyanin production assay in PAO1-L WT and *pqsA* and *pqsR* mutants. Pyocyanin production was measured from cultures grown in 10 ml LB at 37° C shaking at 200 rpm for 16 hours. Pyocyanin was extracted with chloroform and measured at OD_{520}. +/- Error bars represent the standard deviation of biological triplicates.

A selection of PqsR antagonists was tested in laboratory strains PAO1-L and PA14 using the wild type strains. All compounds were tested at 3 times the IC_{50} values calculated from the mCTX::P*pqsA*-lux reporter in PAO1-L and showed significant inhibition (Figure 4.4), especially in PAO1-L were it correlated well with the potency of the compounds (Figure 3.7).

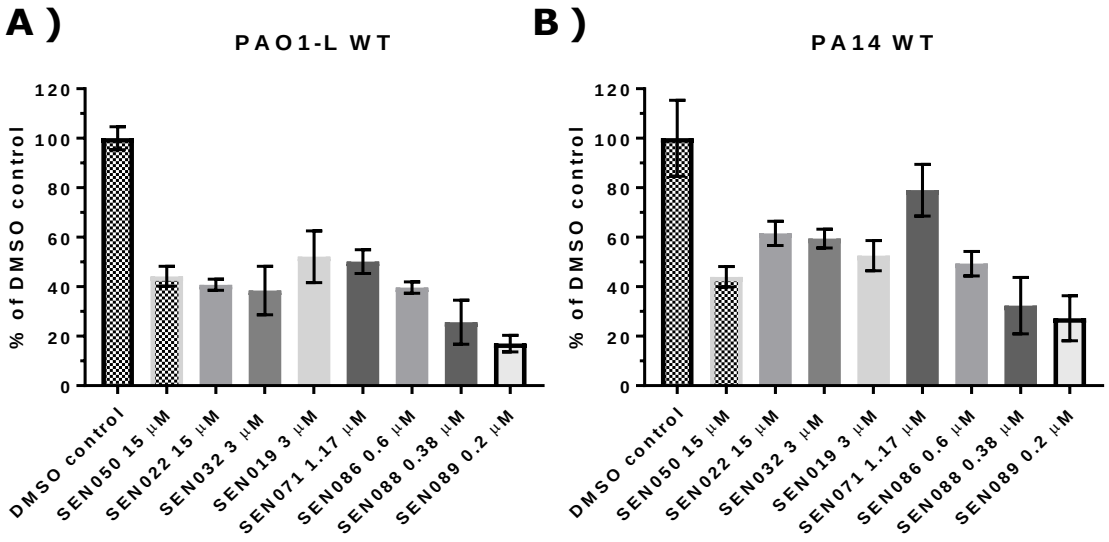

Figure 4.4. Pyocyanin production assay in A) PAO1-L and B) PA14 with different compounds. Pyocyanin production was measured from cultures grown in 10 ml LB at 37° C shaking at 200 rpm for 16 hours. All compounds were added at the beginning of the incubation at 3 times their IC_{50}. All compounds presented significant inhibition of pyocyanin production, especially in PAO1-L WT. *-/ Error bars represent the standard deviation of biological triplicates.

The two compounds that were originally selected (SEN019 and SEN032) together with the lead compound SEN089 and SEN066 belonging to a different compound family, were tested on the clinical isolates and compared to the two laboratory strains using three times the IC_{50} value of PAO1-L WT. Results indicate varying degrees of inhibition by all compounds, highly depending on the strain tested (Figure 4.5).

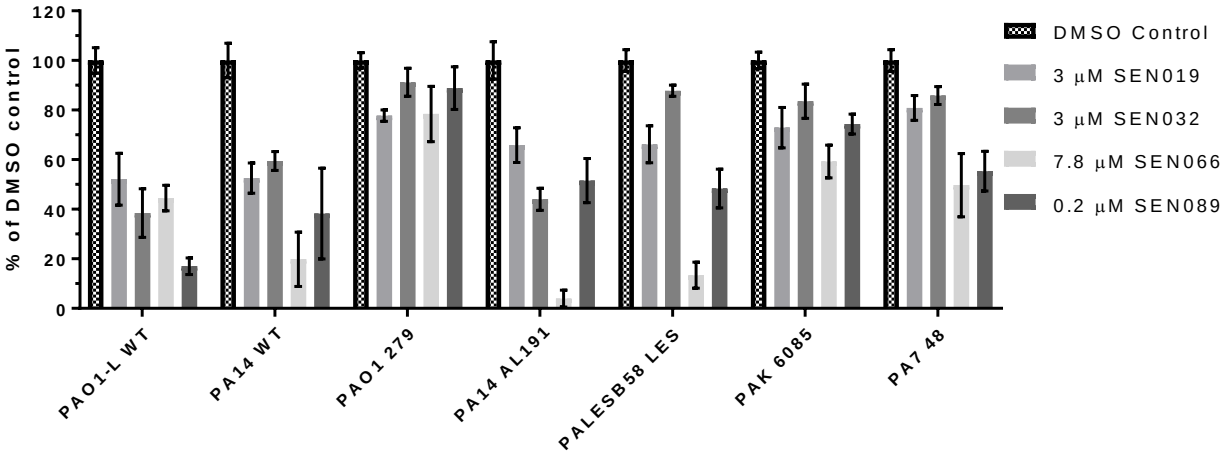

Figure 4.5. Pyocyanin production in laboratory and clinical strains with several PqsR antagonists. The assay was performed from cultures grown in 100 ml glass flasks with 10 ml LB at 37° C shaking at 200 rpm for 16 hours. All compounds were added at the beginning of the incubation at 3 times their IC_{50}. PAO1 279 had the highest production (not shown) and was the most resistant strain. +/- Error bars represent the standard deviation of biological triplicates.

4.3.4. Impact of PqsR antagonists on 2-alkyl-4-quinoline production in different *P. aeruginosa* strains

The most direct way to measure the impact of the PqsR antagonists on the inhibition of the *pqsABCDE* operon is by measuring the levels of the QS signal molecules themselves. Although there are by-products derived from the 2-alkyl-4-quinoline (AQ) biosynthetic pathway (such as HQNO), the main components are the signal molecules HHQ and PQS which in a typical quorum-sensing fashion are upregulated by the effector PqsR (MvfR) (Pesci *et al.* 1999; Déziel *et al.* 2004).

The SEN inhibitors were added to cultures from the different *P. aeruginosa* strains grown in LB at the beginning of growth and after 16 hours of incubation AQs were extracted with solvents and their levels determined by mass spectrometry. A relative quantification was carried out comparing the mean peak area relative to that of an internal standard added at a

known concentration. The data obtained shows that the level of HHQ inhibition is directly correlated with the strength of each tested compound, however this is not as obvious when analysing the impact on PQS levels in part due to the large error bars (Figure 4.6).

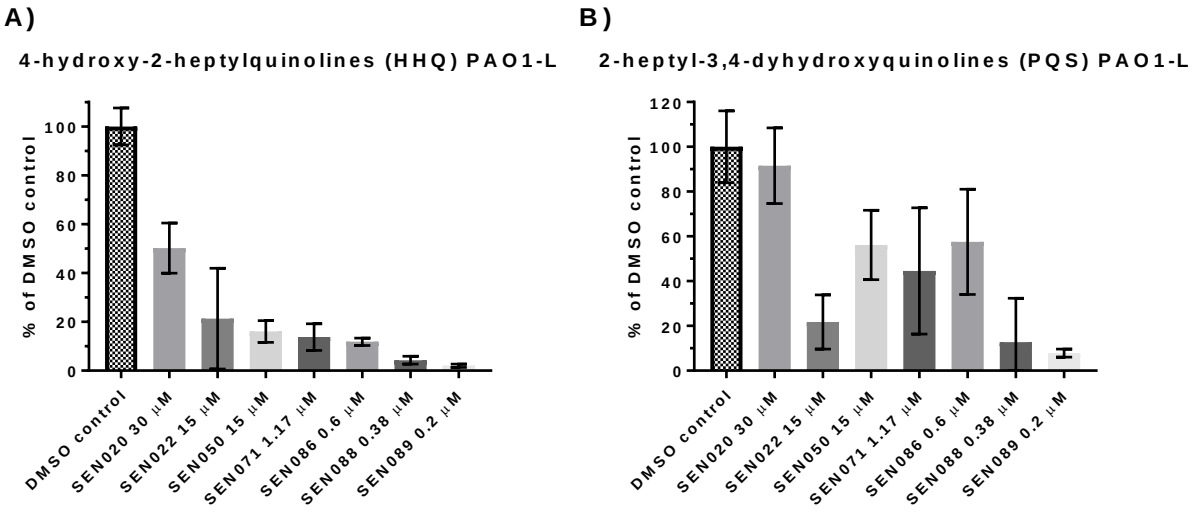

Figure 4.6. Relative quantification of 2-alkyl-4quinolines produced by PAO1-L with different compounds. Bacteria were grown for 16 hours at 37° C shaking in a 50 ml falcon with 5 ml of LB. Quantification was performed by LC-MS/MS analysis of 100 µL of filtered SN extracted thrice with 0.5 ml of acidified ethyl acetate. Deuterated PQS was used as internal standard at 20 nM final concentration. +/- Error bars represent standard deviation between biological triplicates. Data was standardised comparing all samples against the DMSO control group considered to have 100% production.

A further look comparing the best compound SEN089 with the *pqsR* mutant shows that, although significantly higher, the values of HHQ, PQS and even the by-product HQNO are very close to the clean Δ*pqsR* knock-out (Figure 4.7).

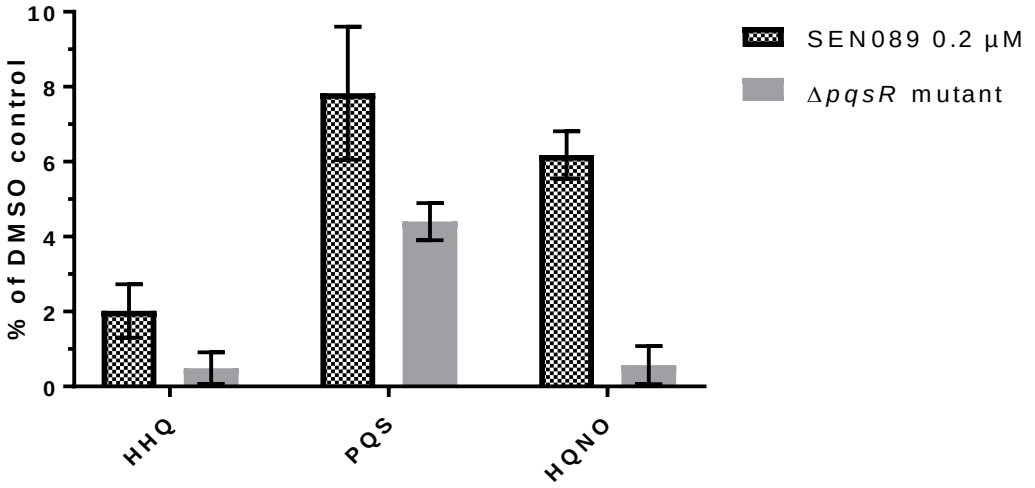

Figure 4.7. Relative quantification of 2-alkyl-4quinolines produced by *P. aeruginosa* with the lead compound SEN089 and pqsR mutant. Bacteria were grown for 16 hours at 37° C shaking in a 50 ml falcon with 5 ml LB. Quantification was performed with LC-MS/MS from 100 µL of filtered SN extracted thrice with 0.5 ml of acidified ethyl acetate. Deuterated PQS was used as internal standard at 20 nM final concentration. Quantification was done for the main molecules HHQ, PQS and the by-product HQNO. +/- Error bars represent the standard deviation between biological replicates. Data was standardised comparing all samples against a DMSO control group considered to have 100% production.

The SEN019, SEN032 and the SEN089 lead compound were tested on the different selected strains in order to see the impact they had on the inhibition of AQ production at three times the IC_{50} value of PAO1-L WT. Results indicate that SEN019 and SEN032 had generally little to no impact over HHQ and PQS expression at 3 µM, SEN089 showed much better inhibition, with the notable exceptions of LES and PAK strains (Figure 4.8). These results are in accordance to what has been observed when performing IC_{50} assays in different strains which showed significantly different values (Table 4.2).

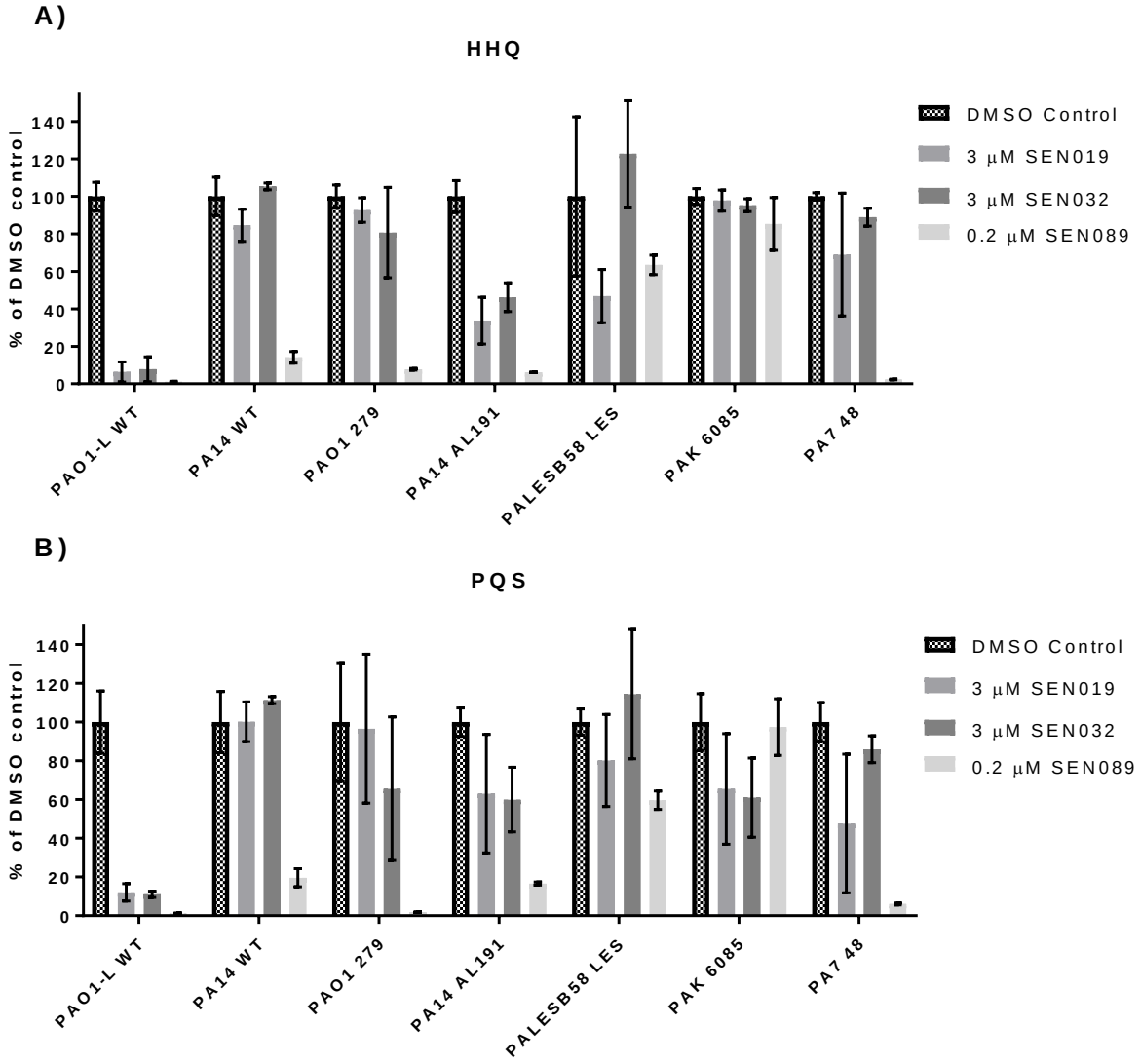

Figure 4.8. Relative quantification of AQs produced by different *P. aeruginosa* strains with different SENBIOTAR PqsR antagonists. Bacteria were grown for 16 hours at 37° C shaking in 50 ml falcons with 5 ml LB. Quantification was performed with LC-MS/MS from 100 µL of filtered SN extracted thrice with 0.5 ml of acidified ethyl acetate. Deuterated PQS was used as internal standard at 20 nM final concentration. **A)** HHQ and **B)** PQS. +/- Error bars represent the standard deviation between biological replicates. Data was standardised comparing all samples against the DMSO control group. PA14, PAO1 279 and PALESB58 LES were particularly resistant to some of the antagonists at those concentrations.

The by-product HQNO, synthesised by PqsL was also significantly affected in all strains tested with the lead compound SEN089 at 200 nM (Figure 4.9). This provides further evidence that the whole PQS pathway is blocked from early steps in all strains, underlining the relevance of PqsR regulation in the pathway.

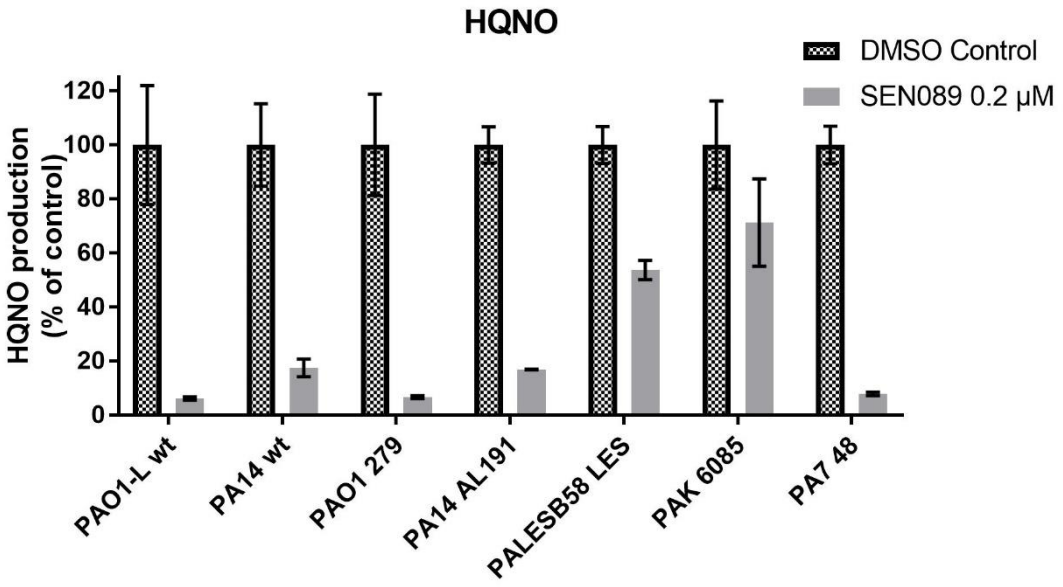

Figure 4.9. Relative quantification of 4-hydroxy-2-heptylquinoline N oxide (HQNO) produced by different *P. aeruginosa* strains with 200 nM SEN089. Bacteria were grown for 16 hours at 37° C shaking in 50 ml falcons with 5 ml LB. Quantification was performed with LC-MS/MS from 100 µL of filtered SN extracted thrice with 0.5 ml of acidified ethyl acetate. D4-PQS was used as internal standard at 20 nM final concentration. +/- Error bars represent the standard deviation of biological replicates. Data was standardised against the DMSO control group. SEN089 was a strong inhibitor of HQNO in all strains except PAK (29% decrease).

4.3.5. Impact of PqsR antagonists on other phenotypes

4.3.5.1. Pyoverdine production

It has been demonstrated that PQS has iron chelating properties (Bredenbruch *et al.* 2006), however, *Pseudomonas spp.* employs pyoverdine as its main siderophore to obtain iron as well as being a very relevant virulence factor involved in host colonisation mechanisms (Meyer and Abdallah 1978; Poole and McKay 2003; Visca, Imperi and Lamont 2007). Pyoverdine can be easily measured by an absorbance reading of filtered supernatant at OD_{405}. In *P. aeruginosa* this siderophore is not under regulation of the *pqs* system, however, it was interesting to see if the antagonists had any impact over pyoverdine production through the potential alteration of free iron availability upon inhibition of PQS biosynthesis or if the compounds had unspecific activity. Results show that generally, there are no major significant differences in the production of pyoverdine in presence of SEN compounds, with the exception of SEN032

in PA14 WT (Figure 4.10). The compounds tested do not have secondary activity that impacts pyoverdine production.

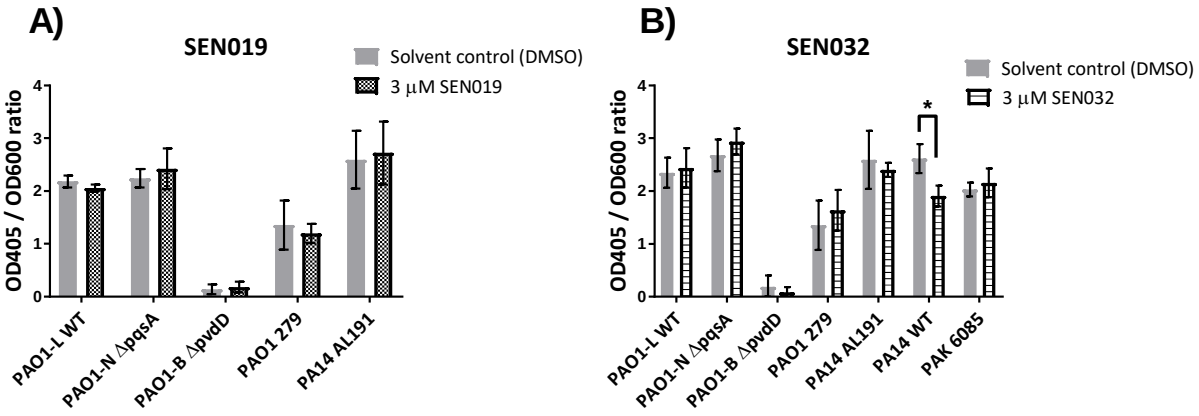

Figure 4.10. Pyoverdine production of *P. aeruginosa* in LB. Cultures were grown at 37° C shaking for 16 hours in 100 ml glass flasks with 10 ml of casamino acids media (CAA) with 0.18 % DMSO, A) 3 μM SEN019 or B) 3 μM SEN032. Pyoverdine was read by measuring the absorbance of filtered (0.22 μm) SNs at OD_{405}. The Δ*pvdD* mutant was used as a negative control. +/- Error bars represent the standard deviation of technical triplicates of biological triplicates. T-tests were performed between each pair, * represents *p* value < 0.05.

4.3.5.2. Elastase production

Elastase is a common virulence factor which production is under positive regulation by quorum sensing systems, including *pqs* (Calfee, Coleman and Pesci 2001; Diggle *et al.* 2007). An elastin-Congo red assay was performed to test if inhibition of the *pqs* system had a significant impact on elastase activity. Interestingly, under the conditions tested, addition of SEN019 and SEN032 did not show a significant difference on elastase production in either the WT or the *pqsA* mutant. Furthermore, there was hardly any difference between the WT strain and the *pqsA* mutant in the DMSO control strains (Figure 4.11). This could be happening because of the *las* and *rhl* systems still controlling *lasB* expression regardless of the *pqs* system deficiency. This figure also shows the levels of elastase in a *lasR* mutant as a reference.

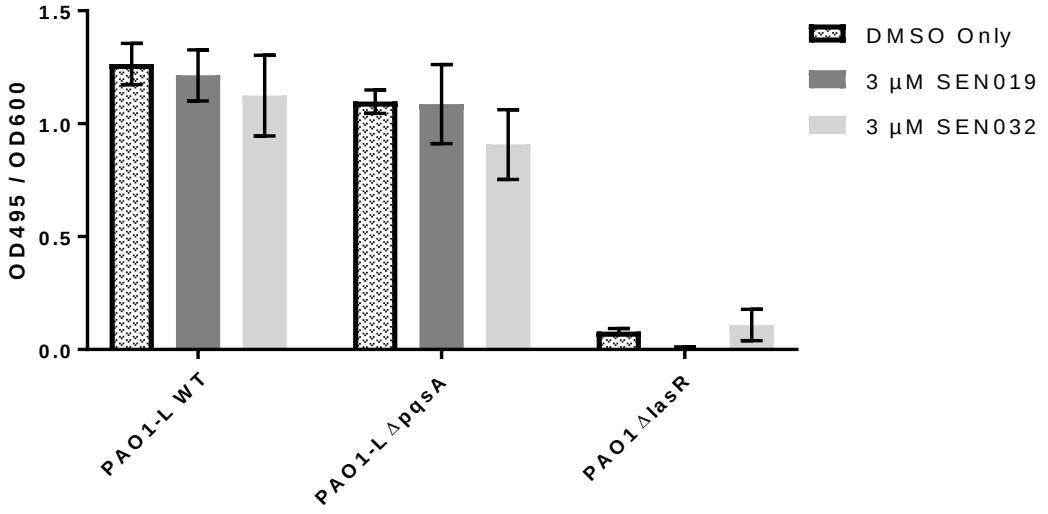

Figure 4.11. Elastase activity assay in *P. aeruginosa*. Elastase production was measured from cultures grown in 100 ml glass flasks with 10 ml LB at 37° C shaking at 200 rpm for 16 to 18 hours in presence of 0.28 % DMSO or 3 µM SEN019. Elastase activity was measured after incubating the filtered supernatant for 4 hours with Elastin-Congo red and measuring the absorbance at OD_{495}. The PAO1-B Δ*lasR* mutant is used as an elastase negative control since elastase production is strongly regulated by the *las* system. +/- Error bars represent standard deviation from biological triplicates.

4.3.5.3. Protease production

The elastin-Congo red assay showed no significant difference on elastase activity when the antagonists were added (Figure 4.11). In order to see if there were any other proteases affected by the compounds, a more general assay was performed. For this reason, an azocasein degradation assay was chosen as it is a general protease substrate. Similarly to the elastase assay, no differences could be observed among the groups even with a significant increase in the concentration of SEN019 used (Figure 4.12).

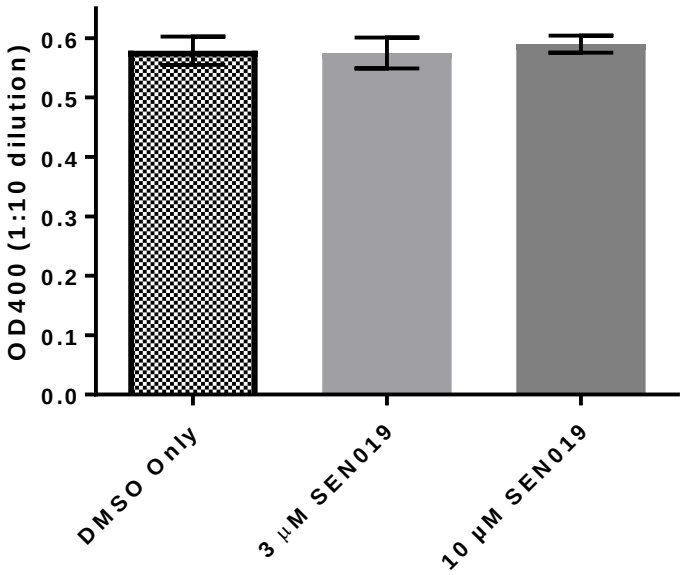

Figure 4.12. Azocasein assay for protease activity of PAO1-L. The assay was performed after overnight growth (approx. 16 hours) in 100 ml glass flasks with 10 ml LB at 37°C and 200 rpm. +/- Error bars indicate standard deviation from biological replicates.

4.3.5.4. Lectin expression

LecA is an important virulence factor produced by *P. aeruginosa*, with high affinity to hydrophobic galactose residues. Its presence is necessary to establish and maintain biofilm architecture and it has been observed to cause significant damage to lung epithelial cells (Bajolet-Laudinat *et al.* 1994; Diggle *et al.* 2006; Chemani *et al.* 2009). Several regulatory factors control the expression of *lecA* including the *pqs* system (Diggle *et al.* 2003). For this reason, mCTX::P*lecA*-*lux* transcriptional reporters were built in PAO1-L in order to test if the inhibition of the system by the SEN088 antagonist had any significant impact over *lecA* expression.

The activity of the *lecA* promoter was measured to determine the impact of SEN089 on it. Bioreporter data was presented as area under the curve from the relative light units obtained over 24 hours. The results indicate that there was a significant but very light repression in the transcription of this gene in both PAO1-L and PA14 (Figure 4.13). However, a similar inhibition was observed in a Δ*pqsA* mutant, suggesting that the small but significant impact of SEN088 over *lecA* expression may not be related to the inhibition of *pqsA* expression.

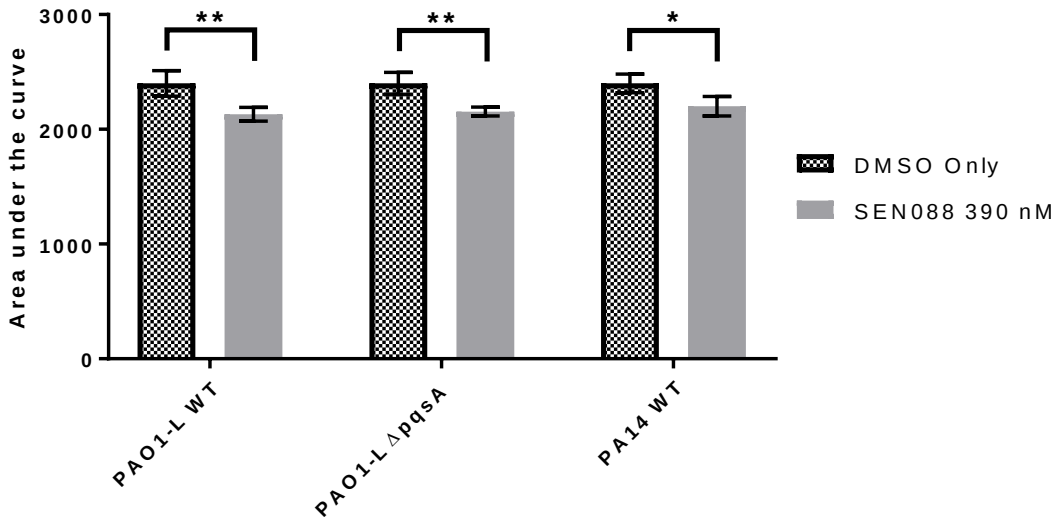

Figure 4.13. Activity of the *lecA* promoter in different strains of *P. aeruginosa*. Reporters are based on mCTX::P*lecA*-lux Tet^R construct. Data was normalised by comparing the compounds to the expression of "DMSO Only" group with mCTX::P*lecA*-lux Tet^R. Constitutive expression was monitored with strains which had the mCTX::P*km*-lux Tet^R construct to ensure there were no biases caused by an effect on the lux operon *per se*. The area under the curve value was extracted from the curve of all data points up to 24 h. +/- Error bars represent the standard deviation between biological triplicates. A series of t-tests were performed to determine statistical significance in each group (*) represents *p* value < 0.05 and (**) *p* value < 0.01

4.3.6. Impact of PqsR inhibitors on cell lysis

4.3.6.1. Impact of PqsR inhibitors on *hol and lys* expression

The *pqs* system of *P. aeruginosa* regulates the release of eDNA in biofilms through a poorly defined system of autolysis spatially defined within the biofilm (D'Argenio *et al.* 2002; Allesen-Holm *et al.* 2006; Yang *et al.* 2009). One of the eDNA release mechanisms through cell lysis is mediated by the activation of the cryptic prophage genes PA0614 (*hol*) and PA0629 (*lys*) (Turnbull *et al.* 2016). Lux-based transcriptional reporters for these genes were constructed and introduced in a wild type and Δ*pqsR* genetic backgrounds to see if the antagonists had a significant impact in their expression through PqsR inhibition.

Results show that both genes have an increased expression in the *pqsR* mutant, which is closely correlated to the significant increase observed when the wild type is treated with SEN089 (Figure 4.14). This data is in accordance to that published by Turnbull *et al.*, 2016 and suggests that

PqsR has a small but significant role in the regulation of *hol* and *lys* expression.

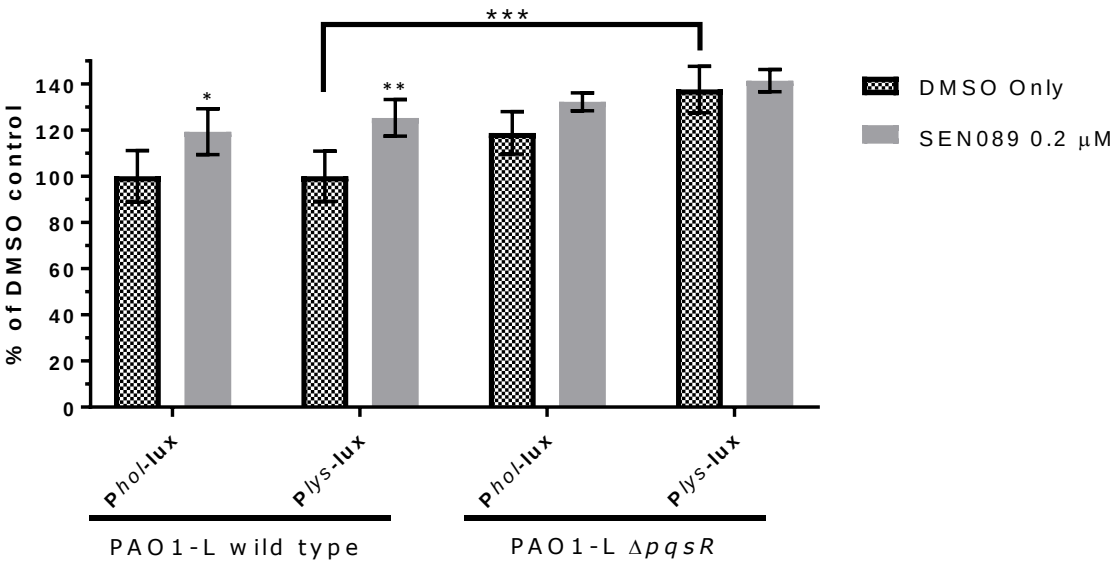

Figure 4.14. Expression of *hol* (PA0614) and *lys* (PA0629) genes in presence of 0.2 µM SEN089 in PAO1-L WT and ΔpqsR. Bacteria were grown static in a 96-well polystyrene plate in 200 µL of LB. A TECAN™ plate reader was used to measure luminescence. The area under the curve was calculated from the RLUs / OD_{600} values for each sample and normalised against the control sample (DMSO only WT P*hol* or P*lys*). +/- Error bars represent standard deviation from biological triplicates. (*) indicates a p value < 0.05, (**) indicates $p < 0.01$ and (***) indicates $p < 0.005$ from a two way ANOVA test.

4.3.6.2. Cell lysis phenotype

Colony biofilms grown on Congo red plates are a straight forward method to observe any potential phenotypic differences in large microcolonies which usually reach very high cell density. Under these conditions, *P. aeruginosa* Δ*pqsL* colony biofilms form lytic plaques, a phenotype that can be reversed by the suppression of PQS levels (D'Argenio *et al.* 2002). The compound SEN089 was used to test if the mutant phenotype could be reversed. Results evidenced that small concentrations of PqsR antagonist SEN089 have a very significant impact on the Δ*pqsL* phenotype and the mutant is complemented fully at 1 µM (Figure 4.15). PAO1-L WT has no lytic plaques because the HHQ and PQS concentrations are lower than those found in a Δ*pqsL* mutant and PAO1-L Δ*pqsR* has the whole PQS pathway inactivated so it has negligible AQ levels. The disappearance of these lytic plaques suggests that the antagonist is effectively blocking the activation of a prophage which could have implications in biofilm development (eDNA

release) and dispersal. Moreover, the classic Congo-red colouring was significantly lighter around the Δ*pqsR* colonies.

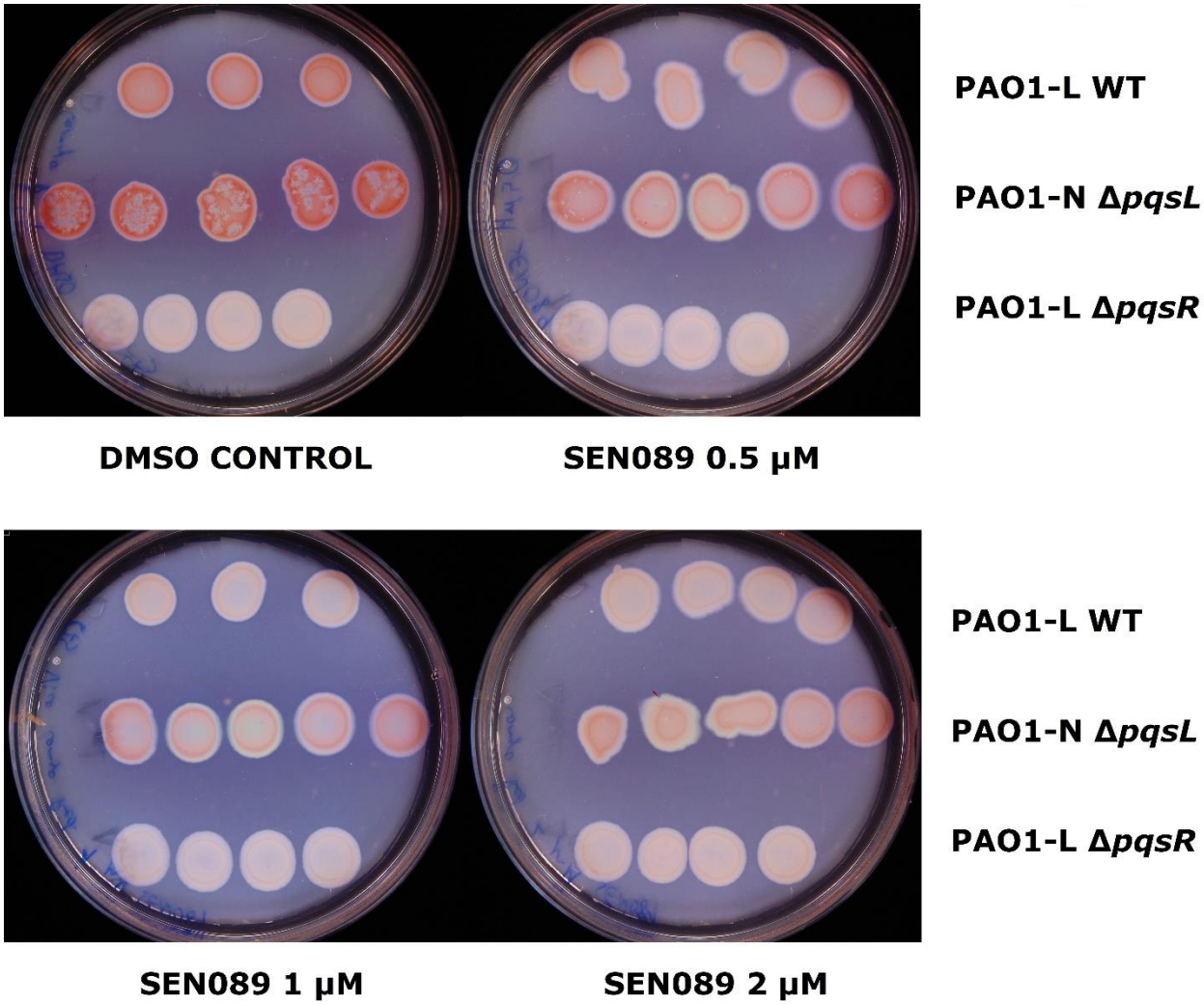

Figure 4.15. Cell lysis phenotype in pseudomonas colony biofilms grown in Congo-red plates. 10 µl of overnight cultures were dropped in Congo-red agar plates and grown at 37°C for 24 hours before taking pictures of the plates. The top row of colonies are PAO1-L WT, middle row are the PAO1-N Δ*pqsL* and bottom row are PAO1-L Δ*pqsR*. A few lytic plaques can still be observed in some of the *pqsL* mutant colonies at 0.5 µM, none were observable at 1 or 2 µM.

4.4. Discussion

In this chapter, several compounds were tested in different *P. aeruginosa* strains in order to determine their impact over a wide range of phenotypes, under direct regulation of the *pqs* system or otherwise, and to compare the efficiency of the PqsR antagonist compounds when used at a fixed concentration in different genomic backgrounds, with a special emphasis made on the lead compound SEN089.

4.4.1. Selection of clinical isolates and compounds

Laboratory strains can provide a great deal of information but can undergo significant genetic changes to adapt to the lifestyle outside the host environment and hence there is a risk for new drugs working on these strains being ineffective on clinical isolates. Therefore, representative clinical isolates from the five different *P. aeruginosa* groups and subgroups were selected to test the SENBIOTAR PqsR antagonists in a range of assays. The chosen isolates had high production levels of AQs and significant levels of pyocyanin. Most came from different regions and all were isolated from cystic fibrosis patients (Table 4.1). Work with these isolates provided key evidence that there are huge differences in the efficacy of a given compound depending on the strain tested.

SEN089, SEN019 and SEN032 were the three compounds tested in all isolates available, with the inclusion of SEN066 in the pyocyanin production assays (Figure 4.5). The PAO1-L IC_{50} of SEN089 is 67 nM, the one for SEN019 is 1.088 μM, for SEN032 is 2.234 μM and SEN066 has a value of 2.583 μM (Figure 3.7). While SEN089 is the most active compound currently available in the SENBIOTAR programme, there are several other compounds that could have been used within the nanomolar range, yet SEN019 and SEN032 were the two most commonly used. This raises the question over the reasons for the choice of compounds. SEN019 and SEN032 were the first active compounds available to work with and therefore a wide array of assays was performed using them while other compounds were developed, optimised and tested for activity. Moreover, these compounds also belong to different chemical families. Testing a compound from each main group provides the added information of potential inter-group disparities.

4.4.2. IC_{50} values of different strains

The clinical relevance of the PAO1-L laboratory strain is limited (Stover *et al.* 2000), furthermore, it has been shown that several *P. aeruginosa* strains present very significant phenotypic differences (Kukavica-Ibrulj *et al.* 2008). For this reason, the IC_{50} for several compounds was tested in other strains. PA14 WT showed the largest differences, although it also had the

most incomplete dataset (Table 4.2). PAK had values always above those of PAO1-L WT whereas PALESB58 had consistently lower IC_{50} values. Notably, PA14 AL191, PAO1 279 and PA7 48 had some IC_{50} values above and below PAO1-L WT levels (Table 4.2). It is worth pointing out that the SEN08- family did not show a consistent trend as SEN086 had higher IC_{50} than PAO1-L WT in PA7 48 but lower in PAO1 279 with inverted results for SEN088, this suggests that the defining characteristics of this family of compounds are less relevant for activity than the individual differences between compounds.

The pqsA and *pqsR* analysis did not provide any obvious explanation for these differences (below). Moreover, the IC_{50} values obtained correlated rather poorly with pyocyanin and even AQ quantitation assays (Table 4.2 compared to Figure 4.2, Figure 4.5 and Figure 4.8). This difference was particularly puzzling with the *pqsA*-lux reporters themselves as they were the same used for the IC_{50} values and highlight a potential technical difference between assays. PA14 AL191 and PALESB58 LES showed the most significant differences, with the IC_{50} values of SEN019 and SEN032 equal or lower than PAO1-L WT, but showing strong resilience against the compounds in pyocyanin and AQ production. The reasons behind this effect are currently unknown and if technical variability is ruled out it could be hinting at strong differences on the role of PqsR regulation between strains.

Finally, it is worth pointing out that these assays were always carried in LB media, this rich media highly impacts the phenotype of bacteria growing in it and the results could have been different if minimal media was used, considering that the relevance of QS systems in certain situations can be highly dependent on the nutrients available (Cezairliyan and Ausubel 2017; Meylan *et al.* 2017). It would be very interesting to obtain the IC_{50} values for SEN089 (which showed much better activity in the other isolates particularly inhibiting AQ production) and to perform some of the phenotypic assays using the corresponding IC_{50}s for each strain to see if results correlate.

4.4.3. Bioinformatic analysis of *pqsR* and *pqsA* in selected *P. aeruginosa* strains

As differences were expected between strains, the sequences for *pqsR* (PA1003) and *pqsA* (PA0996) were analysed *in silico* (Figure 7.1 and Figure 7.2). This included a fraction of their upstream region to include the promoter area. The analysis tried to identify any genotypic cues that could be related to phenotypic differences. The *in silico* analysis can provide useful information when developing and optimising PQS antagonists as it can potentially pin point the specific reasons why there are differences in AQ production, overall virulence and sensitivity to antagonists.

The *pqsR* alignment showed that the regulator was well conserved among strains (Table 4.3), most of the mismatches or insertions were found far in the upstream region after an existing *las/rhl* box but before the defined promoter region. Most mismatches in the gene were silent mutations. The only missense mutation of this alignment could be found in PA14 AL191, a G>A which changes A288V. A brief look at the amino acid sequence shows that the 288 amino acid (aa) is not part of the active site pocket (Figure 4.16) and furthermore, alanine and valine are very similar non-polar amino acids so it is highly unlikely that this change has any significant impact on the phenotype of PA14 AL191. The degree of conservation of PqsR among this phylogenetically distinct strains further highlights the relevance of the regulator for the physiology of PA.

The analysis of the *pqsA* open reading frame along with the 500 nucleotides upstream provided more mismatches within the 2054 nucleotides aligned (Table 4.4). Most of them are silent but there is a significant amount of missense substitutions too.

One of the most notable changes is a substitution present in all isolates compared to the PAO1-L reference sequence in one of the nucleotides inside the predicted *las*/*rhl* box. This probably has no relevance beyond the fact that the sequence from the PAO1-L should not be taken as consensus, however, the small number of sequences compared makes it not possible to confirm it. This particular venue was not further explored as it moved away from the main aims of the project.

The most dissimilar *pqsA* sequence was from PALESB58 with four mismatches, one of them was an amino acid substitution from C>T leading to R354C (Table 4.4). The aa change is significant because cysteine (C) is a polar, uncharged amino acid which can create disulphide bonds. According to the NCBI conserved domains database (CDD), the 354 residue is right before a dimer interphase binding site (Figure 4.16). PqsA has been previously reported as a monomer (Coleman *et al.* 2008), however, their study was performed using only the type strain PAO1. The presence of a cysteine in that region could create a strong disulphide bond which could promote the formation of a dimeric PqsA. However, this mismatch is not found in any other strains. Although it is unlikely that a full conformational change is found specifically in this strain, it is worth pointing out that PALESB58 LES is described as the strongest producer of HHQ (Table 4.1) and its production is among the most resistant to SEN032 and the lead compound SEN089 (Figure 4.8). Nevertheless, phenotypic data collected here does not provide any significant evidence that this substitution has a major impact and the structure of PqsA from LES should be analysed individually.

PA14 AL191 and PA7 are the only other two strains with missense mutations in *pqsA*. They share a mutation not found in other strains and have another unique for each.

The unique substitution within *pqsA* in PA14 AL191 is a G>A, this changes G285S (Table 4.4). Glycine (G) and serine (S) are uncharged but S is also polar which could help maintain solubility and protein stability. The significant difference in polarity between these two amino acids could also modify the structure of that region and bonding affinity since this amino acid is located within the predicted AMP-binding synthesis / ligase domain (Winsor *et al.* 2016) (Figure 4.16). This strain is the only one who appears to be more sensitive to SEN032 in the P*pqsA*-lux reporter (Figure 4.2), and this is backed by the pyocyanin production assay (Figure 4.5), although there are very few other significant phenotypic differences that suggest this mutation is relevant.

The substitution in *pqsA* that is unique to PA7 48 is A345T. Alanine (A) is a simple non-polar aliphatic amino acid while threonine (T) is a polar, uncharged amino acid. The position in the aa chain is relatively isolated from active, binding, or other known sites (Figure 4.16). PA7 48 is the lowest producer of HHQ of the clinical isolates although it has the highest overall pyocyanin production (Table 4.1). Nevertheless, no significant phenotypes that could be somehow linked to the mutations found here could be observed. The differences between AQ levels and pyocyanin could be caused by different expression levels of PqsE (Farrow *et al.* 2008; Rampioni *et al.* 2010, 2016).

PA14 AL191 and PA7 48 share a common missense G>A substitution which leads to R347Q. In this position, arginine (R) is substituted by glutamine (Q). The change in the aa charge in this position does not seem to have any significant impact over the tested phenotypes.

PAK and PAO1 279 do not have any missense mutations in the analysed sequences, however, they both have a robust AQ production (Figure 4.8) and the HQNO production of PAK is the least inhibited of the group (Figure 4.9). Furthermore, both strains (especially PAO1 279) also have a robust pyocyanin production (Figure 4.5). Hence, the analysis of *pqsA* and *pqsR* does not provide any clues regarding the particular characteristics of these isolates.

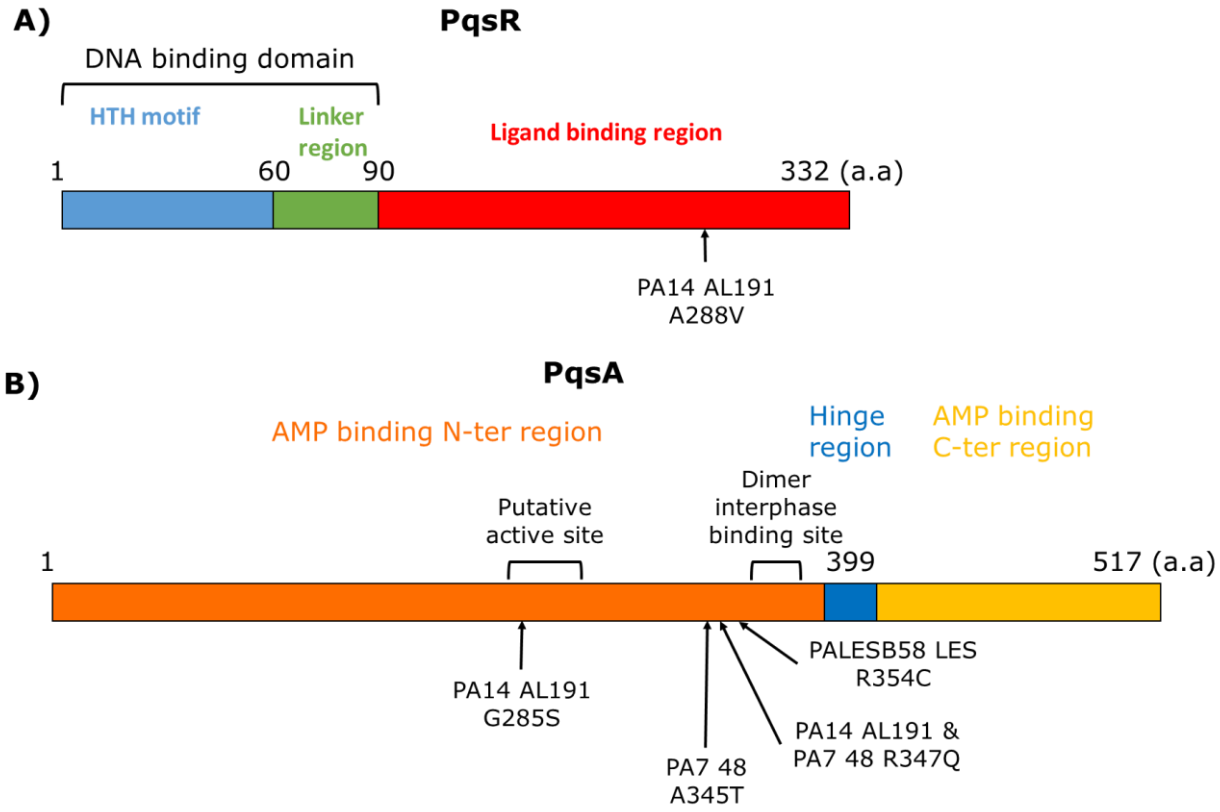

Figure 4.16. Linear diagram of A) PqsA and B) PqsR with missense mutations highlighted. General regions are colour coded for clarity. The numbers indicate the amino acid (a. a.), only two regions of interest are shown in the PqsA diagram but others exist and can be found looking for the conserved domains of the amino acid sequence (aa sequence analysed in the CDD domain of the NCBI). The arrows indicate the strain, exact position and aa change of each missense mutation found.

This suggests that any genotypic differences accounting for the phenotypic variation between strains do not appear to be found in the *pqsA* and *pqsR* sequences analysed, they could be located elsewhere or not be transcriptomic entirely, being of proteomic nature. It must be taken into account that the rest of the PQS operon as well as *pqsH* (PA2587) was not aligned and analysed for further mismatches and substitutions. This could shed more light or provide evidence over differences on HHQ and PQS expression. Furthermore, the comparison was limited to the sequences of the available strains, a larger set could provide more information regarding the conservation of some changes such as that seen in the *pqsA las/rhl* box. Any potential differences in the protein structure could be determined by protein purification and non-denaturing gel analysis.

4.4.4. SEN compounds impact over major *pqs* system indicators – Pyocyanin and 2-Alkyl-4-quinoline production

The strong regulation by PqsR makes pyocyanin an ideal candidate to monitor PqsR inhibition (Pesci *et al.* 1999). The assay to determine the levels of this virulence factor is robust and relatively simple to perform. A large pool of active compounds was tested on laboratory strains PAO1-L and PA14 and results show a very good correlation between inhibition and compound potency, especially in PAO1-L (Figure 4.4), evidencing the strong regulation of pyocyanin by PqsR.

Differences in efficacy with PA14 WT can be attributed to different IC_{50} values for each strain. These differences became much more obvious when some compounds were tested in clinical isolates where SEN089 was not always the most potent inhibitor even when the IC_{50} in PAO1-L is a whole order of magnitude lower than the other compounds (Figure 4.5). Interestingly, SEN066 performed consistently well over all the strains tested at the chosen concentration. SEN066 was one of the last compounds to be developed and a member of a whole different group. The IC_{50} is much higher than the lead compound but the impact on pyocyanin production makes it an interesting compound to further study and develop. Another thing to note is the resilience of pyocyanin production by PAO1 279 (Figure 4.5), this clinical isolate was among the strongest producers of this virulence factor (Table 4.1) and it is possible that there are significant differences in the regulation of *phz*- or *phnAB* genes, involved in pyocyanin production, in this isolate.

As good as pyocyanin is for an indicator, the measurement of AQs as the signals made by PqsABCDE is the most direct quantification of the activity of the *pqs* system itself as well as the impact of PqsR antagonists. Nevertheless, the analysis comes with some limitations when compared to pyocyanin. The extractions are a simple method but have much higher inherent variability and require the use of an LC-MS/MS system which can be more time consuming (Soukarieh *et al.* 2018a). Due the importance of the method, a large batch of compounds was tested in PAO1-L in a similar

fashion than the pyocyanin assays. However, they were not tested in PA14 and SEN066 was not analysed for its impact in clinical isolates.

The correlation between the IC_{50} of the compounds and the HHQ quantification was much better than that of PQS, the latter showing much higher variability (Figure 4.6). PQS synthesis is catalysed by PqsH (PA2587) as the last step in the PQS production pathway (Schertzer, Brown and Whiteley 2010), This step is under LasR regulation rather than PqsR (Gallagher *et al.* 2002). Furthermore, the characteristics of PQS make it bind strongly to the HPLC column in the LC-MS/MS system, increasing the variability of the quantitation assays (N. Halliday personal communication).

The AQ production of a wild type PAO1-L grown with 3 times the IC_{50} of lead compound SEN089 was compared with a clean *pqsR* knock-out. While the inhibition does not reach that of the mutant in terms of HHQ, PQS and HQNO levels, it is very close to it (Figure 4.7). The similarities show how strong is the PqsR inhibition with the lead when is used even at the low concentrations (200 nM). The fact that the by-product HQNO is also affected shows that the whole pathway is highly inhibited from the early steps. The effectivity at this concentration highlights the advancements in antagonist development, as until recently, publications always reported the use of high concentrations of inhibitors (Klein *et al.* 2012; Ilangovan *et al.* 2013; Zender *et al.* 2013; Starkey *et al.* 2014; Thomann *et al.* 2016) with a notable exception from Lu *et al.* 2012 (albeit only in *E. coli*). Only in the past year, publications have started using much lower concentrations to obtain significant impacts (Allegretta *et al.* 2017; Kitao *et al.* 2018; Soukarieh *et al.* 2018a). This thesis follows this last trend with very significant activities at low concentrations corresponding to 3 times the IC_{50} which are much closer to therapeutic doses.

None of the nine publications that were just cited have included any work performed in clinical isolates and the vast majority used PA14 with a few using PAO1 or *E. coli* reporters in the 2012-13 publications, only one used PAO1-L and PA14 (Soukarieh *et al.* 2018a). This can highly limit the relevance of the studies in significantly different *P. aeruginosa* genomic backgrounds like the clinical isolates. Data provided in this thesis shows

that correlation between potency and HHQ inhibition is lost when the compounds are tested on clinical isolates (Figure 4.8). Some strains, including the laboratory strain PA14, show high resistance to HHQ or PQS inhibition in presence of SEN019 or SEN032. It is difficult to say for some strains if there is a real biological difference behind the technical variability, however in some others the resistance is quite obvious, including the laboratory strain PA14. These results show how important it is to work at the right concentrations of compounds in order to obtain significant results, especially in overproducing strains such as the chosen ones. On the other hand, it should be noted that SEN089 is generally a very good inhibitor in all strains at 200 nM with the exception of PAK which is practically unaffected.

A further look at HQNO production was done with SEN089 and the different strains. Results show that the inhibition patterns are similar to those for HHQ and PQS (Figure 4.9). This result provides strong evidence that the inhibition by SEN089 is very tight and shuts down the whole AQ pathway. Furthermore, it is worth noting that the effect of SEN089 over different strains was more universal, making it stand out more from the other tested antagonists.

4.4.5. Impact over secondary phenotypes – Compound specificity towards the *pqs* system

In order to test if the compounds had any secondary impact over other phenotypes that are known to be co-regulated by other systems or not under PqsR regulation, a series of quick phenotypic assays were performed. The assays were centred on important virulence factors such as pyoverdine and proteases. The collected data here provides strong evidence that the compounds tested have no significant impact over these phenotypes and therefore their action is strictly related to PqsR inhibition alone (Figure 4.10, Figure 4.11, Figure 4.12 and Figure 4.13).

It is interesting to point the slight but significant inhibitory effect in elastase (Figure 4.11) and lectin expression (Figure 4.13) even in *pqsA* mutants. These virulence factors have been suggested to be under PqsE regulation in a PQS-independent manner (Farrow *et al.* 2008; Rampioni *et al.* 2010).

Particularly *lecA* has been shown to be highly promoted upon overexpression of *pqsE* but not by other members of the *pqs* system. This could suggest that there could be a small secondary inhibitory effect on PqsE itself (Rampioni *et al.* 2016). Previous data has shown that basal levels of *pqsE* are expressed in *pqsA* mutants (Rampioni *et al.* 2010, 2016) and it is thus hypothesised that there might still be enough PqsE to have a small but significant biological effect. Additionally, unpublished data from Ass. Prof. Luisa Martinez Pomares has also shown that *pqsE* can be expressed in *pqsA* mutants under specific experimental conditions. This could explain the *lecA* inhibition in the *pqsA* mutant (Figure 4.13). However, this remains unconfirmed and no other experiments have been performed exploring the relationship between the SENBIOTAR antagonists and PqsE.

4.4.6. PA autolysis and the *pqs* system

The last phenotype to be tested was the ability for the cells to lyse at high population densities. This is a complex phenotype which covers a wide range of mechanisms. Autolysis is an important mechanism for eDNA release (Ma *et al.* 2009) that has been previously associated with PQS (D'Argenio *et al.* 2002; Allesen-Holm *et al.* 2006). However, the individual steps and regulation leading to it are still largely unknown. Furthermore, the release of eDNA has been shown not to be under the exclusive regulation of the *pqs* system (Heurlier *et al.* 2005; Allesen-Holm *et al.* 2006; Turnbull *et al.* 2016).

The relation between cell lysis and *pqs* inhibition was studied at a transcriptional level through the use of transcriptional reporters of two key components of a lytic prophage and at the phenotypic level with a simple colony biofilm test.

The endolysin Lys (PA0629) and the delivery holin Hol (PA0614) are two proteins with an important role in explosive cell lysis (Turnbull *et al.* 2016). Found in an R- and F- pyocin locus, these genes are activated by the stress response protein RecA and therefore were selected to be tested with the lead compound.

Hol, *lys* and other prophage-derived systems (pyocins) are necessary for the production of membrane vesicles which have been observed to work as

PQS delivery system (Mashburn and Whiteley 2005). Here, transcriptional data is provided showing that inhibition of PqsR upregulates *lys* and *hol* promoters (Figure 4.14), which could imply an increase in membrane vesicle production, in agreement with Turnbull *et al.* 2016 findings.

Unfortunately, due to time constraints the analysis of the molecular mechanisms for eDNA production and the role of *pqs* was not fully explored and requires further work. A much broader range of systems and conditions should be tested, including but not limited to oxygen and / or iron availability, stress / unstressed conditions and expression of other relevant prophages and known autolysis mechanisms.

To assess if the compound had any impact on autolysis, a colony morphology test was performed using a Δ*pqsL* mutant. These mutants overproduce PQS and exhibit visible lytic plaques in very high cell density conditions (D'Argenio *et al.* 2002; Allesen-Holm *et al.* 2006). The assay performed in this study shows how the addition of even low concentrations of SEN089 reverts the lytic phenotype of Δ*pqsL* mutant (Figure 4.15).

The prophages Bacto1 and Pf4 (originally known as Pf1) are encoded in the *P. aeruginosa* PAO1 genome (Stover *et al.* 2000). Unpublished work by Rampioni G., reported that the prophage Pf4 is activated by HHQ accumulation, like in the *pqsL* mutant that has high levels of AQ production because it is incapable of synthesising HQNO. The activation of prophage Pf4 is not trivial because it has been linked to a wide range of phenotypes related to biofilm survival and dispersal through switching to hyper infective dispersed physiological state (Chua *et al.* 2014; Nanda, Thormann and Frunzke 2015).

Taken together, this data suggests that at least two prophage-mediated autolytic systems are found in *P. aeruginosa*. Assuming that autolysis is the main source of MVs, each mechanism would produce different types of MVs, depending on the needs of the population. The R- and F- pyocin loci system is independent of *pqs* regulation and it could be possible that the observed changes in expression (Figure 4.14) are tied to substrate competition with the Pf4 based system which is dependent of PqsR. Moreover, it has been suggested that PQS itself may physically interact with outer membranes to

directly stimulate MV formation (Schwechheimer and Kuehn 2015). The high hydrophobicity of AQs make PQS-related MVs a logical delivery system and there is experimental evidence that this is how the vast majority of PQS moves out of the cells (Mashburn and Whiteley 2005). The regulatory mechanism of this fraction of MVs or the triggering conditions are currently unknown, nevertheless, it is possible that oxygen could play an important role since it is the limiting factor for PqsH activation and catalysis of HHQ to PQS (Schertzer, Brown and Whiteley 2010).

4.4.7. New model for the role of *pqs* system in CF lungs

A new model for the role of the *pqs* system in *P. aeruginosa* growing in CF lungs in microaerophilic conditions is hereby proposed based on initial suggestions by Schertzer, Brown and Whiteley 2010. Still, the absence of O_2 is a key element for this model which does not try to explain the role of *pqs* in aerobic biofilms.

Initially, *P. aeruginosa* preferentially colonises hypoxic microenvironments where biofilms develop in microaerophilic conditions (Worlitzsch *et al.* 2002; Alvarez-Ortega and Harwood 2007). Furthermore, intra-biofilm oxygen gradients are also commonplace and positively correlate to metabolic activity (Borriello *et al.* 2004). Thus, it is hypothesised that PQS production is largely inhibited under these conditions and HHQ signalling is very limited due lack of PQS-related MVs as a delivery mechanism (Mashburn and Whiteley 2005). In the absence of available oxygen, PQS-independent MVs will be predominant, mostly related to biofilm maintenance and development (Turnbull *et al.* 2016). The sudden availability of oxygen through potential biofilm (or mucus) shearing or oxidative bursts from the immune response would rapidly activate PQS production thanks to the pool of active PqsH (Schertzer, Brown and Whiteley 2010). This includes PQS-related MVs necessary for signal translocation. PQS activated bacteria undertake a physiological change as they become dispersed (Chua *et al.* 2014), overexpressing certain virulence factors and activating the oxidative stress response (Maura *et al.* 2016) at the cost of becoming more immunogenic.

This model describes the *pqs* system as a proactive defensive mechanism readily active to answer sudden changes in oxygen availability upon already established biofilms. This study provides evidence that a functioning *pqs* system under oxygenic conditions is required for some virulence factors (Figure 4.4) but not others that may further increase a localised immune response (Figure 4.11). It also shows that genes related to PQS-independent MVs are upregulated in the absence of PQS (Figure 4.14).

It should be taken into account however that the *pqs* system has two key switches PqsR and PqsE without total regulation overlap (Farrow *et al.* 2008; Rampioni *et al.* 2016). To the author's knowledge there are currently no publications regarding the coordination of the PqsR/PqsE regulator couple, if they work in tandem or compete for shared targets and their affinity to them.

Moreover, Mashburn and Whiteley research suggests that PQS, but not HHQ, is necessary to produce PQS-related MVs although both can be found inside. Since both are PqsR-binding autoinducers, it could be that: HHQ regulation needs the presence of PQS, HHQ is relegated to intracellular signalling, or is delivered through a PQS-independent system. In oxygenic conditions HHQ and PQS would work in tandem whereas in hypoxia or anaerobiosis where $[O_2] < PqsH\ K_M$, HHQ would be the main *pqs* autoinducer.

4.4.8. Conclusion and future directions

The compounds tested have shown to have a significant impact over the AQ production of PAO1-L wild type laboratory strain and most of the other isolates. Especially relevant is the overall strength of the lead compound SEN089. However, there are some isolates that have proven to be much more resilient to the PqsR inhibition.

The phenotype most tightly linked to the *pqs* system is pyocyanin production and its inhibition was also heavily correlated to AQ production. However, the inhibitory effects become less obvious as phenotypes get more complex and involve multiple poorly understood mechanisms such as autolysis.

This study provides a significant volume of evidence showing that the compounds accomplish the desired *pqs* system inhibition even at low concentrations without known secondary activity. The overall impact on more complex phenotypes is not as significant but this is only related to the real role that the *pqs* system may play for other phenotypes in standard laboratory conditions.

The use of genotypically different strains has also brought to relevance the importance of performing the major assays using different models. Laboratory strains are very good basic models, however, they will hardly represent other groups found in completely different environments such as clinical isolates. This is especially relevant in studies like this one which aims to settle the bases for the development of usable PqsR inhibitors to work in a CF environment, ideally against persistent strains.

The research shown here aims to work as a benchmark for the first steps towards *in vitro* compound testing. As with most research, time has been the most limiting factor when performing the assays, a more complete approach would include at least the basic AQ and pyocyanin assays in each isolate using their own IC_{50} values for a better inter-strain comparison, and a more in depth study of the differences between HHQ and PQS regulation, the autolysis phenotype and different experimental conditions such as microaerophilic or iron-limited conditions.

5. Chapter 5: *P. aeruginosa* biofilms, antibiotic sensitivity and antagonist additive effect

5.1. Introduction

A more in depth look at the biofilm development of *P. aeruginosa*, its composition and unique characteristics of this bacterial lifestyle is thoroughly explained in the main introduction of this thesis.

5.1.1. *P. aeruginosa* biofilms

As most microorganisms, *P. aeruginosa* (PA) favours the formation of biofilms upon colonisation of a surface and due to its ubiquity (Botzenhart and Döring 1993; Mann and Wozniak 2012), it is able to colonise a wide range of different environments. *P. aeruginosa* rose to prominence as a model organism particularly in cystic fibrosis (CF) (Govan and Deretic 1996), although it can also be found in wound infections, becoming chronic in immunocompromised patients (Gjødsbøl *et al.* 2006; James *et al.* 2008). The development of *P. aeruginosa* biofilms is a complex process where the formation of the extracellular matrix is a critical stage for a successful biofilm (Flemming, Neu and Wozniak 2007; Ma *et al.* 2009) and QS has been shown to play a key role in biofilm formation (Pearson, Pesci and Iglewski 1997; De Kievit *et al.* 2001; Spoering and Gilmore 2006; Williams *et al.* 2007; Ueda and Wood 2009; Shrout *et al.* 2012).

5.1.2. Role of *pqs* in biofilm development

The *pqs* system is a major component of the *P. aeruginosa* QS signalling network (Lee and Zhang 2014). The *pqs* system regulates a wide range of virulence factors, some of which are strictly under *pqs* regulation (Cao *et al.* 2001; Maura *et al.* 2016). Its exact involvement in biofilm development has not been thoroughly studied but literature links the *pqs* system to extracellular DNA release (D'Argenio *et al.* 2002; Allesen-Holm *et al.* 2006; Yang *et al.* 2009; Thomann *et al.* 2016). Nevertheless, the global regulatory mechanism remains unresolved as other PQS-independent autolytic and DNA release mechanisms have been observed (Turnbull *et al.* 2016).

Extracellular DNA (eDNA) is a key component of the biofilm matrix along with exopolysaccharides Pel, Psl, alginate, lipid vesicles and secreted proteins (Whitchurch *et al.* 2002; Ma *et al.* 2009; Toyofuku *et al.* 2012). Release of eDNA appears to be constant through the whole matrix development and maintenance and its structure develops along the Psl network to maintain the whole biofilm architecture (Mann and Wozniak 2012). However, previous published evidence has shown that its presence in structured biofilms is highly localised (Yang *et al.* 2007; Parsek and Tolker-Nielsen 2008). Chemically, the presence of eDNA in the matrix lowers its pH and creates a cationic poor environment (Ma *et al.* 2009; Wilton *et al.* 2015). Mechanically, the high number of hydrogen bonds available makes it able to create strong bonds with many molecules and the surface (Tseng *et al.* 2018). eDNA helps making the matrix sticky and ductile. Biologically, eDNA is used by the cells to create organised migration fronts to expand the biofilm, the correct formation of hollow microcolonies that allow a normal dispersal and as potential carbon and phosphate source under starvation conditions (Finkel and Kolter 2001; Parsek and Tolker-Nielsen 2008; Mulcahy, Charron-Mazenod and Lewenza 2010; Gloag *et al.* 2013). Taking everything together, it is clear that eDNA is essential for the correct development of the biofilm and protection of the bacteria against antibiotics or other harsh environmental conditions like pH (Wilton *et al.* 2015).

The matrix development of flat biofilms has not been studied in as much detail as those forming mushroom-like microcolonies under flow conditions (Ma *et al.* 2009; Wei and Ma 2013). In these structures, it is commonly accepted that eDNA comes from a regulated autolytic process of a defined subpopulation within the biofilm found in the stalk of the microcolony (Parsek and Tolker-Nielsen 2008). Little is known regarding how the eDNA becomes an integral part of all the matrix and the regulatory mechanisms of autolysis in *P. aeruginosa* are ill defined.

In summary, the current model for eDNA release establishes that, upon certain cues (internal or external) a subset of cells undergo autolysis releasing their chromosomal DNA (Allesen-Holm *et al.* 2006). Autolysis is one of the mechanisms to generate membrane vesicles (MVs) with a

defined pool of proteins and virulence factors inside (Schooling and Beveridge 2006; Schooling, Hubley and Beveridge 2009). Furthermore, autolysis events happen all the time in a relatively stochastic manner. This set of events may be important for the maintenance of the matrix and involve MVs with different contents (Turnbull *et al.* 2016). The release of eDNA and autolysis is regulated by *pqs* under specific conditions. Moreover, it has been observed that the addition of external PQS to mature biofilms induces dispersal (Bjarnsholt *et al.* 2010). Unpublished experimental data has shown that this happens with as little as 5 μM of PQS.

5.1.3. Biofilm growth models: Constant flow and static

Biofilm growth models can be generally divided in two main groups depending on whether bacteria are grown under a constant flow of fresh media, or static, not dissimilar to batch or semi-batch processes (if fresh media is added at certain times). Generally, the choice of model depends on the aim of the assay, for instance, continuous flow biofilms are often grown for imaging purposes, as under these conditions bacteria tend to develop highly structured biofilms that includes mushroom-like shapes as the cases reported by Parsek & Tolker-Nielsen, 2008; Ma *et al.*, 2009; Reffuveille *et al.*, 2014. These biofilms can also be quantified often through software tools such as Comstat2 which allows the measurement of values such as biomass or thickness (Heydorn *et al.* 2000; Vorregaard 2008). Nevertheless, constant-flow systems are usually expensive and limited to small number of samples, conditions and replicates. Moreover, any quantitation performed from CLSM pictures of microcolonies could be argued to have human-induced bias, as a completely randomised imaging process might image areas without any growth.

The use of static models effectively overcomes some of these limitations. Most static models are based on multi-well systems like microtiter plates or chambered glass slides, with a wide range of variants. This method offers great flexibility and can be considered more high throughput due to the large number of samples and replicates that one plate usually fits (Rollet,

Gal and Guzzo 2009; Frei, Breitbach and Blackwell 2012; Thomann *et al.* 2016; Berlanga, Gomez-Perez and Guerrero 2017).

Static biofilms grow significantly different to the ones under constant flow and sometimes imaging can be challenging. However, there are published examples of microscopy and quantitation performed exclusively with static biofilms (Fuxman Bass *et al.* 2010).

Notable exceptions exist that grow biofilms in innovative ways, providing interesting information regarding often overlooked topics like biofilm expansion and migration such as an interstitial biofilm model developed by Gloag *et al.*, 2013.

5.1.3.1. Microfluidics biofilms: Bioflux™ (Fluxion Biosciences)

Bioflux™ (Fluxion Biosciences) is a commercially available system that can be used to grow constant flow biofilms (Tremblay *et al.* 2015). The system is considered as microfluidics due the size of the channels and flow rates used. A pump pushes filtered air towards a well plate, the air pushes down the fresh media in the inlet that will flow at a programmable sheer force towards the outlet where waste is collected. Meanwhile, the sample grows within the connecting channel, which contains a wider part in the middle called viewing window, this part has the exact width to fit in a 20X magnification objective (Figure 5.1).

In this project, two plate types of 48 and 24 wells were used. The 48-well plate had space for 24 samples as each channel had one inlet and one outlet. On the other hand, the 24-well plate had two inlets and therefore only 8 samples could be analysed at a time. With two inlets, changes in media or gradients can be programmed. The viewing window of the channel is 70 µm tall, which allows enough space to develop small and structured microcolonies on the bottom and top (Figure 5.1).

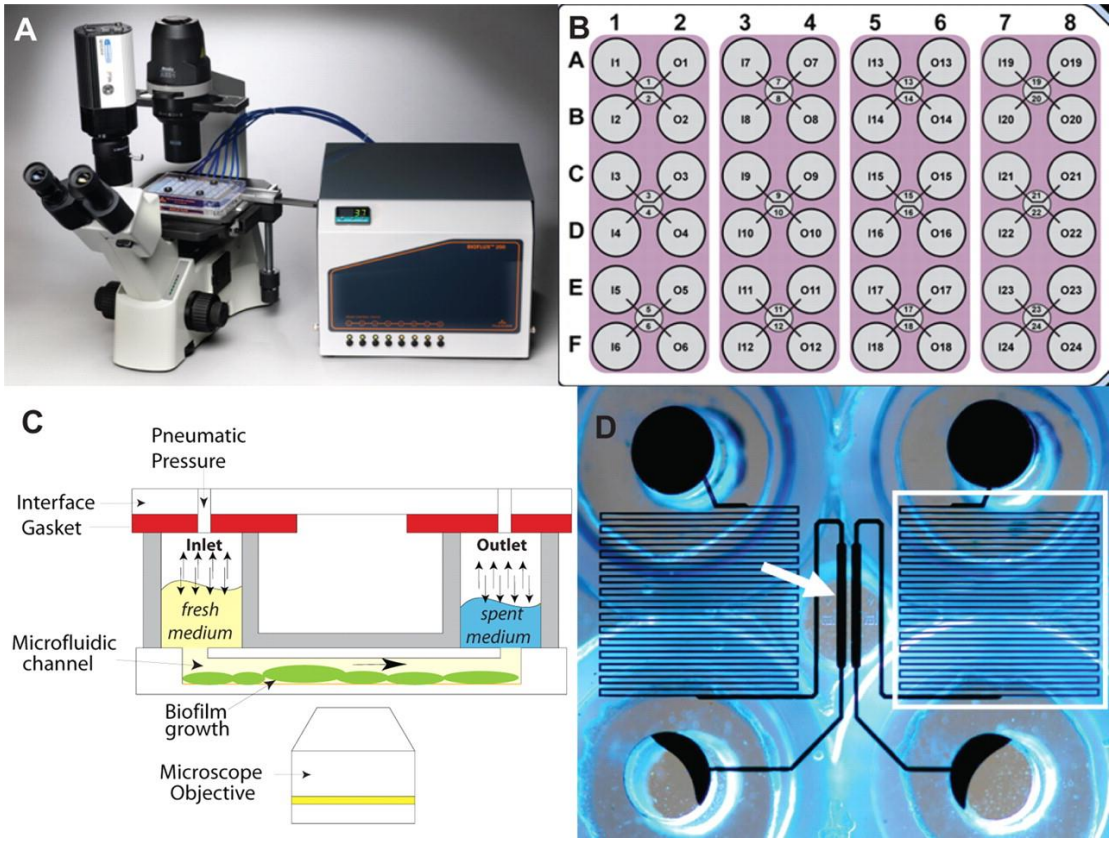

Figure 5.1. Bioflux™ 200 microfluidics system. A) Pump and temperature platform next to optical microscope. A 48 well plate can be observed connected to the pump. B) 48 well plate distribution as seen in the Fluxion™ software. C) Schematic representation of biofilm growth in one channel, including inlet, viewing window and outlet. D) Picture of two channels with their corresponding inlet and outlets, white arrow indicates viewing window and white square shows serpentine grid to prevent inlet contamination.

Bioflux™ is a useful system to grow biofilms with small volumes of media allowing growth monitoring over time as well as high-resolution microscopy facilitated by the imaging surface (180 µm cover slip glass). However, this system presents major drawbacks: The initial seeding has to be empirically fine-tuned to prevent over- or under-reaching as it could lead to a second major biological issue such as the blocking of channels in the case of highly mucoid biofilms. In addition, there can also be problems with contamination from highly motile bacteria capable of swimming upstream. The unidirectional flow makes the biofilm behind the growth front significantly affected by a decreasing nutrient gradient and an increasing biological signal gradient, this can also introduce strong biases during quantitation and imaging. Finally, the system is highly sensitive to air bubbles that could block entire channels and invalidate the results.

Because of these reasons, optimisation is required to obtain reproducible data from this system. However, it can provide very detailed data on biofilm architecture over time.

5.1.3.2. Static biofilms

Static biofilms are cost-effective and easy to set up. The static mode of growth provides a very specific set of conditions where the biofilm grows very differently from constant flow. Oxygen availability is one of the major differences between models as it can become depleted in 96-well plates (Cotter, O'Gara and Casey 2009). The absence of oxygen is extremely significant because *P. aeruginosa* biofilms develop differently in environments that are either aerobic or anaerobic (Furiga *et al.* 2016). Notably, anaerobic biofilms are potentially closer to those observed in the cystic fibrotic environment, in which the mucus has been reported to provide an anaerobic environment (Worlitzsch *et al.* 2002). A strong gradient of nutrients is also generated, and the dispersed cells will swim confined in the well until they die and the biomass falls to the bottom of the well, or they attach to another part of the well, quickly colonising the whole surface.

Because of the cyclic nature of the biofilm (Stoodley *et al.* 2002), it is safe to assume that after maturation and dispersal of the first microcolonies, there will be constant, simultaneous events of dispersal and attachment, making the actual biofilm development difficult to track down. The information provided by assays such as crystal violet (CV) shows a snapshot of the state of the biofilm at that particular time point but gives no further information regarding how the biofilm developed until then. Another interesting point to take into account is the washes performed for these biofilms. In some models, most of the biomass can easily be removed through washes, leaving only the irreversibly attached cells in the well. Imaging or quantitation of washed samples will only provide data of the remaining biofilm. This might be useful if total clearance is sought (Frei, Breitbach and Blackwell 2012; Thomann *et al.* 2016) or surface attachment is analysed (Berlanga, Gomez-Perez and Guerrero 2017) but might not provide accurate information regarding differences in other structural parts of the biofilm that are not strongly bound to the surface attached layers.

5.1.4. Antibiotic treatment of biofilms

The vast majority of infections involve development of biofilms (Percival *et al.* 2014). The high resistance of this lifestyle to antibiotics has been known since the first detailed description by Costerton *et al.*, 1995 who reported that biofilm cells were at least 500 times more resistant than their planktonic counterparts. Moreover, they also play a major role in chronic wounds and infections (James *et al.* 2008) and are a source of persister cells (Lewis 2007, 2008). A large wealth of resources is currently invested in developing alternative or adjuvant therapeutic strategies but antibiotics remain the main treatment against chronic infections that does not involve physically removing the infected area (Ciofu *et al.* 2017).

Two often used antibiotics against P*. aeruginosa* infections are ciprofloxacin and tobramycin. Both are only effective against metabolically active cells and have been used to treat biofilms, but they belong to very different families (Ciofu *et al.* 2017). Colistin is another interesting antibiotic because it has been observed to mostly affect the dormant subpopulation in the stalk and inner layers of microcolonies, making it an appealing choice for combinatory therapy (Pamp *et al.* 2008). Nevertheless, for this work, only ciprofloxacin and tobramycin were tested.

5.1.4.1. Ciprofloxacin

Ciprofloxacin is a very prominent fluoroquinolone (Acar and Goldstein 1997). As other fluoroquinolones, ciprofloxacin binds to two type IIA topoisomerases: DNA gyrase (Gyr) and topoisomerase IV (Topo IV). These topoisomerases are critical to maintain a correct DNA topology, unwinding the circular chromosome during its replication. Gyr and Topo IV cut a strand of dsDNA in the middle of the protein complex to let another dsDNA strand move through from one end to the other of the complex, in a two-gate, unidirectional mechanism with ATP and Mg^{2+} as required cofactors (a detailed review of the system was done by Sissi & Palumbo, 2010).

Tolerance to this antibiotic can increase during dormancy as it significantly decreases the relevance of Gyr and Topo IV in that physiology. The lower metabolic activity decreases DNA restructuration events so DNA remains supercoiled. Moreover, lower quantities of ATP will also decrease the

activity rate of the type IIA topoisomerases, strongly limiting the efficiency of ciprofloxacin in biofilms (Walters *et al.* 2003; Williamson *et al.* 2012). Similarly, resistance can emerge through specific mutations in type IIA topoisomerases.

Secondary resistance mechanisms involve changes in membrane permeability (porins), increase in efflux pump activity and acquisition of resistance cassettes found in mobile elements like plasmids (Jacoby 2005; Heeb *et al.* 2011).

5.1.4.2. Tobramycin

Tobramycin is a widely used aminoglycoside antibiotic, obtained by basic hydrolysis of factor 5' from the nebramycin antibiotic complex of *Streptomyces tenebrarius* (Koch, Davis and Rhoades 1973), now *Streptoalloteichus tenebrarius* (Tamura *et al.* 2008). Tobramycin binds to the A-site of the 30S ribosomal subunit (Yang *et al.* 2006), thus, rendering translation unachievable since tRNAs cannot dock at the ribosome.

The effectiveness of tobramycin is tied to the metabolic state of the cell as its bactericidal effect depends on translation. Dormant cells will be much more tolerant to higher concentrations of tobramycin as their translation is highly supressed (Walters *et al.* 2003; Williamson *et al.* 2012). External metabolic activation can sensitise bacteria to tobramycin but this sensitisation is nutrient-dependent as the addition of glyxolate, a component of the TCA cycle, actually increases resistance to tobramycin since it inhibits respiration directly impairing aminoglycoside uptake (Taber *et al.* 1987; Meylan *et al.* 2017).

The chemical structure of tobramycin makes it a polycationic molecule, this allows tobramycin to strongly interact with negatively charged molecules such as the eDNA found in the matrix. This interaction chelates tobramycin limiting cellular uptake within the biofilm (Mulcahy, Charron-Mazenod and Lewenza 2008). Tobramycin can also be immobilised in the periplasm by the presence of glucans (Ciofu *et al.* 2017). Nevertheless, the most common resistance mechanism is enzymatic modification while changes on the A-site or the ribosome in general are not usually observed due the housekeeping status of this system (Kotra, Haddad and Mobashery 2000).

Synergy between tobramycin and inhibition of the *pqs* system has been recently sought after (Maura and Rahme 2017; Soukarieh *et al.* 2018a). However, relationship between tobramycin sensitivity and the *pqs* system has not been elucidated yet, although could be mediated by *pqs* regulation of eDNA release (D'Argenio *et al.* 2002; Allesen-Holm *et al.* 2006; Yang *et al.* 2009; Thomann *et al.* 2016).

5.2. Aims of the chapter

This chapter aims to determine if the presence of SEN PqsR antagonists has a significant impact on *P. aeruginosa* biofilms, their development and sensitivity to treatment with ciprofloxacin or tobramycin. More specifically, work presented here is intended to:

- Establish and optimise a robust biofilm model that can be imaged by microscopy in which a number of biofilm parameters including cell death can be measured.
- Compare the biofilms grown in presence of SEN compounds to control groups to determine their impact on growth and biofilm structures.
- Determine whether SEN compounds can sensitise biofilms to antibiotics and alter their structural integrity.

5.3. Results

5.3.1. Biofilm model set up using SEN compounds

All the biofilm pictures presented in this work were selected as representative images from a larger pool taken from biological replicates.

5.3.1.1. Controlled flow microfluidics biofilm model: Bioflux™

The microfluidics system Bioflux™ was chosen to grow biofilms under a constant flow of fresh media to observe potential differences in microcolony formation. The presence of constant flow results in the removal of dispersed cells and prevents accumulation of extracellular signalling molecules and metabolites from the biofilm.

The use of the Bioflux™ system in 24- and 48-well plate configurations did not present any differences in biofilm growth and hence no distinction

between these plates is made in this chapter. In a preliminary experiment, using this system, SEN019 and SEN032 were added at 3xIC_{50} to biofilms grown for 17 hours (Figure 5.2). The addition of compounds to already developed biofilms did not change the biofilm conformation nor increase dispersal.

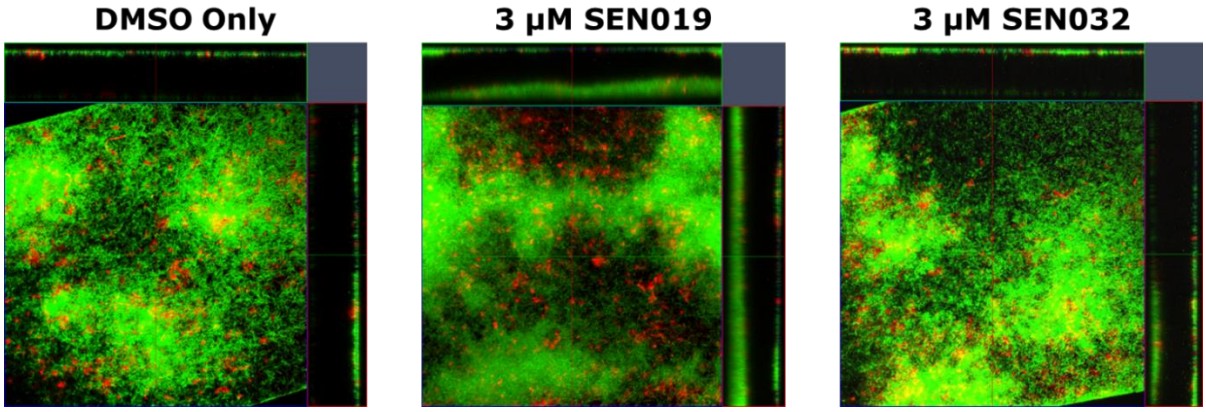

Figure 5.2. PAO1-L 17 h old biofilms from Bioflux. PAO1-L mTn7::*gfp* grown in a Bioflux system (0-20 dyn) for 17 h at 0.5 dyn with LB 10% at 37° C. Compounds were added from time 0 Pictures taken at 20X, green is Gfp fluorescence and red is PI fluorescence. Solvent control group had an equivalent volume of DMSO to that used for compounds. Images taken with CLSM at 20X. **A)** is the control with only DMSO added, **B)** had 3 µM SEN019 added and **C)** 3 µM SEN032**.**

The Bioflux model enables constantly feeding fresh media and the plates are optimised for microscopy visualisation up to super resolution levels. Microcolonies within the channel are suspended in media so the native structure of the biofilm and the dispersed cells can be observed through time.

An example of the structure of a PAO1-L biofilm can be observed in Figure 5.3 using Bioflux. This image shows several microcolonies protruding from the biofilm and the propidium iodide stained DNA mainly from eDNA but also from dead cells.

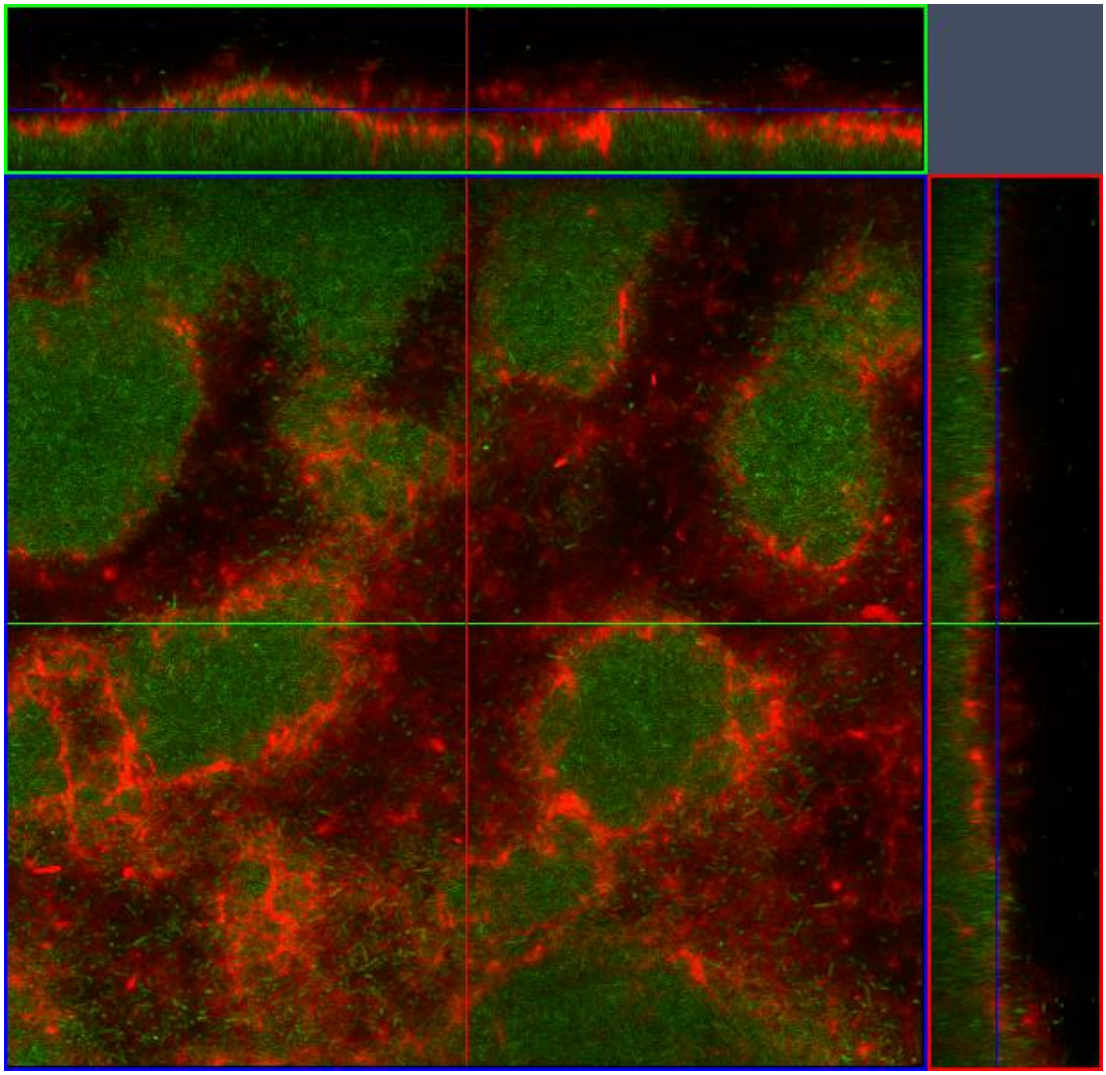

Figure 5.3. 40X LSCM image of a PAO1-L microfluidics biofilm. Image taken from a *Pseudomonas aeruginosa* mTn7::*gfp* Gm^R. The biofilm was grown in a Bioflux system for a total of 21 hours at 37° C in presence of SEN019 3 μM, the media used was LB 10% at 0.4 dyn/cm^2. Counterstain was done with PI (red) which stained dead cells and eDNA alike.

3D representations usually provide less information than an orthogonal (ortho) representation which allows to specific sections to be analysed through the Z stack and the side planes of the sample. Nonetheless they can sometimes complement the information provided by the orthogonal plane by providing a more visual representation.

In order to observe the potential impact in older biofilms in our studies, PAO1-L was grown for three days in presence or absence of SEN019. Biofilms grown in presence of SEN019 seem to have less PI staining likely due to reduced eDNA (Figure 5.4).

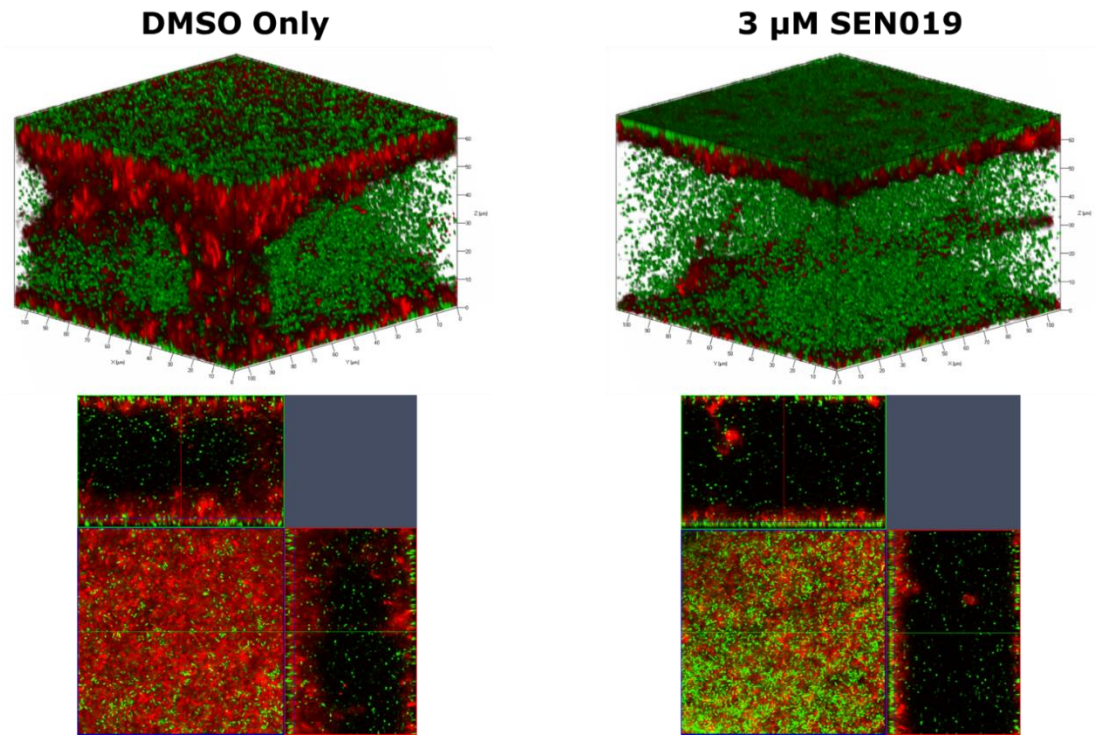

Figure 5.4. 3 day old PAO1-L microfluidics biofilms at 40X in 3D and ortho representation. Image taken from a *P. aeruginosa* mTn7::*gfp* Gm^R. The biofilm was grown in a Bioflux system for a total of 72 hours at 37° C in presence of hit compound SEN019 3 µM or an equivalent volume of DMSO, LB 10% was used at 0.4 dyn. Counterstain was done with PI (red) which stained dead cells and eDNA. Fresh media was added periodically to avoid running air through the system.

5.3.1.2. Static biofilm models

5.3.1.2.1. Biofilms on 8-well chamber slides

The use of 8-well chamber slides was chosen to assess visualisation of static biofilms using a simple method. This model enables biofilms to grow in smaller volumes of media. The visualisation was performed at 10X without removing the media so the biofilm architecture was not disturbed. Subline PAO1-W and strain PA14 were used instead of PAO1-L as they have been shown to develop better biofilms in some models in the presence of MOPS, glucose and CAAs. Biofilms were grown for 6 and 17 hours and imaged.

When biofilms grown for 6 and 17 hours were washed with PBS most of the cells were removed suggesting that the biofilm is not firmly attaching to this surface (Figure 5.5).

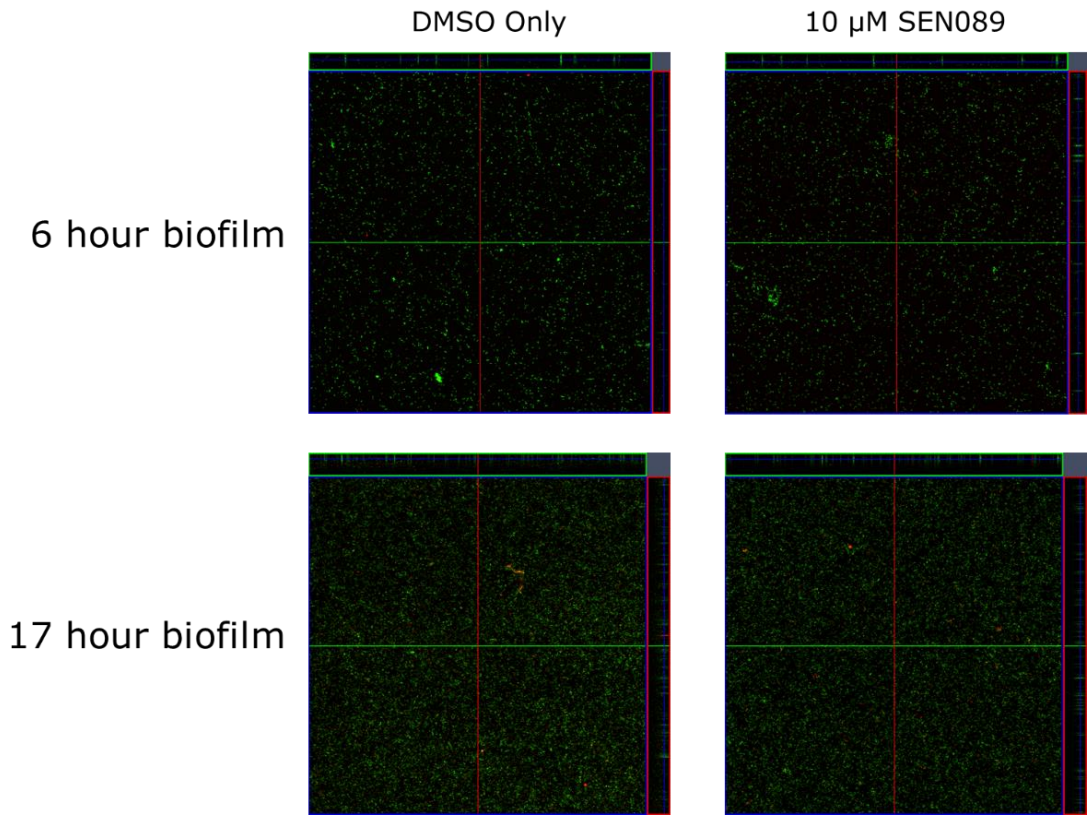

Figure 5.5. PAO1-W 8 well chamber slide washed biofilms. WT strains tagged with mTn7::*gfp* Gm^R were grown in MOPS 0.4 % D-Glucose and 0.2 % CAA for 6 hours at 60 rpm 37° C from OD_{600} 0.05 with 1 μM PI. Images were taken using a ZEISS 700 confocal microscope at 10X magnification. Green represents Gfp fluorescence whereas red is PI fluorescence. The wash was performed by removing the media and washing once with 1 volume of PBS with a micro pipette.

Data shows that a biofilm mat is already formed as early as 6 hours, with PA14 producing more developed biofilms than PAO1-W and also presenting chimney-like structures rich in PI fluorescence (Figure 5.6). The addition of 10 μM SEN089 did not have any impact on the biofilm at this stage.

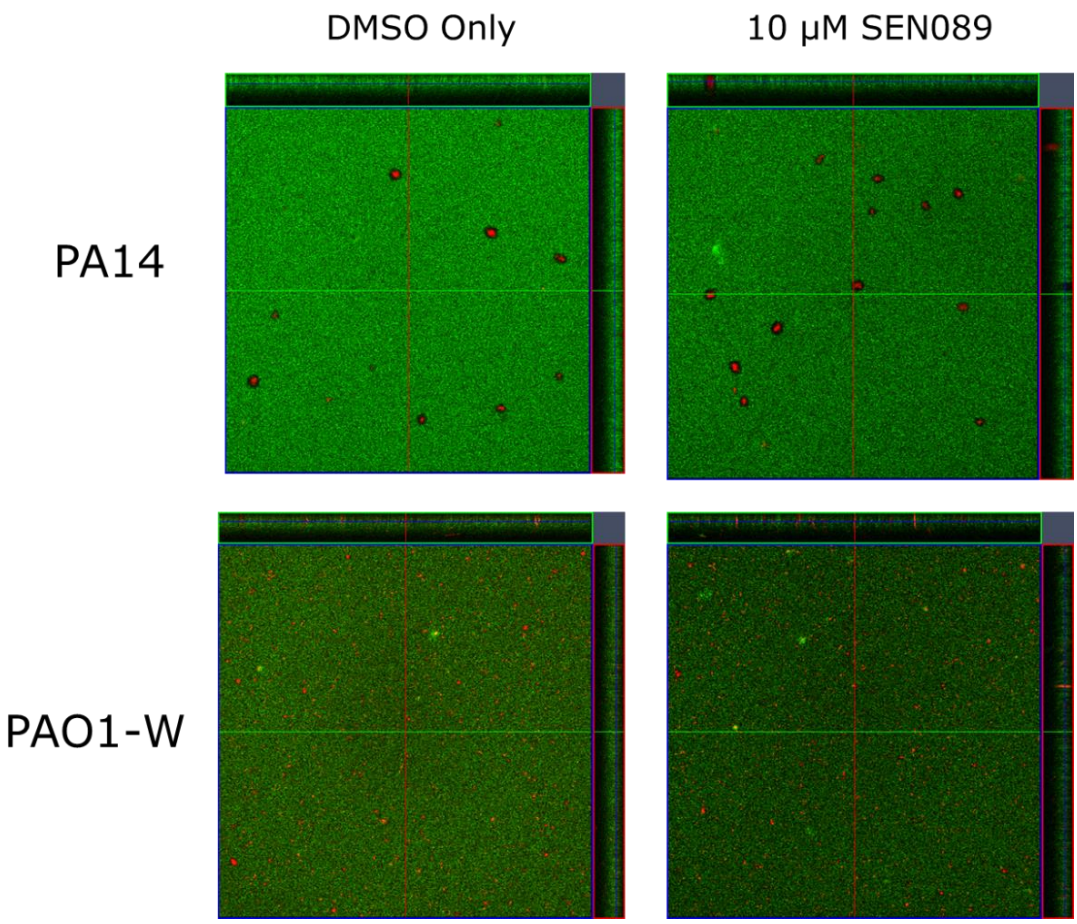

Figure 5.6. PA14 and PAO1-W 6 hour old biofilms. WT strains tagged with mTn7::*gfp* Gm^R were grown in MOPS 0.4 % D-Glucose and 0.2 % CAA for 6 hours at 60 rpm 37° C from OD_{600} 0.05 with 1 μM PI. Images were taken using a ZEISS 700 confocal microscope at 10X magnification. Green represents Gfp fluorescence whereas red is PI fluorescence.

When biofilms were grown for 17 hours PA14 biofilms grown in presence of SEN089 were similar to the control group but the chimney structures were not present or had much smaller diameters. In contrast, PAO1-W control group presented a thin layer of PI fluorescence (possibly due to some eDNA) and addition of SEN089 eliminated this layer and produced a more rugose surface (Figure 5.7).

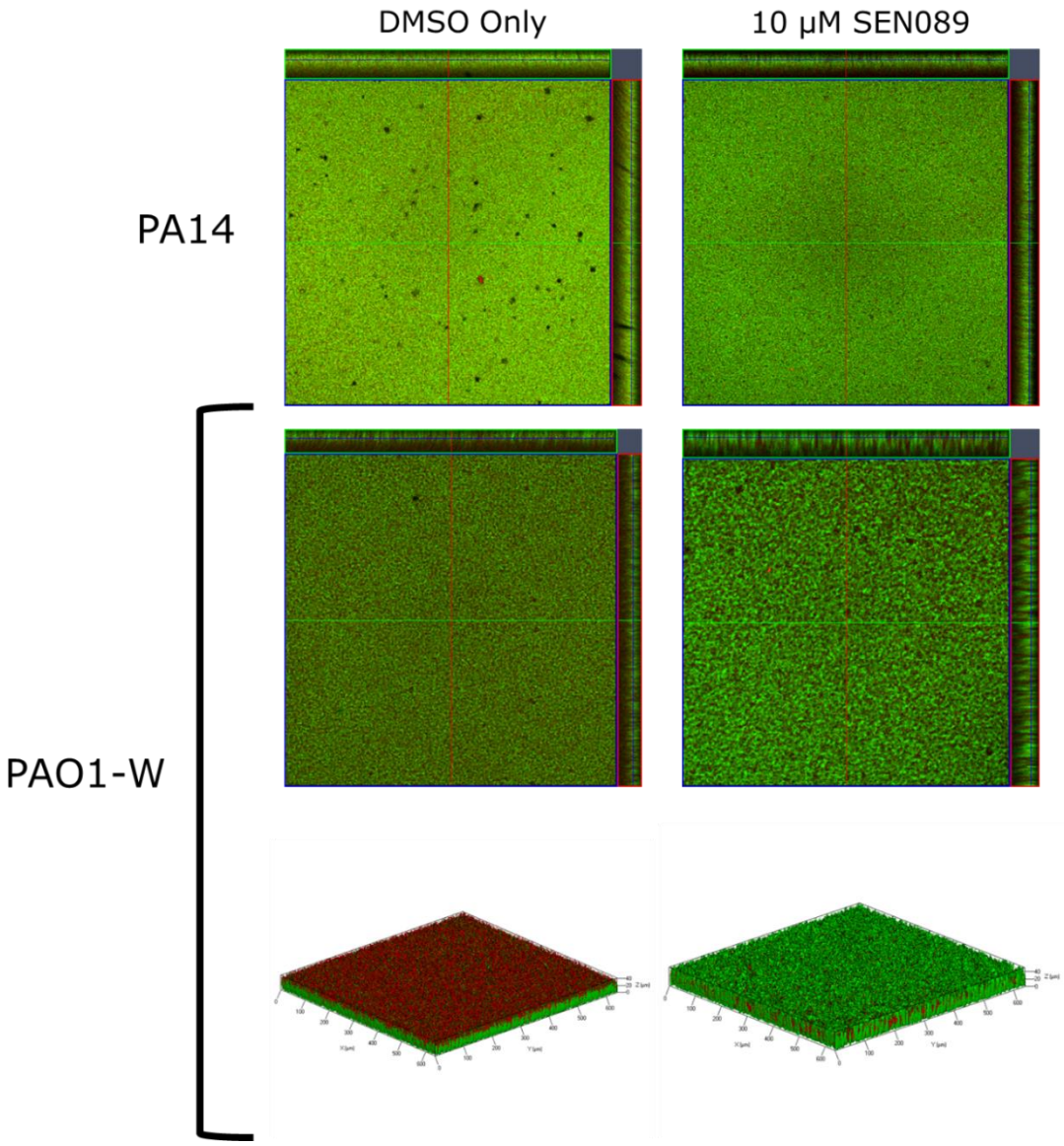

Figure 5.7. PA14 and PAO1-W 17 hour old biofilms. WT strains tagged with mTn7::*gfp* Gm^R were grown in MOPS 0.4 % D-Glucose and 0.2 % CAA for 17 hours at 60 rpm 37° C from OD_{600} 0.05 with 1 µM PI. Images were taken using a ZEISS 700 confocal microscope at 10X magnification. Green represents Gfp fluorescence whereas red is PI fluorescence.

5.3.1.2.2. Crystal violet 96-well plate total biomass

Crystal violet (CV) is a well-known approach for biofilm biomass quantitation (O'Toole and Kolter 1998b) and can be subjected to higher throughput analysis. Unfortunately, the assay is highly variable and over the years many laboratories have performed slight modifications or adaptations so nowadays there is no accepted standard method. The protocol performed here followed Thomann *et al.*, 2016 guidelines.

To assess this method (described in materials and methods) SEN019 was used to start with. This compound did not show any significant impact on CV levels compared to the DMSO control when used at 3 μM (Figure 5.8), a concentration which showed high activity in planktonic bioassays (Chapter 4: 4-hydroxy-2-alkylquinoline phenotype regulation and antagonist mediated interference).

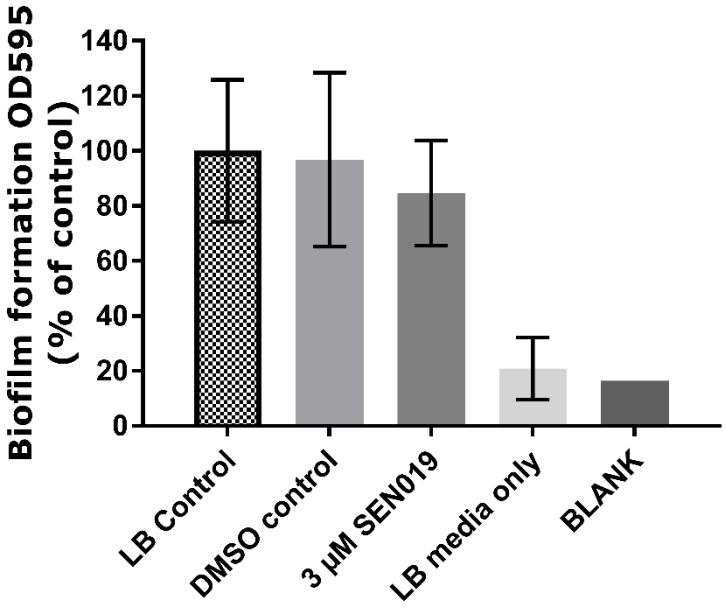

Figure 5.8. Crystal violet assays in PAO1-L. Bacteria were grown for 20 h in 200 μl of LB in 96 well polystyrene plates at 37° C static. Results represent biological triplicates. DMSO control had 0.1 % DMSO concentration. The LB control was used as 100% biofilm formation. +/- Error bars represent the standard deviation between biological triplicates.

To further assess the validity of this model for testing SEN compounds, SEN088 was added at increasing concentrations (0, 3.1, 10, 31, 100 and 310 μM) to PAO1-L static biofilms grown in the 96-well plates with two different media combinations. M63/LB media at 95:5 ratio was done following the protocol by Thomann *et al.* (2016) whereas LB 10% was also tested as it did not promote as much biofilm growth in PAO1-L. Results show that there is a positive correlation between SEN088 concentration and biofilm formation when increasing concentrations of SEN088 are used in LB 10% (Figure 5.9). The M63/LB media promoted a very strong biofilm and showed that SEN088 did not have a strong effect on CV levels even at concentrations many times over their P*pqsA* expression IC_{50} (129 nM) (Figure 5.9).

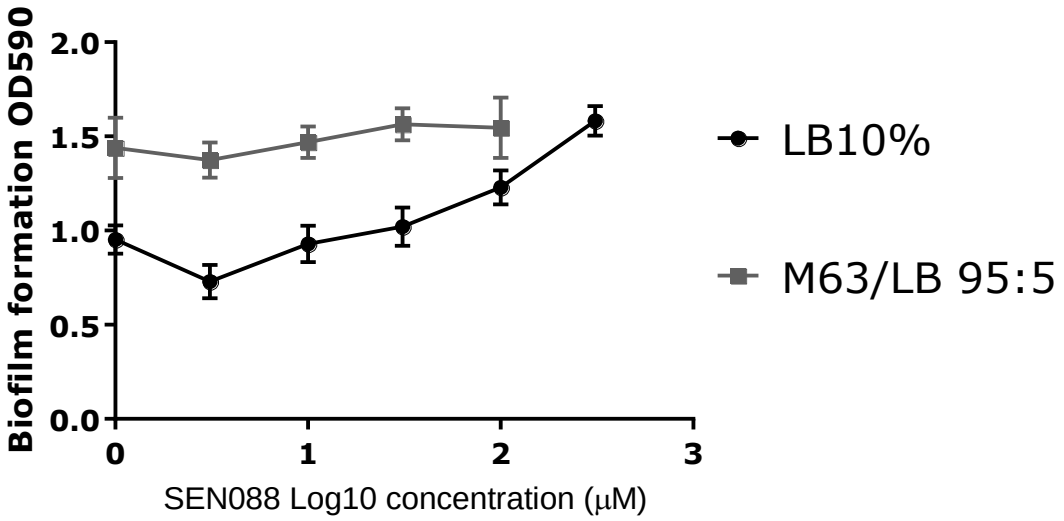

Figure 5.9. 48h PAO1-L WT biofilms stained with CV 0.1% under different concentrations of SEN088. Biofilms were grown in polystyrene 96 well plates using 200 µL of media at 37°C for 48 hours in presence of SEN088 since time 0, fresh media was added after 24 hours. SEN088 concentrations tested were as follows: 0, 3.1, 10, 31, 100 and 310 µM. +/- Error bars represent standard deviation of eight biological replicates.

5.3.2. Assessing possible enhancement effects between antibiotics and SEN PqsR antagonists on biofilms

One of the aims of this study was to evaluate whether some of the SEN compounds identified with low IC_{50}s could increase the activity of ciprofloxacin and tobramycin as they are commonly used to treat *P. aeruginosa* infections.

5.3.2.1. Bioflux qualitative analysis using ciprofloxacin and SEN combinations

Ciprofloxacin is a fluoroquinolone antibiotic that is commonly used in CF *P. aeruginosa* infections. Therefore, several biofilm models were used to thoroughly test ciprofloxacin treatments after being grown in presence of SEN compounds.

In the initial experiment PAO1-L Gfp was grown for 14 hours in the Bioflux system. Under these conditions the antibiotic showed a strong impact on the biofilm after only 40 minutes (Figure 5.10). This assay did not include PI as counterstain, however ciprofloxacin blocks membrane division and induces abnormal elongation which can be clearly observed in the imaged samples. There was a significant difference in the amount of remaining cells

between groups when ciprofloxacin was added on its own or in combination with SEN019 suggesting the possibility of a synergistic effect. However, these results could not be replicated using exactly the same conditions for yet unknown reasons.

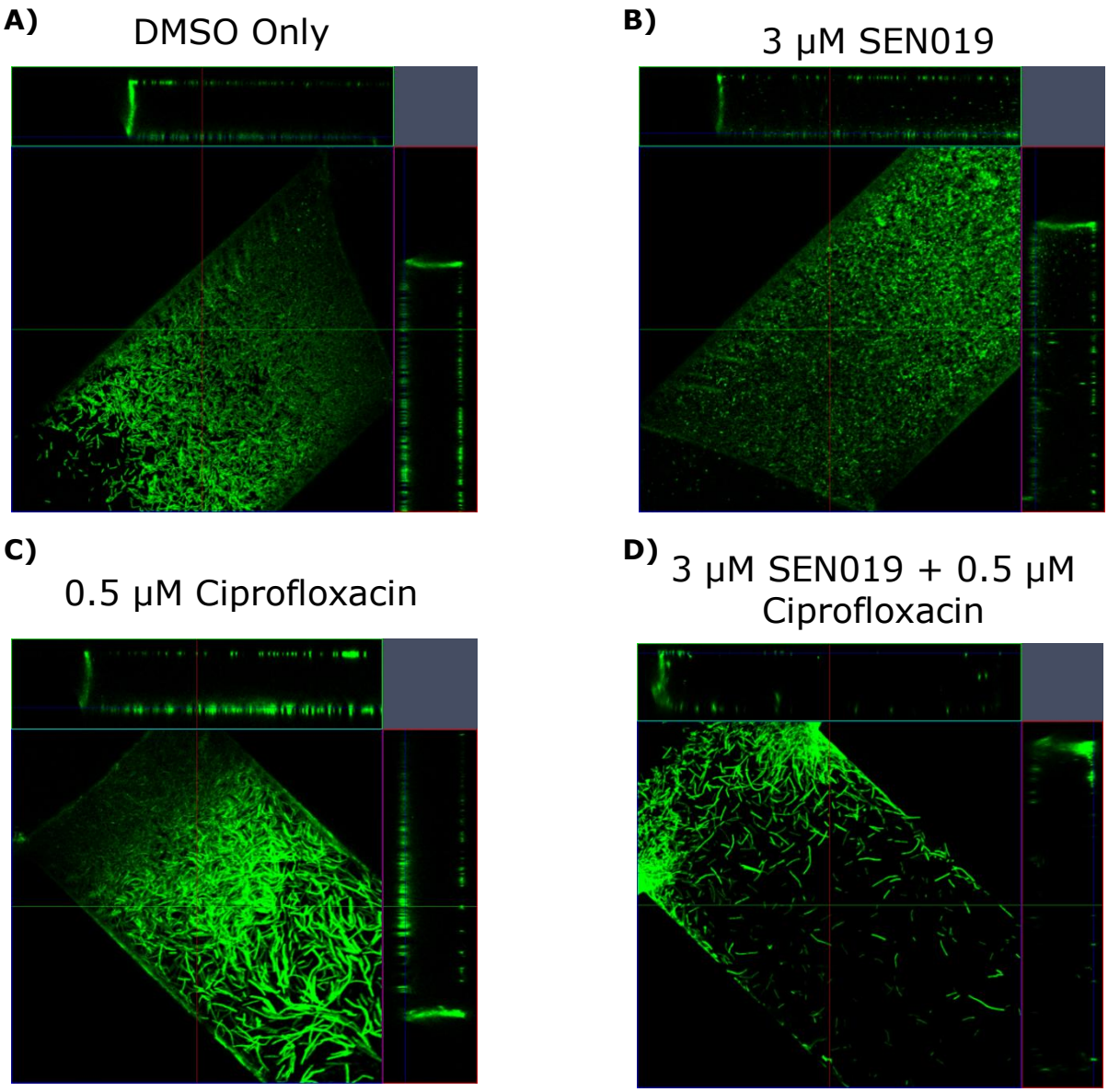

Figure 5.10 PAO1-L biofilms incubated with and without 3 µM SEN019 and / or ciprofloxacin. Ciprofloxacin was added to PAO1-L mTn7::*gfp* 14 h old biofilms and incubated for further 40 minutes in LB 10% with: **A)** DMSO, **B)** 3 µM SEN019, **C)** 0.5 µM ciprofloxacin or **D)** a combination of SEN019 and ciprofloxacin. Elongation of the cells corresponds to the action of ciprofloxacin which inhibits bacterial division.

Another set of Bioflux assays was therefore performed, treating 15 hour old biofilms with 0.5 µM ciprofloxacin but this time for two hours before imaging. The antibiotic concentration and incubation times were increased to further promote the potential synergistic effects. Bacterial growth was improved from previous assays and the addition of PI stain enabled the

imaging of dead cells as well as the biofilm matrix. Elongated cells could be observed dispersed in the interphase and on the outer layers of the microcolonies. PI fluorescence was stronger in groups with SEN019 or SEN032 which also presented elongated cells in deeper layers of the microcolonies (Figure 5.11).

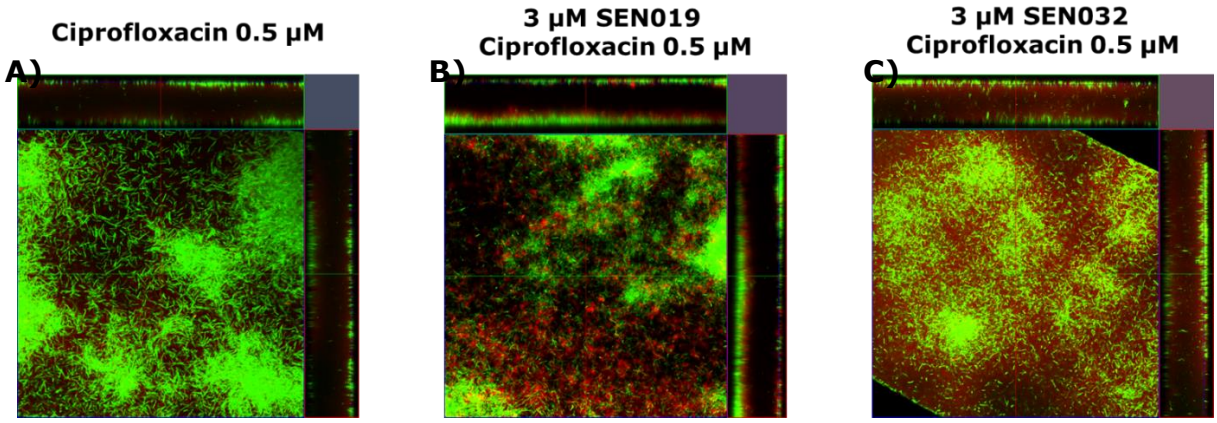

Figure 5.11. PAO1-L biofilms incubated with SEN019 or SEN032 and treated with ciprofloxacin. Ciprofloxacin (0.5 µM) was added to PAO1-L mTn7::*gfp* 15 h old biofilms followed by further 2 hour incubation in LB 10%. **A)** DMSO solvent control or **B)** SEN019 or **C)** SEN032 were added from time 0. Elongation of the cells corresponds to the action of ciprofloxacin which inhibits bacterial division. Pictures were taken at 20X, green is Gfp fluorescence and red is PI fluorescence. Untreated controls can be observed in Figure 5.2**.**

To test whether the synergistic effect could be observed in biofilms that had not been pre-sensitised with SEN compounds, biofilms were grown in absence of any compound for 15 hours before treating simultaneously with ciprofloxacin and SEN019 or SEN032. All groups presented the elongated cell phenotype caused by the action of ciprofloxacin. Results showed that there were no observable differences between groups with the combinatory therapy and the ciprofloxacin control (Figure 5.12). It is worth pointing out the increased growth in the SEN019 sample, this difference can be attributed to biological variability as all groups were initially grown under the same conditions, the cells observed are equally affected by ciprofloxacin but the structure of the microcolony remains largely unchanged.

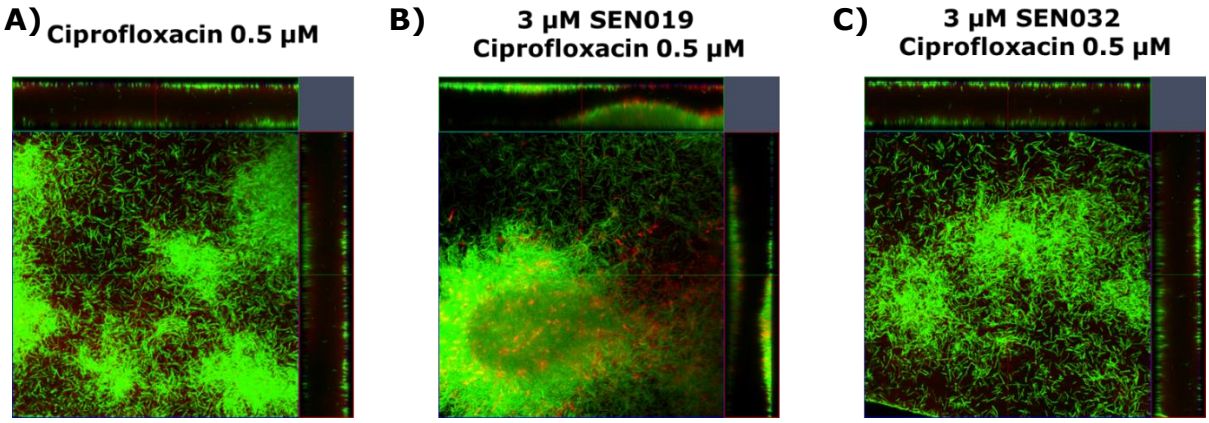

Figure 5.12. PAO1-L biofilms treated with ciprofloxacin and SEN019 or SEN032 without previous compound exposure. PAO1-L mTn7::*gfp* biofilms were grown in LB 10% for 15 hours at 0.5 dyn 37°C without any compound before being incubated for further 2 hours with 0.5 µM Ciprofloxacin and 3 µM **B)** SEN019 or **C)** SEN032. Cell elongation corresponds to the action of ciprofloxacin which inhibits bacterial division. Pictures were taken at 20X, green and red are Gfp and PI fluorescence, respectively. Untreated controls can be observed in Figure 5.2.

5.3.2.2. Bioflux qualitative analysis using tobramycin and SEN combinations

Tobramycin is an aminoglycoside often used against *Pseudomonas*. A Bioflux assay was performed where PAO1-L biofilms were allowed to grow for 15 hours before being treated with a low dosage of tobramycin for 2 more hours. Results showed that PI fluorescence presented a different distribution in the presence of SEN compounds where it concentrated in the edges of the microcolonies whereas the control group treated with tobramycin showed a PI distribution seemingly unrelated to the Gfp fluorescence, suggesting that under these conditions the microcolonies of the control group are largely unaffected (Figure 5.13).

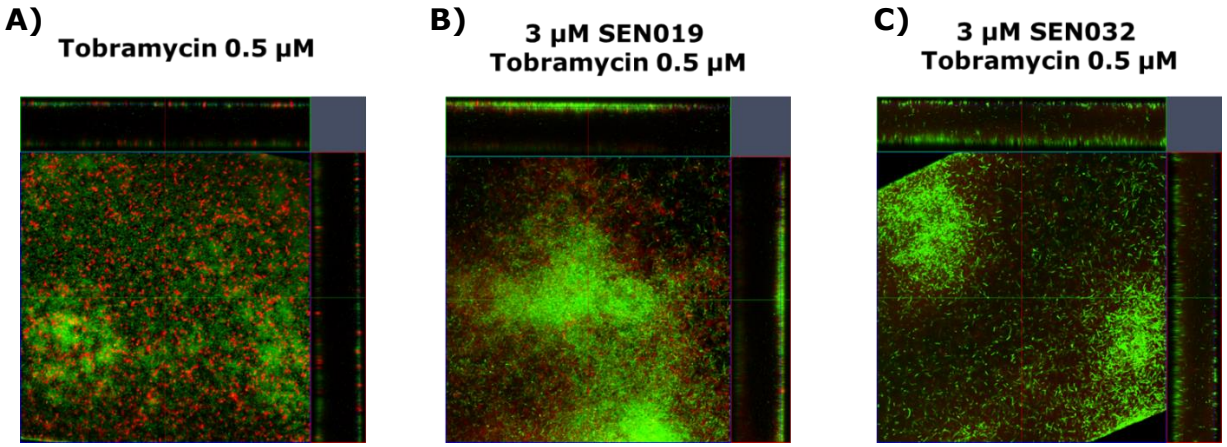

Figure 5.13. PAO1-L biofilms incubated with SEN019 or SEN032 and treated with tobramycin. PAO1-L mTn7::*gfp* 15 h old biofilms were incubated for further 2 hours in LB 10% with 0.5 µM Tobramycin. **A)** DMSO, **B)** SEN019 or **C)** SEN032 were added from time 0. Pictures were taken at 20X, the green is Gfp and red is PI fluorescence, respectively. Untreated controls can be observed in Figure 5.2.

The previous images were taken at 20X magnification (Figure 5.13), in order to more closely examine the effect of tobramycin in microcolonies, 40X images were taken of biofilms grown with SEN compounds for 17 hours and then treated with tobramycin for longer (4h). Several microcolonies were imaged and two representative ones were selected in the same plane for comparison. Results showed significant differences in the levels of cell death (Figure 5.14). Microcolonies showed that even after 4 hours, tobramycin could not kill cells in the innermost parts of the microcolony. On the other hand, the microcolony that had grown in presence of SEN019 had PI staining in all strata of the microcolony (Figure 5.14).

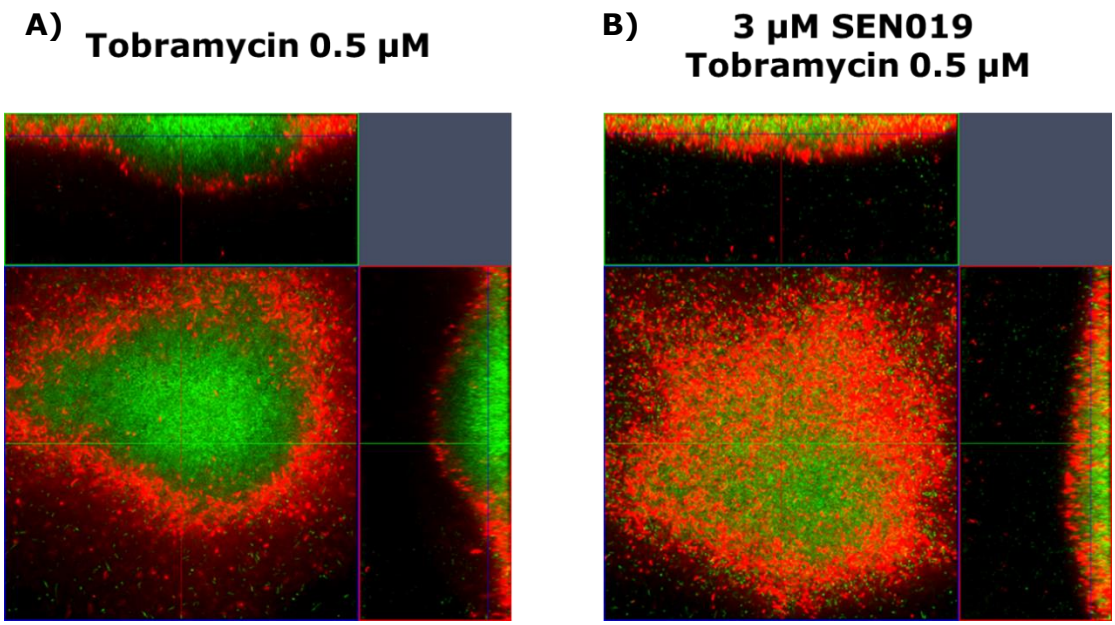

Figure 5.14 Tobramycin treated PAO1-L microcolonies. Biofilms were grown for 17 hours in a bioflux system at 37°C, constant 0.4 dyn flow of LB 10% media, antibiotic was added after 17 hours of growth and incubated for 4 more hours. **A)** DMSO or **B)** SEN019 were added from time 0. Green corresponds to Gfp and red to PI fluorescence. Image was taken at 40X magnification.

In a similar fashion to what has been shown with ciprofloxacin above (Figure 5.12), Biofilms were allowed to grow without compound for 15 hours, before being treated for 2 hours simultaneously with tobramycin and SEN019 or SEN032 to investigate the effect this treatment approach would have in matured biofilms. Results showed that tobramycin did not present obvious enhanced activity on its own or in combination with the SEN compounds (Figure 5.15).

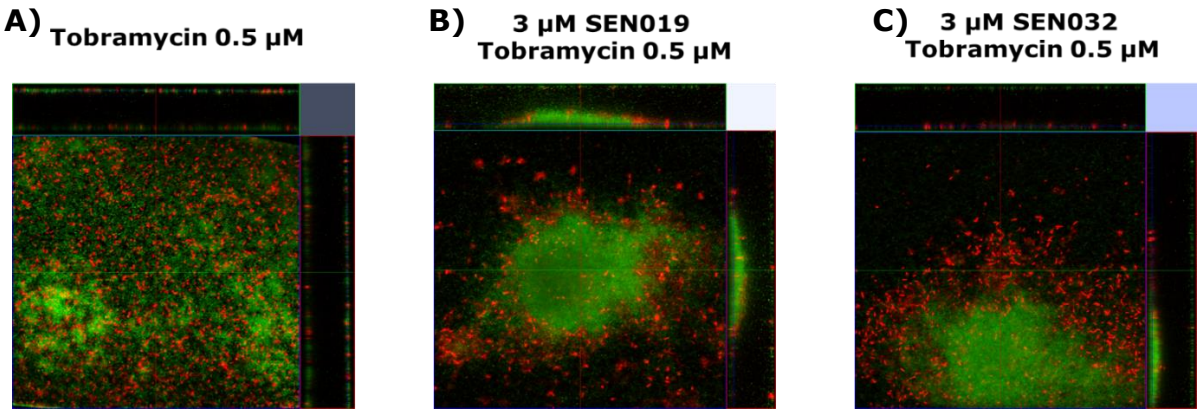

Figure 5.15. PAO1-L biofilms treated with tobramycin and SEN019 or SEN032 without previous compound exposure. PAO1-L mTn7::*gfp* biofilms were grown in LB 10% for 15 hours at 0.5 dyn 37°C without any compound before being incubated for further 2 hours with **A)** 0.5 µM tobramycin and **B)** 3 µM SEN019 or **C)** SEN032. Pictures were taken at 20X, the green represents Gfp and red PI fluorescence. Untreated controls can be observed in Figure 5.2.

In an effort to observe the impact of tobramycin in much older biofilms, bacteria were allowed to grow in the Bioflux system for 48 hours before treating them with 0.5 μM tobramycin for another 24 hours. Results showed a significant prevalence of PI fluorescence coming mostly from binding to eDNA, which was covering the entirety of the flow chamber in the tobramycin control group, but appeared localised to the top and bottom of the biofilm in the group grown in the presence of tobramycin and SEN019 (Figure 5.16). Moreover, it seemed that the SEN019 group had a higher number of dispersed cells in the interphase compared to the control group, although this could be the result of the much thinner matrix (Figure 5.16).

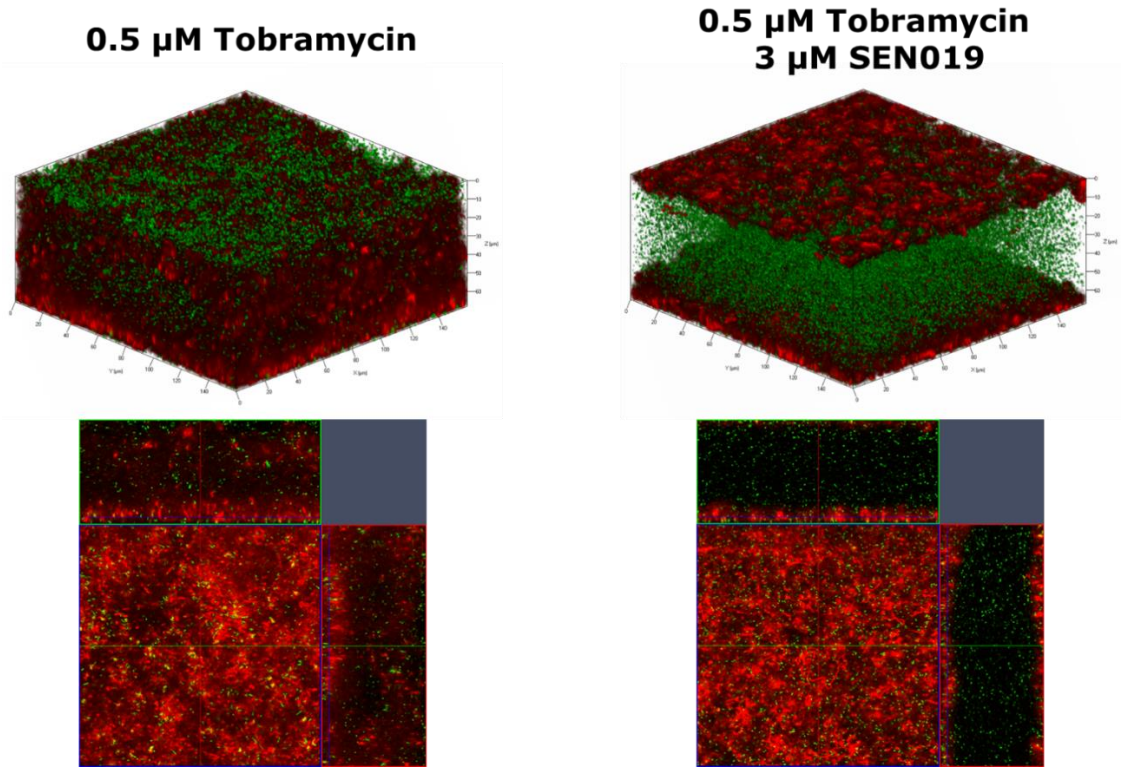

Figure 5.16. 3 day old PAO1-L biofilms, treated with tobramycin. Images at 40X in 3D and ortho representation taken from a P. aeruginosa mTn7::*gfp* Gm^R microfluidics biofilms. The biofilm was allowed to grow in a Bioflux system for 48 hours at 37° C in the presence of SEN019 3 μM or an equivalent volume of DMSO before adding 0.5 μM tobramycin for another 24 hours. The media used was LB 10% at 0.4 dyn. Counterstain was done with PI (red) which stained the DNA of dead cells and eDNA alike. Fresh media was added periodically to avoid running air through the system. Untreated controls can be observed in Figure 5.4.

5.3.2.3. Bioflux quantitative analysis of the impact of SEN compounds and antibiotics combinations on biofilms

Comstat2 was used to quantify biomass and surface from the Z stack images obtained from CLSM. All images used for quantitation were modified with ZEN lite black edition™, interpolating the brightness to 30.00 and contrast level to 90.00 (out of 100) from their original values to improve and standardise the relative pixel intensity distribution.

5.3.2.3.1. Biofilm biomass

Biofilm biomass quantitation is an important measurement to determine the overall impact of different biofilm treatments and growth conditions. Gfp biomass data correlates to the amount of bacteria present in the sample whereas PI data can provide data regarding dead cells and eDNA although it is not possible to differentiate between them.

Biofilms were grown for 17 hours before being treated with antibiotic for another 4 hours at the same flow rate. A large pool of samples was quantified, Gfp fluorescence was highly variable in untreated biofilms (Figure 5.17). The addition of SEN019 did not seem to have a significant effect on biofilm development. Biofilms treated with ciprofloxacin had lower average values in Gfp and PI when SEN019 was present, the differences were significant in the Gfp channel. Another significant difference was observed between tobramycin groups when SEN019 was present, both fluorescences had lower averages and less scatter (Figure 5.17). The addition of antibiotics significantly decreased the Gfp fluorescence compared to the control groups, particularly the SEN019 + tobramycin group which was also significant when compared with the tobramycin group. The PI fluorescence from the tobramycin groups was significantly lower than the DMSO control, especially the SEN019 + tobramycin which also was significantly lower than the SEN019 untreated control and the tobramycin only groups. Finally, the PI fluorescence of the ciprofloxacin group was not significantly different from the DMSO control, but the combinatory SEN019 + ciprofloxacin was, nevertheless, the difference with the SEN019 group was not significant.

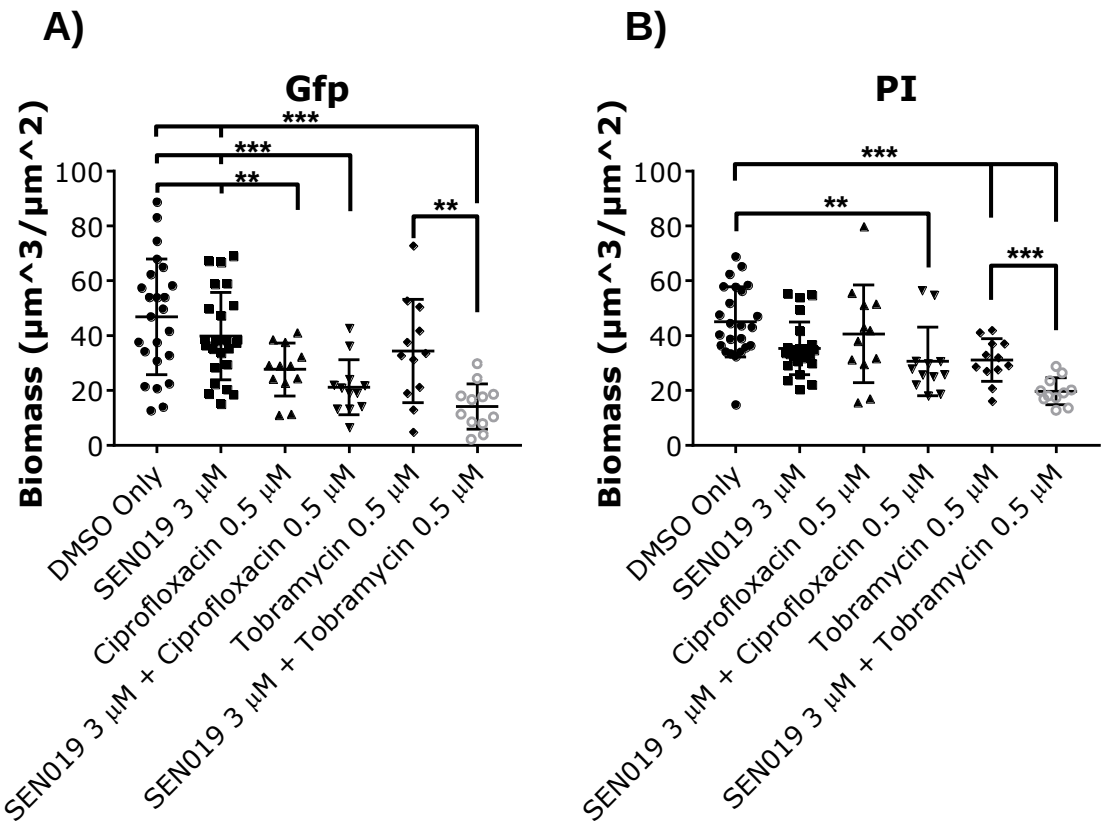

Figure 5.17. Biomass data from PAO1-L WT biofilms grown in presence of 3µM SEN019. PAO1-L mTn7::*gfp* Gm^R biofilms were grown in Bioflux for 17 hours at 37°C 0.4 dyn/cm^2 and treated with 0.5 µM acidified ciprofloxacin or 0.5 µM tobramycin for 4 hours, control conditions had 0.5% DMSO instead of SEN019. Confocal microscopy data was analysed with Comstat2. A) Gfp corresponds to green fluorescent protein. B) PI is Propidium iodide stained bacteria and eDNA. Data has been trimmed to remove significant outliers. Welch's t tests were performed for statistical significance, (**) $p<0.01$, (***) $p<0.005$.

5.3.2.3.2. Biofilm surface coverage and surface to biovolume ratio

Another useful measurement to quantify biofilms is the surface coverage and the surface to biovolume ratio. The surface area of a biofilm can provide information regarding how far spread the biofilm was in the particular sample imaged which has direct implications in its structure. Taking it one step further, dividing the surface area by the total volume can provide insightful information regarding how the biofilm is structured. A higher surface-to-biovolume value means that most of the fluorescence is distributed and spread, while lower values imply that the fluorescence is concentrated. In an easy analogy, a sheet of paper will have higher surface-to-biovolume value than a ball with the same exact surface, because the sheet of paper has much lower volume than the ball.

Quantitation showed that antibiotic treatment lowered the surface area values and usually increased the surface to biovolume ratios. This effect was more prominent in SEN019 groups. Samples treated with tobramycin and SEN019 also presented very low scatter of surface area and surface to biovolume ratios as previously observed with the biomass quantitation (Figure 5.17). Notably, when Gfp surface values where divided by those of PI, the scatter was slightly corrected and results showed that samples treated with tobramycin had lower ratios than the other groups. This means that the surface covered by PI fluorescence compared to the Gfp is higher in these groups than the others, suggesting that tobramycin has a higher impact on biofilm PI fluorescence than ciprofloxacin (Figure 5.18C).

For the surface to biovolume ratio analysis, the group treated with tobramycin and SEN019 presented a higher ratio than the other groups in the Gfp fluorescence which suggests that the Gfp fluorescence concentrates in certain points under these conditions (Figure 5.18D). There was also an increase in the PI fluorescence, however the tobramycin only group also presented a similar increase with no significant differences (Figure 5.18E). There were no significant differences when the ratio between fluorescences was analysed (Figure 5.18F).

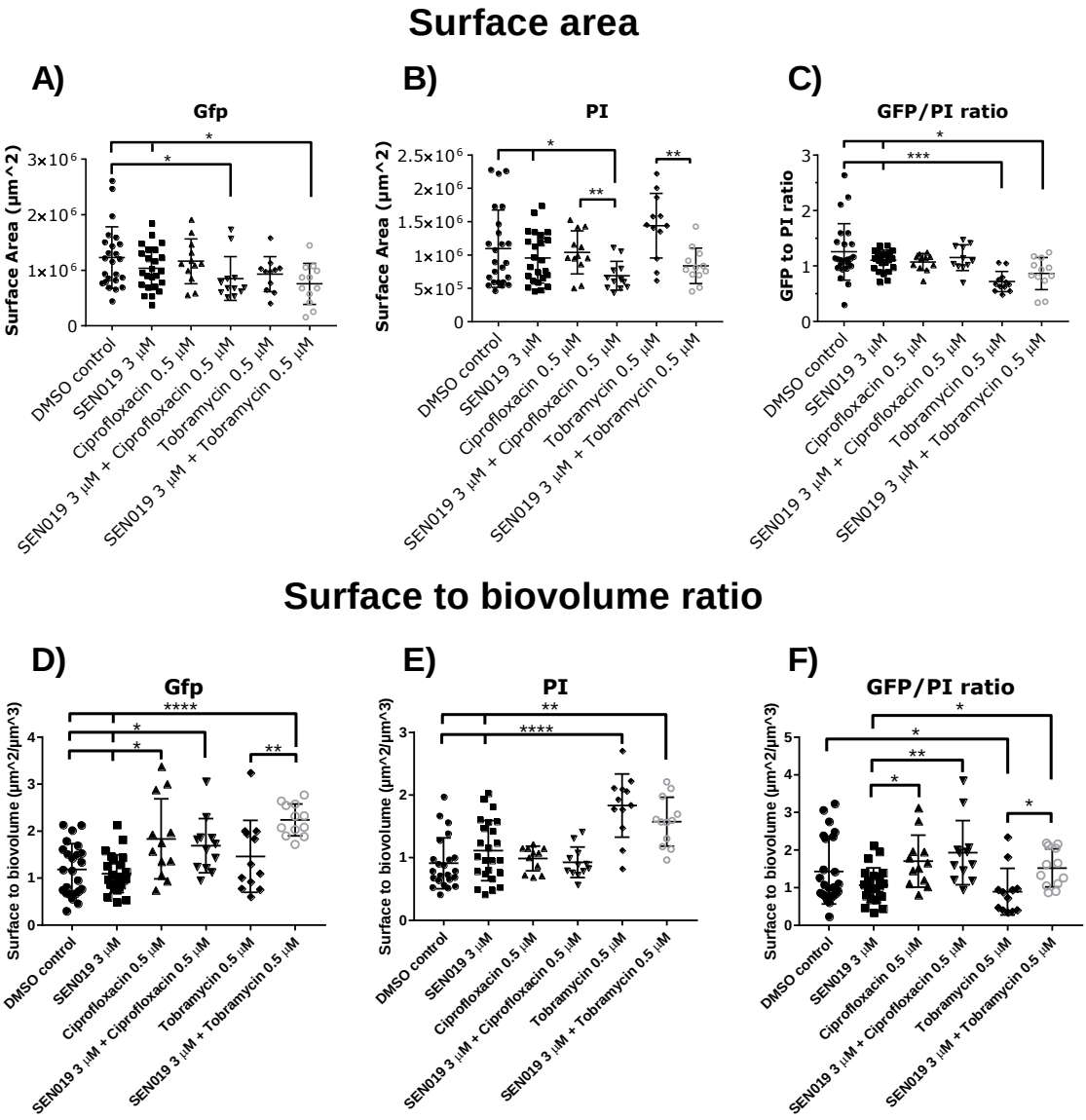

Figure 5.18. Surface area and surface to biovolume data from PAO1-L WT biofilms grown in presence of 3µM SEN019. PAO1-L mTn7::*gfp* Gm^R biofilms were grown in Bioflux for 17 hours at 37°C 0.4 dyn and treated with 0.5 µM acidified ciprofloxacin or 0.5 µM tobramycin on their own or in combination with 3 µM SEN019 for 4 hours (control condition was 0.5 % DMSO). Confocal microscopy data was analysed with Comstat2. **A)** Surface values for Gfp. **B)** Surface values for PI fluorescence, related to dead cells and eDNA. **C)** Is the ratio between surface values for each fluorescence. **D)** and **E)** are surface to biovolume ratios of Gfp and PI respectively and **F)** is surface to biovolume values of Gfp divided by those of PI. Significant outliers were removed. Welch's t tests were performed for statistical significance, (*) $p<0.05$, (**) $p<0.01$, (***) $p<0.005$, (****) $p<0.001$.

5.3.2.4. Testing SEN compounds with antibiotics under static biofilm conditions

Using some of the biofilm models described above, the impact of combinations of SEN compounds with ciprofloxacin and tobramycin was tested under static conditions.

5.3.2.4.1. SEN compounds with ciprofloxacin

Crystal violet assays were used to quantify any potential enhancement between ciprofloxacin and the PqsR antagonists in static biofilms. The assay was performed in M63/LB and LB10% media in 96 well plates. Biofilm formation according to the CV staining assay was significantly stronger in the M63/LB media, furthermore results showed that the addition of SEN088 decreased biofilms, more so in the samples grown in LB10%. However, the concentrations of SEN088 used highly exceeded the IC_{50} values determined in planktonic cultures for inhibition of P*pqsA* expression (Figure 5.19).

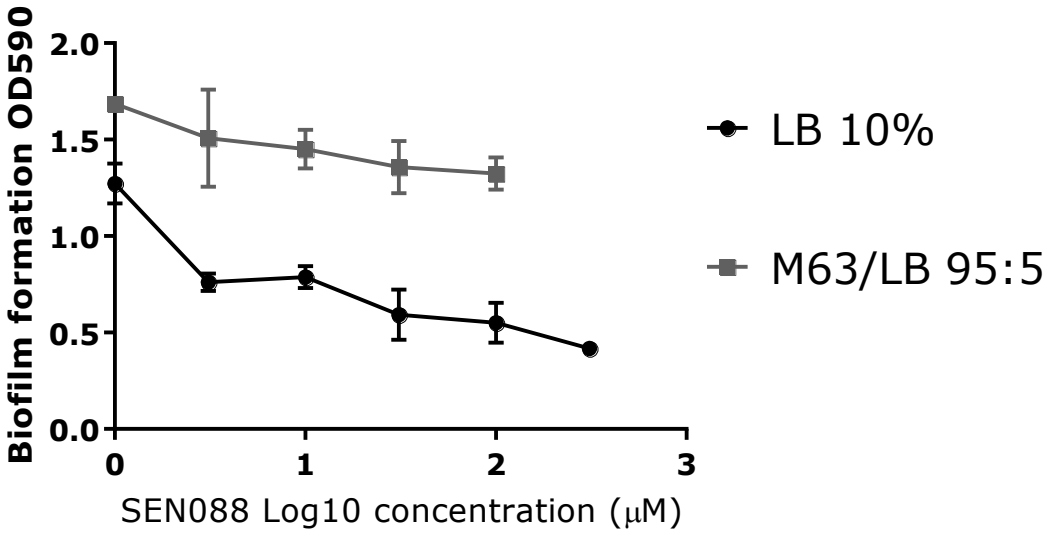

Figure 5.19. PAO1-L WT biofilms stained with Crystal violet assay treated with ciprofloxacin and different concentrations of SEN088. Biofilms were grown in polystyrene based 96 well plates using 200 µL of media at 37°C for 48 hours, the media was changed after the first 24 hours and acidified ciprofloxacin (0.5 µM concentration). SEN088 was added from time 0. SEN088 concentrations tested were as follows: 0, 3.1, 10, 31, 100 and 310 µM. +/- Error bars represent the standard deviation of four biological replicates.

To ensure the optimal concentration of antibiotic was used in these experiments, a range of ciprofloxacin concentrations was tested in the static biofilm model. Two experiments were performed, adding ciprofloxacin at times 0 or at 24 hours and incubating for further 24 hours. These experiments were performed without adding any SEN compound. The addition of ciprofloxacin from time 0 showed that at 1 µM the biomass of the group actually increased compared to the control after 48 hours in antibiotic but further concentrations almost completely killed off all bacteria with barely any CV being retained (Figure 5.20A). The addition of ciprofloxacin after 24 hours showed an increase on biomass again at 1 µM

but further concentrations remained within 90% of the control except the 100 µM concentration which was at 83% (Figure 5.20B).

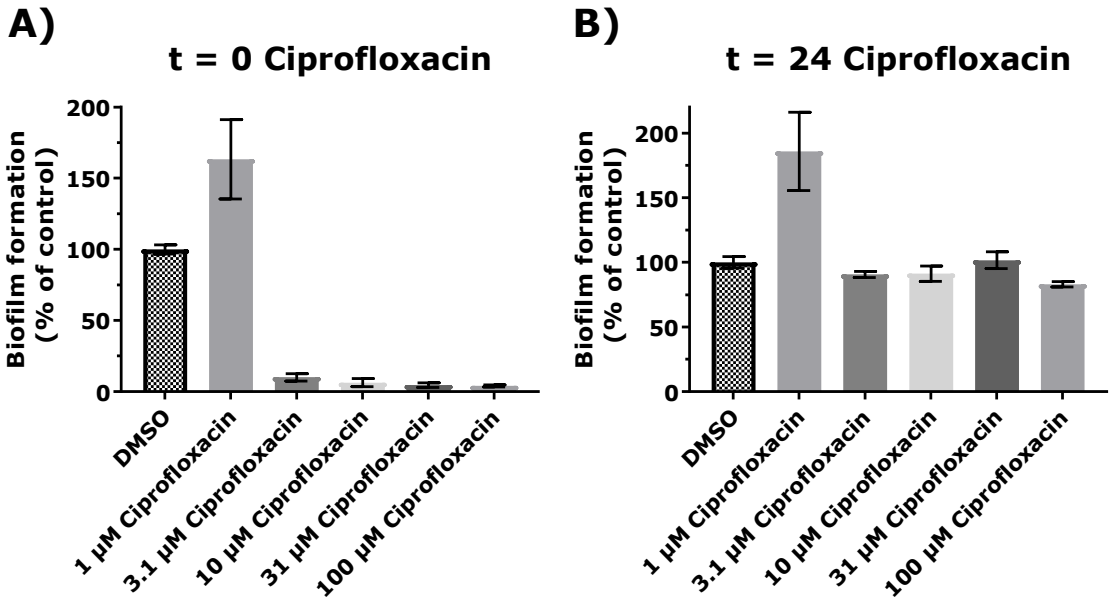

Figure 5.20. PAO1-L WT biofilms stained with CV 0.1% treated with increasing concentrations of ciprofloxacin added at t 0 or 24h. Biofilms were grown in polystyrene 96 well plates using 200 µL of media (M63/LB at 95:5 ratio) at 37°C for 48 hours, the media was changed after the first 24 hours. **A)** Ciprofloxacin was added from t 0 or **B)** after 24 h growth in clean media. +/- Error bars represent the standard deviation of biological triplicates.

3.1 µM Ciprofloxacin was selected as the working concentration and added to PAO1-L biofilms pre-grown for 24 hours under static under static conditions followed by further 24 hours incubation. The SEN088 or SEN089 compounds were used at concentrations of 10 and 30 µM. The addition of ciprofloxacin did not significantly change biofilm formation except at 30 µM SEN088, notably, the addition of SEN088 or SEN089 increased total biomass (Figure 5.21).

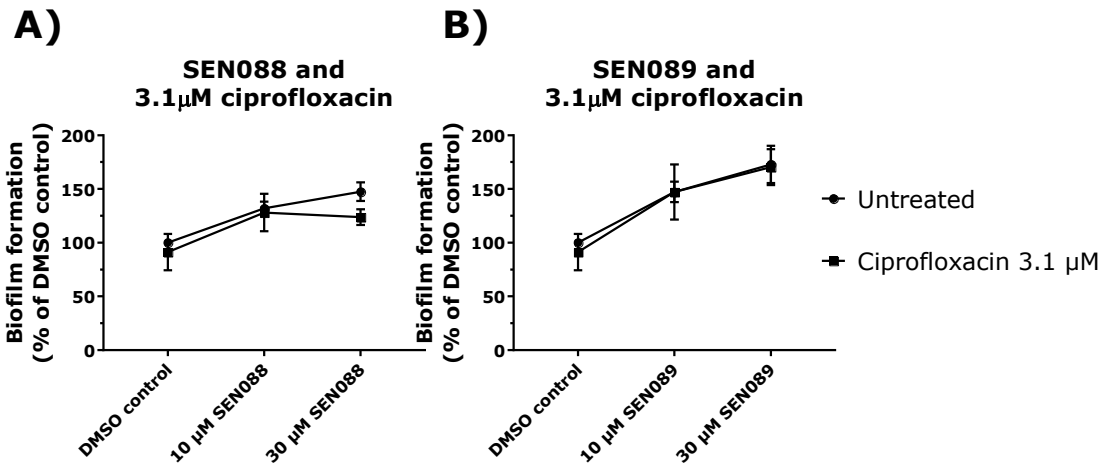

Figure 5.21. PAO1-L WT biofilms stained with CV 0.1% with 10 or 30 μM SEN088 and SEN089 from time 0 and 31 μM ciprofloxacin from t 24h. Biofilms were grown in polystyrene 96 well plates using 200 μL of media (M63/LB at 95:5 ratio) at 37°C for 48 hours, the media was changed after the first 24 hours. +/- Error bars represent standard deviation of four biological replicates.

5.3.2.4.2. SEN compounds with tobramycin

CV was used to quantify the impact of tobramycin on static biofilms grown in 96 well plates. An assay with increasing concentrations of SEN088 (0, 3.1, 10, 31, 100 and 310 μM to fit a logarithmic scale) and a small dosage of tobramycin showed that biomass increased along with the SEN088 concentrations in both media (Figure 5.22). It is noteworthy that the biofilm formation of the control LB10% group was originally rather high and control levels were only restored with 100 and 310 μM SEN088, the reasons for this are currently not known. Unfortunately, the 310 μM SEN088 M63/LB samples could not be measured because the values were too high for the dilution factor used.

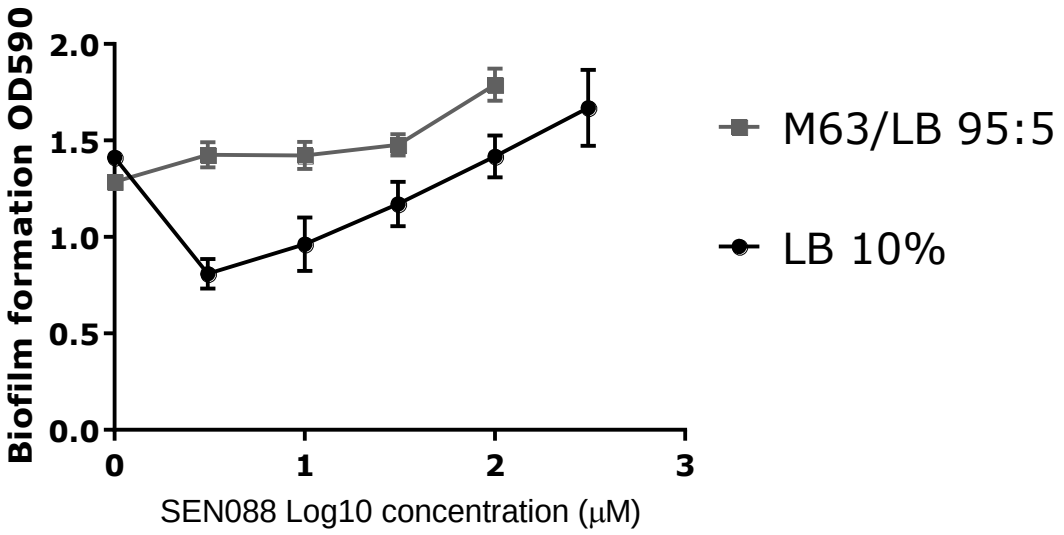

Figure 5.22. PAO1-L WT biofilms stained with CV 0.1% treated with tobramycin and different concentrations of SEN088. Biofilms were grown in polystyrene 96 well plates using 200 µL of media at 37°C for 48 hours with SEN088 added from time 0. The media was changed after the first 24 hours and the antibiotic (0.5 µM concentration) was added then for the remaining 24 hours. +/- Error bars represent the standard deviation of four biological replicates.

To identify the optimal concentration of tobramycin to use in these experiments a range concentrations of this antibiotic were tested in the 96 well static biofilm model. Tobramycin was added at times 0 and at 24 hours in separate assays. PAO1-L biofilm growth was not inhibited by the addition of tobramycin from time 0 until 31 µM antibiotic concentration was used and the biomass was significantly increased at 10 µM (Figure 5.23A). When tobramycin was added after 24 hours, the biofilm was not cleared at any concentration tested, only at 100 µM did the biomass show a 30% decrease, notably there was a significant increase in biomass at 10 µM (Figure 5.23B). The working concentration for tobramycin was thereby chosen to be 31 µM as it was the first concentration to have an impact at t=0, to test if the addition of PqsR antagonist from the beginning of growth could create a visible synergistic effect upon addition of the antibiotic at 24 hours.

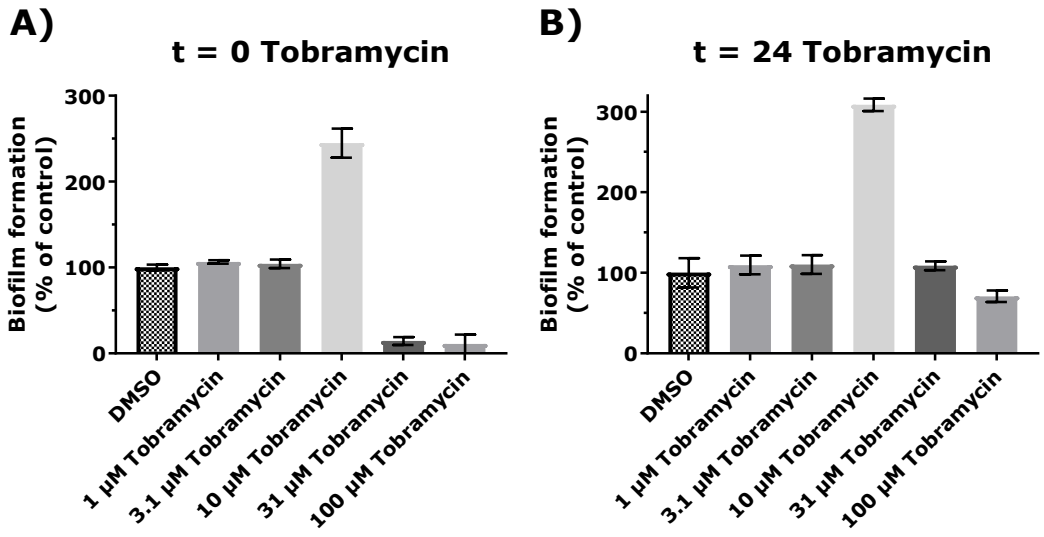

Figure 5.23. PAO1-L WT biofilms stained with CV 0.1% treated with increasing concentrations of tobramycin added at t 0 or 24h. Biofilms were grown in polystyrene 96 well plates using 200 µL of media (M63/LB at 95:5 ratio) at 37°C for 48 hours, the media was changed after the first 24 hours. **A)** Tobramycin was added from t 0 or **B)** after 24 h growth in clean media. +/- Error bars represent the standard deviation of biological triplicates.

Static PAO1-L biofilms were grown for 24 hour in the presence of the SEN compounds or DMSO after which 31 µM of tobramycin was added and incubated for a further 24 hours. SEN088 or SEN089 were tested at 10 or 30 µM concentrations. Tobramycin significantly decreased biofilm formation in the DMSO control and the addition of 10 or 30 µM of SEN088 further decreased it in presence of the antibiotic (Figure 5.24A). On the other hand, the addition of SEN089 at 10 µM had no significant impact and at 30 µM there was a slight increase in biofilm formation (Figure 5.24B). The compounds on their own had a positive impact on this phenotype at 30 µM (Figure 5.24).

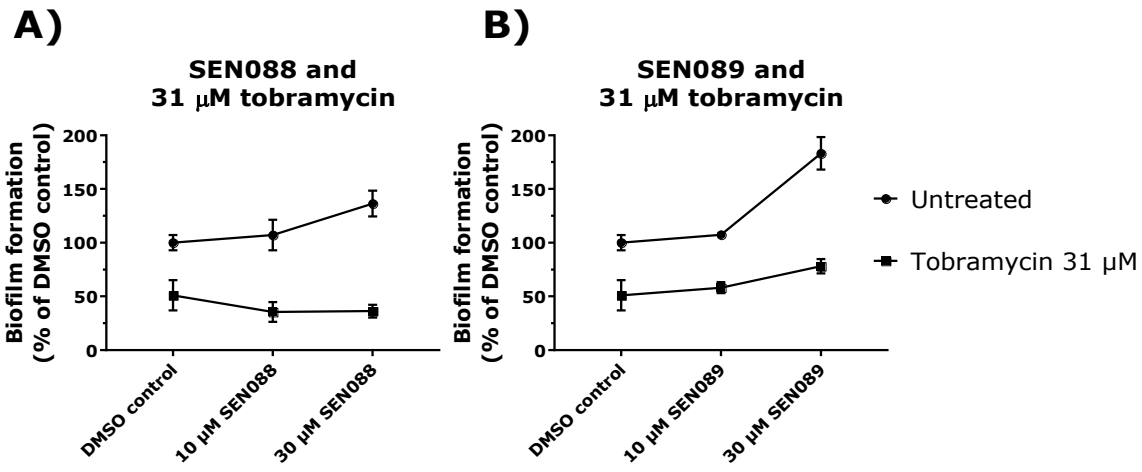

Figure 5.24. PAO1-L WT biofilms stained with CV 0.1% with 10 or 30 µM SEN088 and SEN089 from time 0 and 3.1 µM tobramycin from t 24h. Biofilms were grown in polystyrene 96 well plates using 200 µL of media (M63/LB at 95:5 ratio) at 37°C for 48 hours, the media was changed after the first 24 hours. +/- Error bars represent standard deviation of four biological replicates.

5.3.3. Assessing the impact of SEN compounds and antibiotics on other biofilm parameters

To better understand the impact of the SEN/antibiotic combinations on biofilms, metabolic activity, dispersal and physical shearing as well as the production of eDNA were measured using some of the above biofilm models.

5.3.3.1. Determination of metabolic activity by ATP quantitation

Measuring ATP levels is useful to quantify the overall metabolic activity of the biofilm biomass. The resulting data should be considered as the average activity of the remaining biofilm after a wash has been performed and analysed, taken into account that there are two distinct metabolic states (active and dormant) found within most biofilms (Pamp *et al.* 2008). Dead cells will only show very low remaining activity (if any). However, the assay has two limitations. The addition of some antibiotics, especially at subinhibitory concentrations, can cause significant bacterial stress and increase their metabolic rate. Moreover, dormant cells in the stalk or base layers of the biofilms are the main source of persisters (Wood, Knabel and Kwan 2013).

The impact of tobramycin on ATP production was assessed in a media that strongly promoted biofilm formation. Biofilms were grown in 96-well polystyrene plates with a range of antibiotic concentrations for 48 hours. During the first day, the biofilm was grown in M63/LB 95:5 only and tobramycin was added after 24 hours. Results showed an ATP increase at 3.1 and 10 μM (Figure 5.25). Notably, there is partial resemblance to the data obtained from CV biofilm assays carried out in a previous experiment (Figure 5.23B).

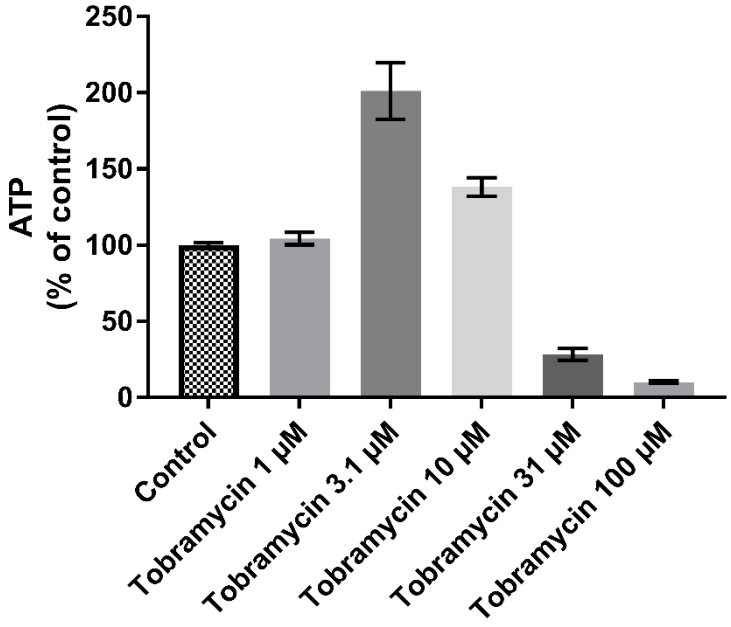

Figure 5.25. ATP levels of PAO1-L WT biofilms treated with increasing concentrations of tobramycin. Biofilms were grown in 96-well polystyrene plates using 200 μL of media at 37°C for 48 hours, the media was changed after the first 24 hours and tobramycin was added then. ATP measurements were done using the BacTiter-Glo™ Microbial cell viability assay from Promega™. +/- Error bars represent standard deviation of four biological replicates.

SEN089 was then tested at 10 and 30 μM in combination with 20 μM tobramycin. This concentration of antibiotic was chosen in order to have a relative decrease in ATP from the control and at the same time be able to clearly observe potential differences when the compounds were added. Samples grown with SEN089 without antibiotic showed a ≈50% increase in ATP at 10 or 30 μM SEN089. The addition of 20 μM tobramycin decreased the ATP to 13% in the control group but the SEN089 groups remained at around 30% of the control (Figure 5.26). It should be noted that the decrease in ATP due to tobramycin was significantly larger in SEN089

groups than in the control, 1.305 $\times 10^5$ in the control vs 1.803 and 1.797 $\times 10^5$ in 10 and 30 µM SEN089 (Figure 5.26).

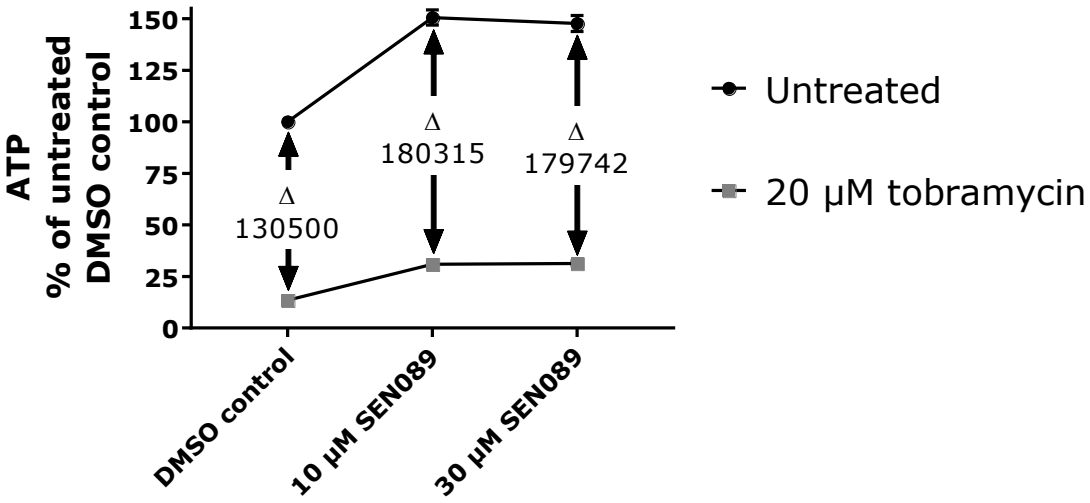

Figure 5.26. ATP levels of PAO1-L WT biofilms treated with SEN089 and 20 µM of tobramycin. Biofilms were grown in polystyrene 96 well plates using 200 µL of media at 37°C for 24 hours after which media was changed and tobramycin added followed by a further 24 hours incubation. SEN089 was present through the 48 hours of incubation. ATP measurements were done using the BacTiter-Glo™ Microbial cell viability assay from Promega™. All values are standardised against the DMSO control group which is assumed to have 100% ATP production. Δ values represent differences between untreated and treated raw values in RLUs. +/- Error bars represent standard deviation of four biological replicates. Some error bars are shorter than the height of the symbol.

5.3.3.2. Dispersed cells and Biofilm physical shearing

Microscopy analysis of biofilms grown in the presence of SEN compounds had shown structural differences in some biofilm models even if growth itself was not impaired. It was therefore hypothesised that their resistance to physical pulling forces and shearing would be significantly different between treated and untreated biofilms.

PAO1-L biofilms were initially grown in Bioflux for 15 hours, just enough to allow an early mature biofilm to develop. Biofilms were then treated with 0.5 µM ciprofloxacin or tobramycin for 2 h and a strong wash was applied afterwards at 20 dyn/cm^2 for 5 minutes to determine how much of the biofilm could be sheared off. Surprisingly, the control group still presented a significant number of intact and healthy microcolonies. On the other hand, biofilms grown in presence of 3 µM SEN019 had less microcolonies (Figure 5.27). Treatment with ciprofloxacin proved to be particularly effective against biofilm integrity with biofilms being washed away in both

ciprofloxacin groups. Treatment with tobramycin showed a few remaining microcolonies although they were mostly formed by dead cells, however, biofilms grown in SEN019 and treated with tobramycin were extremely sensitive to washing, the channel was almost completely clear and very few attached cells could be observed (Figure 5.27).

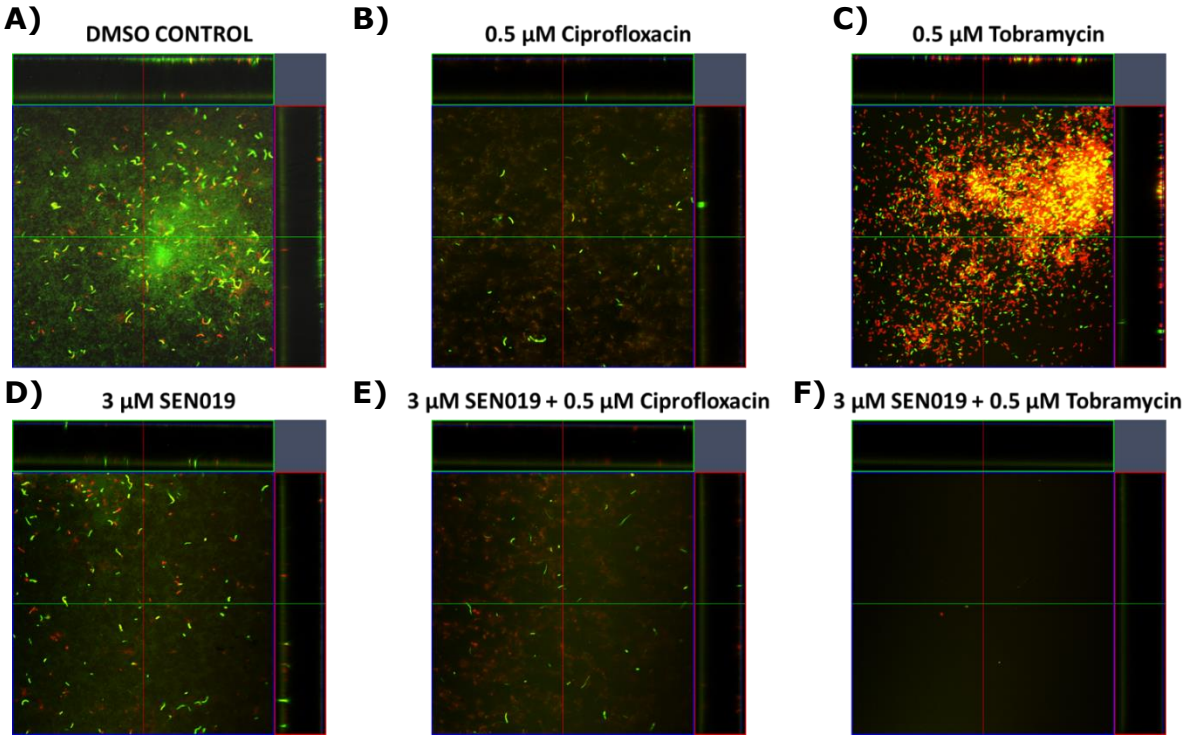

Figure 5.27. PAO1-L washed biofilms. PAO1-L WT 15 h old biofilms grown in the Bioflux system were incubated for further 2 hours in LB 10% with 0.5 µM ciprofloxacin or tobramycin including 1 µM PI and Syto9. SEN compounds and DMSO were added from time 0. After incubation, a wash was performed by running fresh media at 20 dyn/cm^2 for 5 minutes. Pictures taken at 20X magnification, green is syto9 and red is PI fluorescence. **A)** shows the untreated control, **B)** was treated with ciprofloxacin and **C)** with tobramycin, **D)** was untreated but grown with SEN019, **E)** was grown with SEN019 and ciprofloxacin and **F)** with SEN019 and tobramycin.

To test the resistance to shearing force in much more mature biofilms, PAO1-L was grown for 48 hours in the Bioflux system in the presence of SEN019 or DMSO at which point 0.5 µM tobramycin was incorporated into the medium and incubated with flow for a further 24 hours. After the incubation period, the chambers were washed at 20 dyn/cm^2 for 15 minutes. Incubation for 3 days using this model showed the presence of very thick matrix which embeds only a few remaining bacteria. However, it cannot be ruled out that more bacteria are present within the matrix but their metabolic activity may be so low that the expression of the Gfp reporter is below detection. Biofilms grown under these conditions were always much more resilient to shearing forces than their younger

counterparts. The untreated groups retained a significant portion of the biofilm still attached to the channel, particularly the DMSO control group which also presented a larger number of dispersed cells in the interphase (Figure 5.28). When the biofilms were treated with tobramycin for the last day and then washed, a much smaller fraction remained. Z stacks obtained after washing showed that the control group had a much greater number of cells suspended in the interphase and very few and small microcolonies remained attached. However, most of those still presented healthy bacteria within. On the other hand, biofilms that had been grown with SEN019 showed much smaller numbers of dispersed cells in the interphase and similar levels of microcolonies remained attached, nevertheless it was noteworthy that the vast majority of the cells found within those were dead as revealed by the PI fluorescence (Figure 5.28).

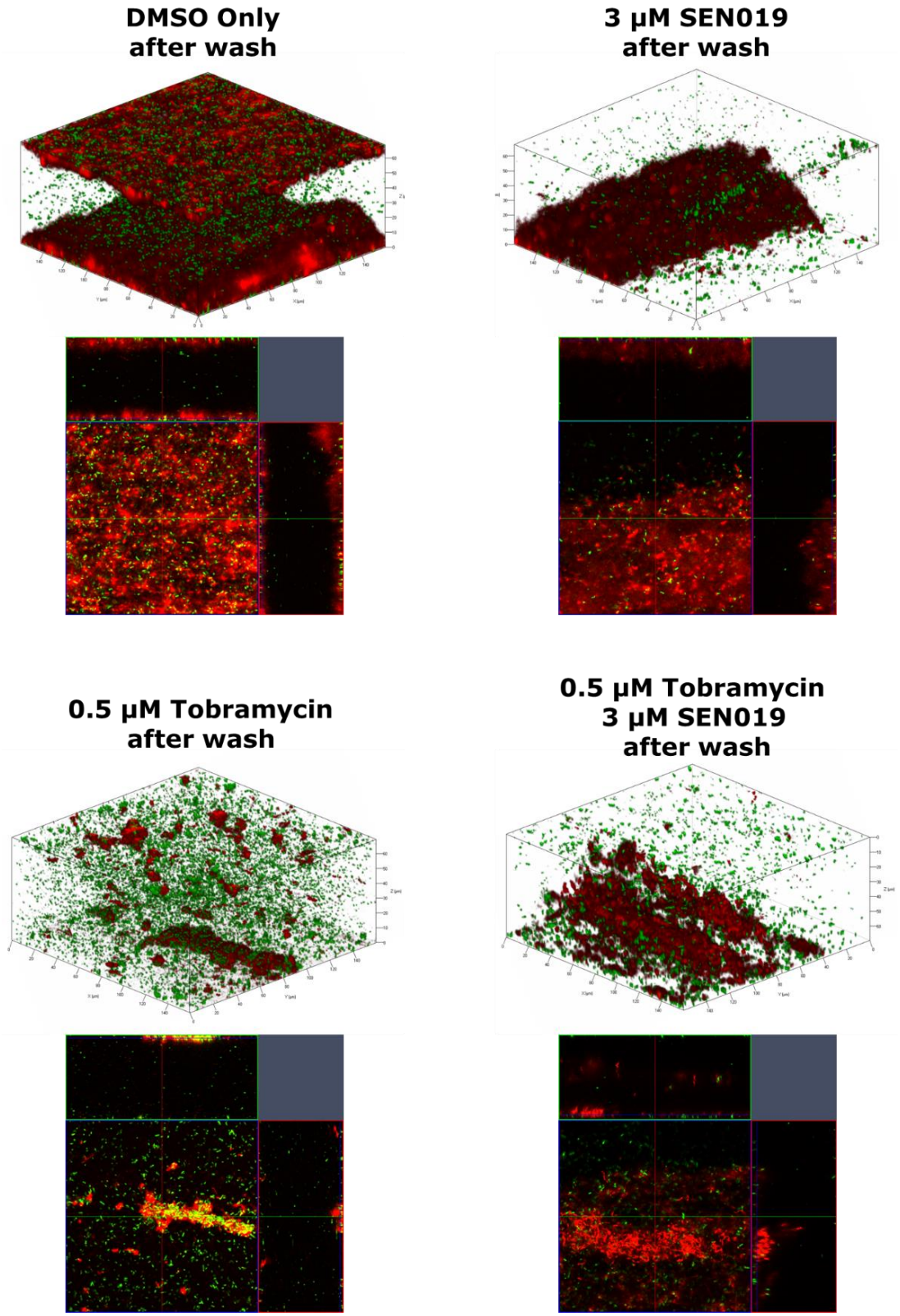

Figure 5.28. Washed PAO1-L biofilms with and without SEN019 and tobramycin. Images at 40X in 3D and orthogonal representation taken from a P. aeruginosa mTn7::*gfp* Gm^R microfluidics biofilms. The biofilm was allowed to grow in a Bioflux system for 72 hours at 37° C in LB 10% at 0.4 dyne with 3 µM SEN019 or an equivalent volume of DMSO. Samples treated with 0.5 µM tobramycin were in contact with the antibiotic during the last 24 hours of incubation. The biofilm was washed for 15 minutes at 20 dyn/cm^2. Counterstain was done with PI (red) which stained dead cells and eDNA alike. Fresh media was added periodically to avoid running air through the system.

5.3.3.3. Determination of natural biofilm dispersal and impact of physical shearing

Cells from the assay from Figure 5.27 were analysed in the flow cytometer for absolute cell counts after pooling together all replicates in their corresponding groups. Samples grown for a total of 17 hours (15 h growth with SEN019 or DMSO followed by 2 h of antibiotic treatment) had their outlet waste collected and also the wash after running it for 5 minutes at 20 dyn/cm^2. Results for the dispersed fraction showed that the SEN019 groups had higher total cell counts in almost all conditions, however, the amount of syto9, live cells dispersed was the same in the control and SEN019 groups (Figure 5.29A). In the total cells count of the biofilm fraction, only the untreated groups presented major differences, with biofilms grown in the presence of SEN019 having lower counts than their control counterparts. The tobramycin total counts were similar to the untreated levels, while the ciprofloxacin counts were lower than the other groups. This could be due to the reduced biofilm formation or to the size of the elongated cells that skipped quantitation (Figure 5.29B). Syto9 counts were higher for groups not treated with antibiotics, although the SEN019 had slightly lower counts than the DMSO control. The ciprofloxacin groups presented the lowest bacterial counts, however the tobramycin groups had the biggest differences between DMSO control and SEN019. Interestingly, PI stain was significantly lower in the SEN019 biofilm fractions, especially in groups treated with antibiotic (Figure 5.29B).

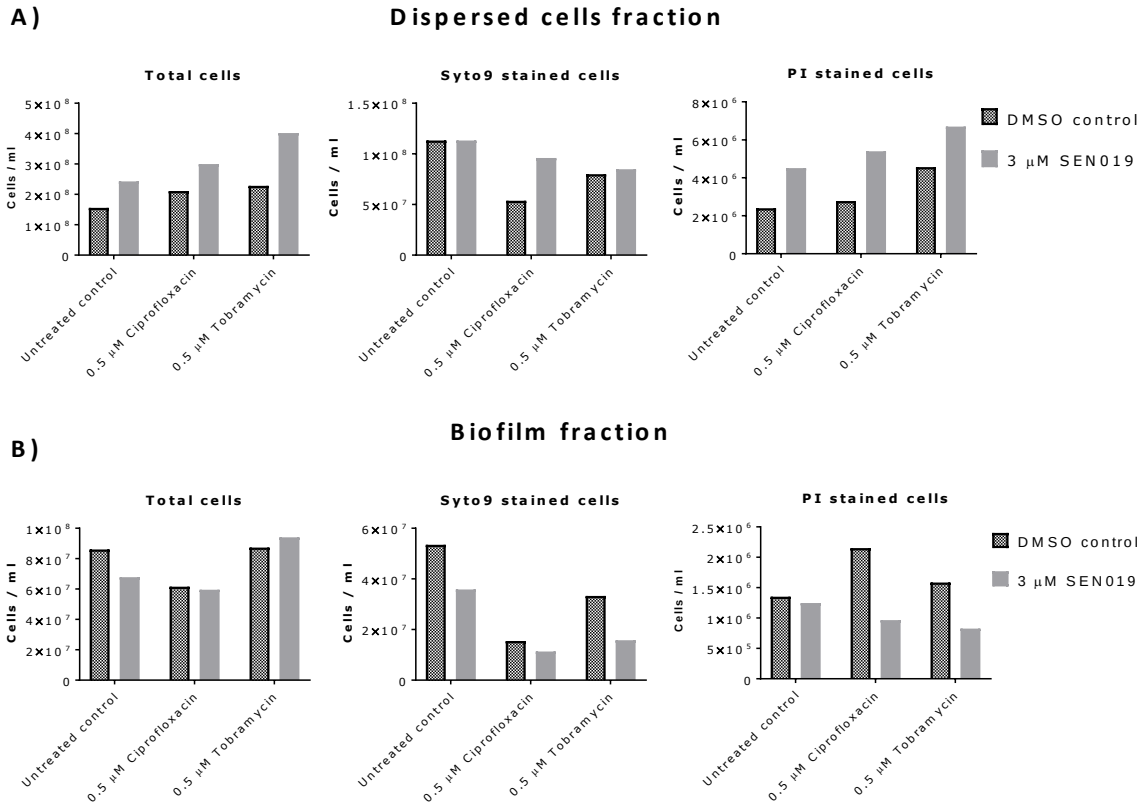

Figure 5.29. Flow cytometry cell counts of washed biofilms and dispersed cells. PAO1-L WT cells were grown in a 48 well Bioflux microfluidics system with LB 10% for 15 hours at 37 °C and 0.5 dyn before being treated for another 2 hours with 0.5 µM Ciprofloxacin or Tobramycin. Some biofilms were grown in presence of either 3 µM SEN019 or DMSO from time 0. Samples were stained with Syto9 and PI with the Live/Dead Backlight® stain, Total cells are the total sum of both groups. A) The waste from the outlet was collected and labelled as Dispersed cells fraction. B) The Biofilm fraction was collected after washing the channel with fresh media at 20 dyn/cm^2 for 5 minutes. There are no error bars because the results are absolute counts of pooled replicates.

5.3.4. Impact of SEN compounds on eDNA levels

5.3.4.1. Visualisation of eDNA on untreated biofilms

The sensitivity of the microscopy system used is high enough to detect the eDNA stained with PI in the extracellular matrix. This can provide very useful insights regarding the biofilm structure, however, it can also introduce biases in dead biomass quantitation. It has been observed that most of the PI fluorescence comes from eDNA rather than dead cells, as can be seen in Figure 5.30 and also in Figure 5.3.

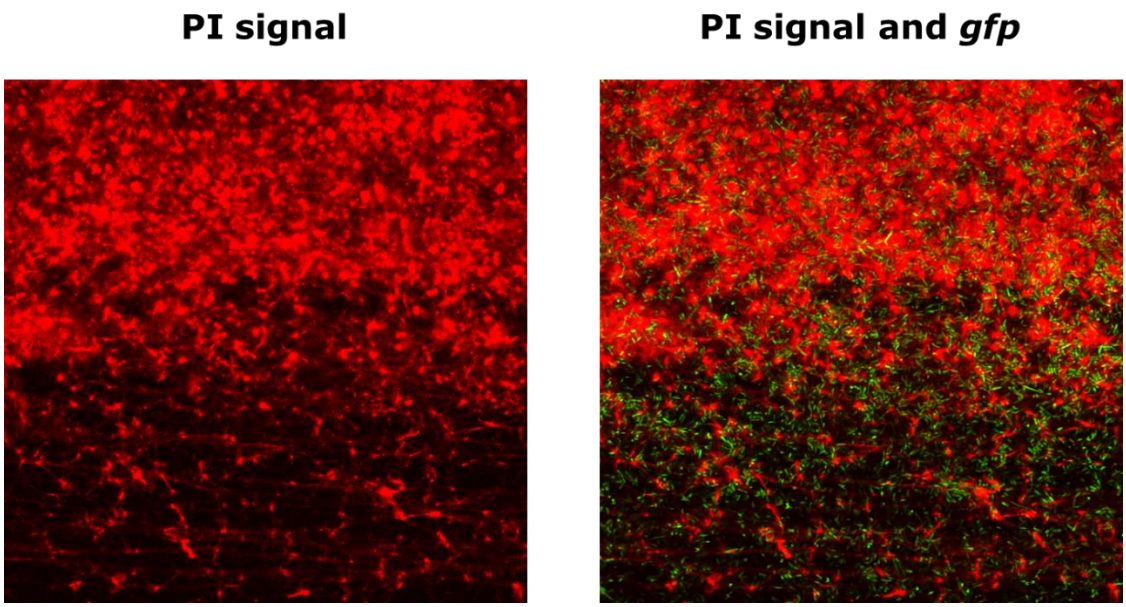

Figure 5.30. PAO1-L microfluidics biofilm slide at 40X. Image taken from PAO1-L WT mTn7::*gfp* Gm^R. The biofilm was grown in a Bioflux system for a total of 72 hours at 37° C in control conditions, the media used was LB 10% at 0.4 dyn. Counterstain was done with PI (red) which stained dead cells and eDNA alike. Fresh media was added periodically to avoid running air through the system.

5.3.4.2. Suspended DNA from planktonic cells treated with SEN compounds

One of the hypothesised impacts on biofilm structure by the PqsR antagonists is the reduction of autolysis, which would generate less eDNA. In order to quickly assess this, an assay which extracted DNA from the filtered supernatant of planktonic cells that had been grown overnight in LB was performed.

Results revealed that under these conditions, the addition of compounds did not have any significant impact on the suspended DNA found in the media (Figure 5.31). The potential eDNA attached to the cells was not quantified as it was discarded with the pellet.

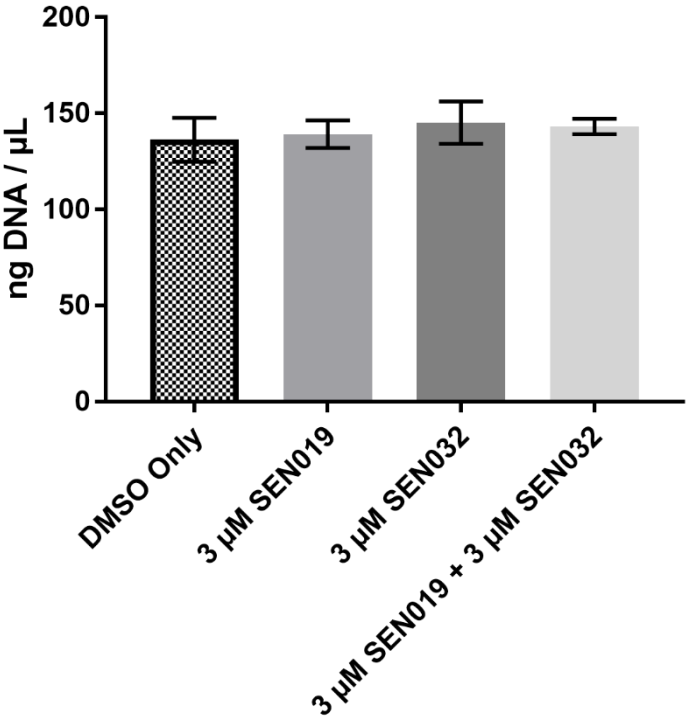

Figure 5.31. DNA concentration from filtered supernatants of PAO1-L WT. Bacteria were grown for 16 hours at 37° C and 200 rpm in 100 glass flasks with 10 ml of LB. Conditions tested were DMSO as solvent control (final concentration 0.1 %), 3 µM of SEN019, 3 µM of SEN032 and a combination of both at 3 µM each. 450 µL of filtered SN were used for the quantitation. +/- Error bars represent the standard deviation of biological triplicates.

5.3.4.3. eDNA in biofilms treated with SEN compounds

To better assess the eDNA production in biofilms, a static, 96-well plate system was chosen. Ethidium homodimer (etho) can be used to measure the presence of eDNA and dead cells in the culture as it is a high affinity DNA binding dye that only penetrates cells if membranes are disrupted. PAO1-L WT was grown in biofilm-promoting media M63/LB at 95:5 ratio (Thomann *et al.* 2016) for 24 hours. A measure of etho fluorescence was taken every 30 minutes and assumed to be mostly coming from eDNA rather than dead cells as previously observed (Figure 5.30).

Results showed a significant decrease in etho fluorescence when the cultures were grown in the presence of 1 µM SEN089 (Figure 5.32). Values used to calculate the area under the curve were divided by the OD_{600} to normalise any potential growth differences (for which there were none in

any sample). Therefore, it could be assumed that the differences in the etho assay came directly from a reduction of eDNA in the medium.

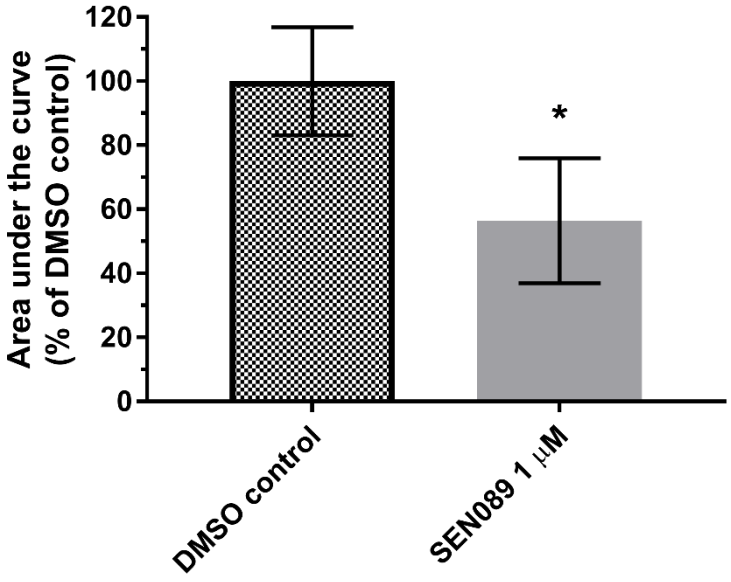

Figure 5.32. Ethidium homodimer fluorescence from PAO1-L WT cultures. Bacteria were grown for 24 hours at 37°C static in a polystyrene 96 well plate in 200 µL of M63 media mixed with LB in a 95:5 ratio. A TECAN™ plate reader was used to measure the fluorescence of etho by exciting at 535 nm and detecting the emission at 595 nm. The area under the curve was calculated from the absolute values of the sample values minus background divided by the OD_{600}. +/- Error bars represent standard deviation from biological triplicates. (*) indicates a $p < 0.05$ from a t test with Welch's correlation. The etho fluorophore is a cell impermeable indicator for the quantity of DNA found in the sample as it only presents fluorescence upon binding to DNA.

This approach would not be ideal to test in samples including antibiotics because under those circumstances, the dead cell fraction would become the dominant source of etho fluorescence and it would invalidate the method as an eDNA measuring assay.

5.4. Discussion

Results obtained show that the addition of SEN compounds significantly alters the structure of the biofilms in PAO1-L, PAO1-W and PA14, the impact of these alterations depends on the media tested which falls in line with previously described results (Shrout *et al.* 2006, 2012). The quantitation of biofilms highlighted significant differences between antibiotics probably because of their mechanism of action, since ciprofloxacin is not as cell-disruptive as tobramycin, the PI levels remained closer to the controls in some instances. Nevertheless, it has been evidenced that the incubation with SEN compounds sensitises biofilms to

the action of ciprofloxacin and tobramycin. This additive effect has also been recently reported elsewhere in literature (Thomann *et al.* 2016; Maura and Rahme 2017; Soukarieh *et al.* 2018a) showing that PqsR and the *pqs* system are emerging targets for the development of supporting therapeutic molecules.

The work performed in this chapter can be divided in three major parts: method optimisation, biofilm quantitation and antibiotic treatments.

The optimisation process required extensive repeats of several biofilm models and the setup of a robust non-biased approach. Most chosen pictures were post-processed to increase brightness and decrease contrast without modifying the metadata of the files used for quantitation in other software such as Comstat2 and just altered for visualisation purposes when required. The use of Comstat2 quantitation seemed to produce a high level of variability as shown in Figure 5.17 and Figure 5.18 hence the project moved towards the use of static biofilms, which provided similar answers through much simpler methods.

Finally, assessing the impact of antibiotics on biofilms grown in the presence of SENBIOTAR compounds was a cornerstone of the project. The initial concentration of antibiotics tested for biofilms, 0.5 µM, was chosen from previous experiments performed in the laboratory. This concentration was subinhibitory but still had a clear impact over microcolonies and some synergistic effect could be observed (Figure 5.10, Figure 5.11, Figure 5.13, Figure 5.14 and Figure 5.16). Nevertheless, quantitation of these conditions did not show obvious differences corresponding to what was observed, prompting the use of other quantitation methods in static biofilm models. A range of antibiotic and compound concentrations was tested in the new models to obtain the optimal working concentrations for each condition.

5.4.1. Comstat2 - quantitation of CLSM pictures

Comstat2 is a common tool for biofilm quantitation that can provide useful data in a range of variables, including biomass and surface area (Heydorn *et al.* 2000; Vorregaard 2008). Recent publications from the author's group has made use of this tool with significant success (Soukarieh *et al.* 2018a)

Because of the way that Comstat2 analyses data, quantitation is not related to fluorescence intensity *per se*. A threshold is set (manually or automatic) and any pixel with intensity values above that will be considered signal, any with lower intensity will be considered as no signal (Heydorn *et al.* 2000; Vorregaard 2008). This is a useful approach for general quantitation but heavily suffers from technical limitations during the imaging process.

In low fluorescence intensity conditions, the fluorescence is only slightly above the background and the thresholding process may introduce a significant bias where some fluorescence will be read as background, therefore obtaining lower measurements. In high intensity conditions, oversaturation means that some fluorescence will bleed out of the actual source and be overestimated (Vorregaard 2008).

Very careful imaging must therefore be performed in order to prevent serious over or underestimations while analysing with Comstat2. The ideal picture for quantitation will have a clean background with close to no fluorescence (blue, in a heat gradient visualisation), most of the signal should be light grey and white, with spots of red (oversaturation) expected from where fluorescence is densest (like the centre of a microcolony) (Heydorn *et al.* 2000; Klausen *et al.* 2003b). This is called relative pixel intensity distribution, if the relative pixel intensity of the images is not satisfactory, the metadata can be post-processed later, modifying brightness and contrast. This change should be clearly stated as it can significantly alter the quantitation process (Figure 5.33).

It should be noted that PI fluorescence can present some bias at the magnification used (40x) because it binds to DNA, also staining eDNA from the matrix, explaining the high PI fluorescence in biofilms grown without antibiotics (Figure 5.3 and Figure 5.33).

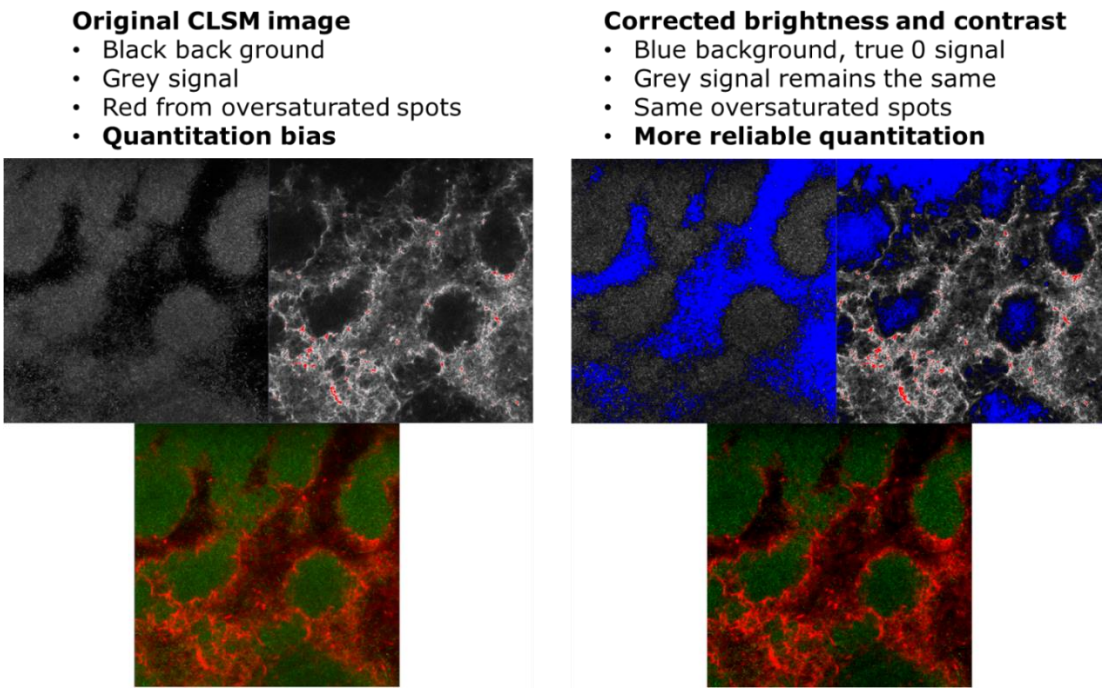

Figure 5.33. Original and corrected relative pixel intensity distribution of a CLSM biofilm 2D picture. A slice of a *P. aeruginosa* biofilm Z stack was pictured in a split configuration, with blue to red heat range indicator for Gfp and PI fluorescence and the standard green and red for the collated image. The blue in the range indicator corresponds to signal intensity 0, signal is represented from black to white as intensity grows stronger to the point of overexposure represented in red. A black background with dark grey signal will often cause issues with threshold dependent quantitation methods, as it will be difficult to separate. The original image was corrected by interpolating brightness to 30 and contrast to 90 to accentuate the separation between signal and background.

5.4.2. Microfluidics biofilm heterogeneity

The microfluidics model is a great tool to grow biofilms under a constant flow of fresh media, nevertheless it must be taken into account that its directionality can induce bias in the downstream parts of the chamber, this becomes a larger issue the longer the biofilm is grown for (Azevedo *et al.* 2017). Experimental observations from this body of work have evidenced that the leading edge of the biofilm will always receive fresh media and show more development than the following parts which receive downstream signals from the leading microcolonies that could potentially include dispersal effectors, biasing the assay. In all microfluidics samples, the furthermost downstream part of the biofilm was generally covered in PI stained matrix, with very few, dim bacteria in it, even in biofilms less than a day old. It is not possible to say if this was originated *in situ* or was the result of partial clogging from biofilm shearing. On the other hand, the leading edge will always be formed by younger microcolonies with more active cells and less developed biofilm matrix.

The requirement of multiple images for quantitation can often clash with the limited space offered by viewing channels in narrow flow systems such as Bioflux. In practice, this is the main source of variability during the quantitation process as observed in Figure 5.17. A solution would be to take only a few images from the leading edge of the biofilm for each biological replicate.

Nevertheless, this variation can provide some useful information. A very high standard deviation is tied to a heterogeneous biofilm, with microcolonies of different sizes and shapes that can sometimes be connected (Figure 5.2). It is interesting to observe that untreated biofilms had the largest standard deviations in the Gfp quantitation whereas biofilms subject to antibiotic treatment tended to present a lower scatter in the fluorescence (Figure 5.17).

5.4.3. Microfluidics biofilms biomass and surface

Biomass measurements showed that the groups under antibiotic treatment had lower Gfp values than their control counterparts, showing the bactericidal effect of the antibiotics over the biofilm which was particularly significant in the combinatory therapies (Figure 5.17A). Furthermore, tobramycin groups had some significant differences among them. The SEN019 + tobramycin group showed a lower level of Gfp and PI fluorescence (Figure 5.17). This suggests that there is higher biofilm clearance when tobramycin is added to SEN019 grown biofilms. The fact that ciprofloxacin groups did not present significant differences could be related to the biofilm not being disrupted although the SEN019 + ciprofloxacin presented lower averages which made it more significantly different from the control groups.

Surface measurements consisted of surface area and surface to volume ratios. Both variables provide useful information regarding the biofilm structure and distribution within the sample. In a similar fashion than biomass, surface area values presented strong variability. There are no significant differences in the surface area of the biofilm when it was grown in the presence of compound (Figure 5.18). The addition of tobramycin seemed to have the strongest impact over biofilm structure, while

ciprofloxacin did not seem to change much the surface area values. This is particularly obvious when comparing the surface area Gfp / PI ratios, with tobramycin groups being distinct from the others (Figure 5.18). This confirms the differences in PI fluorescence observed when tobramycin is added (Figure 5.13), as cells die and are stained in PI, it becomes much more widely distributed and so Comstat2 shows that the PI surface values are higher than Gfp and the ratio results below 1 (Figure 5.18C).

The addition of ciprofloxacin did not yield significant visual differences in PI fluorescence after two hours treatment, possibly because ciprofloxacin does not disrupt bacterial integrity (Figure 5.10) (Mason *et al.* 1995). In these groups, most, but not all, of the PI fluorescence will come from the matrix staining (Figure 5.11), which might be a reason why the surface and surface to volume values for PI are very close to those of the control, albeit with much less scatter (Figure 5.18). Moreover, it is very likely that the cell elongation caused by ciprofloxacin (Mason *et al.* 1995) generated overestimates in Gfp fluorescence quantitation, since a single bacterial cell could grow multiple times their normal size (Figure 5.10).

Comparing biomass and surface data can provide information regarding the biofilm structure. The higher intensity distributed over a larger areas shows that biofilm development was bigger in those samples. Imaging of overnight biofilms did not show growth differences with SEN019 (Figure 5.2). This is supported by Comstat2 quantitation data (Figure 5.17 and Figure 5.18).

In the biofilm quantitation, the control and SEN019 groups had no significant differences in Gfp or PI fluorescence in either biomass, surface area or surface to biovolume (Figure 5.17 and Figure 5.18) as it was observed in CLSM (Figure 5.2). SEN019 in combination with tobramycin was the group with lower biomass values but interestingly, had the highest Gfp surface to biovolume ratio and second highest in PI, showing that the biofilm structure is more sensitive to the action of tobramycin when grown in SEN019 since the remaining fluorescence is tightly grouped (Figure 5.17 and Figure 5.18).

Variability found in Comstat2 quantitation does not benefit the clarity of the conclusions towards the established hypotheses. However the author considered that it was relevant to show the distribution of individual data points so the reader might get an idea of the problems that researchers often face when quantifying microscopy data. Moreover this work also aims to be an example of the complexity of quantifying CLSM images, which is often lost in published material. Therefore the author recommends that any CLSM complex quantification data is taken as supporting evidence that should be well complemented with auxiliary assays and overlapping measurements, as has been intended in this chapter.

5.4.4. Crystal violet Static biofilm quantitation

Static biofilms models were chosen to increase the output of the assays in order to test more conditions with a higher number of replicates. This allowed the generation of much larger volumes of data thanks to crystal violet quantification which allows to measure total attached biomass (O'Toole and Kolter 1998b).

The concentrations required to observe any significant change in biofilm formation were much higher in biofilms than planktonic cells. An assay performed with SEN019 at its usual concentration showed there were no significant differences (Figure 5.8) so a series of increasing concentrations of SEN088 was tested. The IC_{50} of SEN088 in PAO1-L WT is 129 nM (Figure 3.7) but in the CV staining assay, biofilm formation only significantly increased at about 10 μM (Figure 5.9). The addition of increasing concentrations of the SEN compound had a positive, unexpected impact on crystal violet staining. This was more significant when LB10% was used, a media that did not promote as much biofilm development as M63/LB 95:5 which has been previously used to grow biofilms (Thomann *et al.* 2016). The main difference between media is the presence of M63 minimal media. The iron content of M63 is 1.798 μM and the iron content of LB has been estimated to be 13.4 μM (Grant and Pramer 1962). In LB 10% the final concentration of iron is 1.34 μM whereas in the M63 / LB mixture the final concentration is 1.77 times that, at 2.378 μM. This significant increase in iron content could be the explanation as this is a limiting factor that highly

promotes the development of biofilms in some instances (Berlutti *et al.* 2005).

Crystal violet stains all biomass and therefore it is not easy to assess if the increase in staining comes from live bacteria, dead cells or the extracellular matrix. Nevertheless, since PQS has been linked to autolysis in some instances (D'Argenio *et al.* 2002; Allesen-Holm *et al.* 2006; Yang *et al.* 2009), the production of eDNA could be affected. These biofilms would be structurally different and potentially present reduced dispersal rates. Moreover, exogenously added PQS has been shown to promote biofilm dispersal by activating the *pqs* system which controls autolysis and eDNA production (Dong *et al.* 2008; Bjarnsholt *et al.* 2010). This could be one of the reasons why there is an increase in biomass in the presence of high concentrations of SEN088 (Figure 5.9). Further visualisation assays proved that the addition of high concentrations of SEN089 had a significant impact over static biofilm structures with special emphasis to the eDNA found in the matrix of PAO1-W (Figure 5.7). This change could not be observed in younger biofilms (Figure 5.6), implying that the differences appear during development between 6 and 17 hours.

5.4.5. Enhancement of antibiotic treatments

The addition of SEN compounds to the growth media increased the sensitivity of biofilms towards the antibiotic treatment. Significant differences could be visually assessed with both ciprofloxacin (Figure 5.10 and Figure 5.11) and tobramycin (Figure 5.13, Figure 5.14 and Figure 5.16). However, these differences were only observed when the biofilm had been grown from the beginning in the presence of the compound. Combination treatment of previously grown biofilms that had not been in contact with SEN compounds did not increase their sensitivity after 2 hours of treatment (Figure 5.12 and Figure 5.15). Unfortunately, due to time constrains, no minimum inhibitory concentration (MIC) and minimum bactericidal concentration (MBC) assays could be performed.

5.4.5.1. Ciprofloxacin treatment

5.4.5.1.1. Ciprofloxacin in microfluidics biofilms

The addition of ciprofloxacin to biofilms had a clear impact on cell morphology as observed in all samples, even at low concentrations of antibiotic (Figure 5.10, Figure 5.11 and Figure 5.12). The blocking of the DNA IIA topoisomerases by ciprofloxacin makes the most metabolically active layers susceptible (Høiby *et al.* 2010) and activates the DNA repair mechanisms which indirectly increases the fluorescent intensity from bacteria (Figure 5.10).

Qualitative and quantitative data show that the addition of ciprofloxacin at 0.5 μM significantly decreased the Gfp biomass (Figure 5.10 and Figure 5.17A). Results suggest that the incubation with SEN019 sensitises the biofilm to ciprofloxacin, enhancing its biofilm clearance properties, however the biomass differences with the ciprofloxacin only group were not significant, suggesting that the effect is not very strong under the tested conditions (Figure 5.17).

The addition of ciprofloxacin increases the Gfp surface to biovolume ratio but not the surface area, meaning that there is a decrease in volume (Figure 5.18D). With a significant decrease in biomass and no changes in the surface area, it appears that ciprofloxacin degrades the biofilm as some microcolonies will start emptying. This can also be observed in one of the images showing a large microcolony that has been grown in control conditions and treated with ciprofloxacin and SEN019 at the same time (Figure 5.12). This could be because of the changes on morphology by the affected cells or because of the strong impact over QS that ciprofloxacin has (Skindersoe *et al.* 2008), but it has not been explored in more depth here. Growth in the presence of SEN019 increased the significance and extent of the action of ciprofloxacin when compared to the control group. The surface area of this group was significantly smaller than the control in both Gfp and PI fluorescence whereas the Gfp to biovolume ratio remained high, further confirming a synergistic effect (Figure 5.18).

Taking all together, there is enough quantitative and visual data to attest that growth in presence of SEN compounds sensitises microfluidics biofilms

as the microcolonies present a compromised structural integrity, degrade and disperse (quantitative data: Figure 5.17 and Figure 5.18; qualitative data: Figure 5.10 and Figure 5.11).

5.4.5.1.2. Ciprofloxacin in static biofilms

Static biofilms grow in completely different conformations (Figure 5.6 and Figure 5.7), developing a thick layer that often lacks structure and can be very resistant to antibiotics (Macià, Rojo-Molinero and Oliver 2014). Synergy between SEN088 and ciprofloxacin was observed at high concentrations of compound (Figure 5.19). A recent study by Thomann *et al.* (2016) showed increased activity between their dual inhibitor (PqsR and D, IC_{50} = 15 µM) and ciprofloxacin using a higher concentration of the antibiotic (0.5 µM used here vs 1 µM in their study) and compound (50 µM). This study followed the same CV protocol of Thomann *et al.* (2016) and required 31 µM of PqsR antagonist with 0.5 µM ciprofloxacin to reach similar clearance levels. The necessity to use comparatively high concentrations of PqsR antagonists could be caused by a lower relative relevance of the *pqs* system in this model compared to microfluidics. Interestingly, data from this work indicates that the inhibition of PqsR does not inhibit biofilm formation *per se*, however another recently published PqsR antagonist has been observed to inhibit biofilm formation on its own (Maura and Rahme 2017). The structure and binding to PqsR of this antagonist is significantly different than the ones used in this work (Ilangovan *et al.* 2013; Kitao *et al.* 2018), therefore it is hypothesised that this small but significant difference has important implications for biofilm formation. It is interesting to observe an increase in biofilm formation when ciprofloxacin is added at 1 µM (Figure 5.20A). It is possible that the increase in biofilm biomass comes from impaired motility by dispersed cells (Gupta, Chhibber and Harjai 2016). These cells would fall and get stuck at the bottom of the well since they are not washed away in static models.

The addition of ciprofloxacin to day-old biofilms grown in M63:LB 95:5 had little impact to their CV assay values even after another day of incubation at concentrations up to 100 µM (Figure 5.20B), suggesting that the thick biofilms developed under this conditions were extremely resilient to the antibiotic. It is not known if this was through an active mechanism or the

matrix. The previously observed increase on biomass for ciprofloxacin added at 1 μM also appeared here, which suggests that the resistance to the antibiotic does not come from dormancy as the population could still react. A reduction of 30% was only achieved at 100 μM. It is unlikely that the strain developed resistance to ciprofloxacin because of the sensitivity shown to it at time 0 (Figure 5.20A). Furthermore, it is unknown if these samples are viable or if most of the biomass was dead. However, considering that the CV assay contains several washing steps, it is safe to assume that biofilms grown static become recalcitrant after one day of growth and are potentially a source of persisters (De la Fuente-Núñez *et al.* 2013; Wood, Knabel and Kwan 2013). After these assays, a working concentration of 3.1 μM ciprofloxacin was chosen to be tested along with SEN compounds, hypothesising that the addition of compounds weakens the biofilm structural integrity and this acts synergistically with ciprofloxacin and could be quantified as a decrease in biofilm formation.

SEN088 and SEN089 were tested at 10 and 30 μM, with and without ciprofloxacin, however no major differences could be observed (Figure 5.21). The addition of SEN compounds seems to increase biofilm formation but the only significant differences in biofilm biomass were observed when SEN088 was added at 30 μM (Figure 5.21A). It is very possible that the extensive biofilm development that PAO1-L shows in M63:LB 95:5 media played a role in this assay which was not repeated in LB10% due to time constrains. A significant difference with published material that shows biofilm inhibition with PqsR antagonists on their own is the strain tested as those experiments have based most work in PA14 (Thomann *et al.* 2016; Maura and Rahme 2017).

The addition of SEN compounds to static biofilm models does not have as much impact on the integrity because the matrix development is different (Figure 5.3 compared to Figure 5.7). It appears that the *pqs* system does not play a significant role in the integrity of static grown biofilms.

5.4.5.2. Tobramycin treatment

5.4.5.2.1. Tobramycin in microfluidics biofilms

Biofilms grown in the presence of SEN compounds showed PI stained bacteria in deeper layers of the microcolonies (Figure 5.13 and Figure 5.14). Aminoglycosides have been reported to have poor biofilm permeability (Shigeta *et al.* 1997). Nevertheless, a recent study using high concentrations of tobramycin (92 µM vs the 0.5 µM used here) showed that this antibiotic penetrated well into the biofilm and was even retained by the matrix and active in deeper layers with lower oxygen concentration (Cao *et al.* 2015). However, the study did not show the impact of eDNA chelating properties over tobramycin. The presence of dead cells in the innermost areas of microcolonies grown with SEN019 is particularly significant and could be because of decreased chelation as eDNA production is inhibited so tobramycin reaches all parts of the microcolonies with enough concentration to cause cellular death, providing strong evidence of enhancement (Figure 5.14). It is unlikely that the compounds increase biofilm permeability as no link has been established between the regulation of alginate production and the *pqs* system.

In 72h old biofilms, SEN019 prevented the development of a thick extracellular matrix as the control group presented (Figure 5.4) and more cells could be observed in the interphase. In tobramycin-treated biofilms, SEN019 groups had less cells embedded within the matrix than in the control group (Figure 5.16) which contrasts with what was observed in the untreated biofilms, where the SEN019 had a larger number of Gfp active cells embedded (Figure 5.4), suggesting that older biofilms are also more sensitive to tobramycin.

Quantitation data from Comstat2 shows that the decrease in Gfp and PI biomass was particularly significant in the SEN019 + tobramycin group (Figure 5.17). The biomass data, combined with the very low surface values of both tobramycin groups (Figure 5.18) provide quantitative evidence that the activity of this antibiotic has a strong impact on biofilm structure. The presence of SEN019 also makes differences more significant (Figure 5.17 and Figure 5.18), the Gfp surface to biovolume ratio of the combination of

SEN019 with tobramycin is notably high, meaning that most of the Gfp biomass is relatively less structured than the control providing quantitative evidence to the compromised structure hypothesis.

Hence, quantitative data presented in this work provides strong supportive evidence to microscopy observations, confirming that microfluidics biofilms grown in presence of SEN compounds are more sensitive to tobramycin even at low concentrations of antibiotic (quantitative data: Figure 5.17 and Figure 5.18. Visual data: Figure 5.13, Figure 5.14 and Figure 5.16).

5.4.5.2.2. Tobramycin in static biofilms

The tobramycin treatment of static biofilms with increasing SEN088 concentrations did not seem to change the pattern previously observed without antibiotic treatment (with antibiotic: Figure 5.22 and without antibiotic Figure 5.9) suggesting that 0.5 µM is not effective in this static model. Therefore, multiple tobramycin concentrations were tested added at 0 and 24 h (Figure 5.23). PAO1-L biofilms showed increased resilience to tobramycin compared to ciprofloxacin. At time 0, control levels of biofilm formation were achieved up to 10 µM of tobramycin and at that concentration there was a significant increase in biomass, comparable to what was observed in ciprofloxacin. This suggests that threshold subinhibitory concentrations of antibiotic could promote static biofilm formation (Figure 5.20 and Figure 5.23) although published data has shown that subinhibitory concentrations of ciprofloxacin can disperse 7-day old biofilms (Gupta, Chhibber and Harjai 2016). PAO1-L did not grow when tobramycin was added at 31 or 100 µM. The addition of tobramycin after 24 hours of growth also presented increased biofilm formation at 10 µM, however 31 µM of tobramycin did not clear the biofilm (although the viability of it is unknown) and 100 µM only had a 30% reduction (Figure 5.23).

SEN088 at 10 µM presented improved biofilm clearance with 31 µM of tobramycin but this did not increase with 30 µM of SEN088, which could be due to antagonist saturation (Figure 5.26A). Interestingly, the lead compound SEN089 only showed increased activity with tobramycin at 30 µM, but then the untreated samples had much greater biofilm formation

than the treated. This large difference in staining could be related to a larger accumulation of biomass in the presence of 30 μM SEN089 which is then more sensitive to the action of tobramycin than the biofilms grown in absence of SEN089 (Figure 5.26B). Nevertheless it is possible that these results and the lack of correlation between increased activity and compound potency is related to a lower relevance of the *pqs* system in this model.

Results suggest that the presence of SEN compounds has a small synergistic effect to the action of the antibiotic for which PAO1-L has shown high resilience (Figure 5.23), even when the compounds alone increase CV biomass (Figure 5.9). Finally, the chosen growth media is also an important condition when performing this assays as it can have a very significant impact on biofilm development and the relevance of different regulatory systems such as *pqs* (Davies *et al.* 1998; De Kievit *et al.* 2001; Shrout *et al.* 2006; Gupta and Schuster 2012).

5.4.6. ATP quantitation of static biofilms

Bacteria increase their metabolism in the presence of subinhibitory concentrations of tobramycin that are still high enough to cause a degree of cellular death (Figure 5.25) (Stewart *et al.* 2015; Ciofu *et al.* 2017). Moreover, the addition of compound also increases the ATP measurements (Figure 5.26) without significant changes in the total biomass (Figure 5.9). This could imply that the inhibition of the *pqs* system during biofilm development inhibits the creation of metabolically distinct subpopulations, which could have a strong impact on the biofilm development and long term antibiotic resistances (Williamson *et al.* 2012; Chiang *et al.* 2013; Wood, Knabel and Kwan 2013; Stewart *et al.* 2015).

Biofilms grown in the presence of SEN089 and treated with tobramycin also had a significant increase in ATP compared to the control groups (Figure 5.26). The increase in ATP could be linked to the submission of the biofilm to stress conditions. Interestingly, the difference between treated and untreated was larger than in the DMSO control, suggesting that whilst more active, they are also more sensitive to tobramycin. These results are in

accordance to published data linking higher metabolic activity to increased sensitivity to ciprofloxacin and tobramycin (Walters *et al.* 2003).

5.4.7. SEN compounds sensitise biofilms to pull forces

Most of the work linking the *pqs* system to biofilm suggests a role in the matrix formation and maintenance which can indirectly impact dispersal through autolysis and eDNA release (D'Argenio *et al.* 2002; Allesen-Holm *et al.* 2006; Häussler and Becker 2008; Bjarnsholt *et al.* 2010; Xu *et al.* 2016). Thus it was hypothesised that biofilms grown in presence of a PqsR inhibitor compound would present a significantly different biofilm structure. Work done during this research has provided strong supportive evidence to this hypothesis as has been summarised so far. Synergy with tobramycin and ciprofloxacin was tested (above), but to further put the structural integrity to test, microfluidics biofilms were set against the strongest sheer forces available for a short amount of time.

Very significant differences between biofilms in the presence and absence of SEN compounds have been observed, particularly those treated with tobramycin (Figure 5.27 and Figure 5.28). The lack of matrix regulation by *pqs* through the biofilm development makes the structure more sensitive to this forces, which could improve the clearance by expectoration in CF patients, especially those being treated with tobramycin. The major components related to biofilm attachment are alginate, proteins and cell appendages (Moradali, Ghods and Rehm 2017) but data provided in this thesis suggests that eDNA and possibly membrane vesicles (MVs) play a small but significant role as those are the main matrix components under *pqs* regulation (D'Argenio *et al.* 2002; Mashburn and Whiteley 2005).

Flow cytometry was performed with the aim to quantify the amount of dispersed cells and those from the detached biofilm fraction. To the author's knowledge, this was an approach that has not been reported before in literature and it would still require thorough optimisation. One of the major caveats is that the samples may contain big lumps of detached biomass that may block the flow cytometer or be discarded by the software analysis. On the other hand, significant morphological changes induced by

the antibiotics (like cell elongation by ciprofloxacin, or the contrary by tobramycin) can also influence final counts if the software's size window is not properly set.

The data indicates that biofilms with SEN019 have more dispersed PI stained cells (Figure 5.29A) which could suggest an inability to retain dead bacteria within the biofilm. It is possible that the absence of these cells had an impact in the biofilm as has previously been discussed. Under these circumstances, bacteria that would otherwise go through normal autolysis and release autolysis-mediated MVs and eDNA would not complete the process due the lack of a fully functional *pqs* system (D'Argenio *et al.* 2002; Mashburn and Whiteley 2005; Häussler and Becker 2008; Ma *et al.* 2009; Toyofuku *et al.* 2014). However it has to be considered that there are *pqs*-independent autolysis mechanisms also involved in biofilm formation although the differences are currently unknown (Turnbull *et al.* 2016). The increase of PI-labelled bacteria in antibiotic-treated SEN019 groups could be a mixture of the aforementioned cells and further evidence of enhanced activity (Figure 5.29A). The biofilm fraction presents lower total counts in untreated SEN019 samples compared to the control (Figure 5.29B). Notably, Comstat2 quantitative data showed slightly lower biomass and surface area values (Figure 5.17 and Figure 5.18) especially in the PI fluorescence which is in accordance to flow cytometry data and strengthens the significance of these results.

No further conclusions can be confidently drawn from this assay. However, the use of flow cytometry as a tool for total cell quantitation is an interesting prospect that should be explored further. The method can quickly quantify with exactitude large sets of samples and the potential issues with the biofilm fraction could be solved with some biofilm degrading pre-treatment with, for example, small concentrations of DNAse. Furthermore, size and fluorescence intensity sorting could potentially be used to quantify subpopulations separately.

5.4.8. SEN compounds inhibit eDNA formation in biofilms

In a healthy biofilm, most of the PI fluorescence detected actually comes from staining the eDNA fraction of the matrix, with little to no overlapping Gfp fluorescence from bacteria (Figure 5.30). Considering that eDNA production has been linked to *pqs* in multiple publications (D'Argenio *et al.* 2002; Mashburn-Warren *et al.* 2008; Thomann *et al.* 2016; Maura and Rahme 2017), the quantity of eDNA was measured in planktonic and biofilm models. The eDNA from planktonic cultures had no significant differences (Figure 5.31), which indicates that the role of *pqs* in autolysis and eDNA is limited within the biofilm. This was further supported by ethidium homodimer (etho) staining of a static biofilm showing a significant fluorescence decrease (Figure 5.32). Ethidium homodimer was chosen as opposed to propidium iodide because etho has a greater fluorescence yield than PI under the same wavelength, therefore giving a stronger fluorescence that allows for more sensitivity. This data provides evidence that all the previously observed changes in biofilm architecture and sensitivity by growth in presence of *pqs* inhibitors may be caused by an impaired eDNA release that would directly affect the matrix characteristics and is in accordance with the last published results with other PqsR antagonists (Thomann *et al.* 2016; Maura and Rahme 2017).

5.4.9. Conclusion and future directions

The more technical side of this chapter has been presented in the spirit of showing a successful approach to method optimisation, with special emphasis on CLSM quantitation using Comstat2, including its pros and cons. Furthermore, multiple biofilm quantitation models have been developed, including novel approaches to microfluidics using flow cytometry.

The use of many different models and three different strains has increased the complexity of the data analysis but ultimately provides much more robust evidence that the observed results are significant in a wide range of backgrounds.

This study provides sufficient evidence to confirm that the incubation of *P. aeruginosa* biofilms in presence of SEN PqsR antagonists reduce the amount of eDNA released in the biofilm matrix, possibly through the inhibition of *pqs* mediated eDNA release. Structural differences have been observed after 6 to 17 hours of growth and up to three days of incubation. This does not have an impact on bacterial growth *per se* but the resulting biofilm might present lower numbers of cells as its structure is affected. The biofilm has a more active metabolism but is structurally weakened, making it more sensitive to physical shearing forces as well as the action of ciprofloxacin and tobramycin, two antibiotics from different families and mechanisms of action. It is possible that the correct development of the matrix or the *pqs* system itself are necessary for the formation and maintenance of active and dormant subpopulations.

Unfortunately, the wide range of models tested prevented a more in-depth analysis of some particularly interesting results. The complexity of the biofilm lifestyle also makes it hard to establish the impact of *pqs* inhibition from a molecular point of view. Moreover, static biofilms have been proven to be particularly insensitive to SEN compounds and antibiotics, and differences were observed only when using concentrations many times over the IC_{50} values obtained from planktonic cultures as reported by other groups (Høiby *et al.* 2010; Moradali, Ghods and Rehm 2017).

Several important topics remain to be analysed in depth. An important point would be the addition of SEN compounds to already grown biofilms. This was only very briefly tested in this study, but longer incubation periods should be tried to determine if the impact over biofilm architecture is linked to its original development or can also occur in pre-established biofilms. Testing the compounds on alginate-overproducing mucoid strains would also provide important information regarding the capacity to significantly alter the matrix of these phenotypically-distinct strains, so relevant in chronic CF environments (Govan and Deretic 1996; Mann and Wozniak 2012). Testing microfluidics in anaerobic biofilms and / or with higher concentrations of both antibiotic and inhibitor compound could also provide more information regarding a potential synergy in more transferrable conditions. The flow cytometry quantitation of the dispersed fraction and

potentially the biofilm is also an interesting tool that could be further optimised and expanded and would provide strong, direct evidence regarding biofilm dispersal rates as well as physical shearing resistance.

Finally, an approach left untouched in this work has been the evolution of long-term biofilms and the development of spontaneous mutations and persisters. An impact over biofilm structure and metabolism over a long period of time could have strong implications for the mutation rates and generation of persisters, highly improving the outcome of treatments of chronic infections (Driffield *et al.* 2008; Conibear, Collins and Webb 2009; Mandsberg *et al.* 2009).

6. General discussion

The *pqs* quorum sensing system of *P. aeruginosa* is a major regulatory network, controlling the expression of genes involved in virulence, biofilms, oxidative stress and iron acquisition (Déziel *et al.* 2005; Yang *et al.* 2007; Häussler and Becker 2008; Lee and Zhang 2014). The main autoinducer of the system is 2-heptyl-3,4-dihydroxyquinoline (PQS) but its precursor, 4-hydroxy-2-heptylquinoline (HHQ) can also bind and activate the effector which is a LysR-type transcriptional regulator named PqsR (originally MvfR) (Déziel *et al.* 2004). When the autoinducers bind to PqsR it becomes functional and binds directly to the promoter regions with the corresponding box, one of these is the promoter region of the *pqsABCDE* operon which contains most (but not all) the genes related to the PQS biosynthetic pathway. A major by-product of this pathway is 2-heptyl-4-hydroxyquinoline *N*-oxide (HQNO) which works as a biostatic element that enhances *Pseudomonas* competitiveness, but has no signal function (Rampioni *et al.* 2016). The precursor HHQ is much less active than PQS but it does not act as a signal molecule, instead it can only feed the positive feedback loop increasing the concentrations of AQs (Déziel *et al.* 2004; Rampioni *et al.* 2016). The synthesis of PQS is performed by PqsH, a monooxygenase that introduces a hydroxyl group at the position 3 of HHQ to convert it to PQS in an oxygen dependent manner. Interestingly, *pqsH* is activated by the *las* system and it is produced even in anaerobic conditions where it remains inactive until O_2 becomes available (Déziel *et al.* 2004; Schertzer, Brown and Whiteley 2010).

PQS, HHQ and HQNO are detected extracellularly in the sputum, plasma and urine of CF patients (Barr *et al.* 2015). However, these molecules are highly hydrophobic so evidence so far suggests that they are transported in membrane vesicles (MVs) although other mechanisms could not be discarded (Mashburn and Whiteley 2005). The production of MVs is part of the biology of *P. aeruginosa* that has not received major attention, although they are constantly produced in biofilms and biologically functional due to their contents (lipids like LPS, proteins like proteases, and DNA) (Kadurugamuwa & Beveridge, 1995; Schooling & Beveridge, 2006;

Schooling, Hubley, & Beveridge, 2009; Kulp & Kuehn, 2010). The production of MVs is a regulated and non-stochastic mechanism that results in a specific set of contents and LPS. In *P. aeruginosa*, the regulation over MV production is not fully described, and although there is data that closely relates them to the *pqs* system (Mashburn and Whiteley 2005), other publications show that their production is not dependent of *pqs* (Turnbull *et al.* 2016), however, it is not known under which conditions each type is produced. Interestingly, a recent publication suggested that PQS plays a role in a newly described iron acquisition mechanism by transferring the chelated iron from PQS to the protein TseF (PA2734) (Lin *et al.* 2017). This protein is found in MVs and can deliver the iron to intracellular siderophores. *P. aeruginosa* could use *pqs*-related MVs as iron scavenging platforms. It is expected that the inhibition of *pqs* would inhibit this iron uptake pathway as TseF can collect iron exclusively from chelated PQS (Lin *et al.* 2017). It is therefore hypothesised that iron works as the environmental switch that favours the production of *pqs*-dependent MVs to the detriment of others.

In various environments from underwater pipes to lungs, the establishment of biofilms in an undesired surface is a very troublesome problem. The physiological characteristics of the biofilm and the physicochemical characteristics of the extracellular matrix in which they are embedded make the community exceptionally resilient and creates a friendly microenvironment in otherwise very hostile environments. All major regulatory networks of *P. aeruginosa* are involved in one stage or the other of the biofilm lifestyle, although their relevance depends on the growth conditions. The *las* and *rhl* QS systems seem to play a role in the initial establishment and resistance to dispersal agents (De Kievit *et al.* 2001), while the *pqs* system is more involved in the biofilm structure and dispersal through regulation of iron scavenging systems and eDNA (Bjarnsholt *et al.* 2010). Other very important regulators involved in the biofilms are cAMP, c-di-GMP, RpoN, RsmZ and GacA/S (Rasamiravaka *et al.* 2015). Notwithstanding this, the external factors such as iron availability, oxygen concentration or the carbon source are critical components that will guide the biofilm development (Toyofuku *et al.* 2016), making the choice of an

appropriate biofilm model *in vitro* the most important part of experimental design when working with biofilms.

The work presented here has aimed at providing more information regarding the impact of the inhibition of the *pqs* system in several phenotypes as well as in biofilms, this information can also be used to further expand the current knowledge regarding the role of *pqs* in some particularly poorly understood mechanisms like autolysis. The PqsR antagonists were obtained from the *in silico* screening followed by *in vitro* validation and further chemical optimisation. The first studied hit SEN016 had a reasonable micromolar IC_{50} value in PAO1-L, with the first generations between 1 and 10 μM. Further chemical optimisation led to the discovery of another generation with potency in nanomolar range, the SEN08- family with 67 nM IC_{50} for the lead compound SEN089. The PqsR ligand binding domain ($PqsR_{LBD}$) was expressed and purified as previously described (Ilangovan *et al.* 2013), this was used for isothermal titration calorimetry assays (ITC) with the compounds for which IC_{50} data was available, showing that most but not all of the antagonists bound to the active site of the protein. M64, a benzamine–benzimidazole (BB) derived compound, is a published PqsR antagonist that binds to the $PqsR_{LBD}$ with a $K_{(D)}$ of 5.4 nM and has a pyocyanin IC_{50} of 600 nM (Starkey *et al.* 2014; Kitao *et al.* 2018). X-ray co-crystallography data showed that M64 could trigger a conformational change of the active site to fit its bulky hydrophobic tail that makes it interact with adjacent regions of the active site. M64 showed activity in several laboratory and clinical isolates, inhibiting virulence production and even persister formation, providing evidence that the inhibition of PqsR has a strong impact over virulence in acute and chronic infections (Starkey *et al.* 2014; Kitao *et al.* 2018). SEN089, the lead compound of this project, has a $K_{(D)}$ value of 2.66 nM and an IC_{50} of 67 nM, showing better affinity and activity than M64. Unfortunately, crystallography data is not available but the structure is significantly different from M64. The binding of SEN08 should resemble the QZN binding reported by Ilangovan *et al.* 2013 (SEN089 structure not shown). Interestingly, the compounds SEN022 and SEN066 did not show binding to $PqsR_{LBD}$ although SEN022 was obtained from chemical

optimisation of SEN016 and the rest of the optimised compounds bound whereas SEN066 was one of the original hits that showed activity in the initial round of validation. SEN066, with an IC_{50} of 1.013 μM, was shown to inhibit pyocyanin production in all tested strains and it is unlikely that the inhibition happens through PqsE inactivation because the IC_{50} data is calculated from a *pqsA*-lux reporter, and PqsE actively represses *pqsA* (Rampioni *et al.* 2016). SEN022 also showed significant inhibition of pyocyanin in PAO1-L and PA14. Moreover, the presence of SEN022 also inhibited HHQ and PQS production. It is likely that SEN066 also inhibits AQ production although this has not been assessed. The reasons behind this inhibition are not currently known. It is unlikely that SEN022 or SEN066 have secondary activities in the *las* system because it only controls PQS levels through *pqsH* regulation (Lee and Zhang 2014), therefore the concentration of HHQ would not be affected, whereas the inhibition of *rhl* could explain the decrease in pyocyanin but not on AQs themselves since *rhl* has been observed to inhibit *pqs* (Cao *et al.* 2001). It is possible that these compounds bind elsewhere of PqsR, unfortunately there is no published work regarding the purification of the full PqsR protein because of its insolubility (Maddocks and Oyston 2008). ITC assays could be performed if the whole protein was purified, with further crystallography experiments if there was binding. Alternatively, the antagonists could also bind to other enzymes of the PQS biosynthetic pathway. Surface plasmon resonance (SPR) would be an excellent alternative to the use of ITC to study the kinetics of these compounds with different proteins (Douzi 2017).

The lead compound SEN089 on the other hand binds to the $PqsR_{LBD}$ and is extremely active at very low concentrations. 200 nM of SEN089 inhibited the production of pyocyanin in all strains. At this concentration, in rich media (LB) and aerobic conditions, the AQ production of PAO1-L WT was close to the production detected in a Δ*pqsR* mutant. The inhibition was also significant in the clinical isolates. Furthermore, the addition of SEN089 decreased eDNA production in a static biofilm model. Concluding, the lead compound SEN089 has strong *pqs* inhibitory activity at nanomolar concentrations and has a significant impact over biofilms at 1 and 10 μM. These results make SEN089 an ideal candidate for further testing on

synergy assays with antibiotics and other biofilm models like microfluidics which would be very useful to emulate catheter-associated infections. Testing SEN089 with and without oxygen, to study the relevance of *pqs* inhibition in anaerobic conditions. Moreover, previous research has shown that PqsR antagonists can significantly decrease the number of persister cells from a culture (Starkey *et al.* 2014), an effect of particular importance for the clinical environment. If time allowed, the analysis of SEN089 over persisters should be assessed.

The results obtained in this body of work also provide evidence that autolysis in *P. aeruginosa* is not a phenotype controlled through a single mechanism. The appearance of autolysis seems to be strictly mediated by prophages and the production of pyocins. Autolysis is an important system for *P. aeruginosa* as it has been shown to be involved in the release of eDNA and outer membrane vesicles (MVs) (D'Argenio *et al.* 2002; Turnbull *et al.* 2016). Turnbull *et al.* showed a mechanism of eDNA and MVs release through explosive cell lysis that did not depend on *pqs* and as a matter of fact, was slightly enhanced in Δ*pqsA* mutants. Some of the genes identified in their work were the endolysin PA0629 (*lys*) and the holin transporter PA0614 (*hol*), lux reporters for these genes were built in wild type and Δ*pqsR* backgrounds to corroborate this (Turnbull *et al.* 2016). Results obtained here are in accordance with Turnbull *et al*. data, showing a slight increase in expression in the *pqsR* mutant compared to the wild type, and a similar increase in the wild type grown in presence of SEN089 so the inhibition of the *pqs* system would increase autolysis. Nevertheless, another autolysis assay showed that the inhibition of *pqs* decreased the autolysis found in colony biofilms. This apparent contradiction could be explained considering that the autolysis regulated by *pqs* is a cell density and iron dependent mechanism through the prophage Pf4 (Stover *et al.* 2000, Rampioni G., *et al.* unpublished) whilst the R- and F- cryptic prophages (of which *lys* and *hol* are part) mediate explosive autolysis through a *pqs* independent system. Since the *pqs* autolysis is more tightly controlled by cell density and iron than its counterpart, it is possible that the *pqs*-independent release of MVs, eDNA and other iron acquisition systems occurs during the initial stages of biofilm establishment and

formation. On the other hand, the *pqs*-dependent autolysis is activated once the biofilm is more mature and has grown enough to reach the required cell density. PQS has been observed to promote biofilm formation through increasing iron bioavailability (Tettmann *et al.* 2016). Linking this information with the described iron acquisition *pqs*-dependent pathway (Lin *et al.* 2017), suggests that both MV production systems are not completely exclusive and coexist in an equilibrium, potentially determined by iron content. Moreover, an autolysis system that releases MVs and eDNA independently of *pqs* ensures that these important components are released regardless of oxygen.

This hypothesis supports the observations performed in biofilm assays as the inhibition of *pqs* showed no structural differences in the early biofilms but they become obvious later on more mature cultures. Older biofilms grown in the presence of PqsR antagonist SEN019 had a significantly smaller amount of eDNA and were more sensitive to antibiotics and shearing forces. Unfortunately, the effects of iron content have not been assessed in this research.

The doses of compounds to treat biofilms had to be increased for a robust biological effect, so for example SEN089 with an active dose of 200 nM in planktonic cultures, was raised to 10 μM in biofilm assays. There is several factors behind this. For one, there is no data regarding how the compound diffuses through the biofilm matrix and at which active concentration reaches the cells inside the microcolonies (Rampioni *et al.* 2017). Also considering the effect of efflux pumps, it is worth highlighting that the action of resistance-nodulation-division (RND) pump inhibitors, phenylalanine-arginine β-naphthylar, have been observed to increase the action of SEN089 against a PAK CF isolate (one of the more resistant strains) (Nigel Halliday, personal communication).

The chosen experimental conditions are key elements for any research, specifically for biofilms and the role of QS in them. It has been observed that media composition such as the carbon source use could have an impact on biofilm formation (Shrout *et al.* 2006). To the author's knowledge, the impact of external factors to the *pqs* system has not been properly

addressed. There is evidence that pyocyanin production is significantly influenced by the carbon source, although this appears to be in a *pqs* independent manner through post-transcriptional regulation by the catabolite repression control system (crc) (Huang *et al.* 2012). Another very important factor is oxygen, standard experimental conditions are aerobic, under which PQS is fully synthesised (Schertzer, Brown and Whiteley 2010), similar conditions can be expected in constant flow biofilms that are fed with fresh, aerobic media, while static biofilms are more likely to present oxygen stratification, which in turn has been observed within the microcolonies themselves (Cotter, O'Gara and Casey 2009). This leads to the hypothesis that the PQS production is significantly different between models which in turn will lead to different results from *pqs* inhibition. In multi-day static models, the media is often changed periodically to maintain growth, the addition of new media provides newly available oxygen (Cotter, O'Gara and Casey 2009; Steenackers *et al.* 2016). An assay with the observation after several of such events may be biased by these if the groups react differently and only factors as total biomass are analysed. For this particular work, it is possible that the addition of fresh, aerobic media activates PqsH that will trigger PQS synthesis (Schertzer, Brown and Whiteley 2010), activating *pqs*-dependent autolysis and coordinating dispersal, the inhibition of *pqs* will have a significant impact over this mechanism, resulting in different dispersal and biofilm structures.

An underexplored aspect of *pqs* regulation is its role in the formation of persister cells. The relationship is well documented and has been observed in separate publications from different groups (Starkey *et al.* 2014; Allegretta *et al.* 2017), nevertheless, the reason behind this effect is not known precisely. The other major QS systems, *las* and *rhl*, but also pyocyanin itself, have also been related to the formation of this subpopulation (Möker, Dean and Tao 2010). The relationship between pyocyanin and persisters is interesting because it could be the link from which *pqs* controls this trait. However, to the author's knowledge there are no studies on the formation of persisters in *pqs* negative mutants complemented in trans with pyocyanin. PQS is a pro-oxidant but one of the mechanisms under regulation by *pqs* is the oxidative stress response

(Bredenbruch *et al.* 2006; Häussler and Becker 2008). Notably, the oxidative stress mechanism is a key element in the generation of antibiotic resistances, mutants of the oxidative stress response are sensitised to the action of antibiotics and the addition of PQS increases this because of the pro-oxidative effect (Nguyen *et al.* 2011). It is possible that the presence of *pqs* maintains a functional oxidative stress system that ultimately helps protect the population and develop resistances (thanks to its pro-oxidative action). Moreover, the (p)ppGpp mediated stress response is a key component for the formation of persisters, yet the alarmone actively inhibits the *pqs* system (Schafhauser *et al.* 2014). It is unknown why this duality is observed regarding the role of *pqs* in the development of persisters. Unfortunately, no experiments have been performed for cellular stress and the impact of *pqs* inhibition in these circumstances and the area remains open for further investigation.

All the clinical isolates used in this work had functional *las*, *rhl* and *pqs* systems, with most of them expressing high levels of AQs. The reason behind this was to test the compounds in a clinically relevant isolate from a chronically infected patient that might be responsive to *pqs* inhibition. However, the CF lung is a complex environment encasing diverse communities of which *P. aeruginosa* can be dominant (Yi-Chia 2014). The microbial community evolves with the patient and it must be pointed out that a significant fraction of the isolates from chronically infected lungs present loss of function mutations in the *las, rhl*, and *pqs* systems (Chung *et al.* 2012). Interestingly, *P. aeruginosa* strains still dominate the CF chronic lung community regardless of the loss of some QS systems, especially *lasR* (Heurlier *et al.* 2005; Feltner *et al.* 2016). In those particular conditions, QS regulation may not play a major role in the fitness of the population, or its loss of function may help with community cooperation. This could have important implications and should be considered when developing QS inhibitors. Little is known regarding why this happens but a possible hypothesis is that it could be caused by reaching a homeostatic point in which the community becomes so recalcitrant and the inflammatory damage so high that the bacteria does not need to regulate the systems involved in survival and dispersion. However, some of the

phenotypes under QS regulation manage to remain active regardless of the presence of QS, an example of this is pyocyanin, whose production has been observed to remain high even in some *pqs* loss of function mutants (Feltner *et al.* 2016). It is unknown if these systems mutated to remain active in the absence of QS systems after they mutated or remain active through secondary mechanisms that ensure redundancy in critical components or through signal cross feed if mutations are in the biosynthetic genes (mutant can still respond). Thus, the role of QS and in particular *pqs* in chronic infections, may not be as obvious as thought due to other players that contribute in the maintenance of a core set of components critical for the isolate. If this were true, it could limit the efficacy of *pqs* inhibitors in clinical backgrounds that favoured the appearance of QS loss of function mutations.

Besides QS mutants, mucoid strains are also clinical isolates commonly found in the CF lung (Schurr *et al.* 1996). Mucoid strains are characterised for their overproduction of alginate and develop in chronic infection environments, sometimes as response to antibiotic treatment (Evans and Linker 1973). The overproduction of alginate generates a very different biofilm matrix, much thicker and stickier, it offers enhanced protection against external elements although it limits the dispersal capabilities of the population (Bjarnsholt *et al.* 2009). The biofilm structure of these strains is expected to be significantly different (Wozniak *et al.* 2003). Moreover the oxygen availability might be more limited because of the physical barrier that the highly hydrated matrix creates, thus the relative role of *pqs* within these biofilms is expected to be significantly different and the compounds may be less likely to reach bacteria in the inner strata of mature biofilms. However, it is possible that this is not important. If these inner layers are anaerobic, the *pqs* system remains on standby (as suggested previously in the new proposed model for the role of *pqs* in biofilms) and any potential regulation by the *pqs* system will happen in the upper layers where cells are more active and have more oxygen available (Xu *et al.* 1998). Incidentally, if there were limitations in the compound distribution within the biofilm, it will be concentrated in the upper layers, precisely where it can show effect (Shigeta *et al.* 1997; Cao *et al.* 2015). In the case of

dispersal or sudden breakage of the biofilm, the inner layers will be exposed and their *pqs* system can re-activate as oxygen is available again (Schertzer, Brown and Whiteley 2010), however, if there is enough concentration of PqsR antagonist in the immediate environment, it will translocate to inhibit *pqs*, blocking any *pqs* mediated response to the breakage event. This hypothesis has a major limitation by assuming that the compound remains readily available in the media. It is possible that the hydrophobic nature gives it a relatively low half-life in the lumen (Soukarieh *et al.* 2018a), making it translocate and accumulate quickly in the outer regions of the biofilm or elsewhere in the system so the *pqs* mediated response of the inner regions may be activated without inhibition in case of sudden oxygen availability. This hypothesis remains untested but highlights the complexity of *pqs* inhibition and its biological impact in mucoid strains which are of paramount clinical relevance (Govan and Deretic 1996).

All this variability is a very important factor to take into account in any research linked to a clinical objective. Even with a representative sample of isolates from CF chronic infections, the behaviour of the isolates in laboratory conditions may be completely different. Thus it is very important to use models that replicate the natural environment (Azevedo *et al.* 2017). This approach aims to reduce potential biases introduced by the experimental design.

As with most research projects, time constraints were the main limiting factor, they limited the capability to perform IC_{50} assays of all compounds in the other strains. This would provide significant information regarding the strain heterogeneity of the *pqs* system. Furthermore, many biofilm models were only tested with PAO1-L or PA14 but not on clinical isolates, which could provide very useful information regarding the biofilm characteristics of these strains and the biological impact of *pqs* inhibition. Finally, the large scope of this project also limited the exploration of secondary venues that aroused along the way such as: A more in depth look at the *pqs* regulated autolysis, the phenotypic and biofilm assays in

anaerobic conditions or an exhaustive analysis over how SEN066 and SEN022 inhibit the *pqs* system.

6.1. Summary of findings, new hypotheses and future venues

Ten PqsR antagonists were tested in this project to ensure that the phenotypes observed upon *pqs* inhibition were robust between antagonists as well as correlated with their calculated potency. Table 6.1 presents a summary of the compounds tested, their activity and IC_{50} values as well as phenotypic and biofilm assays performed (if any). More detailed data regarding the information found in the table can be found in the previous results chapters.

SEN019 and SEN032 were the compounds used for most phenotypic and biofilm assays, followed by SEN089. The most repeated assay was Pyocyanin as a direct measure of *pqs* activity (Table 6.1).

Table 6.1. Table of PqsR antagonists from SENBIOTAR project. Phenotypic assays are colour coded according the effect on the strain, green indicates overproduction compared to the control, red indicates inhibition and black indicates differences are not significant.

Name	Inhibition at 10 µM	IC_{50} PAO1-L	IC_{50} other strains	Phenotypic assays	Biofilm assays
SEN089		67 nM		**Pyocyanin:** PAO1-L, PA14, PAO1 279, PA14 AL191, LESB58, PAK 6085 and PA7 48. **AQ quantitation:** PAO1-L, PA14, PAO1 279, PA14 AL191, LESB58, PAK 6085 and PA7 48. **P*hol* and P*lys* expression:** PAO1-L and PAO1-L Δ*pqsR*. **Cell lysis phenotype:** PAO1-L, PAO1-L Δ*pqsL* and PAO1-L Δ*pqsR*.	**8 well microchambers:** PAO1-W and PA14. **24 well polystyrene plates:** PAO1-L, PAO1-W and PA14. **96 well microtiter plates:** PAO1-L.
SEN088		129 nM	**PAO1 279** 147 nM **PA7 48** 107 nM	**Pyocyanin:** PAO1-L and PA14. **AQ quantitation:** PAO1-L. **P*lecA* expression:** PAO1-L, PAO1-L Δ*pqsA* and PA14.	**96 well microtiter plates:** PAO1-L
SEN086		200 nM	**PA14** 437 nM **PAO1 279** 184 nM **PA14 AL191** 544 nM **LESB58** 171 nM **PAK 6085** 333 nM **PA7 48** 312 nM	**Pyocyanin:** PAO1-L and PA14. **AQ quantitation:** PAO1-L.	
SEN071		390 nM		**Pyocyanin:** PAO1-L and PA14. **AQ quantitation:** PAO1-L.	
SEN019		1.088 µM	**PA14** 8.25 µM **PAO1 279** 2.341 µM **PA14 AL191** 1.089 µM	**Pyocyanin:** PAO1-L, PA14, PAO1 279, PA14 AL191, LESB58, PAK 6085 and PA7 48. **AQ quantitation:**	**Bioflux microfluidics:** PAO1-L. **Flow cytometry:** PAO1-L.

			LESB58 846 nM **PAK 6085** 1.113 µM **PA7 48** 1.141 µM	PAO1-L, PA14, PAO1 279, PA14 AL191, LESB58, PAK 6085 and PA7 48. **Pyoverdine:** PAO1-L, PAO1-N Δ*pqsA*, PAO1-B Δ*pvdD*, PAO1 279 and PA14 AL191. **Elastase:** PAO1-L, PAO1-L Δ*pqsA* and PAO1 Δ*lasR*. **Azocasein:** PAO1-L.	
SEN032		2.234 µM	**PAO1 279** 1.539 µM **PA14 AL191** 711 nM **LESB58** 645 nM **PAK 6085** 2.703 µM **PA7 48** 1.13 µM	**Pyocyanin:** PAO1-L, PA14, PAO1 279, PA14 AL191, LESB58, PAK 6085 and PA7 48. **AQ quantitation:** PAO1-L, PA14, PAO1 279, PA14 AL191, LESB58, PAK 6085 and PA7 48. **Pyoverdine:** PAO1-L, PAO1-N Δ*pqsA*, PAO1-B Δ*pvdD*, PA14, PAO1 279, PA14 AL191 and PAK 6085. **Elastase:** PAO1-L, PAO1-L Δ*pqsA* and PAO1 Δ*lasR*.	**Bioflux microfluidics:** PAO1-L.
SEN066		2.583 µM		**Pyocyanin:** PAO1-L, PA14, PAO1 279, PA14 AL191, LESB58, PAK 6085 and PA7 48.	
SEN022		5 µM		**Pyocyanin:** PAO1-L and PA14. **AQ quantitation:** PAO1-L.	
SEN050	70%	5 µM		**Pyocyanin:** PAO1-L and PA14. **AQ quantitation:** PAO1-L.	
SEN020	23%				

The major findings from this body of work can be summarised as follows:

- A PqsR antagonist compound has been developed with an IC_{50} of 67 nM in PAO1-L wt. This compound is effective in all isolates tested and in biofilms at concentrations of 10 μM or less.

- Compounds SEN066 and SEN022 have been shown to not bind to the $PqsR_{LBD}$ but actively inhibit the *pqs* system as they modulate AQ and pyocyanin production through an unknown mechanism.

- The inhibition of the *pqs* system has a significant impact on the biofilm structure and sensitivity to tobramycin, ciprofloxacin and physical shearing.

- The inhibition of the *pqs* system reduces the amount of eDNA released by cultures grown in static, 96 well microtiter plates.

- PQS plays a significant role in a cell density dependent mechanism of autolysis. The inhibition of *pqs* promotes the expression of other known autolytic mechanisms based on pyocins from prophages R- and F-.

- Different clinical isolates show differential sensitivity to the inhibition of *pqs* by SENBIOTAR compounds. These differences do not have a genomic origin.

Several new hypotheses and future directions have arisen from the data available. These have been discussed in the discussions from the previous chapters and in the general discussion, the main ones are summarised here as follows:

- Autolysis in *P. aeruginosa* is a complex mechanism regulated by two or more systems, one of which is *pqs* controlled. In absence of *pqs,* the other mechanism is upregulated, however the triggers that decide which mechanism works and when are currently not known. It is hypothesised that different autolysis mechanisms release different types of MVs.

- A new model has been proposed attempting to describe the role of PQS in the CF lung. The colonisation of hypoxic environments in the CF lung relegates the *pqs* system to a secondary role where it remains on standby with a pool of PqsH that will convert HHQ to PQS upon contact with a high enough concentration of oxygen. These events will occur if the biofilm breaks or is under heavy ROS attack, activating all the *pqs* related virulence and dispersal factors. Thus the *pqs* system is a mechanism of defence and persistence used by *P. aeruginosa*.

- In aerobic conditions, the inhibition of *pqs* modulates eDNA production which has a significant impact over the sensitivity to antibiotics and makes the biofilm more susceptible to shearing forces, while the biomass of the biofilm may increase under certain circumstances because dispersal is not properly regulated. Furthermore the loss of regulated dispersal makes the biofilm react differently towards changes in the environment, making it less adaptable and more susceptible to sudden changes.

- IC_{50} assays with SEN089 and other important compounds should be performed on the clinical isolates.

- A comprehensive study should be performed to determine how SEN066 and SEN022 inhibit the *pqs* system. By expanding the phenotypic tests performed with these compounds and their impact on other targets such as *las, rhl* or PqsE.

- SEN089 should be tested in a Bioflux microfluidics system to assess its relevance in other types of infections such as catheter-associated.

- The impact of *pqs* inhibition with SENBIOTAR compounds towards formation of persisters should be assessed. By comparing the formation of this subpopulation to control groups.

- The impact of *pqs* inhibition with SENBIOTAR compounds on cultures grown in anaerobic or microaerophilic conditions should be

determined. This would include the study of both planktonic and biofilm development in those conditions.

- Biofilm assays should be performed with the available clinical strains but also with mucoid and QS loss of function mutant strains.

7. Supplementary Data

Figure 7.1. *pqsA* alignment between PAO1 ref. sequence and strains used in this thesis. Mismatches are highlighted in black, The ATG start codon and TAG stop codon are highlighted in yellow.

```
Ref_pqsA          1 GAAGCCTGCAAATGGCAGGCGAGGCGGGGCGGAGCGCTATCGGCCCGATGGATGGCCGCCTGCTTCCAGGCATGCCGTCGCCCCCTTGGAGCCCAGGCCGAGCGCCTCGAACTG
PAO1-L__WT        1 GAAGCCTGCAAATGGCAGGCGAGGCGGGGCGGAGCGCTATCGGCCCGATGGATGGCCGCCTGCTTCCAGGCATGCCGTCGCCCCCTTGGAGCCCAGGCCGAGCGCCTCGAACTG
PALESB58__LES     1 GAAGCCTGCAAATGGCAGGCGAGGCGGGGCGGAGCGCTATCGGCCCGATGGATGGCCGCCTGCTTCCAGGCATGCCGTCGCCCCCTTGGAGCCCAGGCCGAGCGCCTCGAACTG
PAK__6085         1 GAAGCCTGCAAATGGCAGGCGAGGCGGGGCGGAGCGCTATCGGCCCGATGGATGGCCGCCTGCTTCCAGGCATGCCGTCGCCCCCTTGGAGCCCAGGCCGAGCGCCTCGAACTG
PAO1__279         1 GAAGCCTGCAAATGGCAGGCGAGGCGGGGCGGAGCGCTATCGGCCCGATGGATGGCCGCCTGCTTCCAGGCATGCCGTCGCCCCCTTGGAGCCCAGGCCGAGCGCCTCGAACTG
PA14__AL191       1 GAAGCCTGCAAATGGCAGGCGAGGCGGGGCGGAGCGCTATCGGCCCGATGGATGGCCGCCTGCTTCCAGGCATGCCGTCGCCCCCTTGGAGCCCAGGCCGAGCGCCTCGAACTG
PA7__48           1 GAGGCCTGCAAATGGCAGGCGAGACGGGGTGGAGCGCTATCGGCCGGATGGATGGCCGCCCGCTTCCAGGCATGCCGTCGCCCCCTTGGAGCCCAGGCCGAGCGCCTCGAACTG

Ref_pqsA        115 TGAGATTTGGGAGGCGATTTGCCGAGCAAAGTGGGTTGTCATTGGTTTGCCATCTCATGGGTTCGGACGAGGCCTCGAGCAAGGGTTGTAACGGTTTTTGTCTGGCCAATGGGC
PAO1-L__WT      115 TGAGATTTGGGAGGCGATTTGCCGAGCAAAGTGGGTTGTCATTGGTTTGCCATCTCATGGGTTCGGACGAGGCCTCGAGCAAGGGTTGTAACGGTTTTTGTCTGGCCAATGGGC
PALESB58__LES   115 TGAGATCTGGGAGGCGATTTGCCGAGCAAAGTGGGTTGTCATTGGTTTGCCATCTCATGGGTTCGGACGAGGCCTCGAGCAAGGGTTGTAACGGTTTTTGTCTGGCCAATGGGC
PAK__6085       115 TGAGATCTGGGAGGCGATTTGCCGAGCAAAGTGGGTTGTCATTGGTTTGCCATCTCATGGGTTCGGACGAGGCCTCGAGCAAGGGTTGTAACGGTTTTTGTCTGGCCAATGGGC
PAO1__279       115 TGAGATCTGGGAGGCGATTTGCCGAGCAAAGTGGGTTGTCATTGGTTTGCCATCTCATGGGTTCGGACGAGGCCTCGAGCAAGGGTTGTAACGGTTTTTGTCTGGCCAATGGGC
PA14__AL191     115 TGAGATCTGGGAGGCGATTTGCCGAGCAAAGTGGGTTGTCATTGGTTTGCCATCTCATGGGTTCGGACGAGGCCTCGAGCAAGGGTTGTAACGGTTTTTGTCTGGCCAATGGGC
PA7__48         115 TGAGATCTGGGAGGCGATTTGCCGAGCAAAGTGGGTTGTCATTGGTTTGCCATCTCATGGGTTCGGACGAGGCCTCGAGTAAGGGTTGTAACGGTTTTTGTCTGGCCAGTGGGC

Ref_pqsA        229 TCTTGCGTAAAAAGGCTGCCGCCCTTCTTGCTTGGTTGCCGTTCTCGGATCCCGCGCAGCCCGGTGGGTGTGCCAAATTTCTCGCGGTTTGGATCGCGCCGATTGCCGCGGCCT
PAO1-L__WT      229 TCTTGCGTAAAAAGGCTGCCGCCCTTCTTGCTTGGTTGCCGTTCTCGGATCCCGCGCAGCCCGGTGGGTGTGCCAAATTTCTCGCGGTTTGGATCGCGCCGATTGCCGCGGCCT
PALESB58__LES   229 TCCTGCGTAAAAAGGCTGCCGCCCTTCTTGCTTGGTTGCCGTTCTCGGATCCCGCGCAGCCCGGTGGGTGTGCCAAATTTCTCGCGGTTTGGATCGCGCCGATTGCCGCGGCCT
PAK__6085       229 TCTTGCGTAAAAAGGCTGCCGCCCTTCTTGCTTGGTTGCCGTTCTCGGATCCCGCGCAGCCCGGTGGGTGTGCCAAATTTCTCGCGGTTTGGATCGCGCCGATTGCCGCGGCCT
PAO1__279       229 TCTTGCGTAAAAAGGCTGCCGCCCTTCTTGCTTGGTTGCCGTTCTCGGATCCCGCGCAGCCCGGTGGGTGTGCCAAATTTCTCGCGGTTTGGATCGCGCCGATTGCCGCGGCCT
PA14__AL191     229 TCTTGCGTAAAAAGGCTGCCGCCCTTCTTGCTTGGTTGCCGTTCTCGGATCCCGCGCAGCCCGGTGGGTGTGCCAAATTTCTCGCGGTTTGGATCGCGCCGATTGCCGCGGCCT
PA7__48         229 TCTTGCGTAAAGAGGCTGCCGCCCTTCTTGCTTGGTTGCCGTTCTCGGATCCCGCGCAGTCCGGTGGGTGTGCCAAATTTCTCGCGGTTTGGATAGCGCCGATTGCCGCGGCCT

Ref_pqsA        343 ACGAAGCCCGTGGTTCTTCTCCCCGAAACTTTTTCGTTCGGACTCCGAATATCGCGCTTCGCCCAGCGCCGCTAGTTTCCCGTTCCTGACAAAGCAAGCGCTCTGGCTCAGGTA
PAO1-L__WT      343 ACGAAGCCCGTGGTTCTTCTCCCCGAAACTTTTTCGTTCGGACTCCGAATATCGCGCTTCGCCCAGCGCCGCTAGTTTCCCGTTCCTGACAAAGCAAGCGCTCTGGCTCAGGTA
PALESB58__LES   343 ACGAAGCCCGTGGTTCTTCTCCCCGAAACTTTTTCGTTCGGACTCCGAATATCGCGCTTCGCCCAGCGCCGCTAGTTTCCCGTTCCTGACAAAGCAAGCGCTCTGGCTCAGGTA
PAK__6085       343 ACGAAGCCCTTGGTTCTTCTCCCCGAAACTTTTTCGTTCGGACTCCGAATATCGCGCTTCGCCCAGCGCCGCTAGTTTCCCGTTCCTGACAAAGCAAGCGCTCTGGCTCAGGTA
PAO1__279       343 ACGAAGCCCTTGGTTCTTCTCCCCGAAACTTTTTCGTTCGGACTCCGAATATCGCGCTTCGCCCAGCGCCGCTAGTTTCCCGTTCCTGACAAAGCAAGCGCTCTGGCTCAGGCA
PA14__AL191     343 ACGAAGCCCGTGGTTCTTCTCCCCGAAACTTTTTCGTTCGGACTCCGAATATCGCGCTTCGCCCAGCGCCGCTAGTTTCCCGTTCCTGACAAAGCAAGCGCTCTGGCTCAGGTA
PA7__48         343 ACTAAGCCCGTGGTTCTTCTCCCCGAAACTTTTTCGTTCGGACTCCGAATATCGCGCTTCGCCCAGCGCCGCTAGTTTCCCGTTCCTGACAAAGCAAGCGCTCTGGCTCAGGTA
```

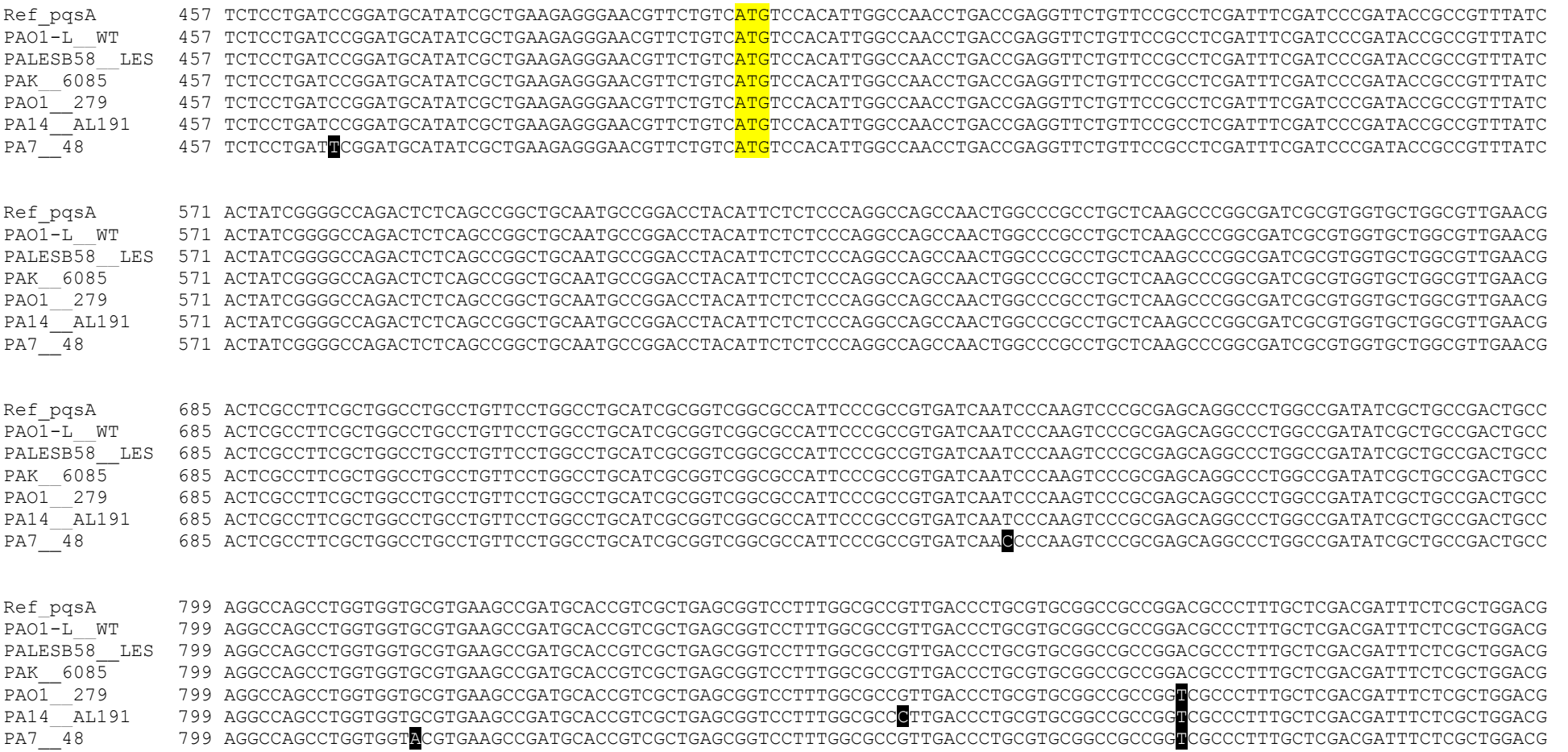
Ref_pqsA 457 TCTCCTGATCCGGATGCATATCGCTGAAGAGGGAACGTTCTGTCATGTCCACATTGGCCAACCTGACCGAGGTTCTGTTCCGCCTCGATTTCGATCCCGATACCGCCGTTTATC
PAO1-L__WT 457 TCTCCTGATCCGGATGCATATCGCTGAAGAGGGAACGTTCTGTCATGTCCACATTGGCCAACCTGACCGAGGTTCTGTTCCGCCTCGATTTCGATCCCGATACCGCCGTTTATC
PALESB58__LES 457 TCTCCTGATCCGGATGCATATCGCTGAAGAGGGAACGTTCTGTCATGTCCACATTGGCCAACCTGACCGAGGTTCTGTTCCGCCTCGATTTCGATCCCGATACCGCCGTTTATC
PAK__6085 457 TCTCCTGATCCGGATGCATATCGCTGAAGAGGGAACGTTCTGTCATGTCCACATTGGCCAACCTGACCGAGGTTCTGTTCCGCCTCGATTTCGATCCCGATACCGCCGTTTATC
PAO1__279 457 TCTCCTGATCCGGATGCATATCGCTGAAGAGGGAACGTTCTGTCATGTCCACATTGGCCAACCTGACCGAGGTTCTGTTCCGCCTCGATTTCGATCCCGATACCGCCGTTTATC
PA14__AL191 457 TCTCCTGATCCGGATGCATATCGCTGAAGAGGGAACGTTCTGTCATGTCCACATTGGCCAACCTGACCGAGGTTCTGTTCCGCCTCGATTTCGATCCCGATACCGCCGTTTATC
PA7__48 457 TCTCCTGATTCGGATGCATATCGCTGAAGAGGGAACGTTCTGTCATGTCCACATTGGCCAACCTGACCGAGGTTCTGTTCCGCCTCGATTTCGATCCCGATACCGCCGTTTATC
Ref_pqsA 571 ACTATCGGGGCCAGACTCTCAGCCGGCTGCAATGCCGGACCTACATTCTCTCCCAGGCCAGCCAACTGGCCCGCCTGCTCAAGCCCGGCGATCGCGTGGTGCTGGCGTTGAACG
PAO1-L__WT 571 ACTATCGGGGCCAGACTCTCAGCCGGCTGCAATGCCGGACCTACATTCTCTCCCAGGCCAGCCAACTGGCCCGCCTGCTCAAGCCCGGCGATCGCGTGGTGCTGGCGTTGAACG
PALESB58__LES 571 ACTATCGGGGCCAGACTCTCAGCCGGCTGCAATGCCGGACCTACATTCTCTCCCAGGCCAGCCAACTGGCCCGCCTGCTCAAGCCCGGCGATCGCGTGGTGCTGGCGTTGAACG
PAK__6085 571 ACTATCGGGGCCAGACTCTCAGCCGGCTGCAATGCCGGACCTACATTCTCTCCCAGGCCAGCCAACTGGCCCGCCTGCTCAAGCCCGGCGATCGCGTGGTGCTGGCGTTGAACG
PAO1__279 571 ACTATCGGGGCCAGACTCTCAGCCGGCTGCAATGCCGGACCTACATTCTCTCCCAGGCCAGCCAACTGGCCCGCCTGCTCAAGCCCGGCGATCGCGTGGTGCTGGCGTTGAACG
PA14__AL191 571 ACTATCGGGGCCAGACTCTCAGCCGGCTGCAATGCCGGACCTACATTCTCTCCCAGGCCAGCCAACTGGCCCGCCTGCTCAAGCCCGGCGATCGCGTGGTGCTGGCGTTGAACG
PA7__48 571 ACTATCGGGGCCAGACTCTCAGCCGGCTGCAATGCCGGACCTACATTCTCTCCCAGGCCAGCCAACTGGCCCGCCTGCTCAAGCCCGGCGATCGCGTGGTGCTGGCGTTGAACG
Ref_pqsA 685 ACTCGCCTTCGCTGGCCTGCCTGTTCCTGGCCTGCATCGCGGTCGGCGCCATTCCCGCCGTGATCAATCCCAAGTCCCGCGAGCAGGCCCTGGCCGATATCGCTGCCGACTGCC
PAO1-L__WT 685 ACTCGCCTTCGCTGGCCTGCCTGTTCCTGGCCTGCATCGCGGTCGGCGCCATTCCCGCCGTGATCAATCCCAAGTCCCGCGAGCAGGCCCTGGCCGATATCGCTGCCGACTGCC
PALESB58__LES 685 ACTCGCCTTCGCTGGCCTGCCTGTTCCTGGCCTGCATCGCGGTCGGCGCCATTCCCGCCGTGATCAATCCCAAGTCCCGCGAGCAGGCCCTGGCCGATATCGCTGCCGACTGCC
PAK__6085 685 ACTCGCCTTCGCTGGCCTGCCTGTTCCTGGCCTGCATCGCGGTCGGCGCCATTCCCGCCGTGATCAATCCCAAGTCCCGCGAGCAGGCCCTGGCCGATATCGCTGCCGACTGCC
PAO1__279 685 ACTCGCCTTCGCTGGCCTGCCTGTTCCTGGCCTGCATCGCGGTCGGCGCCATTCCCGCCGTGATCAATCCCAAGTCCCGCGAGCAGGCCCTGGCCGATATCGCTGCCGACTGCC
PA14__AL191 685 ACTCGCCTTCGCTGGCCTGCCTGTTCCTGGCCTGCATCGCGGTCGGCGCCATTCCCGCCGTGATCAATCCCAAGTCCCGCGAGCAGGCCCTGGCCGATATCGCTGCCGACTGCC
PA7__48 685 ACTCGCCTTCGCTGGCCTGCCTGTTCCTGGCCTGCATCGCGGTCGGCGCCATTCCCGCCGTGATCAACCCCAAGTCCCGCGAGCAGGCCCTGGCCGATATCGCTGCCGACTGCC
Ref_pqsA 799 AGGCCAGCCTGGTGGTGCGTGAAGCCGATGCACCGTCGCTGAGCGGTCCTTTGGCGCCGTTGACCCTGCGTGCGGCCGCCGGACGCCCTTTGCTCGACGATTTCTCGCTGGACG
PAO1-L__WT 799 AGGCCAGCCTGGTGGTGCGTGAAGCCGATGCACCGTCGCTGAGCGGTCCTTTGGCGCCGTTGACCCTGCGTGCGGCCGCCGGACGCCCTTTGCTCGACGATTTCTCGCTGGACG
PALESB58__LES 799 AGGCCAGCCTGGTGGTGCGTGAAGCCGATGCACCGTCGCTGAGCGGTCCTTTGGCGCCGTTGACCCTGCGTGCGGCCGCCGGACGCCCTTTGCTCGACGATTTCTCGCTGGACG
PAK__6085 799 AGGCCAGCCTGGTGGTGCGTGAAGCCGATGCACCGTCGCTGAGCGGTCCTTTGGCGCCGTTGACCCTGCGTGCGGCCGCCGGACGCCCTTTGCTCGACGATTTCTCGCTGGACG
PAO1__279 799 AGGCCAGCCTGGTGGTGCGTGAAGCCGATGCACCGTCGCTGAGCGGTCCTTTGGCGCCGTTGACCCTGCGTGCGGCCGCCGGTCGCCCTTTGCTCGACGATTTCTCGCTGGACG
PA14__AL191 799 AGGCCAGCCTGGTGGTGCGTGAAGCCGATGCACCGTCGCTGAGCGGTCCTTTGGCGCCCTTGACCCTGCGTGCGGCCGCCGGTCGCCCTTTGCTCGACGATTTCTCGCTGGACG
PA7__48 799 AGGCCAGCCTGGTGGTACGTGAAGCCGATGCACCGTCGCTGAGCGGTCCTTTGGCGCCGTTGACCCTGCGTGCGGCCGCCGGTCGCCCTTTGCTCGACGATTTCTCGCTGGACG

```
Ref_pqsA        913 CGCTGGTCGGCCCTGCGGACCTCGATTGGAGTGCCTTCCATCGCCAGGACCCGGCGGCAGCCTGTTTCCTGCAATACACCTCGGGTTCCACCGGGGCGCCCAAGGGGGTGATGC
PAO1-L__WT      913 CGCTGGTCGGCCCTGCGGACCTCGATTGGAGTGCCTTCCATCGCCAGGACCCGGCGGCAGCCTGTTTCCTGCAATACACCTCGGGTTCCACCGGGGCGCCCAAGGGGGTGATGC
PALESB58__LES   913 CGCTGGTCGGTCCTGCGGACCTCGATTGGAGTGCCTTCCATCGCCAGGACCCGGCGGCAGCCTGTTTCCTGCAATACACCTCGGGTTCCACCGGGGCGCCCAAGGGGGTGATGC
PAK__6085       913 CGCTGGTCGGTCCTGCGGACCTCGATTGGAGTGCCTTCCATCGCCAGGACCCGGCGGCAGCCTGTTTCCTGCAATACACCTCGGGTTCCACCGGGGCGCCCAAGGGGGTGATGC
PAO1__279       913 CGCTGGTCGGCCCTGCGGACCTCGATTGGAGTGCCTTCCATCGCCAGGACCCGGCGGCAGCCTGTTTCCTGCAATACACCTCGGGTTCCACCGGGGCGCCCAAGGGGGTGATGC
PA14__AL191     913 CGCTGGTCGGTCCTGCGGACCTCGATTGGAGTGCCTTCCATCGCCAGGACCCGGCGGCAGCCTGTTTCCTGCAATACACCTCGGGTTCCACCGGGGCGCCCAAGGGGGTGATGC
PA7__48         913 CGCTGGTCGGTCCTGCGGACCTCGATTGGAGTGCCTTCCATCGCCAGGACCCGGCGGCAGCCTGTTTCCTGCAATACACCTCGGGTTCCACCGGGGCGCCCAAGGGGGTGATGC
Ref_pqsA       1027 ACAGCCTGCGCAACACGCTCGGTTTCTGCCGGGCGTTCGCTACGGAGTTGCTGGCATTGCAGGCGGGAGACCGGCTGTATTCGATTCCCAAGATGTTCTTCGGCTATGGCATGG

PAO1-L__WT     1027 ACAGCCTGCGCAACACGCTCGGTTTCTGCCGGGCGTTCGCTACGGAGTTGCTGGCATTGCAGGCGGGAGACCGGCTGTATTCGATTCCCAAGATGTTCTTCGGCTATGGCATGG
PALESB58__LES  1027 ACAGCCTGCGCAACACGCTCGGTTTCTGCCGGGCGTTCGCTACGGAGTTGCTGGCATTGCAGGCGGGAGACCGGCTGTATTCGATTCCCAAGATGTTCTTCGGCTATGGCATGG
PAK__6085      1027 ACAGCCTGCGCAACACGCTCGGTTTCTGCCGGGCGTTCGCTACGGAGTTGCTGGCATTGCAGGCGGGAGACCGGCTGTATTCGATTCCCAAGATGTTCTTCGGCTATGGCATGG
PAO1__279      1027 ACAGCCTGCGCAACACGCTCGGTTTCTGCCGGGCGTTCGCTACGGAGTTGCTGGCATTGCAGGCGGGAGACCGGCTGTATTCGATTCCCAAGATGTTCTTCGGCTATGGCATGG
PA14__AL191    1027 ACAGCCTGCGCAACACGCTCGGTTTCTGCCGGGCGTTCGCTACGGAGTTGCTGGCATTGCAGGCGGGAGACCGGCTGTATTCGATTCCCAAGATGTTCTTTGGCTATGGCATGG
PA7__48        1027 ACAGCCTGCGCAACACGCTCGGGTTCTGTCGGGCGTTCGCTACGGAGTTGCTGGCATTGCAGGCGGGAGACCGGCTGTATTCGATTCCCAAGATGTTCTTCGGCTATGGCATGG

Ref_pqsA       1141 GCAACAGCCTGTTCTTTCCCTGGTTCAGCGGAGCCTCGGCGCTGCTCGACGATACCTGGCCGAGCCCGGAGCGGGTTCTGGAGAACCTGGTCGCCTTCCGCCCCCGGGTCCTGT
PAO1-L__WT     1141 GCAACAGCCTGTTCTTTCCCTGGTTCAGCGGAGCCTCGGCGCTGCTCGACGATACCTGGCCGAGCCCGGAGCGGGTTCTGGAGAACCTGGTCGCCTTCCGCCCCCGGGTCCTGT
PALESB58__LES  1141 GCAACAGCCTGTTCTTTCCCTGGTTCAGCGGAGCCTCGGCGCTGCTCGACGATACCTGGCCGAGCCCGGAGCGGGTTCTGGAGAACCTGGTCGCCTTCCGCCCCCGGGTCCTGT
PAK__6085      1141 GCAACAGCCTGTTCTTTCCCTGGTTCAGCGGAGCCTCGGCGCTGCTCGACGATACCTGGCCGAGCCCGGAGCGGGTTCTGGAGAACCTGGTCGCCTTCCGCCCCCGGGTCCTGT
PAO1__279      1141 GCAACAGCCTGTTCTTTCCCTGGTTCAGCGGAGCCTCGGCGCTGCTCGACGATACCTGGCCGAGCCCGGAGCGGGTTCTGGAGAACCTGGTCGCCTTCCGCCCCCGGGTCCTGT
PA14__AL191    1141 GCAACAGCCTGTTCTTTCCCTGGTTCAGCGGAGCCTCGGCGCTGCTCGACGATACCTGGCCGAGCCCGGAGCGGGTCCTGGAGAACCTGGTCGCCTTCCGCCCCCGGGTCCTGT
PA7__48        1141 GCAACAGCCTGTTCTTTCCCTGGTTCAGCGGAGCCTCGGCGCTGCTCGACGATACCTGGCCGAGCCCGGAGCGGGTCCTGGAGAACCTGGTCGCCTTCCGCCCCCGGGTCCTGT

Ref_pqsA       1255 TTGGGGTGCCGGCCATCTATGCCTCGCTGCGTCCGCAGGCCAGGGAGCTGTTGAGCAGCGTGCGCCTGGCGTTTTCCGCCGGCTCGCCGCTGCCGCGCGGCGAGTTCGAATTCT
PAO1-L__WT     1255 TTGGGGTGCCGGCCATCTATGCCTCGCTGCGTCCGCAGGCCAGGGAGCTGTTGAGCAGCGTGCGCCTGGCGTTTTCCGCCGGCTCGCCGCTGCCGCGCGGCGAGTTCGAATTCT
PALESB58__LES  1255 TTGGGGTGCCGGCCATCTATGCCTCGCTGCGTCCGCAGGCCAGGGAGCTGTTGAGCAGCGTGCGCCTGGCGTTTTCCGCCGGCTCGCCGCTGCCGCGCGGCGAGTTCGAATTCT
PAK__6085      1255 TTGGGGTGCCGGCCATCTATGCCTCGCTGCGTCCGCAGGCCAGGGAGCTGTTGAGCAGCGTGCGCCTGGCGTTTTCCGCCGGCTCGCCGCTGCCGCGCGGCGAGTTCGAATTCT
PAO1__279      1255 TTGGGGTGCCGGCCATCTATGCCTCGCTGCGTCCGCAGGCCAGGGAGCTGTTGAGCAGCGTGCGCCTGGCGTTTTCCGCCGGCTCGCCGCTGCCGCGCGGCGAGTTCGAATTCT
PA14__AL191    1255 TTGGGGTGCCAGCCATCTATGCCTCGCTGCGTGCGCAGGCCAGGGCGCTGTTGAGCAGCGTGCGCCTGGCGTTTTCCGCCGGCTCGCCGCTGCCGCGCGGCGAGTTCGAATTCT
PA7__48        1255 TTGGGGTGCCAGCCATCTATGCCTCGCTGCGTGCGCAGGCCAGGGAGCTGTTGAGCAGCGTGCGCCTGGCGTTTTCCGCCGGCTCGCCGCTGCCGCGCGGCGAGTTCGAATTCT
```

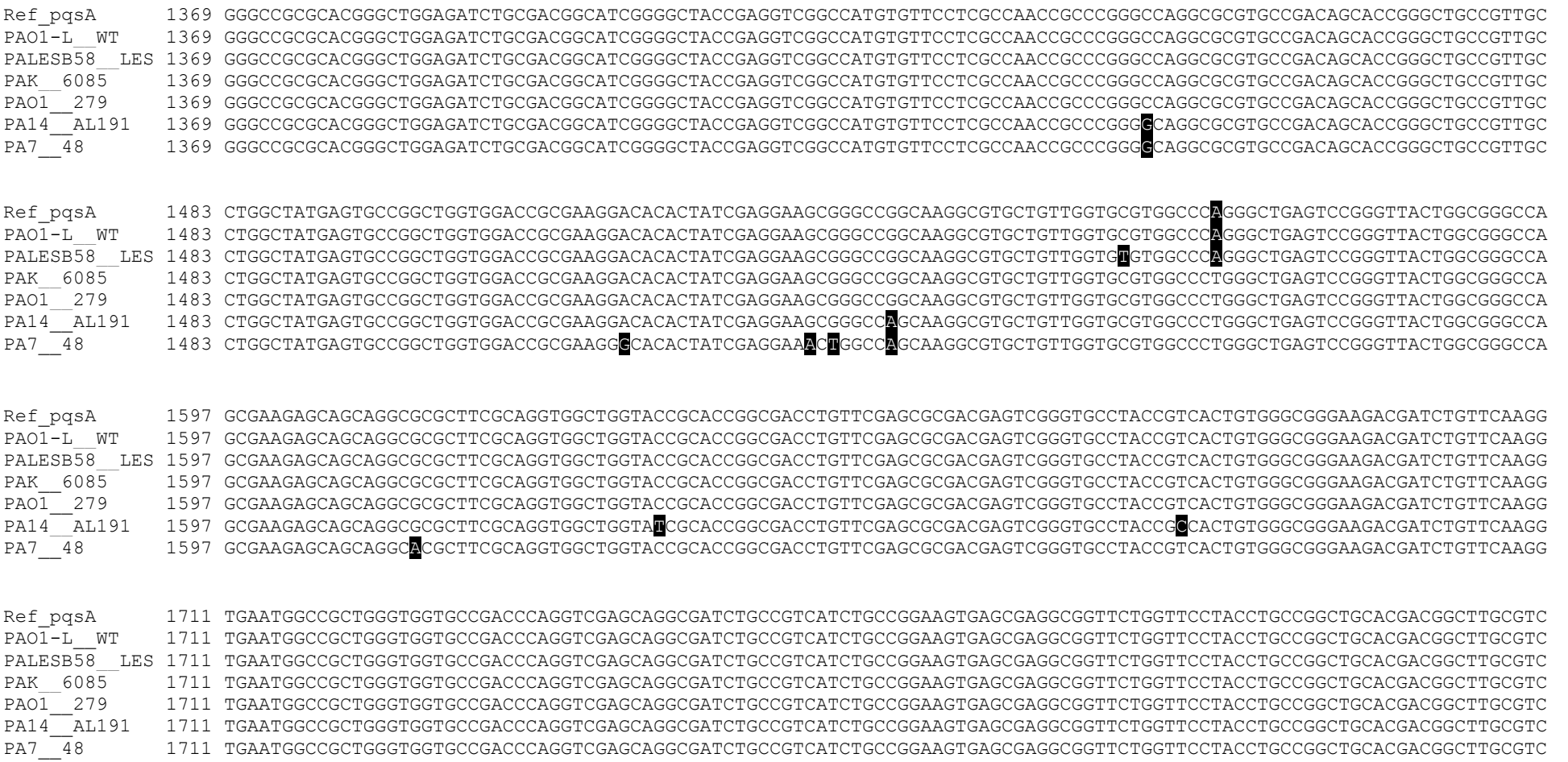
Ref_pqsA 1369 GGGCCGCGCACGGGCTGGAGATCTGCGACGGCATCGGGGCTACCGAGGTCGGCCATGTGTTCCTCGCCAACCGCCCGGGCCAGGCGCGTGCCGACAGCACCGGGCTGCCGTTGC
PAO1-L__WT 1369 GGGCCGCGCACGGGCTGGAGATCTGCGACGGCATCGGGGCTACCGAGGTCGGCCATGTGTTCCTCGCCAACCGCCCGGGCCAGGCGCGTGCCGACAGCACCGGGCTGCCGTTGC
PALESB58__LES 1369 GGGCCGCGCACGGGCTGGAGATCTGCGACGGCATCGGGGCTACCGAGGTCGGCCATGTGTTCCTCGCCAACCGCCCGGGCCAGGCGCGTGCCGACAGCACCGGGCTGCCGTTGC
PAK__6085 1369 GGGCCGCGCACGGGCTGGAGATCTGCGACGGCATCGGGGCTACCGAGGTCGGCCATGTGTTCCTCGCCAACCGCCCGGGCCAGGCGCGTGCCGACAGCACCGGGCTGCCGTTGC
PAO1__279 1369 GGGCCGCGCACGGGCTGGAGATCTGCGACGGCATCGGGGCTACCGAGGTCGGCCATGTGTTCCTCGCCAACCGCCCGGGCCAGGCGCGTGCCGACAGCACCGGGCTGCCGTTGC
PA14__AL191 1369 GGGCCGCGCACGGGCTGGAGATCTGCGACGGCATCGGGGCTACCGAGGTCGGCCATGTGTTCCTCGCCAACCGCCCGGGGCAGGCGCGTGCCGACAGCACCGGGCTGCCGTTGC
PA7__48 1369 GGGCCGCGCACGGGCTGGAGATCTGCGACGGCATCGGGGCTACCGAGGTCGGCCATGTGTTCCTCGCCAACCGCCCGGGGCAGGCGCGTGCCGACAGCACCGGGCTGCCGTTGC
Ref_pqsA 1483 CTGGCTATGAGTGCCGGCTGGTGGACCGCGAAGGACACACTATCGAGGAAGCGGGCCGGCAAGGCGTGCTGTTGGTGCGTGGCCCAGGGCTGAGTCCGGGTTACTGGCGGGCCA
PAO1-L__WT 1483 CTGGCTATGAGTGCCGGCTGGTGGACCGCGAAGGACACACTATCGAGGAAGCGGGCCGGCAAGGCGTGCTGTTGGTGCGTGGCCCAGGGCTGAGTCCGGGTTACTGGCGGGCCA
PALESB58__LES 1483 CTGGCTATGAGTGCCGGCTGGTGGACCGCGAAGGACACACTATCGAGGAAGCGGGCCGGCAAGGCGTGCTGTTGGTGTGTGGCCCAGGGCTGAGTCCGGGTTACTGGCGGGCCA
PAK__6085 1483 CTGGCTATGAGTGCCGGCTGGTGGACCGCGAAGGACACACTATCGAGGAAGCGGGCCGGCAAGGCGTGCTGTTGGTGCGTGGCCCTGGGCTGAGTCCGGGTTACTGGCGGGCCA
PAO1__279 1483 CTGGCTATGAGTGCCGGCTGGTGGACCGCGAAGGACACACTATCGAGGAAGCGGGCCGGCAAGGCGTGCTGTTGGTGCGTGGCCCTGGGCTGAGTCCGGGTTACTGGCGGGCCA
PA14__AL191 1483 CTGGCTATGAGTGCCGGCTGGTGGACCGCGAAGGACACACTATCGAGGAAGCGGGCCAGCAAGGCGTGCTGTTGGTGCGTGGCCCTGGGCTGAGTCCGGGTTACTGGCGGGCCA
PA7__48 1483 CTGGCTATGAGTGCCGGCTGGTGGACCGCGAAGGGCACACTATCGAGGAAACTGGCCAGCAAGGCGTGCTGTTGGTGCGTGGCCCTGGGCTGAGTCCGGGTTACTGGCGGGCCA
Ref_pqsA 1597 GCGAAGAGCAGCAGGCGCGCTTCGCAGGTGGCTGGTACCGCACCGGCGACCTGTTCGAGCGCGACGAGTCGGGTGCCTACCGTCACTGTGGGCGGGAAGACGATCTGTTCAAGG
PAO1-L__WT 1597 GCGAAGAGCAGCAGGCGCGCTTCGCAGGTGGCTGGTACCGCACCGGCGACCTGTTCGAGCGCGACGAGTCGGGTGCCTACCGTCACTGTGGGCGGGAAGACGATCTGTTCAAGG
PALESB58__LES 1597 GCGAAGAGCAGCAGGCGCGCTTCGCAGGTGGCTGGTACCGCACCGGCGACCTGTTCGAGCGCGACGAGTCGGGTGCCTACCGTCACTGTGGGCGGGAAGACGATCTGTTCAAGG
PAK__6085 1597 GCGAAGAGCAGCAGGCGCGCTTCGCAGGTGGCTGGTACCGCACCGGCGACCTGTTCGAGCGCGACGAGTCGGGTGCCTACCGTCACTGTGGGCGGGAAGACGATCTGTTCAAGG
PAO1__279 1597 GCGAAGAGCAGCAGGCGCGCTTCGCAGGTGGCTGGTACCGCACCGGCGACCTGTTCGAGCGCGACGAGTCGGGTGCCTACCGTCACTGTGGGCGGGAAGACGATCTGTTCAAGG
PA14__AL191 1597 GCGAAGAGCAGCAGGCGCGCTTCGCAGGTGGCTGGTATCGCACCGGCGACCTGTTCGAGCGCGACGAGTCGGGTGCCTACCGCCACTGTGGGCGGGAAGACGATCTGTTCAAGG
PA7__48 1597 GCGAAGAGCAGCAGGCACGCTTCGCAGGTGGCTGGTACCGCACCGGCGACCTGTTCGAGCGCGACGAGTCGGGTGCCTACCGTCACTGTGGGCGGGAAGACGATCTGTTCAAGG
Ref_pqsA 1711 TGAATGGCCGCTGGGTGGTGCCGACCCAGGTCGAGCAGGCGATCTGCCGTCATCTGCCGGAAGTGAGCGAGGCGGTTCTGGTTCCTACCTGCCGGCTGCACGACGGCTTGCGTC
PAO1-L__WT 1711 TGAATGGCCGCTGGGTGGTGCCGACCCAGGTCGAGCAGGCGATCTGCCGTCATCTGCCGGAAGTGAGCGAGGCGGTTCTGGTTCCTACCTGCCGGCTGCACGACGGCTTGCGTC
PALESB58__LES 1711 TGAATGGCCGCTGGGTGGTGCCGACCCAGGTCGAGCAGGCGATCTGCCGTCATCTGCCGGAAGTGAGCGAGGCGGTTCTGGTTCCTACCTGCCGGCTGCACGACGGCTTGCGTC
PAK__6085 1711 TGAATGGCCGCTGGGTGGTGCCGACCCAGGTCGAGCAGGCGATCTGCCGTCATCTGCCGGAAGTGAGCGAGGCGGTTCTGGTTCCTACCTGCCGGCTGCACGACGGCTTGCGTC
PAO1__279 1711 TGAATGGCCGCTGGGTGGTGCCGACCCAGGTCGAGCAGGCGATCTGCCGTCATCTGCCGGAAGTGAGCGAGGCGGTTCTGGTTCCTACCTGCCGGCTGCACGACGGCTTGCGTC
PA14__AL191 1711 TGAATGGCCGCTGGGTGGTGCCGACCCAGGTCGAGCAGGCGATCTGCCGTCATCTGCCGGAAGTGAGCGAGGCGGTTCTGGTTCCTACCTGCCGGCTGCACGACGGCTTGCGTC
PA7__48 1711 TGAATGGCCGCTGGGTGGTGCCGACCCAGGTCGAGCAGGCGATCTGCCGTCATCTGCCGGAAGTGAGCGAGGCGGTTCTGGTTCCTACCTGCCGGCTGCACGACGGCTTGCGTC

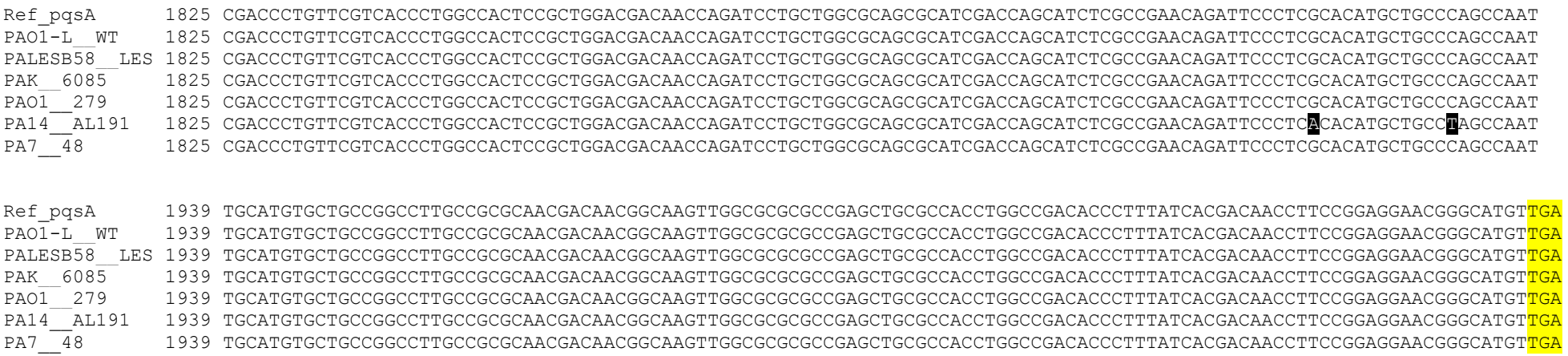

Figure 7.2. *pqsR* alignment between PAO1 ref. sequence and strains used in this thesis. Mismatches are highlighted in black, The ATG start codon and TAG stop codon are highlighted in yellow.

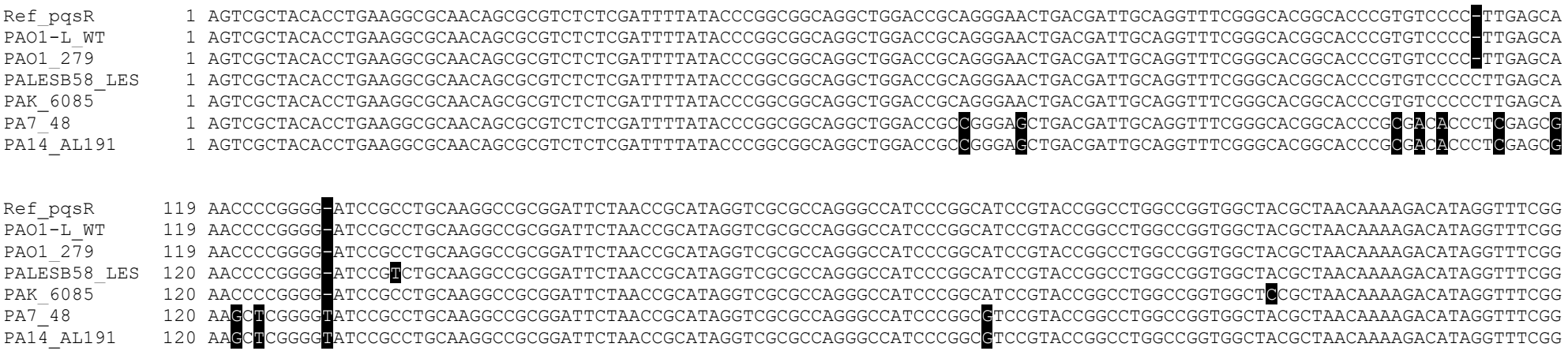


Ref_pqsR 237 TCGTTAGACCTACGCGACATAATTTTTTCGTTTCTTAGAACCGTTCCTGGCTCGGCTCGCTCCACGACCGAACACGACATGCCGGCATGCCAGCGTTAATACTTTGGTATTAGGCCCTT
PAO1-L_WT 237 TCGTTAGACCTACGCGACATAATTTTTTCGTTTCTTAGAACCGTTCCTGGCTCGGCTCGCTCCACGACCGAACACGACATGCCGGCATGCCAGCGTTAATACTTTGGTATTAGGCCCTT
PAO1_279 237 TCGTTAGACCTACGCGACATAATTTTTTCGTTTCTTAGAACCGTCCCTGGCTCGGCTCGCTCCACGACCGAACACGACATGCCGGCATGCCAGCGTTAATACTTTGGTATTAGGCCCTT
PALESB58_LES 238 TCGTTAGACCTACGCGACATAATTTTTTCGTTTCTTAGAACCGTCCCTGGCTCGGCTCGCTCCACGACCGAACACGACATGCCGGCATGCCAGCGTTAATACTTTGGTATTAGGCCCTT
PAK_6085 238 TCGTTAGACCTACGCGACATAATTTTTTCGTTTCTTAGAACCGTCCCTGACTCGGCTCGCTCCACAACCGAACACGACATGCCGGCATGCCAGCGTTAATACTTTGGTATTAGGCCCTT
PA7_48 239 TCGTTAGACCTACGCGACATAATTTTTTCGTTTCTTAGAACCGTCCCTAGCTCGGCTCGCTCCACGACCGAACACGACATGCCGGCATGCCAGCGTTAATACTTTGGTATTAGGCCCTT
PA14_AL191 239 TCGTTAGACCTACGCGACATAATTTTTTCGTTTCTTAGAACCGTCCCTAGCTCGGCTCGCTCCACGACCGAACACGACATGCCGGCATACCAGCGTTAATACTTTGGTATTAGGCACTT
Ref_pqsR 356 GGTATTAACGTTAAATAACCGGTAAATATCCGGATTTTCTTTTCGTCGAATTTACGAGCAATATGAAACATATTTCGTTGAAATAAGCTCTTCTTTCACATAATTATAAAAATATCCTG
PAO1-L_WT 356 GGTATTAACGTTAAATAACCGGTAAATATCCGGATTTTCTTTTCGTCGAATTTACGAGCAATATGAAACATATTTCGTTGAAATAAGCTCTTCTTTCACATAATTATAAAAATATCCTG
PAO1_279 356 GGTATTAACGTTAAATAACCGGTAAATATCCGGATTTTCTTTTCGTCGAATTTACGAGCAATATGAAACATATTTCGTTGAAATAAGCTCTTCTTTCACATAATTATAAAAATATCCTG
PALESB58_LES 357 GGTATTAACGTTAAATAACCGGTAAATATCCGGATTTTCTTTTCGTCGAATTTACGAGCAATATGAAACATATTTCGTTGAAATAAGCTCTTCTTTCACATAATTATAAAAATATCCTG
PAK_6085 357 GGTATTAGCGTTAAATAACCGGTAAATATCCGGATTTTCTTTTCGTCGAATTTACGAGCAATATGAAACATATTTCGTTGAAATAAGCTCTTCTTTCACATAATTATAAAAATATCCTG
PA7_48 358 GGTATTAGCGTTAAATAACCGGTAAATATCCGGATTTTCTTTTCGTCGAATTTACGAGCAATATGAAACATATTTCGTTGAAATAAGCTCTTCTTTCACATAATTATAAAAATATCCTG
PA14_AL191 358 GGTATTAGCGTTAAATAACCGGTAAATATCCGGATTTTCTTTTCGTCGAATTTACGAGCAATATGAAACATATTTCGTTGAAATAAGCTCTTCTTTCACATAATTATAAAAATATCCTG
Ref_pqsR 475 AAACAGAGCCGTCATCCCTCACCTCCAAAACGACGACTCCCCGTGCCGTGCGCCCGCCGCGCAGAAAGCGAGCCGGCGGCCGATTCCACCCTCGCACGCCAGCCCTTGCGCTTCACTGA
PAO1-L_WT 475 AAACAGAGCCGTCATCCCTCACCTCCAAAACGACGACTCCCCGTGCCGTGCGCCCGCCGCGCAGAAAGCGAGCCGGCGGCCGATTCCACCCTCGCACGCCAGCCCTTGCGCTTCACTGA
PAO1_279 475 AAACAGAGCCGTCATCCCTCACCTCCAAAACGACGACTCCCCGTGCCGTGCGCCCGCCGCGCAGAAAGCGAGCCGGCGGCCGATTCCACCCTCGCACGCCAGCCCTTGCGCTTCACTGA
PALESB58_LES 476 AAACAGAGCCGTCATCCCTCACCTCCAAAACGACGACTCCCCGTGCCGTGCGCCCGCCGCGCAGAAAGCGAGCCGGCGGCCGATTCCACCCTCGCACGCCAGCCCTTGCGCTTCACTGA
PAK_6085 476 AAACAGAGCCGTCATCCCTCACCTCCAAAACGACGACTCCCCGTGCCGTGCGCCCGCCGCGCAGAAAGCGAGCCGGCGGCCGATTCCACCCTCGCACGCCAGCCCTTGCGCTTCACTGA
PA7_48 477 AAACAGAGCCGTCATCCCTCACCTCCAAAACGACGACTCCCCGTGCCGTGCGCCCGCCGCGCAGAAAGCGAGCCGGCGGCCGATTCCACCCTCGCACGCCAGCCCTTGCGCTTCACTGA
PA14_AL191 477 AAACAGAGCCGTCATCCCTCACCTCCAAAACGACGACTCCCCGTGCCGTGCGCCCGCCGCGCAGAAAGCGAGCCGGCGGCCGATTCCACCCTCGCACGCCAGCCCTTGCGCTTCACTGA
Ref_pqsR 594 CCGACGGGAGGTTTCCCCGATGAAAACGTCATCCAGAAGACAAGTTGAAACACTCGGGCGCTATCTATCGAGTCCTCGACGCTTCTTCCACAGTAGCGGCAACCTGACCCGATCAAGGG
PAO1-L_WT 594 CCGACGGGAGGTTTCCCCGATGAAAACGTCATCCAGAAGACAAGTTGAAACACTCGGGCGCTATCTATCGAGTCCTCGACGCTTCTTCCACAGTAGCGGCAACCTGACCCGATCAAGGG
PAO1_279 594 CCGACGGGAGGTTTCCCCGATGAAAACGTCATCCAGAAGACAAGTTGAAACACTCGGGCGCTATCTATCGAGTCCTCGACGCTTCTTCCACAGTAGCGGCAACCTGACCCGATCAAGGG
PALESB58_LES 595 CCGACGGGAGGTTTCCCCGATGAAAACGTCATCCAGAAGACAAGTTGAAACACTCGGGCGCTATCTATCGAGTCCTCGACGCTTCTTCCACAGTAGCGGCAACCTGACCCGATCAAGGG
PAK_6085 595 CCGACGGGAGGTTTCCCCGATGAAAACGTCATCCAGAAGACAAGTTGAAACACTCGGGCGCTATCTATCGAGTCCTCGACGCTTCTTCCACAGTAGCGGCAACCTGACCCGATCAAGGG
PA7_48 596 CCGACGGGAGGTTTCCCCGATGAAAACGTCATCCAGAAGACAAGTTGAAACACTCGGGCGCTATCTATCGAGTCCTCGACGCTTCTTCCACAGTAGCGGCAACCTGACCCGATCAAGGG
PA14_AL191 596 CCGACGGGAGGTTTCCCCGATGAAAACGTCATCCAGAAGACAAGTTGAAACACTCGGGCGCTATCTATCGAGTCCTCGACGCTTCTTCCACAGTAGCGGCAACCTGACCCGATCAAGGG

```
Ref_pqsR       713 AAGCGGCACGCGCCACCCAATAAAAGGAATAAGGGATGCCTATTCATAACCTGAATCACGTGAACATGTTCCTCCAGGTCATCGCCTCCGGTTCGATTTCCTCCGCTGCGCGGATCCTG
PAO1-L_WT      713 AAGCGGCACGCGCCACCCAATAAAAGGAATAAGGGATGCCTATTCATAACCTGAATCACGTGAACATGTTCCTCCAGGTCATCGCCTCCGGTTCGATTTCCTCCGCTGCGCGGATCCTG
PAO1_279       713 AAGCGGCACGCGCCACCCAATAAAAGGAATAAGGGATGCCTATTCATAACCTGAATCACGTGAACATGTTCCTCCAGGTCATCGCCTCCGGTTCGATTTCCTCCGCTGCGCGGATCCTG
PALESB58_LES   714 AAGCGGCACGCGCCACCCAATAAAAGGAATAAGGGATGCCTATTCATAACCTGAATCACGTGAACATGTTCCTCCAGGTCATCGCCTCCGGTTCGATTTCCTCCGCTGCGCGGATCCTG
PAK_6085       714 AAGCGGCACGCGCCACCCAATAAAAGGAATAAGGGATGCCTATTCATAACCTGAATCACGTGAACATGTTCCTCCAGGTCATCGCCTCCGGTTCGATTTCCTCCGCTGCGCGGATCCTG
PA7_48         715 AAGCGGCACGCGCCACCCAATAAAAGGAATAAGGGATGCCTATTCATAACCTGAATCACGTGAACATGTTCCTCCAGGTCATCGCCTCCGGTTCGATTTCCTCCGCTGCGCGGATCCTG
PA14_AL191     715 AAGCGGCACGCGCCACCCAATAAAAGGAATAAGGGATGCCTATTCATAACCTGAATCACGTGAACATGTTCCTCCAGGTCATCGCCTCCGGTTCGATTTCCTCCGCTGCGCGGATCCTG

Ref_pqsR       832 CGCAAGTCGCACACCGCGGTCAGCTCGGCGGTCAGCAACCTGGAAATCGACCTGTGCGTGGAGCTGGTCCGTCGGGACGGCTACAAGGTCGAACCCACCGAGCAGGCGCTTCGCCTGAT
PAO1-L_WT      832 CGCAAGTCGCACACCGCGGTCAGCTCGGCGGTCAGCAACCTGGAAATCGACCTGTGCGTGGAGCTGGTCCGTCGGGACGGCTACAAGGTCGAACCCACCGAGCAGGCGCTTCGCCTGAT
PAO1_279       832 CGCAAGTCGCACACCGCGGTCAGCTCGGCGGTCAGCAACCTGGAAATCGACCTGTGCGTGGAGCTGGTCCGTCGGGACGGCTACAAGGTCGAACCCACCGAGCAGGCGCTTCGCCTGAT
PALESB58_LES   833 CGCAAGTCGCACACCGCGGTCAGCTCGGCGGTCAGCAACCTGGAAATCGACCTGTGCGTGGAGCTGGTCCGTCGGGACGGCTACAAGGTCGAACCCACCGAGCAGGCGCTTCGCCTGAT
PAK_6085       833 CGCAAGTCGCACACCGCGGTCAGCTCGGCGGTCAGCAACTTGGAAATCGACCTGTGCGTGGAGCTGGTCCGTCGGGACGGCTACAAGGTCGAACCCACCGAGCAGGCGCTTCGCCTGAT
PA7_48         834 CGCAAGTCGCACACCGCGGTCAGCTCGGCGGTCAGCAACCTGGAAATCGACCTGTGCGTGGAGCTGGTCCGTCGGGACGGCTACAAGGTCGAACCCACCGAGCAGGCGCTTCGCCTGAT
PA14_AL191     834 CGCAAGTCGCACACCGCGGTCAGCTCGGCGGTCAGCAACCTGGAAATCGACCTATGCGTGGAGCTGGTCCGTCGGGACGGCTACAAGGTCGAACCCACCGAGCAGGCGCTTCGCCTGAT

Ref_pqsR       951 CCCTTACATGCGCAGCCTGCTGAACTACCAGCAGCTGATCGGCGACATCGCCTTCAATCTCAACAAGGGTCCGCGCAATCTCCGGGTGCTGCTGGACACCGCCATCCCGCCGTCGTTCT
PAO1-L_WT      951 CCCTTACATGCGCAGCCTGCTGAACTACCAGCAGCTGATCGGCGACATCGCCTTCAATCTCAACAAGGGTCCGCGCAATCTCCGGGTGCTGCTGGACACCGCCATCCCGCCGTCGTTCT
PAO1_279       951 CCCTTACATGCGCAGCCTGCTGAACTACCAGCAGCTGATCGGCGACATCGCCTTCAATCTCAACAAGGGTCCGCGCAATCTCCGGGTGTTGCTGGACACCGCCATCCCGCCGTCGTTCT
PALESB58_LES   952 CCCTTACATGCGCAGCCTGCTGAACTACCAGCAGCTGATCGGCGACATCGCCTTCAATCTCAACAAGGGTCCGCGCAATCTCCGGGTGTTGCTGGACACCGCCATCCCGCCGTCGTTCT
PAK_6085       952 CCCTTACATGCGCAGCCTGCTGAACTACCAGCAGCTGATCGGCGACATCGCCTTCAATCTCAACAAGGGTCCGCGCAATCTCCGGGTGCTGCTGGACACCGCCATCCCGCCGTCGTTCT
PA7_48         953 CCCTTACATGCGCAGCCTGCTGAACTACCAGCAGCTGATCGGCGACATCGCCTTCAATCTCAACAAGGGTCCGCGCAATCTCCGGGTGCTGCTGGACACCGCCATCCCGCCGTCGTTCT
PA14_AL191     953 CCCTTACATGCGCAGCCTGCTGAACTACCAGCAGCTGATCGGCGACATCGCCTTCAATCTCAACAAGGGTCCGCGCAATCTCCGGGTGCTGCTGGACACCGCCATCCCGCCGTCGTTCT

Ref_pqsR      1070 GCGATACGGTGAGCAGCGTACTGCTCGACGATTTCAACATGGTCAGCCTGATACGCACCTCGCCCGCCGATAGCCTGGCGACGATCAAGCAGGACAACGCGGAAATCGATATCGCCATC
PAO1-L_WT     1070 GCGATACGGTGAGCAGCGTACTGCTCGACGATTTCAACATGGTCAGCCTGATACGCACCTCGCCCGCCGATAGCCTGGCGACGATCAAGCAGGACAACGCGGAAATCGATATCGCCATC
PAO1_279      1070 GCGATACGGTGAGCAGCGTACTGCTCGACGATTTCAACATGGTCAGCCTGATACGCACCTCGCCCGCCGATAGCCTGGCGACGATCAAGCAGGACAACGCGGAAATCGATATCGCCATC
PALESB58_LES  1071 GCGATACGGTGAGCAGCGTACTGCTCGACGATTTCAACATGGTCAGCCTGATACGCACCTCGCCCGCCGATAGCCTGGCGACGATCAAGCAGGACAACGCGGAAATCGATATCGCCATC
PAK_6085      1071 GCGATACGGTGAGCAGCGTACTGCTCGACGATTTCAACATGGTCAGCCTGATACGCACCTCGCCCGCCGATAGCCTGGCGACGATCAAGCAGGACAACGCGGAAATCGATATCGCCATC
PA7_48        1072 GCGATACGGTGAGCAGCGTACTGCTCGACGATTTCAACATGGTCAGCCTGATACGCACCTCGCCCGCCGATAGCCTGGCGACGATCAAGCAGGACAACGCGGAAATCGATATCGCCATC
PA14_AL191    1072 GCGATACGGTGAGCAGCGTACTGCTCGACGATTTCAACATGGTCAGCCTGATACGCACCTCGCCCGCCGATAGCCTGGCGACGATCAAGCAGGACAACGCGGAAATCGATATCGCCATC
```

```
Ref_pqsR      1189 ACCATCGACGAGGAACTGAAGATCTCCCGCTTCAACCAGTGCGTGCTCGGCTACACCAAGGCGTTCGTCGTCGCCCATCCGCAGCACCCGTTGTGCAATGCCTCCCTGCACAGCATCGC
PAO1-L_WT     1189 ACCATCGACGAGGAACTGAAGATCTCCCGCTTCAACCAGTGCGTGCTCGGCTACACCAAGGCGTTCGTCGTCGCCCATCCGCAGCACCCGTTGTGCAATGCCTCCCTGCACAGCATCGC
PAO1_279      1189 ACCATCGACGAGGAACTGAAGATCTCCCGCTTCAACCAGTGCGTGCTCGGCTACACCAAGGCGTTCGTCGTCGCCCATCCGCAGCACCCGTTGTGCAATGCCTCCCTGCACAGCATCGC
PALESB58_LES  1190 ACCATCGACGAGGAACTGAAGATCTCCCGCTTCAACCAGTGCGTGCTCGGCTACACCAAGGCGTTCGTCGTCGCCCATCCGCAGCACCCGTTGTGCAATGCCTCCCTGCACAGCATCGC
PAK_6085      1190 ACCATCGACGAGGAACTGAAGATCTCCCGCTTCAACCAGTGCGTGCTCGGCTACACCAAGGCGTTCGTCGTCGCCCATCCGCAGCACCCGTTGTGCAATGCCTCCCTGCACAGCATCGC
PA7_48        1191 ACCATCGACGAGGAACTGAAGATCTCCCGCTTCAACCAGTGCGTGCTCGGCTACACCAAGGCGTTCGTCGTCGCCCATCCGCAGCACCCGTTGTGCAATGCCTCCCTGCACAGCATCGC
PA14_AL191    1191 ACCATCGACGAGGAACTGAAGATCTCCCGCTTCAACCAGTGCGTGCTCGGCTACACCAAGGCGTTCGTCGTCGCCCATCCGCAGCACCCGTTGTGCAATGCCTCCCTGCACAGCATCGC

Ref_pqsR      1308 GAGCCTGGCCAATTACCGGCAGATCAGCCTCGGCAGCCGCTCCGGGCAGCATTCGAACCTGCTGCGGCCGGTCAGCGACAAGGTGCTCTTCGTGGAAAACTTCGACGACATGCTGCGTC
PAO1-L_WT     1308 GAGCCTGGCCAATTACCGGCAGATCAGCCTCGGCAGCCGCTCCGGGCAGCATTCGAACCTGCTGCGGCCGGTCAGCGACAAGGTGCTCTTCGTGGAAAACTTCGACGACATGCTGCGTC
PAO1_279      1308 GAGCCTGGCCAATTACCGGCAGATCAGCCTCGGCAGCCGCTCCGGGCAGCATTCGAACCTGCTGCGGCCGGTCAGCGACAAGGTGCTCTTCGTGGAAAACTTCGACGACATGCTGCGTC
PALESB58_LES  1309 GAGCCTGGCCAATTACCGGCAGATCAGCCTCGGCAGCCGCTCCGGGCAGCATTCGAACCTGCTGCGGCCGGTCAGCGACAAGGTGCTCTTCGTGGAAAACTTCGACGACATGCTGCGTC
PAK_6085      1309 GAGCCTGGCCAATTACCGGCAGATCAGCCTCGGCAGCCGCTCCGGGCAGCATTCGAACCTGCTGCGGCCGGTCAGCGACAAGGTGCTCTTCGTGGAAAACTTCGACGACATGCTGCGTC
PA7_48        1310 GAGCCTGGCCAATTACCGGCAGATCAGCCTCGGCAGCCGCTCCGGGCAGCATTCGAACCTGCTGCGGCCGGTCAGCGACAAGGTGCTCTTCGTGGAAAACTTCGACGACATGCTGCGTC
PA14_AL191    1310 GAGCCTGGCCAATTACCGGCAGATCAGCCTCGGCAGCCGCTCCGGGCAGCATTCGAACCTGCTGCGGCCGGTCAGCGACAAGGTGCTCTTCGTGGAAAACTTCGACGACATGCTGCGTC

Ref_pqsR      1427 TGGTGGAAGCCGGCGTCGGATGGGGCATCGCGCCGCATTATTTCGTCGAGGAACGCCTGCGCAACGGTACCCTGGCAGTCCTCAGCGAACTCTACGAACCGGGCGGCATCGACACCAAG
PAO1-L_WT     1427 TGGTGGAAGCCGGCGTCGGATGGGGCATCGCGCCGCATTATTTCGTCGAGGAACGCCTGCGCAACGGTACCCTGGCAGTCCTCAGCGAACTCTACGAACCGGGCGGCATCGACACCAAG
PAO1_279      1427 TGGTGGAAGCCGGCGTCGGATGGGGCATCGCGCCGCATTATTTCGTCGAGGAACGCCTGCGCAACGGTACCCTGGCAGTCCTCAGCGAACTCTACGAACCGGGCGGCATCGACACCAAG
PALESB58_LES  1428 TGGTGGAAGCCGGCGTCGGATGGGGCATCGCGCCGCATTATTTCGTCGAGGAACGCCTGCGCAACGGTACCCTGGCAGTCCTCAGCGAACTCTACGAACCGGGCGGCATCGACACCAAG
PAK_6085      1428 TGGTGGAAGCCGGCGTCGGATGGGGCATCGCGCCGCATTATTTCGTCGAGGAACGCCTGCGCAACGGTACCCTGGCAGTCCTCAGCGAACTCTACGAACCGGGCGGCATCGACACCAAG
PA7_48        1429 TGGTGGAAGCCGGCGTCGGATGGGGCATCGCGCCGCATTATTTCGTCGAGGAACGCCTGCGCAACGGTACCCTGGCAGTCCTCAGCGAACTCTACGAACCGGGCGGCATCGACACCAAG
PA14_AL191    1429 TGGTGGAAGCCGGCGTCGGATGGGGCATCGCGCCGCATTATTTCGTCGAGGAACGCCTGCGCAACGGTACCCTGGCAGTCCTCAGCGAACTCTACGAACCGGGCGGCATCGACACCAAG

Ref_pqsR      1546 GTGTATTGCTACTACAACACCGCGCTGGAATCCGAGCGCAGCTTCCTGCGCTTTCTCGAAAGCGCCCGCCAGCGCCTGCGCGAACTCGGCCGCCAGCGTTTCGACGATGCGCCGGCCTG
PAO1-L_WT     1546 GTGTATTGCTACTACAACACCGCGCTGGAATCCGAGCGCAGCTTCCTGCGCTTTCTCGAAAGCGCCCGCCAGCGCCTGCGCGAACTCGGCCGCCAGCGTTTCGACGATGCGCCGGCCTG
PAO1_279      1546 GTGTATTGCTACTACAACACCGCGCTGGAATCCGAGCGCAGCTTCCTGCGCTTTCTCGAAAGCGCCCGCCAGCGCCTGCGCGAACTCGGCCGCCAGCGTTTCGACGATGCGCCGGCCTG
PALESB58_LES  1547 GTGTATTGCTACTACAACACCGCGCTGGAATCCGAGCGCAGCTTCCTGCGCTTTCTCGAAAGCGCCCGCCAGCGCCTGCGCGAACTCGGCCGCCAGCGTTTCGACGATGCGCCGGCCTG
PAK_6085      1547 GTGTATTGCTACTACAACACCGCGCTGGAATCCGAGCGCAGCTTCCTGCGCTTTCTCGAAAGCGCCCGCCAGCGCCTGCGCGAACTCGGCCGCCAGCGTTTCGACGATGCGCCGGCCTG
PA7_48        1548 GTGTATTGCTACTACAACACCGCGCTGGAATCCGAGCGCAGCTTCCTGCGCTTTCTCGAAAGCGCCCGCCAGCGCCTGCGCGAACTCGGCCGCCAGCGTTTCGACGATGCGCCGGCCTG
PA14_AL191    1548 GTGTATTGCTACTACAACACCGCGCTGGAATCCGAGCGCAGCTTCCTGCGCTTTCTCGAAAGCGTCCGCCAGCGCCTGCGCGAACTCGGCCGCCAGCGTTTCGACGATGCGCCGGCCTG
```

```
Ref_pqsR      1665 GCAACCGAGCATCGTCGAAACGGCGCAGCGCCGCTCAGGCCCGAAGGCGCTCGCGTACCGCCAGCGCGCCGCACCAGAGTAG
PAO1-L_WT     1665 GCAACCGAGCATCGTCGAAACGGCGCAGCGCCGCTCAGGCCCGAAGGCGCTCGCGTACCGCCAGCGCGCCGCACCAGAGTAG
PAO1_279      1665 GCAACCGAGCATCGTCGAAACGGCGCAGCGCCGCTCAGGCCCGAAGGCGCTCGCGTACCGCCAGCGCGCCGCACCAGAGTAG
PALESB58_LES 1666 GCAACCGAGCATCGTCGAAACGGCGCAGCGCCGCTCAGGCCCGAAGGCGCTCGCGTACCGCCAGCGCGCCGCACCAGAGTAG
PAK_6085      1666 GCAACCGAGCATCGTCGAAACGGCGCAGCGCCGCTCAGGCCCGAAGGCGCTCGCGTACCGCCAGCGCGCCGCACCAGAGTAG
PA7_48        1667 GCAACCGAGCATCGTCGAAACGGCGCAGCGCCGCTCAGGCCCGAAGGCGCTCGCGTACCGCCAGCGCGCCGCACCAGAGTAG
PA14_AL191    1667 GCAACCGAGCATCGTCGAAACGGCGCAGCGCCGCTCAGGCCCGAAGGCGCTCGCGTACCGCCAGCGCGCCGCACCAGAGTAG
```

Bibliography

Acar JF, Goldstein FW. Trends in bacterial resistance to fluoroquinolones. *Clin Infect Dis* 1997;**24 Suppl 1**:S67–73.

Aedekerk S, Diggle SP, Song Z *et al.* The MexGHI-OpmD multidrug efflux pump controls growth, antibiotic susceptibility and virulence in *Pseudomonas aeruginosa* via 4-quinolone-dependent cell-to-cell communication. *Microbiology* 2005;**151**:1113–25.

Albrecht-Gary A, Blanc S, Rochel N *et al.* Bacterial Iron Transport Coordination Properties of Pyoverdine PaA, a Peptidic Siderophore od *Pseudomonas aeruginosa*. *Inorg Chem* 1994;**33**:6391–402.

Allegretta G, Maurer CK, Eberhard J *et al.* In-depth profiling of MvfR-regulated small molecules in *Pseudomonas aeruginosa* after Quorum Sensing inhibitor treatment. *Front Microbiol* 2017;**8**:924.

Allesen-Holm M, Barken KB, Yang L *et al.* A characterization of DNA release in *Pseudomonas aeruginosa* cultures and biofilms. *Mol Microbiol* 2006;**59**:1114–28.

Alvarez-Ortega C, Harwood CS. Responses of *Pseudomonas aeruginosa* to low oxygen indicate that growth in the cystic fibrosis lung is by aerobic respiration. *Mol Microbiol* 2007;**65**:153–65.

Amari DT, Marques CNH, Davies DG. The putative enoyl-coenzyme A hydratase DspI is required for production of the *Pseudomonas aeruginosa* biofilm dispersion autoinducer cis-2-decenoic acid. *J Bacteriol* 2013;**195**:4600–10.

Andersen JB, Sternberg C, Poulsen LK *et al.* New unstable variants of green fluorescent protein for studies of transient gene expression in bacteria. *Appl Environ Microbiol* 1998;**64**:2240–6.

Ansari MI, Harb M, Jones B *et al.* Molecular-based approaches to characterize coastal microbial community and their potential relation to the trophic state of Red Sea. *Sci Rep* 2015;**5**:9001.

Aruni AW, Dou Y, Mishra A *et al.* The Biofilm Community: Rebels with a Cause. *Curr Oral Heal Reports* 2015;**2**:48–56.

Audenaert K, Pattery T, Cornelis P *et al.* Induction of Systemic Resistance to Botrytis cinerea in Tomato by *Pseudomonas aeruginosa* 7NSK2: Role of Salicylic Acid, Pyochelin, and Pyocyanin. *Mol Plant-Microbe Interact* 2002;**15**:1147–56.

Awasthi G, Chester A, Chaturvedi R *et al.* Study on Role of *Pseudomonas aeruginosa* on Heavy Metal Bioremediation. *Int J Pure App Biosci* 2015;**3**:92–100.

Azevedo F, Costa R, Bonaventura D *et al.* Critical review on biofilm methods. *Crit Rev Microbiol* 2017;**43**:313–51.

Baell JB, Holloway GA. New substructure filters for removal of pan assay interference compounds (PAINS) from screening libraries and for their exclusion in bioassays. *J Med Chem* 2010;**53**:2719–40.

Bajolet-Laudinat O, Girod-de Bentzmann S, Tournier JM *et al.* Cytotoxicity of *Pseudomonas aeruginosa* internal lectin PA-I to respiratory epithelial cells in primary culture. *Infect Immun* 1994;**62**:4481–7.

Balasubramanian D, Schneper L, Kumari H *et al.* A dynamic and intricate regulatory network determines *Pseudomonas aeruginosa* virulence. *Nucleic Acids Res* 2013;**41**:1–20.

Banin E, Vasil ML, Greenberg EP. Iron and *Pseudomonas aeruginosa* biofilm formation. *Proc Natl Acad Sci U S A* 2005;**102**:11076–81.

Barken KB, Pamp SJ, Yang L *et al.* Roles of type IV pili, flagellum-mediated motility and extracellular DNA in the formation of mature multicellular structures in *Pseudomonas aeruginosa* biofilms. *Environ Microbiol* 2008;**10**:2331–43.

Barnes RJ, Bandi RR, Chua F *et al.* The roles of *Pseudomonas aeruginosa* extracellular polysaccharides in biofouling of reverse osmosis membranes and nitric oxide induced dispersal. *J Memb Sci* 2014;**466**:161–72.

Barr HL, Halliday N, Cámara M *et al. Pseudomonas aeruginosa* quorum sensing molecules correlate with clinical status in cystic fibrosis. *European Respiratory Journal*. Vol 46. European Respiratory Society, 2015, 1046–54.

Becher A, Schweizer HP. Integration-proficient *Pseudomonas aeruginosa* vectors for isolation of single-copy chromosomal lacZ and lux gene fusions. *Biotechniques* 2000;**29**:948–50, 952.

Bengtsson MM, Wagner K, Schwab C *et al.* Light availability impacts structure and function of phototrophic stream biofilms across domains and trophic levels. *Mol Ecol* 2018, DOI: 10.1111/MEC.14696.

Berlanga M, Gomez-Perez L, Guerrero R. Biofilm formation and antibiotic susceptibility in dispersed cells versus planktonic cells from clinical, industry and environmental origins. *Antonie Van Leeuwenhoek* 2017;**110**:1691–704.

Berlutti F, Morea C, Battistoni A *et al.* Iron availability influences aggregation, biofilm, adhesion and invasion of *Pseudomonas aeruginosa* and Burkholderia cenocepacia. *Int J Immunopathol Pharmacol* 2005;**18**:661–70.

Bhakthavatchalu S, Shivakumar S, Sullia SB. Characterization of multiple plant growth promotion traits of *Pseudomonas aeruginosa* FP6, a potential stress tolerant biocontrol agent. *Sch Res Libr Ann Biol Res* 2013;**4**:214–23.

Bhattacharjee A, Nusca TD, Hochbaum AI. Rhamnolipids mediate an interspecies biofilm dispersal signaling pathway. *ACS Chem Biol* 2016;**11**:3068–76.

Bhattacharya M, Roy SS, Biswas D *et al.* Effect of Mg 2+ ion in protein secretion by magnesium-resistant strains of *Pseudomonas aeruginosa* and Vibrio parahaemolyticus isolated from the coastal water of Haldia port. *FEMS Microbiol Lett* 2000;**185**:151–6.

Bjarnsholt T. The role of bacterial biofilms in chronic infections. *APMIS Suppl* 2013:1–51.

Bjarnsholt T, Jensen PØ, Fiandaca MJ *et al. Pseudomonas aeruginosa* biofilms in the respiratory tract of cystic fibrosis patients. *Pediatr Pulmonol* 2009;**44**:547–58.

Bjarnsholt T, Tolker-Nielsen T, Høiby N *et al.* Interference of *Pseudomonas aeruginosa* signalling and biofilm formation for infection control. *Expert Rev Mol Med* 2010;**12**:e11.

Bleves S, Viarre V, Salacha R *et al.* Protein secretion systems in *Pseudomonas aeruginosa*: A wealth of pathogenic weapons. *Int J Med Microbiol* 2010;**300**:534–43.

Blumer C, Haas D. Mechanism, regulation, and ecological role of bacterial cyanide biosynthesis. *Arch Microbiol* 2000, DOI: 10.1007/s002039900127.

Bojanowski CL, Crookes-Goodson WJ, Robinson JB. Use of bacteriophage to prevent *Pseudomonas aeruginosa* contamination and fouling in Jet A aviation fuel. *Biofouling* 2016;**32**:1163–70.

Boles BR, Thoendel M, Singh PK. Rhamnolipids mediate detachment of *Pseudomonas aeruginosa* from biofilms. *Mol Microbiol* 2005;**57**:1210–23.

Borriello G, Werner E, Roe F *et al.* Oxygen limitation contributes to antibiotic tolerance of *Pseudomonas aeruginosa* in biofilms. *Antimicrob Agents Chemother* 2004;**48**:2659–64.

Botzenhart K, Döring G. Ecology and Epidemiology of *Pseudomonas aeruginosa*. Springer, Boston, MA, 1993, 1–18.

Brandel J, Humbert N, Elhabiri M *et al.* Pyochelin, a siderophore of *Pseudomonas aeruginosa*: Physicochemical characterization of the iron(iii), copper(ii) and zinc(ii) complexes. *Dalt Trans* 2012;**41**:2820–34.

Bredenbruch F, Geffers R, Nimtz M *et al.* The *Pseudomonas aeruginosa* quinolone signal (PQS) has an iron-chelating activity. *Environ Microbiol* 2006;**8**:1318–29.

Burrows LL. *Pseudomonas aeruginosa* twitching motility: type IV pili in action. *Annu Rev Microbiol* 2012;**66**:493–520.

Byrd MS, Pang B, Mishra M *et al.* The *Pseudomonas aeruginosa* exopolysaccharide Psl facilitates surface adherence and NF-kappaB activation in A549 cells. *MBio* 2010;**1**, DOI: 10.1128/mBio.00140-10.

Byrd MS, Sadovskaya I, Vinogradov E *et al.* Genetic and biochemical analyses of the *Pseudomonas aeruginosa* Psl exopolysaccharide reveal overlapping roles for polysaccharide synthesis enzymes in Psl and LPS

production. *Mol Microbiol* 2009;**73**:622–38.

Calfee MW, Coleman JP, Pesci EC. Interference with Pseudomonas quinolone signal synthesis inhibits virulence factor expression by *Pseudomonas aeruginosa*. *Proc Natl Acad Sci U S A* 2001;**98**:11633–7.

Calfee MW, Shelton JG, McCubrey JA *et al.* Solubility and bioactivity of the Pseudomonas quinolone signal are increased by a *Pseudomonas aeruginosa*-produced surfactant. *Infect Immun* 2005;**73**:878–82.

Camilli A, Bassler BL. Bacterial small-molecule signaling pathways. *Science* 2006;**311**:1113–6.

Campodónico VL, Llosa NJ, Grout M *et al.* Evaluation of flagella and flagellin of *Pseudomonas aeruginosa* as vaccines. *Infect Immun* 2010;**78**:746–55.

Cantin AM, Hartl D, Konstan MW *et al.* Inflammation in cystic fibrosis lung disease: Pathogenesis and therapy. *J Cyst Fibros* 2015;**14**:419–30.

Cao B, Christophersen L, Thomsen K *et al.* Antibiotic penetration and bacterial killing in a *Pseudomonas aeruginosa* biofilm model. *J Antimicrob Chemother* 2015;**70**:2057–63.

Cao H, Krishnan G, Goumnerov B *et al.* A quorum sensing-associated virulence gene of *Pseudomonas aeruginosa* encodes a LysR-like transcription regulator with a unique self-regulatory mechanism. *Proc Natl Acad Sci U S A* 2001;**98**:14613–8.

Capuzzi SJ, Muratov EN, Tropsha A. Phantom PAINS: Problems with the Utility of Alerts for Pan- Assay in terference Compound S. *J Chem Inf Model* 2017;**57**:417–27.

Casilag F, Lorenz A, Krueger J *et al.* LasB elastase of *Pseudomonas aeruginosa* acts in concert with alkaline protease AprA to prevent flagellin-mediated immune recognition. *Infect Immun* 2016;**84**:162–71.

Cezairliyan B, Ausubel FM. Investment in secreted enzymes during nutrient-limited growth is utility dependent. *Proc Natl Acad Sci U S A* 2017;**114**:E7796–802.

Charlesworth JC, Beloe C, Watters C *et al.* Quorum sensing in archaea: Recent advances and emerging directions. *Biocommunication of Archaea*. Cham: Springer International Publishing, 2017, 119–32.

Chemani C, Imberty A, De Bentzmann S *et al.* Role of LecA and LecB lectins in *Pseudomonas aeruginosa*-induced lung injury and effect of carbohydrate ligands. *Infect Immun* 2009;**77**:2065–75.

Chen L, Zou Y, She P *et al.* Composition, function, and regulation of T6SS in *Pseudomonas aeruginosa*. *Microbiol Res* 2015a;**172**:19–25.

Chen Y, Yuan M, Mohanty A *et al.* Multiple diguanylate cyclase-coordinated regulation of pyoverdine synthesis in *Pseudomonas aeruginosa*. *Environ Microbiol Rep* 2015b;**7**:498–507.

Chiang W-C, Nilsson M, Jensen PØ *et al.* Extracellular DNA shields against aminoglycosides in *Pseudomonas aeruginosa* biofilms. *Antimicrob Agents Chemother* 2013;**57**:2352–61.

Chiang WC, Pamp SJ, Nilsson M *et al.* The metabolically active subpopulation in *Pseudomonas aeruginosa* biofilms survives exposure to membrane-targeting antimicrobials via distinct molecular mechanisms. *FEMS Immunol Med Microbiol* 2012;**65**:245–56.

Choi Y, Park HY, Park SJ *et al.* Growth phase-differential quorum sensing regulation of anthranilate metabolism in *Pseudomonas aeruginosa*. *Mol Cells* 2011;**32**:57–65.

Chow S, Gu K, Jiang L *et al.* Salicylic acid affects swimming, twitching and swarming sotility in *Pseudomonas aeruginosa*, resulting in decreased biofilm formation. *J experimantal Microbiol Immunol* 2011;**15**:22–9.

Chua SL, Liu Y, Yam JKH *et al.* Dispersed cells represent a distinct stage in the transition from bacterial biofilm to planktonic lifestyles. *Nat Commun* 2014;**5**:4462.

Chung JCS, Becq J, Fraser L *et al.* Genomic variation among contemporary *Pseudomonas aeruginosa* isolates from chronically infected cystic fibrosis patients. *J Bacteriol* 2012;**194**:4857–66.

Ciofu O, Rojo-Molinero E, Macià MD *et al.* Antibiotic treatment of biofilm infections. *APMIS* 2017;**125**:304–19.

Cogen AL, Nizet V, Gallo RL. Skin microbiota: A source of disease or defence? *Br J Dermatol* 2008;**158**:442–55.

Coleman JP, Hudson LL, McKnight SL *et al. Pseudomonas aeruginosa* PqsA is an anthranilate-coenzyme A ligase. *J Bacteriol* 2008;**190**:1247–55.

Colvin KM, Gordon VD, Murakami K *et al.* The pel polysaccharide can serve a structural and protective role in the biofilm matrix of *Pseudomonas aeruginosa*. *PLoS Pathog* 2011;**7**:e1001264.

Conant CG, Schwartz MA, Ionescu-Zanetti C. Well Plate—Coupled Microfluidic Devices Designed for Facile Image-Based Cell Adhesion and Transmigration Assays. *J Biomol Screen* 2010;**15**:102–6.

Conibear TCR, Collins SL, Webb JS. Role of mutation in *Pseudomonas aeruginosa* biofilm development. Buckling A (ed.). *PLoS One* 2009;**4**:e6289.

Cornelis GR. The type III secretion injectisome. *Nat Rev Microbiol* 2006;**4**:811–25.

Cornelis P, Dingemans J. *Pseudomonas aeruginosa* adapts its iron uptake strategies in function of the type of infections. *Front Cell Infect Microbiol* 2013;**3**:75.

Costa SGVAO, Lépine F, Milot S *et al.* Cassava wastewater as a substrate for the simultaneous production of rhamnolipids and polyhydroxyalkanoates by *Pseudomonas aeruginosa*. *J Ind Microbiol Biotechnol* 2009;**36**:1063–72.

Costerton JW, Lewandowski Z, Caldwell DE *et al.* Microbial biofilms. *Annu Rev Microbiol* 1995;**49**:711–45.

Cotter JJ, O'Gara JP, Casey E. Rapid depletion of dissolved oxygen in 96-well microtiter plate *Staphylococcus epidermidis* biofilm assays promotes biofilm development and is influenced by inoculum cell concentration. *Biotechnol Bioeng* 2009;**103**:1042–7.

D'Argenio DA, Calfee MW, Rainey PB *et al.* Autolysis and autoaggregation in *Pseudomonas aeruginosa* colony morphology mutants. *J Bacteriol* 2002;**184**:6481–9.

Dahlin JL, Nissink JWM, Strasser JM *et al.* PAINS in the assay: Chemical

mechanisms of assay interference and promiscuous enzymatic inhibition observed during a sulfhydryl-scavenging HTS. *J Med Chem* 2015;**58**:2091–113.

Dasgupta N, Arora SK, Ramphal R. The Flagellar System of *Pseudomonas aeruginosa*. *Pseudomonas*. Boston, MA: Springer US, 2004, 675–98.

Davey ME, Caiazza NC, O'Toole GA. Rhamnolipid surfactant production affects biofilm architecture in *Pseudomonas aeruginosa* PAO1. *J Bacteriol* 2003;**185**:1027–36.

Davies DG, Parsek MR, Pearson JP *et al.* The involvement of cell-to-cell signals in the development of a bacterial biofilm. *Science (80-)* 1998;**280**:295–8.

Dean CR, Poole K. Cloning and characterization of the ferric enterobactin receptor gene (pfeA) of *Pseudomonas aeruginosa*. *J Bacteriol* 1993;**175**:317–24.

Defoirdt T. Quorum-Sensing Systems as Targets for Antivirulence Therapy. *Trends Microbiol* 2018;**26**:313–28.

Defoirdt T, Boon N, Bossier P. Can bacteria evolve resistance to quorum sensing disruption? Rall GF (ed.). *PLoS Pathog* 2010;**6**:1–6.

Van Delden C, Iglewski BH. Cell-to-cell signaling and *Pseudomonas aeruginosa* infections. *Emerg Infect Dis* 1998;**4**:551–60.

Delepelaire P. Type I secretion in gram-negative bacteria. *Biochim Biophys Acta - Mol Cell Res* 2004;**1694**:149–61.

Deng Y, Wu J, Tao F *et al.* Listening to a new language: DSF-based quorum sensing in Gram-negative bacteria. *Chem Rev* 2011;**111**:160–73.

Déziel E, Gopalan S, Tampakaki AP *et al.* The contribution of MvfR to *Pseudomonas aeruginosa* pathogenesis and quorum sensing circuitry regulation: Multiple quorum sensing-regulated genes are modulated without affecting IasRI, rhIRI or the production of N-acyl-L-homoserine lactones. *Mol Microbiol* 2005;**55**:998–1014.

Déziel E, Lépine F, Milot S *et al.* rhlA is required for the production of a novel biosurfactant promoting swarming motility in *Pseudomonas aeruginosa*: 3-(3-hydroxyalkanoyloxy)alkanoic acids (HAAs), the

precursors of rhamnolipids. *Microbiology* 2003;**149**:2005–13.

Déziel E, Lépine F, Milot S *et al.* Analysis of *Pseudomonas aeruginosa* 4-hydroxy-2-alkylquinolines (HAQs) reveals a role for 4-hydroxy-2-heptylquinoline in cell-to-cell communication. *Proc Natl Acad Sci* 2004;**101**:1339–44.

Diggle SP, Matthijs S, Wright VJ *et al.* The *Pseudomonas aeruginosa* 4-quinolone signal molecules HHQ and PQS play multifunctional roles in quorum sensing and iron entrapment. *Chem Biol* 2007;**14**:87–96.

Diggle SP, Stacey RE, Dodd C *et al.* The galactophilic lectin, LecA, contributes to biofilm development in *Pseudomonas aeruginosa*. *Environ Microbiol* 2006;**8**:1095–104.

Diggle SP, Winzer K, Chhabra SR *et al.* The *Pseudomonas aeruginosa* quinolone signal molecule overcomes the cell density-dependency of the quorum sensing hierarchy, regulates rhl-dependent genes at the onset of stationary phase and can be produced in the absence of LasR. *Mol Microbiol* 2003;**50**:29–43.

Dirckx P, Davies D. The five stages of biofilm development in *Pseudomonas aeruginosa*. *Cent Biofilm Eng Mont State* 2003.

Dobler L, De Carvalho BR, De Sousa Alves W *et al.* Enhanced rhamnolipid production by *Pseudomonas aeruginosa* overexpressing estA in a simple medium. Bose S (ed.). *PLoS One* 2017;**12**:e0183857.

Dobler L, Vilela LF, Almeida R V. *et al.* Rhamnolipids in perspective: Gene regulatory pathways, metabolic engineering, production and technological forecasting. *N Biotechnol* 2016;**33**:123–35.

Dong Y-H, Zhang X-F, An S-W *et al.* A novel two-component system BqsS-BqsR modulates quorum sensing-dependent biofilm decay in *Pseudomonas aeruginosa*. *Commun Integr Biol* 2008;**1**:88–96.

Douzi B. Protein–Protein Interactions: Surface Plasmon Resonance. 2017, 257–75.

Drees SL, Fetzner S. PqsE of *Pseudomonas aeruginosa* acts as pathway-specific thioesterase in the biosynthesis of alkylquinolone signaling molecules. *Chem Biol* 2015;**22**:611–8.

Drees SL, Li C, Prasetya F *et al.* PqsBC, a condensing enzyme in the biosynthesis of the pseudomonas aeruginosa quinolone signal: Crystal structure, inhibition, and reaction mechanism. *J Biol Chem* 2016;**291**:6610–24.

Driffield K, Miller K, Bostock JM *et al.* Increased mutability of *Pseudomonas aeruginosa* in biofilms. *J Antimicrob Chemother* 2008;**61**:1053–6.

Dulcey CE, Dekimpe V, Fauvelle DA *et al.* The end of an old hypothesis: The pseudomonas signaling molecules 4-hydroxy-2-alkylquinolines derive from fatty acids, not 3-ketofatty acids. *Chem Biol* 2013;**20**:1481–91.

Ebadi A, Khoshkholgh Sima NA, Olamaee M *et al.* Effective bioremediation of a petroleum-polluted saline soil by a surfactant-producing *Pseudomonas aeruginosa* consortium. *J Adv Res* 2017;**8**:627–33.

Elliott BW, Cohen C. Isolation and characterization of a lysine-specific protease from *Pseudomonas aeruginosa*. *J Biol Chem* 1986;**261**:11259–65.

Engel LS, Hill JM, Caballero AR *et al.* Protease IV, a unique extracellular protease and virulence factor from *Pseudomonas aeruginosa*. *J Biol Chem* 1998;**273**:16792–7.

Essar DW, Eberly L, Hadero A *et al.* Identification and characterization of genes for a second anthranilate synthase in *Pseudomonas aeruginosa*: Interchangeability of the two anthranilate synthase and evolutionary implications. *J Bacteriol* 1990;**172**:884–900.

Evans LR, Linker A. Production and characterization of the slime polysaccharide of *Pseudomonas aeruginosa*. *J Bacteriol* 1973;**116**:915–24.

Fakruddin M. Biosurfactant: Production and Application. *J Pet Environ Biotechnol* 2012;**03**:1–6.

Farrow JM, Sund ZM, Ellison ML *et al.* PqsE functions independently of PqsR-Pseudomonas quinolone signal and enhances the rhl quorum-sensing system. *J Bacteriol* 2008;**190**:7043–51.

Feinbaum RL, Urbach JM, Liberati NT *et al.* Genome-wide identification of

Pseudomonas aeruginosa virulence-related genes using a Caenorhabditis elegans infection model. *PLoS Pathog* 2012;**8**:e1002813.

Feltner JB, Wolter DJ, Pope CE *et al.* LasR variant cystic fibrosis isolates reveal an adaptable quorum-sensing hierarchy in *Pseudomonas aeruginosa*. *MBio* 2016;**7**:e01513-16.

Fernández D, Rodríguez E, Bassas M *et al.* Agro-industrial oily wastes as substrates for PHA production by the new strain *Pseudomonas aeruginosa* NCIB 40045: Effect of culture conditions. *Biochem Eng J* 2005;**26**:159–67.

Feuillet V, Medjane S, Mondor I *et al.* Involvement of Toll-like receptor 5 in the recognition of flagellated bacteria. *Proc Natl Acad Sci* 2006;**103**:12487–92.

Filloux A. The underlying mechanisms of type II protein secretion. *Biochim Biophys Acta - Mol Cell Res* 2004;**1694**:163–79.

Finkel SE, Kolter R. DNA as a nutrient: novel role for bacterial competence gene homologs. *J Bacteriol* 2001;**183**:6288–93.

Fitridge I, Dempster T, Guenther J *et al.* The impact and control of biofouling in marine aquaculture: a review. *Biofouling* 2012;**28**:649–69.

Flemming H-C, Neu TR, Wozniak DJ. The EPS matrix: the "house of biofilm cells". *J Bacteriol* 2007;**189**:7945–7.

Fletcher MP, Diggle SP, Crusz SA *et al.* A dual biosensor for 2-alkyl-4-quinolone quorum-sensing signal molecules. *Environ Microbiol* 2007;**9**:2683–93.

Florez C, Raab JE, Cooke AC *et al.* Membrane distribution of the Pseudomonas quinolone signal modulates outer membrane vesicle production in *Pseudomonas aeruginosa*. *MBio* 2017;**8**, DOI: 10.1128/mBio.01034-17.

Folkesson A, Jelsbak L, Yang L *et al.* Adaptation of *Pseudomonas aeruginosa* to the cystic fibrosis airway: an evolutionary perspective. *Nat Rev Microbiol* 2012;**10**:841–51.

Frei R, Breitbach AS, Blackwell HE. 2-aminobenzimidazole derivatives strongly inhibit and disperse *Pseudomonas aeruginosa* biofilms. *Angew Chemie - Int Ed* 2012;**51**:5226–9.

Freire E, Mayorga OL, Straume M. Isothermal Titration Calorimetry. *Anal Chem* 1990;**62**:950A–959A.

Friedman L, Kolter R. Two Genetic Loci Produce Distinct Carbohydrate-Rich Structural Components of the *Pseudomonas aeruginosa* Biofilm Matrix. *J Bacteriol* 2004;**186**:4457–65.

Friesner RA, Murphy RB, Repasky MP *et al.* Extra precision glide: Docking and scoring incorporating a model of hydrophobic enclosure for protein-ligand complexes. *J Med Chem* 2006;**49**:6177–96.

Frølund B, Palmgren R, Keiding K *et al.* Extraction of extracellular polymers from activated sludge using a cation exchange resin. *Water Res* 1996;**30**:1749–58.

Fuqua C, Parsek MR, Greenberg EP. Regulation of Gene Expression by Cell-to-Cell Communication: Acyl-Homoserine Lactone Quorum Sensing. *Annu Rev Genet* 2001;**35**:439–68.

Fuqua WC, Winans SC, Greenberg EP. Quorum sensing in bacteria: The LuxR-LuxI family of cell density- responsive transcriptional regulators. *J Bacteriol* 1994;**176**:269–75.

Furiga A, Lajoie B, Hage S El *et al.* Impairment of pseudomonas aeruginosa biofilm resistance to antibiotics by combining the drugs with a new quorum-sensing inhibitor. *Antimicrob Agents Chemother* 2016;**60**:1676–86.

Fuxman Bass JI, Russo DM, Gabelloni ML *et al.* Extracellular DNA: a major proinflammatory component of *Pseudomonas aeruginosa* biofilms. *J Immunol* 2010;**184**:6386–95.

G. Kulkarni A, Kaliwal BB. Bioremediation of Methomyl by Soil Isolate – Pseudomonas Aeruginosa. *IOSR J Environ Sci Toxicol Food Technol* 2015;**8**:01-10.

Gallagher LA, McKnight SL, Kuznetsova MS *et al.* Functions required for extracellular quinolone signaling by *Pseudomonas aeruginosa*. *J*

Bacteriol 2002;**184**:6472–80.

Ganesh Kumar A, Swarnalatha S, Sairam B *et al.* Production of alkaline protease by *Pseudomonas aeruginosa* using proteinaceous solid waste generated from leather manufacturing industries. *Bioresour Technol* 2008;**99**:1939–44.

Geesey GG, Richardson WT, Yeomans HG *et al.* Microscopic examination of natural sessile bacterial populations from an alpine stream. *Can J Microbiol* 1977;**23**:1733–6.

Van Gennip M, Christensen LD, Alhede M *et al.* Inactivation of the rhlA gene in *Pseudomonas aeruginosa* prevents rhamnolipid production, disabling the protection against polymorphonuclear leukocytes. *APMIS* 2009;**117**:537–46.

Van Gerven N, Waksman G, Remaut H. Pili and flagella: Biology, structure, and biotechnological applications. *Prog Mol Biol Transl Sci* 2011;**103**:21–72.

Ghanbari A, Dehghany J, Schwebs T *et al.* Inoculation density and nutrient level determine the formation of mushroom-shaped structures in *Pseudomonas aeruginosa* biofilms. *Sci Rep* 2016;**6**:32097.

Ghoul M, West SA, Diggle SP *et al.* An experimental test of whether cheating is context dependent. *J Evol Biol* 2014, DOI: 10.1111/jeb.12319.

Gibiansky ML, Conrad JC, Jin F *et al.* Bacteria use type IV pili to walk upright and detach from surfaces. *Science* 2010;**330**:197.

Girard G, Bloemberg G V. Central role of quorum sensing in regulating the production of pathogenicity factors in *Pseudomonas aeruginosa*. *Future Microbiol* 2008;**3**:97–106.

Gjødsbøl K, Christensen JJ, Karlsmark T *et al.* Multiple bacterial species reside in chronic wounds: a longitudinal study. *Int Wound J* 2006;**3**:225–31.

Glessner A, Smith RS, Iglewski BH *et al.* Roles of *Pseudomonas aeruginosa* las and rhl quorum-sensing systems in control of twitching motility. *J Bacteriol* 1999;**181**:1623–9.

Gloag ES, Turnbull L, Huang A *et al.* Self-organization of bacterial biofilms is facilitated by extracellular DNA. *Proc Natl Acad Sci* 2013;**110**:11541–6.

Goodman AL, Kulasekara B, Rietsch A *et al.* A signaling network reciprocally regulates genes associated with acute infection and chronic persistence in *Pseudomonas aeruginosa*. *Dev Cell* 2004;**7**:745–54.

Goodman AL, Merighi M, Hyodo M *et al.* Direct interaction between sensor kinase proteins mediates acute and chronic disease phenotypes in a bacterial pathogen. *Genes Dev* 2009;**23**:249–59.

Gould TA, Schweizer HP, Churchill MEA. Structure of the *Pseudomonas aeruginosa* acyl-homoserinelactone synthase LasI. *Mol Microbiol* 2004;**53**:1135–46.

Govan JR, Deretic V. Microbial pathogenesis in cystic fibrosis: mucoid *Pseudomonas aeruginosa* and Burkholderia cepacia. *Microbiol Rev* 1996;**60**:539–74.

Grant CL, Pramer D. Minor element composition of yeast extract. *J Bacteriol* 1962;**84**:869–70.

Grant SG, Jessee J, Bloom FR *et al.* Differential plasmid rescue from transgenic mouse DNAs into Escherichia coli methylation-restriction mutants. *Proc Natl Acad Sci* 1990;**87**:4645–9.

Grosso-Becerra M-V, Santos-Medellín C, González-Valdez A *et al.* *Pseudomonas aeruginosa* clinical and environmental isolates constitute a single population with high phenotypic diversity. *BMC Genomics* 2014;**15**:318.

Gruber JD, Chen W, Parnham S *et al.* The role of 2,4-dihydroxyquinoline (DHQ) in *Pseudomonas aeruginosa* pathogenicity. *PeerJ* 2016;**4**:e1495.

Gupta P, Chhibber S, Harjai K. Subinhibitory concentration of ciprofloxacin targets quorum sensing system of pseudomonas aeruginosa causing inhibition of biofilm formation & reduction of virulence. *Indian J Med Res* 2016;**143**:643–51.

Gupta R, Schuster M. Quorum sensing modulates colony morphology

through alkyl quinolones in *Pseudomonas aeruginosa*. *BMC Microbiol* 2012;**12**:30.

Guttenplan SB, Kearns DB. Regulation of flagellar motility during biofilm formation. *FEMS Microbiol Rev* 2013;**37**:n/a-n/a.

Haenni M, Hocquet D, Ponsin C *et al.* Population structure and antimicrobial susceptibility of *Pseudomonas aeruginosa* from animal infections in France. *BMC Vet Res* 2015;**11**:9.

Häse CC, Finkelstein RA. Bacterial extracellular zinc-containing metalloproteases. *Microbiol Rev* 1993;**57**:823–37.

Häussler S, Becker T. The pseudomonas quinolone signal (PQS) balances life and death in *Pseudomonas aeruginosa* populations. Ausubel FM (ed.). *PLoS Pathog* 2008;**4**:e1000166.

Hay ID, Remminghorst U, Rehm BHA. MucR, a novel membrane-associated regulator of alginate biosynthesis in *Pseudomonas aeruginosa*. *Appl Environ Microbiol* 2009;**75**:1110–20.

Hay ID, Wang Y, Moradali MF *et al.* Genetics and regulation of bacterial alginate production. *Environ Microbiol* 2014;**16**:2997–3011.

He J, Baldini RL, Déziel E *et al.* The broad host range pathogen *Pseudomonas aeruginosa* strain PA14 carries two pathogenicity islands harboring plant and animal virulence genes. *Proc Natl Acad Sci U S A* 2004;**101**:2530–5.

Heeb S, Fletcher MP, Chhabra SR *et al.* Quinolones: From antibiotics to autoinducers. *FEMS Microbiol Rev* 2011;**35**:247–74.

Heurlier K, Dénervaud V, Haenni M *et al.* Quorum-sensing-negative (lasR) mutants of *Pseudomonas aeruginosa* avoid cell lysis and death. *J Bacteriol* 2005;**187**:4875–83.

Heydorn A, Nielsen AT, Hentzer M *et al.* Quantification of biofilm structures by the novel computer program COMSTAT. *Microbiology* 2000;**146**:2395–407.

Hilker R, Munder A, Klockgether J *et al.* Interclonal gradient of virulence in the *Pseudomonas aeruginosa* pangenome from disease and environment. *Environ Microbiol* 2015;**17**:29–46.

Hoang TT, Karkhoff-Schweizer RR, Kutchma AJ *et al.* A broad-host-range Flp-FRT recombination system for site-specific excision of chromosomally-located DNA sequences: application for isolation of unmarked *Pseudomonas aeruginosa* mutants. *Gene* 1998;**212**:77–86.

Hodgkinson JT, Gross J, Baker YR *et al.* A new Pseudomonas quinolone signal (PQS) binding partner: MexG. *Chem Sci* 2016;**7**:2553–62.

Hoegy F, Mislin GLA, Schalk IJ. Pyoverdine and pyochelin measurements. *Methods Mol Biol* 2014;**1149**:293–301.

Hoge R, Pelzer A, Rosenau F *et al.* Weapons of a pathogen: Proteases and their role in virulence of *Pseudomonas aeruginosa*. *Curr Res Technol Educ Top Appl Microbiol Microb Biotechnol* 2010;**45**:383–95.

Høiby N, Bjarnsholt T, Givskov M *et al. Antibiotic Resistance of Bacterial Biofilms*., 2010:322–32.

Høiby N, Bjarnsholt T, Moser C *et al.* ESCMID* guideline for the diagnosis and treatment of biofilm infections 2014. *Clin Microbiol Infect* 2015;**21**:S1–25.

Holloway BW. Genetic Recombination in *Pseudomonas aeruginosa*. *Microbiology* 1955;**13**:572–81.

Hotterbeekx A, Kumar-Singh S, Goossens H *et al.* In vivo and In vitro Interactions between *Pseudomonas aeruginosa* and Staphylococcus spp. *Front Cell Infect Microbiol* 2017;**7**:106.

Housseini B Issa K, Phan G, Broutin I. Functional Mechanism of the Efflux Pumps Transcription Regulators From *Pseudomonas aeruginosa* Based on 3D Structures. *Front Mol Biosci* 2018;**5**:q.

Huang J, Sonnleitner E, Ren B *et al.* Catabolite repression control of pyocyanin biosynthesis at an intersection of primary and secondary metabolism in *Pseudomonas aeruginosa*. *Appl Environ Microbiol* 2012;**78**:5016–20.

Iiyama K, Takahashi E, Lee JM *et al.* Alkaline protease contributes to pyocyanin production in *Pseudomonas aeruginosa*. *FEMS Microbiol Lett* 2017;**364**, DOI: 10.1093/femsle/fnx051.

Ilangovan A, Fletcher MM, Rampioni G *et al.* Structural Basis for Native

Agonist and Synthetic Inhibitor Recognition by the *Pseudomonas aeruginosa* Quorum Sensing Regulator PqsR (MvfR). Ausubel FM (ed.). *PLoS Pathog* 2013;**9**:e1003508.

Imamura Y, Yanagihara K, Tomono K *et al.* Role of *Pseudomonas aeruginosa* quorum-sensing systems in a mouse model of chronic respiratory infection. *J Med Microbiol* 2005;**54**:515–8.

Jackson KD, Starkey M, Kremer S *et al.* Identification of psl, a locus encoding a potential exopolysaccharide that is essential for *Pseudomonas aeruginosa* PAO1 biofilm formation. *J Bacteriol* 2004;**186**:4466–75.

Jacoby GA. Mechanisms of Resistance to Quinolones. *Clin Infect Dis* 2005;**41**:S120–6.

James GA, Swogger E, Wolcott R *et al.* Biofilms in chronic wounds. *Wound Repair Regen* 2008;**16**:37–44.

Jasial S, Hu Y, Bajorath J. How Frequently Are Pan-Assay Interference Compounds Active? Large-Scale Analysis of Screening Data Reveals Diverse Activity Profiles, Low Global Hit Frequency, and Many Consistently Inactive Compounds. *J Med Chem* 2017;**60**:3879–86.

Jennings LK, Storek KM, Ledvina HE *et al.* Pel is a cationic exopolysaccharide that cross-links extracellular DNA in the *Pseudomonas aeruginosa* biofilm matrix. *Proc Natl Acad Sci* 2015;**112**:11353–8.

Jensen PØ, Givskov M, Bjarnsholt T *et al.* The immune system vs. *Pseudomonas aeruginosa* biofilms. *FEMS Immunol Med Microbiol* 2010;**59**:292–305.

Jeong H, Barbe V, Lee CH *et al.* Genome Sequences of Escherichia coli B strains REL606 and BL21(DE3). *J Mol Biol* 2009;**394**:644–52.

Ji C, Sharma I, Pratihar D *et al.* Designed small-molecule inhibitors of the anthranilyl-CoA synthetase PqsA block quinolone biosynthesis in pseudomonas aeruginosa. *ACS Chem Biol* 2016;**11**:3061–7.

Jimenez PN, Koch G, Thompson JA *et al.* The multiple signaling systems regulating virulence in *Pseudomonas aeruginosa*. *Microbiol Mol Biol Rev*

2012;**76**:46–65.

Jones S, Yu B, Bainton NJ *et al.* The lux autoinducer regulates the production of exoenzyme virulence determinants in Erwinia carotovora and *Pseudomonas aeruginosa*. *EMBO J* 1993;**12**:2477–82.

Joo H-S, Otto M. Molecular basis of in vivo biofilm formation by bacterial pathogens. *Chem Biol* 2012;**19**:1503–13.

Kadurugamuwa JL, Beveridge TJ. Virulence factors are released from *Pseudomonas aeruginosa* in association with membrane vesicles during normal growth and exposure to gentamicin: A novel mechanism of enzyme secretion. *J Bacteriol* 1995;**177**:3998–4008.

Kanehisa M, Furumichi M, Tanabe M *et al.* KEGG: New perspectives on genomes, pathways, diseases and drugs. *Nucleic Acids Res* 2017;**45**:D353–61.

Kang C, Wu P, Li Y *et al.* Understanding the role of clay minerals in the chromium(VI) bioremoval by *Pseudomonas aeruginosa* CCTCC AB93066 under growth condition: microscopic, spectroscopic and kinetic analysis. *World J Microbiol Biotechnol* 2015;**31**:1765–79.

Kang D, Kirienko DR, Webster P *et al.* Pyoverdine, a siderophore from *Pseudomonas aeruginosa*, translocates into C. elegans, removes iron, and activates a distinct host response. *Virulence* 2018;**9**:804–17.

Kato J, Kim H-E, Takiguchi N *et al. Pseudomonas aeruginosa* as a model microorganism for investigation of chemotactic behaviors in ecosystem. *J Biosci Bioeng* 2008;**106**:1–7.

Kefala K, Kotsifaki D, Providaki M *et al.* Purification, crystallization and preliminary X-ray diffraction analysis of the C-terminal fragment of the MvfR protein from *Pseudomonas aeruginosa*. *Acta Crystallogr Sect F Struct Biol Cryst Commun* 2012;**68**:695–7.

Kesarwani M, Hazan R, He J *et al.* A quorum sensing regulated small volatile molecule reduces acute virulence and promotes chronic infection phenotypes. Coburn J (ed.). *PLoS Pathog* 2011;**7**:e1002192.

De Kievit TR, Gillis R, Marx S *et al.* Quorum-sensing genes in *Pseudomonas aeruginosa* biofilms: their role and expression patterns. *Appl Environ*

Microbiol 2001;**67**:1865–73.

Kim SK, Lee JH. Biofilm dispersion in *Pseudomonas aeruginosa*. *J Microbiol* 2016;**54**:71–85.

Kim SK, Park HY, Lee JH. Anthranilate deteriorates the structure of *Pseudomonas aeruginosa* biofilms and antagonizes the biofilm-enhancing indole effect. *Appl Environ Microbiol* 2015;**81**:2328–38.

Kiratisin P, Tucker KD, Passador L. LasR, a transcriptional activator of *Pseudomonas aeruginosa* virulence genes, functions as a multimer. *J Bacteriol* 2002;**184**:4912–9.

Kitao T, Lepine F, Babloudi S *et al.* Molecular insights into function and competitive inhibition of pseudomonas aeruginosa multiple virulence factor regulator. *MBio* 2018;**9**:e02158-17.

Klausen M, Aaes-Jørgensen A, Molin S *et al.* Involvement of bacterial migration in the development of complex multicellular structures in *Pseudomonas aeruginosa* biofilms. *Mol Microbiol* 2003a;**50**:61–8.

Klausen M, Heydorn A, Ragas P *et al.* Biofilm formation by *Pseudomonas aeruginosa* wild type, flagella and type IV pili mutants. *Mol Microbiol* 2003b;**48**:1511–24.

Klein T, Henn C, De Jong JC *et al.* Identification of small-molecule antagonists of the pseudomonas aeruginosa transcriptional regulator PqsR: Biophysically guided hit discovery and optimization. *ACS Chem Biol* 2012;**7**:1496–501.

Koch B, Jensen LE, Nybroe O. A panel of Tn7-based vectors for insertion of the gfp marker gene or for delivery of cloned DNA into Gram-negative bacteria at a neutral chromosomal site. *J Microbiol Methods* 2001;**45**:187–95.

Koch K, Davis F, Rhoades J. NEBRAMYCIN: SEPARATION OF THE COMPLEX AND IDENTIFICATION OF FACTORS 4, 5, AND 5′. *J Antibiot (Tokyo)* 1973;**XXVI**:745–51.

Kon Y, Tsukada H, Hasegawa T *et al.* The role of *Pseudomonas aeruginosa* elastase as a potent inflammatory factor in a rat air pouch inflammation model. *FEMS Immunol Med Microbiol* 1999;**25**:313–21.

Kotra LP, Haddad J, Mobashery S. Aminoglycosides: perspectives on mechanisms of action and resistance and strategies to counter resistance. *Antimicrob Agents Chemother* 2000;**44**:3249–56.

Kotresha D, Vidyasagar GM. Isolation and characterisation of phenol-degrading *Pseudomonas aeruginosa* MTCC 4996. *World J Microbiol Biotechnol* 2008;**24**:541–7.

Kukavica-Ibrulj I, Bragonzi A, Paroni M *et al.* In vivo growth of *Pseudomonas aeruginosa* strains PAO1 and PA14 and the hypervirulent strain LESB58 in a rat model of chronic lung infection. *J Bacteriol* 2008;**190**:2804–13.

Kulp A, Kuehn MJ. Biological Functions and Biogenesis of Secreted Bacterial Outer Membrane Vesicles. *Annu Rev Microbiol* 2010;**64**:163–84.

De la Fuente-Núñez C, Reffuveille F, Fernández L *et al.* Bacterial biofilm development as a multicellular adaptation: Antibiotic resistance and new therapeutic strategies. *Curr Opin Microbiol* 2013;**16**:580–9.

LaFayette SL, Houle D, Beaudoin T *et al.* Cystic fibrosis–adapted *Pseudomonas aeruginosa* quorum sensing lasR mutants cause hyperinflammatory responses. *Sci Adv* 2015;**1**, DOI: 10.1126/sciadv.1500199.

Lanzer M, Bujard H. Promoters largely determine the efficiency of repressor action. *Proc Natl Acad Sci U S A* 1988;**85**:8973–7.

Lau GW, Hassett DJ, Ran H *et al.* The role of pyocyanin in *Pseudomonas aeruginosa* infection. *Trends Mol Med* 2004;**10**:599–606.

Lee J, Zhang L. The hierarchy quorum sensing network in *Pseudomonas aeruginosa*. *Protein Cell* 2014;**6**:26–41.

Leid JG, Willson CJ, Shirtliff ME *et al.* The Exopolysaccharide Alginate Protects *Pseudomonas aeruginosa* Biofilm Bacteria from IFN- -Mediated Macrophage Killing. *J Immunol* 2005;**175**:7512–8.

Lenney W, Gilchrist FJ. *Pseudomonas aeruginosa* and cyanide production. *Eur Respir J* 2011;**37**:482–3.

Lesic B, Lépine F, Déziel E *et al.* Inhibitors of pathogen intercellular signals as selective anti-infective compounds. *PLoS Pathog* 2007;**3**:1229–39.

Lewis K. Persister cells, dormancy and infectious disease. *Nat Rev Microbiol* 2007;**5**:48–56.

Lewis K. Multidrug Tolerance of Biofilms and Persister Cells. Springer, Berlin, Heidelberg, 2008, 107–31.

Lin J, Zhang W, Cheng J *et al.* A Pseudomonas T6SS effector recruits PQS-containing outer membrane vesicles for iron acquisition. *Nat Commun* 2017;**8**:14888.

Llamas MA, Imperi F, Visca P *et al.* Cell-surface signaling in Pseudomonas: Stress responses, iron transport, and pathogenicity. *FEMS Microbiol Rev* 2014;**38**:569–97.

Lu C, Kirsch B, Maurer CK *et al.* Optimization of anti-virulence PqsR antagonists regarding aqueous solubility and biological properties resulting in new insights in structure-activity relationships. *Eur J Med Chem* 2014a;**79**:173–83.

Lu C, Kirsch B, Zimmer C *et al.* Discovery of antagonists of PqsR, a key player in 2-alkyl-4-quinolone- dependent quorum sensing in *Pseudomonas aeruginosa*. *Chem Biol* 2012;**19**:381–90.

Lu C, Maurer CK, Kirsch B *et al.* Overcoming the unexpected functional inversion of a PqsR antagonist in *Pseudomonas aeruginosa*: An in vivo potent antivirulence agent targeting pqs quorum sensing. *Angew Chemie - Int Ed* 2014b;**53**:1109–12.

Ma L, Conover M, Lu H *et al.* Assembly and development of the *Pseudomonas aeruginosa* biofilm matrix. *PLoS Pathog* 2009;**5**:e1000354.

Ma L, Jackson KD, Landry RM *et al.* Analysis of *Pseudomonas aeruginosa* conditional psl variants reveals roles for the psl polysaccharide in adhesion and maintaining biofilm structure postattachment. *J Bacteriol* 2006;**188**:8213–21.

Macià MD, Rojo-Molinero E, Oliver A. Antimicrobial susceptibility testing in biofilm-growing bacteria. *Clin Microbiol Infect* 2014;**20**:981–90.

Maddocks SE, Oyston PCF. Structure and function of the LysR-type transcriptional regulator (LTTR) family proteins. *Microbiology*

2008;**154**:3609–23.

Maeda T, García-Contreras R, Pu M *et al.* Quorum quenching quandary: Resistance to antivirulence compounds. *ISME J* 2012;**6**:493–501.

Mah T-F, Pitts B, Pellock B *et al.* A genetic basis for *Pseudomonas aeruginosa* biofilm antibiotic resistance. *Lett to Nat* 2003;**426**:1–5.

Mahanta N, Gupta A, Khare SK. Production of protease and lipase by solvent tolerant *Pseudomonas aeruginosa* PseA in solid-state fermentation using Jatropha curcas seed cake as substrate. *Bioresour Technol* 2008;**99**:1729–35.

Mahenthiralingam E, Campbell ME, Speert DP. Nonmotility and phagocytic resistance of *Pseudomonas aeruginosa* isolates from chronically colonized patients with cystic fibrosis. *Infect Immun* 1994;**62**:596–605.

Maleki S, Almaas E, Zotchev S *et al.* Alginate Biosynthesis Factories in *Pseudomonas fluorescens*: Localization and Correlation with Alginate Production Level. *Appl Environ Microbiol* 2016;**82**:1227–36.

Mandsberg LF, Ciofu O, Kirkby N *et al.* Antibiotic resistance in *Pseudomonas aeruginosa* strains with increased mutation frequency due to inactivation of the DNA oxidative repair system. *Antimicrob Agents Chemother* 2009;**53**:2483–91.

Mann EE, Wozniak DJ. Pseudomonas biofilm matrix composition and niche biology. *FEMS Microbiol Rev* 2012;**36**:893–916.

van Mansfeld R, Jongerden I, Bootsma M *et al.* The population genetics of *Pseudomonas aeruginosa* isolates from different patient populations exhibits high-level host specificity. *PLoS One* 2010;**5**:e13482.

Marquart ME, Caballero AR, Chomnawang M *et al.* Identification of a novel secreted protease from *Pseudomonas aeruginosa* that causes corneal erosions. *Investig Ophthalmol Vis Sci* 2005;**46**:3761–8.

Mashburn-Warren L, Howe J, Garidel P *et al.* Interaction of quorum signals with outer membrane lipids: Insights into prokaryotic membrane vesicle formation. *Mol Microbiol* 2008;**69**:491–502.

Mashburn LM, Whiteley M. Membrane vesicles traffic signals and facilitate

group activities in a prokaryote. *Nature* 2005;**437**:422–5.

Mason DJ, Power EG, Talsania H *et al.* Antibacterial action of ciprofloxacin. *Antimicrob Agents Chemother* 1995;**39**:2752–8.

Mathee K. Forensic investigation into the origin of pseudomonas aeruginosa PA14 — Old but not lost. *J Med Microbiol* 2018;**67**:1019–21.

Matsukawa M, Greenberg EP. Putative exopolysaccharide synthesis genes influence *Pseudomonas aeruginosa* biofilm development. *J Bacteriol* 2004;**186**:4449–56.

Maura D, Hazan R, Kitao T *et al.* Evidence for direct control of virulence and defense gene circuits by the pseudomonas aeruginosa quorum sensing regulator, MvfR. *Sci Rep* 2016;**6**:34083.

Maura D, Rahme LG. Pharmacological inhibition of the *Pseudomonas aeruginosa* MvfR quorum-sensing system interferes with biofilm formation and potentiates antibiotic-mediated biofilm disruption. *Antimicrob Agents Chemother* 2017;**61**:e01362-17.

Mavrodi D V, Bonsall RF, Delaney SM *et al.* Functional analysis of genes for biosynthesis of pyocyanin and phenazine-1-carboxamide from *Pseudomonas aeruginosa* PAO1. *J Bacteriol* 2001;**183**:6454–65.

McDougald D, Rice SA, Barraud N *et al.* Should we stay or should we go: mechanisms and ecological consequences for biofilm dispersal. *Nat Rev Microbiol* 2012;**10**:39–50.

McKnight SL, Iglewski BH, Pesci EC. The Pseudomonas quinolone signal regulates rhl quorum sensing in *Pseudomonas aeruginosa*. *J Bacteriol* 2000;**182**:2702–8.

Meliani, Bensoltane. Review of Pseudominas attachment and biofilm formation in food industry. *Poult Fish Wildl Sci* 2015;**3**:1–7.

Melville S, Craig L. Type IV Pili in Gram-Positive Bacteria. *Microbiol Mol Biol Rev* 2013;**77**:323–41.

Merhej V, Georgiades K, Raoult D. Postgenomic analysis of bacterial pathogens repertoire reveals genome reduction rather than virulence factors. *Brief Funct Genomics* 2013;**12**:291–304.

Meyer J-M, Stintzi A, De Vos D *et al.* Use of siderophores to type pseudomonads: the three *P aeruginosa* pyoverdine systems. *Microbiology* 1997;**143**:35–43.

Meyer JM, Abdallah MA. The Fluorescent Pigment of *Pseudomonas fluorescens*: Biosynthesis, Purification and Physicochemical Properties. *J Gen Microbiol* 1978;**107**:319–28.

Meylan S, Porter CBM, Yang JH *et al.* Carbon Sources Tune Antibiotic Susceptibility in *Pseudomonas aeruginosa* via Tricarboxylic Acid Cycle Control. *Cell Chem Biol* 2017;**24**:195–206.

Michalska M, Wolf P. Pseudomonas Exotoxin A: Optimized by evolution for effective killing. *Front Microbiol* 2015;**6**:963.

Mielczarek, E. V.; McGrayne SB. *Iron, Nature's Universal Element. Why People Need Iron & Animals Make Magnets*. Rutgers University Press, 2000.

Mihai MM, Holban AM, Giurcăneanu C *et al.* Microbial Biofilms: Impact On Pathogenesis Of Periodontitis, Cystic Fibrosis, Chronic Wounds And Medical Device-Related Infections. *Curr Top Med Chem* 2015.

Minandri F, Imperi F, Frangipani E *et al.* Role of iron uptake systems in *Pseudomonas aeruginosa* virulence and airway infection. *Infect Immun* 2016;**84**:2324–35.

Minaxi, Saxena J. Characterization of *Pseudomonas aeruginosa* RM-3 as a potential biocontrol agent. *Mycopathologia* 2010;**170**:181–93.

Mishra M, Byrd MS, Sergeant S *et al. Pseudomonas aeruginosa* Psl polysaccharide reduces neutrophil phagocytosis and the oxidative response by limiting complement-mediated opsonization. *Cell Microbiol* 2012;**14**:95–106.

Möker N, Dean CR, Tao J. *Pseudomonas aeruginosa* increases formation of multidrug-tolerant persister cells in response to quorum-sensing signaling molecules. *J Bacteriol* 2010;**192**:1946–55.

Monds RD, O'Toole GA. The developmental model of microbial biofilms: ten years of a paradigm up for review. *Trends Microbiol* 2009;**17**:73–87.

Moradali MF, Ghods S, Rehm BHA. *Pseudomonas aeruginosa* Lifestyle: A

Paradigm for Adaptation, Survival, and Persistence. *Front Cell Infect Microbiol* 2017;**7**:39.

Morales-Espinosa R, Soberón-Chávez G, Delgado-Sapién G *et al.* Genetic and phenotypic characterization of a *Pseudomonas aeruginosa* population with high frequency of genomic islands. *PLoS One* 2012;**7**:e37459.

Moran NA. Microbial Minimalism Genome Reduction in Bacterial Pathogens. *Cell* 2002;**108**:583–6.

Mukherjee AK, Bordoloi NK. Biodegradation of benzene, toluene, and xylene (BTX) in liquid culture and in soil by *Bacillus subtilis* and *Pseudomonas aeruginosa* strains and a formulated bacterial consortium. *Environ Sci Pollut Res* 2012;**19**:3380–8.

Mulcahy H, Charron-Mazenod L, Lewenza S. Extracellular DNA chelates cations and induces antibiotic resistance in *Pseudomonas aeruginosa* biofilms. *PLoS Pathog* 2008;**4**:e1000213.

Mulcahy H, Charron-Mazenod L, Lewenza S. *Pseudomonas aeruginosa* produces an extracellular deoxyribonuclease that is required for utilization of DNA as a nutrient source. *Environ Microbiol* 2010;**12**:1621–9.

Murray TS, Kazmierczak BI. *Pseudomonas aeruginosa* exhibits sliding motility in the absence of type IV pili and flagella. *J Bacteriol* 2008;**190**:2700–8.

Nanda AM, Thormann K, Frunzke J. Impact of spontaneous prophage induction on the fitness of bacterial populations and host-microbe interactions. *J Bacteriol* 2015;**197**:410–9.

Nealson KH, Platt T, Hastings JW. Cellular control of the synthesis and activity of the bacterial luminescent system. *J Bacteriol* 1970;**104**:313–22.

Ng W-L, Bassler BL. Bacterial quorum-sensing network architectures. *Annu Rev Genet* 2009;**43**:197–222.

Nguyen AT, O'Neill MJ, Watts AM *et al.* Adaptation of iron homeostasis pathways by a *Pseudomonas aeruginosa* pyoverdine mutant in the

cystic fibrosis lung. *J Bacteriol* 2014;**196**:2265–76.

Nguyen D, Joshi-Datar A, Lepine F *et al.* Active starvation responses mediate antibiotic tolerance in biofilms and nutrient-limited bacteria. *Science (80-)* 2011;**334**:982–6.

Nguyen DHK, Pham VTH, Truong VK *et al.* Role of topological scale in the differential fouling of: *Pseudomonas aeruginosa* and *Staphylococcus aureus* bacterial cells on wrinkled gold-coated polystyrene surfaces. *Nanoscale* 2018;**10**:5089–96.

Nickzad A, Déziel E. The involvement of rhamnolipids in microbial cell adhesion and biofilm development - an approach for control? *Lett Appl Microbiol* 2014;**58**:447–53.

Nitschke M, Costa SGVAO. Biosurfactants in food industry. *Trends Food Sci Technol* 2007;**18**:252–9.

O'Sullivan BP, Freedman SD. Cystic fibrosis. *Lancet* 2009;**373**:1891–904.

O'Toole GA, Kolter R. Flagellar and twitching motility are necessary for *Pseudomonas aeruginosa* biofilm development. *Mol Microbiol* 1998a;**30**:295–304.

O'Toole GA, Kolter R. Initiation of biofilm formation in *Pseudomonas fluorescens* WCS365 proceeds via multiple, convergent signalling pathways: a genetic analysis. *Mol Microbiol* 1998b;**28**:449–61.

Ochsner UA, Vasil ML, Alsabbagh E *et al.* Role of the *Pseudomonas aeruginosa* oxyR-recG operon in oxidative stress defense and DNA repair: OxyR-dependent regulation of katB-ankB, ahpB, and ahpC-ahpF. *J Bacteriol* 2000;**182**:4533–44.

Okshevsky M, Meyer RL. The role of extracellular DNA in the establishment, maintenance and perpetuation of bacterial biofilms. *Crit Rev Microbiol* 2015;**41**:341–52.

Ołdak E, Trafny EA. Secretion of proteases by *Pseudomonas aeruginosa* biofilms exposed to ciprofloxacin. *Antimicrob Agents Chemother* 2005;**49**:3281–8.

Ostroff RM, Vasil AI, Vasil ML. Molecular comparison of a nonhemolytic and a hemolytic phospholipase C from *Pseudomonas aeruginosa*. *J*

Bacteriol 1990;**172**:5915–23.

Pamp SJ, Gjermansen M, Johansen HK *et al.* Tolerance to the antimicrobial peptide colistin in *Pseudomonas aeruginosa* biofilms is linked to metabolically active cells, and depends on the pmr and mexAB-oprM genes. *Mol Microbiol* 2008;**68**:223–40.

Pamp SJ, Tolker-Nielsen T. Multiple roles of biosurfactants in structural biofilm development by *Pseudomonas aeruginosa*. *J Bacteriol* 2007;**189**:2531–9.

Parsek MR, Tolker-Nielsen T. Pattern formation in *Pseudomonas aeruginosa* biofilms. *Curr Opin Microbiol* 2008;**11**:560–6.

Pasqua M, Visaggio D, Lo Sciuto A *et al.* Ferric uptake regulator Fur is conditionally essential in *Pseudomonas aeruginosa*. *J Bacteriol* 2017;**199**, DOI: 10.1128/JB.00472-17.

Paulsen IT, Press CM, Ravel J *et al.* Complete genome sequence of the plant commensal *Pseudomonas fluorescens* Pf-5. *Nat Biotechnol* 2005;**23**:873–8.

Pearson JP, Gray KM, Passador L *et al.* Structure of the autoinducer required for expression of *Pseudomonas aeruginosa* virulence genes. *Proc Natl Acad Sci U S A* 1994;**91**:197–201.

Pearson JP, Passador L, Iglewski BH *et al.* A second N-acylhomoserine lactone signal produced by *Pseudomonas aeruginosa*. *Proc Natl Acad Sci U S A* 1995;**92**:1490–4.

Pearson JP, Pesci EC, Iglewski BH. Roles of *Pseudomonas aeruginosa las* and *rhl* quorum-sensing systems in control of elastase and rhamnolipid biosynthesis genes. *J Bacteriol* 1997;**179**:5756–67.

Percival SL, Williams DW, Randle J *et al. Biofilms in Infection Prevention and Control: A Healthcare Handbook*. Elsevier, 2014.

Pérez Silva RM, Ábalos Rodríguez A, Gómez Montes De Oca JM *et al.* Biosorption of chromium, copper, manganese and zinc by *Pseudomonas aeruginosa* AT18 isolated from a site contaminated with petroleum. *Bioresour Technol* 2009;**100**:1533–8.

Persat A, Inclan YF, Engel JN *et al.* Type IV pili mechanochemically regulate

virulence factors in *Pseudomonas aeruginosa*. *Proc Natl Acad Sci* 2015;**112**:7563–8.

Pesci EC, Milbank JB, Pearson JP *et al.* Quinolone signaling in the cell-to-cell communication system of *Pseudomonas aeruginosa*. *Proc Natl Acad Sci U S A* 1999;**96**:11229–34.

Polkade A V., Mantri SS, Patwekar UJ *et al.* Quorum sensing: An under-explored phenomenon in the phylum Actinobacteria. *Front Microbiol* 2016;**7**:131.

Poole K, McKay GA. Iron acquisition and its control in *Pseudomonas aeruginosa*: Many roads lead to Rome. 2003;**8**.

Priyam A, Woodcroft BJ, Rai V *et al.* Sequenceserver: a modern graphical user interface for custom BLAST databases. *bioRxiv* 2015.

Purevdorj-Gage B, Costerton WJ, Stoodley P. Phenotypic differentiation and seeding dispersal in non-mucoid and mucoid *Pseudomonas aeruginosa* biofilms. *Microbiology* 2005;**151**:1569–76.

Quiñones B, Dulla G, Lindow SE. Quorum Sensing Regulates Exopolysaccharide Production, Motility, and Virulence in Pseudomonas syringae. *Mol Plant-Microbe Interact* 2005;**18**:682–93.

Radhapriya P, Ramachandran A, Anandham R *et al. Pseudomonas aeruginosa* RRALC3 enhances the biomass, nutrient and carbon contents of Pongamia pinnata seedlings in degraded forest soil. Berg G (ed.). *PLoS One* 2015;**10**:e0139881.

Rahim R, Ochsner UA, Olvera C *et al.* Cloning and functional characterization of the *Pseudomonas aeruginosa* rhlC gene that encodes rhamnosyltransferase 2, an enzyme responsible for di-rhamnolipid biosynthesis. *Mol Microbiol* 2001;**40**:708–18.

Rahmani-Badi A, Sepehr S, Fallahi H *et al.* Dissection of the cis-2-decenoic acid signaling network in *Pseudomonas aeruginosa* using microarray technique. *Front Microbiol* 2015;**6**:383.

Rampioni G, Falcone M, Heeb S *et al.* Unravelling the Genome-Wide Contributions of Specific 2-Alkyl-4-Quinolones and PqsE to Quorum Sensing in *Pseudomonas aeruginosa*. *PLoS Pathog*

2016;**12**:e1006029.

Rampioni G, Leoni L, Williams P. The art of antibacterial warfare: Deception through interference with quorum sensing-mediated communication. *Bioorg Chem* 2014;**55**:60–8.

Rampioni G, Pillai CR, Longo F *et al.* Effect of efflux pump inhibition on *Pseudomonas aeruginosa* transcriptome and virulence. *Sci Rep* 2017;**7**:11392.

Rampioni G, Pustelny C, Fletcher MP *et al.* Transcriptomic analysis reveals a global alkyl-quinolone-independent regulatory role for PqsE in facilitating the environmental adaptation of *Pseudomonas aeruginosa* to plant and animal hosts. *Environ Microbiol* 2010;**12**:1659–73.

Rampioni G, Schuster M, Greenberg EP *et al.* RsaL provides quorum sensing homeostasis and functions as a global regulator of gene expression in *Pseudomonas aeruginosa*. *Mol Microbiol* 2007;**66**:1557–65.

Raposo A, Pérez E, de Faria CT *et al.* Food Spoilage by Pseudomonas spp.-An Overview. *Foodborne Pathogens and Antibiotic Resistance*. Hoboken, NJ, USA: John Wiley & Sons, Inc., 2017, 41–71.

Rasamiravaka T, Labtani Q, Duez P *et al.* The formation of biofilms by pseudomonas aeruginosa: A review of the natural and synthetic compounds interfering with control mechanisms. *Biomed Res Int* 2015;**2015**:1–17.

Read RC, Roberts P, Munro N *et al.* Effect of *Pseudomonas aeruginosa* rhamnolipids on mucociliary transport and ciliary beating. *J Appl Physiol* 1992;**72**:2271–7.

Reffuveille F, De La Fuente-Nűnez C, Mansour S *et al.* A broad-spectrum antibiofilm peptide enhances antibiotic action against bacterial biofilms. *Antimicrob Agents Chemother* 2014;**58**:5363–71.

Rehm BHA. *Pseudomonas: Model Organism, Pathogen, Cell Factory*. John Wiley & Sons, 2008.

Rohmer L, Hocquet D, Miller SI. Are pathogenic bacteria just looking for food? Metabolism and microbial pathogenesis. *Trends Microbiol* 2011;**19**:341–8.

Rollet C, Gal L, Guzzo J. Biofilm-detached cells, a transition from a sessile to a planktonic phenotype: a comparative study of adhesion and physiological characteristics in *Pseudomonas aeruginosa*. *FEMS Microbiol Lett* 2009;**290**:135–42.

Römling U, Kader A, Sriramulu DD *et al.* Worldwide distribution of *Pseudomonas aeruginosa* clone C strains in the aquatic environment and cystic fibrosis patients. *Environ Microbiol* 2005;**7**:1029–38.

Safdari MS, Kariminia HR, Ghobadi Nejad Z *et al.* Study Potential of Indigenous *Pseudomonas aeruginosa* and *Bacillus subtilis* in Bioremediation of Diesel-Contaminated Water. *Water Air Soil Pollut* 2017;**228**:37.

Sahner JH, Brengel C, Storz MP *et al.* Combining in silico and biophysical methods for the development of *Pseudomonas aeruginosa* quorum sensing inhibitors: An alternative approach for structure-based drug design. *J Med Chem* 2013;**56**:8656–64.

Sakthipriya N, Doble M, Sangwai JS. Systematic investigations on the biodegradation and viscosity reduction of long chain hydrocarbons using *Pseudomonas aeruginosa* and *Pseudomonas fluorescens*. *Environ Sci Process Impacts* 2016;**18**:386–97.

Sambrook J, Russell DW. *Molecular Cloning: A Laboratory Manual*. CSHL Press, 2001.

Sandoz KM, Mitzimberg SM, Schuster M. Social cheating in *Pseudomonas aeruginosa* quorum sensing. *Proc Natl Acad Sci* 2007;**104**:15876–81.

Sang S, Yang Z, Wang L *et al.* SemaTyP: A knowledge graph based literature mining method for drug discovery. *BMC Bioinformatics* 2018;**19**:193.

Sasirekha B, Srividya S. Siderophore production by *Pseudomonas aeruginosa* FP6, a biocontrol strain for *Rhizoctonia solani* and *Colletotrichum gloeosporioides* causing diseases in chilli. *Agric Nat Resour* 2016;**50**:250–6.

Sauer K, Camper AK, Ehrlich GD *et al. Pseudomonas aeruginosa* displays multiple phenotypes during development as a biofilm. *J Bacteriol* 2002;**184**:1140–54.

Schafhauser J, Lepine F, McKay G *et al.* The stringent response modulates 4-hydroxy-2-alkylquinoline biosynthesis and quorum-sensing hierarchy in *Pseudomonas aeruginosa*. *J Bacteriol* 2014;**196**:1641–50.

Schertzer JW, Boulette ML, Whiteley M. More than a signal: non-signaling properties of quorum sensing molecules. *Trends Microbiol* 2009;**17**:189–95.

Schertzer JW, Brown SA, Whiteley M. Oxygen levels rapidly modulate *Pseudomonas aeruginosa* social behaviours via substrate limitation of PqsH. *Mol Microbiol* 2010;**77**:1527–38.

Schooling SR, Beveridge TJ. Membrane vesicles: An overlooked component of the matrices of biofilms. *J Bacteriol* 2006;**188**:5945–57.

Schooling SR, Charaf UK, Allison DG *et al.* A role for rhamnolipid in biofilm dispersion. *Biofilms* 2004;**1**:91–9.

Schooling SR, Hubley A, Beveridge TJ. Interactions of DNA with biofilm-derived membrane vesicles. *J Bacteriol* 2009;**191**:4097–102.

Schurr MJ. Which bacterial biofilm exopolysaccharide is preferred, Psl or alginate? *J Bacteriol* 2013;**195**:1623–6.

Schurr MJ, Yu H, Martinez-Salazar JM *et al.* Control of AlgU, a member of the sigma E-like family of stress sigma factors, by the negative regulators MucA and MucB and *Pseudomonas aeruginosa* conversion to mucoidy in cystic fibrosis. *J Bacteriol* 1996;**178**:4997–5004.

Schuster M, Greenberg EP. A network of networks: quorum-sensing gene regulation in *Pseudomonas aeruginosa*. *Int J Med Microbiol* 2006;**296**:73–81.

Schuster M, Greenberg EP. Early activation of quorum sensing in *Pseudomonas aeruginosa* reveals the architecture of a complex regulon. *BMC Genomics* 2007;**8**:287.

Schwechheimer C, Kuehn MJ. Outer-membrane vesicles from Gram-negative bacteria: Biogenesis and functions. *Nat Rev Microbiol* 2015;**13**:605–19.

Scott NE, Hare NJ, White MY *et al.* Secretome of transmissible *Pseudomonas aeruginosa* AES-1R grown in a cystic fibrosis lung-like

environment. *J Proteome Res* 2013;**12**:5357–69.

Sharon C, Furugoh S, Yamakido T *et al.* Purification and characterization of a lipase from *Pseudomonas aeruginosa* KKA-5 and its role in castor oil hydrolysis. *J Ind Microbiol Biotechnol* 1998;**20**:304–7.

Shigematsu T, Fukushima J, Oyama M *et al.* Iron-mediated regulation of alkaline proteinase production in *Pseudomonas aeruginosa*. *Microbiol Immunol* 2001;**45**:579–90.

Shigeta M, Tanaka G, Komatsuzawa H *et al.* Permeation of antimicrobial agents through pseudomonas aeruginosa biofilms: A simple method. *Chemotherapy* 1997;**43**:340–5.

Shrout JD, Chopp DL, Just CL *et al.* The impact of quorum sensing and swarming motility on *Pseudomonas aeruginosa* biofilm formation is nutritionally conditional. *Mol Microbiol* 2006;**62**:1264–77.

Shrout JD, Tolker-Nielsen T, Givskov M *et al.* The contribution of cell-cell signalling and motility to bacterial biofilm formation. *MRS Bull* 2012;**36**:367–73.

Simon R, Priefer U, Pühler A. A Broad Host Range Mobilization System for In Vivo Genetic Engineering: Transposon Mutagenesis in Gram Negative Bacteria. *Bio/Technology* 1983;**1**:784–91.

Singh AK, Mallick N. Exploitation of inexpensive substrates for production of a novel SCL–LCL-PHA co-polymer by *Pseudomonas aeruginosa* MTCC 7925. *J Ind Microbiol Biotechnol* 2009;**36**:347–54.

Sissi C, Palumbo M. In front of and behind the replication fork: bacterial type IIA topoisomerases. *Cell Mol Life Sci* 2010;**67**:2001–24.

Skaar EP. The battle for iron between bacterial pathogens and their vertebrate hosts. *PLoS Pathog* 2010;**6**:1–2.

Skindersoe ME, Alhede M, Phipps R *et al.* Effects of antibiotics on quorum sensing in *Pseudomonas aeruginosa*. *Antimicrob Agents Chemother* 2008;**52**:3648–63.

Smalheiser NR. Literature-based discovery: Beyond the ABCs. *J Am Soc Inf Sci Technol* 2012;**63**:218–24.

Soberón-Chávez G, Lépine F, Déziel E. Production of rhamnolipids by *Pseudomonas aeruginosa*. *Appl Microbiol Biotechnol* 2005;**68**:718–25.

Sommer T, Hübner H, El Kerdawy A *et al.* Identification of the beer component hordenine as food-derived dopamine D2 receptor agonist by virtual screening a 3D compound database. *Sci Rep* 2017;**7**:44201.

Sonawane A, Jyot J, Ramphal R. *Pseudomonas aeruginosa* LecB is involved in pilus biogenesis and protease IV activity but not in adhesion to respiratory mucins. *Infect Immun* 2006;**74**:7035–9.

Soukarieh F, Vico Oton E, Dubern J-F *et al.* In Silico and in Vitro-Guided Identification of Inhibitors of Alkylquinolone-Dependent Quorum Sensing in *Pseudomonas aeruginosa*. *Molecules* 2018a;**23**:257.

Soukarieh F, Williams P, Stocks MJ *et al. Pseudomonas aeruginosa* Quorum Sensing Systems as Drug Discovery Targets: Current Position and Future Perspectives. *Journal of Medicinal Chemistry*. http://pubs.acs.org/doi/10.1021/acs.jmedchem.8b00540. Published July 27, 2018b. Accessed September 13, 2018.

Spoering AL, Gilmore MS. Quorum sensing and DNA release in bacterial biofilms. *Curr Opin Microbiol* 2006;**9**:133–7.

Starkey M, Lepine F, Maura D *et al.* Identification of Anti-virulence Compounds That Disrupt Quorum-Sensing Regulated Acute and Persistent Pathogenicity. Whiteley M (ed.). *PLoS Pathog* 2014;**10**:e1004321.

Steenackers HP, Parijs I, Foster KR *et al.* Experimental evolution in biofilm populations. *FEMS Microbiol Rev* 2016;**40**:373–97.

Stewart GS, Williams P. lux genes and the applications of bacterial bioluminescence. *J Gen Microbiol* 1992;**138**:1289–300.

Stewart PS, Franklin MJ, Williamson KS *et al.* Contribution of stress responses to antibiotic tolerance in *Pseudomonas aeruginosa* biofilms. *Antimicrob Agents Chemother* 2015;**59**:3838–47.

Stintzi A, Cornelis P, Hohnadel D *et al.* Novel pyoverdine biosynthesis gene(s) of *Pseudomonas aeruginosa* PAO. *Microbiology* 1996;**142**:1181–90.

Stintzi A, Evans K, Meyer J-M *et al.* Quorum-sensing and siderophore biosynthesis in *Pseudomonas aeruginosa*: lasR/lasI mutants exhibit reduced pyoverdine biosynthesis. *FEMS Microbiol Lett* 1998;**166**:341–5.

Stintzi A, Johnson Z, Stonehouse M *et al.* The pvc gene cluster of *Pseudomonas aeruginosa*: role in synthesis of the pyoverdine chromophore and regulation by PtxR and PvdS. *J Bacteriol* 1999;**181**:4118–24.

Stoodley P, Sauer K, Davies DG *et al.* Biofilms as complex differentiated communities. *Annu Rev Microbiol* 2002;**56**:187–209.

Storz MP, Maurer CK, Zimmer C *et al.* Validation of PqsD as an anti-biofilm target in pseudomonas aeruginosa by development of small-molecule inhibitors. *J Am Chem Soc* 2012;**134**:16143–6.

Stover CK, Pham XQ, Erwin AL *et al.* Complete genome sequence of *Pseudomonas aeruginosa* PAO1, an opportunistic pathogen. *Nature* 2000;**406**:959–64.

Studier FW, Moffatt BA. Use of bacteriophage T7 RNA polymerase to direct selective high-level expression of cloned genes. *J Mol Biol* 1986;**189**:113–30.

Sulochana MB, Jayachandra SY, Kumar SA *et al.* Siderophore as a Potential Plant Growth-Promoting Agent Produced by *Pseudomonas aeruginosa* JAS-25. *Appl Biochem Biotechnol* 2014:297–308.

Sutherland IW. Biofilm exopolysaccharides: a strong and sticky framework. *Microbiology* 2001;**147**:3–9.

Taber HW, Mueller JP, Miller PF *et al.* Bacterial uptake of aminoglycoside antibiotics. *Microbiol Rev* 1987;**51**:439–57.

Tamura T, Ishida Y, Otoguro M *et al.* Classification of "Streptomyces tenebrarius" Higgins and Kastner as Streptoalloteichus tenebrarius nom. rev., comb. nov., and emended description of the genus Streptoalloteichus. *Int J Syst Evol Microbiol* 2008;**58**:688–91.

Tang A, Caballero AR, Marquart ME *et al. Pseudomonas aeruginosa* small protease (PASP), a keratitis virulence factor. *Investig Ophthalmol Vis*

Sci 2013;**54**:2821–8.

Tang A, Marquart ME, Fratkin JD *et al.* Properties of PASP: A pseudomonas protease capable of mediating corneal erosions. *Investig Ophthalmol Vis Sci* 2009;**50**:3794–801.

Tettmann B, Niewerth C, Kirschhöfer F *et al.* Enzyme-mediated quenching of the Pseudomonas Quinolone Signal (PQS) promotes biofilm formation of pseudomonas aeruginosa by increasing iron availability. *Front Microbiol* 2016;**7**:1978.

Thomann A, De Mello Martins AGG, Brengel C *et al.* Application of Dual Inhibition Concept within Looped Autoregulatory Systems toward Antivirulence Agents against *Pseudomonas aeruginosa* Infections. *ACS Chem Biol* 2016;**11**:1279–86.

Thomas J, Thanigaivel S, Vijayakumar S *et al.* Pathogenecity of *Pseudomonas aeruginosa* in Oreochromis mossambicus and treatment using lime oil nanoemulsion. *Colloids Surfaces B Biointerfaces* 2014;**116**:372–7.

Tielker D, Hacker S, Loris R *et al. Pseudomonas aeruginosa* lectin LecB is located in the outer membrane and is involved in biofilm formation. *Microbiology* 2005;**151**:1313–23.

Toyofuku M, Inaba T, Kiyokawa T *et al.* Environmental factors that shape biofilm formation. *Biosci Biotechnol Biochem* 2016;**80**:7–12.

Toyofuku M, Roschitzki B, Riedel K *et al.* Identification of Proteins Associated with the *Pseudomonas aeruginosa* Biofilm Extracellular Matrix. *J Proteome Res* 2012;**11**:4906–15.

Toyofuku M, Zhou S, Sawada I *et al.* Membrane vesicle formation is associated with pyocin production under denitrifying conditions in *Pseudomonas aeruginosa* PAO1. *Environ Microbiol* 2014;**16**:2927–38.

Tremblay J, Richardson A-P, Lépine F *et al.* Self-produced extracellular stimuli modulate the *Pseudomonas aeruginosa* swarming motility behaviour. *Environ Microbiol* 2007;**9**:2622–30.

Tremblay YDN, Vogeleer P, Jacques M *et al.* High-throughput microfluidic method to study biofilm formation and host-pathogen interactions in

pathogenic Escherichia coli. *Appl Environ Microbiol* 2015;**81**:2827–40.

Tripathy S, Kumar N, Mohanty S *et al.* Characterisation of *Pseudomonas aeruginosa* isolated from freshwater culture systems. *Microbiol Res* 2007;**162**:391–6.

Troxell B, Hassan HM. Transcriptional regulation by Ferric Uptake Regulator (Fur) in pathogenic bacteria. *Front Cell Infect Microbiol* 2013;**3**:59.

Trunk K, Benkert B, Quäck N *et al.* Anaerobic adaptation in *Pseudomonas aeruginosa*: Definition of the Anr and Dnr regulons. *Environ Microbiol* 2010;**12**:1719–33.

Tseng BS, Reichhardt C, Merrihew GE *et al.* A Biofilm Matrix-Associated Protease Inhibitor Protects *Pseudomonas aeruginosa* from Proteolytic Attack. *MBio* 2018;**9**, DOI: 10.1128/mBio.00543-18.

Tsuda M, Miyazaki H, Nakazawa T. Genetic and physical mapping of genes involved in pyoverdin production in *Pseudomonas aeruginosa* PAO. *J Bacteriol* 1995;**177**:423–31.

Turnbull L, Toyofuku M, Hynen AL *et al.* Explosive cell lysis as a mechanism for the biogenesis of bacterial membrane vesicles and biofilms. *Nat Commun* 2016;**7**:11220.

Tyson GW, Chapman J, Hugenholtz P *et al.* Community structure and metabolism through reconstruction of microbial genomes from the environment. *Nature* 2004;**428**:37–43.

Ueda A, Wood TK. Connecting quorum sensing, c-di-GMP, pel polysaccharide, and biofilm formation in *Pseudomonas aeruginosa* through tyrosine phosphatase TpbA (PA3885). *PLoS Pathog* 2009;**5**:e1000483.

Velázquez-Campoy A, Ohtaka H, Nezami A *et al.* Isothermal Titration Calorimetry. *Current Protocols in Cell Biology*. Vol 23. Hoboken, NJ, USA: John Wiley & Sons, Inc., 2004, 17.8.1-17.8.24.

Venturi V. Regulation of quorum sensing in Pseudomonas. *FEMS Microbiol Rev* 2006;**30**:274–91.

Visaggio D, Pasqua M, Bonchi C *et al.* Cell aggregation promotes pyoverdine-dependent iron uptake and virulence in *Pseudomonas*

aeruginosa. *Front Microbiol* 2015;**6**:902.

Visca P, Imperi F, Lamont IL. Pyoverdine siderophores: from biogenesis to biosignificance. *Trends Microbiol* 2007;**15**:22–30.

Voggu L, Schlag S, Biswas R *et al.* Microevolution of cytochrome bd oxidase in Staphylococci and its implication in resistance to respiratory toxins released by Pseudomonas. *J Bacteriol* 2006;**188**:8079–86.

Vorregaard M. Comstat2 - a modern 3D image analysis environment for biofilms. *PhD thesis* 2008.

Voynow JA, Fischer BM, Zheng S. Proteases and cystic fibrosis. *Int J Biochem Cell Biol* 2008;**40**:1238–45.

Wagner S, Sommer R, Hinsberger S *et al.* Novel Strategies for the Treatment of *Pseudomonas aeruginosa* Infections. *J Med Chem* 2016;**59**:5929–69.

Walters MC, Roe F, Bugnicourt A *et al.* Contributions of antibiotic penetration, oxygen limitation, and low metabolic activity to tolerance of *Pseudomonas aeruginosa* biofilms to ciprofloxacin and tobramycin. *Antimicrob Agents Chemother* 2003;**47**:317–23.

Wandersman C, Delepelaire P. Bacterial Iron Sources: From Siderophores to Hemophores. *Annu Rev Microbiol* 2004;**58**:611–47.

Wei Q, Ma LZ. Biofilm matrix and its regulation in *Pseudomonas aeruginosa*. *Int J Mol Sci* 2013;**14**:20983–1005.

Weng LK, Bayer ME, London WT. Interaction of hepatitis B surface antigen (Australia antigen) with membrane vesicles of *Pseudomonas aeruginosa*. *Infect Immun* 1975;**12**:180–6.

Werner E, Roe F, Bugnicourt A *et al.* Stratified growth in *Pseudomonas aeruginosa* biofilms. *Appl Environ Microbiol* 2004;**70**:6188–96.

Whitchurch CB, Tolker-Nielsen T, Ragas PC *et al.* Extracellular DNA required for bacterial biofilm formation. *Science* 2002;**295**:1487.

Whitehead NA, Barnard AML, Slater H *et al.* Quorum-sensing in Gram-negative bacteria. *FEMS Microbiol Rev* 2001;**25**:365–404.

Wilderman PJ, Vasil AI, Johnson Z *et al.* Characterization of an

endoprotease (PrpL) encoded by a PvdS-regulated gene in *Pseudomonas aeruginosa*. *Infect Immun* 2001;**69**:5385–94.

Williams BJ, Dehnbostel J, Blackwell TS. *Pseudomonas aeruginosa*: Host defence in lung diseases. *Respirology* 2010;**15**:1037–56.

Williams P, Bainton NJ, Swift S *et al.* Small molecule-mediated density-dependent control of gene expression in prokaryotes: bioluminescence and the biosynthesis of carbapenem antibiotics. *FEMS Microbiol Lett* 1992;**100**:161–7.

Williams P, Winzer K, Chan WC *et al.* Look who's talking: communication and quorum sensing in the bacterial world. *Philos Trans R Soc Lond B Biol Sci* 2007;**362**:1119–34.

Williamson KS, Richards LA, Perez-Osorio AC *et al.* Heterogeneity in *Pseudomonas aeruginosa* biofilms includes expression of ribosome hibernation factors in the antibiotic-tolerant subpopulation and hypoxia-induced stress response in the metabolically active population. *J Bacteriol* 2012;**194**:2062–73.

Wilton M, Charron-Mazenod L, Moore R *et al.* Extracellular DNA Acidifies Biofilms and Induces Aminoglycoside Resistance in *Pseudomonas aeruginosa*. *Antimicrob Agents Chemother* 2015;**60**:544–53.

Winsor GL, Griffiths EJ, Lo R *et al.* Enhanced annotations and features for comparing thousands of *Pseudomonas* genomes in the Pseudomonas genome database. *Nucleic Acids Res* 2016;**44**:D646–53.

Witzgall F, Ewert W, Blankenfeldt W. Structures of the N-Terminal Domain of PqsA in Complex with Anthraniloyl- and 6-Fluoroanthraniloyl-AMP: Substrate Activation in Pseudomonas Quinolone Signal (PQS) Biosynthesis. *ChemBioChem* 2017;**18**:2045–55.

Wood TK, Knabel SJ, Kwan BW. Bacterial persister cell formation and dormancy. *Appl Environ Microbiol* 2013;**79**:7116–21.

Worlitzsch D, Tarran R, Ulrich M *et al.* Effects of reduced mucus oxygen concentration in airway Pseudomonas infections of cystic fibrosis patients. *J Clin Invest* 2002;**109**:317–25.

Wozniak DJ, Sprinkle AB, Baynham PJ. Control of *Pseudomonas aeruginosa*

algZ expression by the alternative sigma factor AlgT. *J Bacteriol* 2003;**185**:7297–300.

Wozniak DJ, Wyckoff TJO, Starkey M *et al.* Alginate is not a significant component of the extracellular polysaccharide matrix of PA14 and PAO1 *Pseudomonas aeruginosa* biofilms. *Proc Natl Acad Sci U S A* 2003;**100**:7907–12.

Xiao G, Déziel E, He J *et al.* MvfR, a key *Pseudomonas aeruginosa* pathogenicity LTTR-class regulatory protein, has dual ligands. *Mol Microbiol* 2006;**62**:1689–99.

Xu KD, Stewart PS, Xia F *et al.* Spatial physiological heterogeneity in *Pseudomonas aeruginosa* biofilm is determined by oxygen availability. *Appl Environ Microbiol* 1998;**64**:4035–9.

Xu N, Yu S, Moniot S *et al.* Crystallization and preliminary crystal structure analysis of the ligand-binding domain of PqsR (MvfR), the Pseudomonas quinolone signal (PQS) responsive quorum-sensing transcription factor of *Pseudomonas aeruginosa*. *Acta Crystallogr Sect F Struct Biol Cryst Commun* 2012;**68**:1034–9.

Xu X, Yu H, Zhang D *et al.* Role of ppGpp in *Pseudomonas aeruginosa* acute pulmonary infection and virulence regulation. *Microbiol Res* 2016;**192**:84–95.

Yang G, Trylska J, Tor Y *et al.* Binding of aminoglycosidic antibiotics to the oligonucleotide A-site model and 30S ribosomal subunit: Poisson-Boltzmann model, thermal denaturation, and fluorescence studies. *J Med Chem* 2006;**49**:5478–90.

Yang L, Barken KB, Skindersoe ME *et al.* Effects of iron on DNA release and biofilm development by *Pseudomonas aeruginosa*. *Microbiology* 2007;**153**:1318–28.

Yang L, Hu Y, Liu Y *et al.* Distinct roles of extracellular polymeric substances in *Pseudomonas aeruginosa* biofilm development. *Environ Microbiol* 2011;**13**:1705–17.

Yang L, Nilsson M, Gjermansen M *et al.* Pyoverdine and PQS mediated subpopulation interactions involved in *Pseudomonas aeruginosa* biofilm formation. *Mol Microbiol* 2009;**74**:1380–92.

Yeung ATY, Torfs ECW, Jamshidi F *et al.* Swarming of *Pseudomonas aeruginosa* is controlled by a broad spectrum of transcriptional regulators, including MetR. *J Bacteriol* 2009;**191**:5592–602.

Yi-Chia L. Understanding chronic inflammatory diseases in the human lung: the cystic fibrosis and idiopathic pulmonary fibrosis paradigms. *Univ Nottingham* 2014.

Zahler R. Aryloxyacetylindoles and analogs as antibiotic tolerance inhibitors. 2016.

Zegans ME, Wozniak D, Griffin E *et al. Pseudomonas aeruginosa* exopolysaccharide psl promotes resistance to the biofilm inhibitor polysorbate 80. *Antimicrob Agents Chemother* 2012;**56**:4112–22.

Zender M, Klein T, Henn C *et al.* Discovery and biophysical characterization of 2-amino-oxadiazoles as novel antagonists of PqsR, an important regulator of *Pseudomonas aeruginosa* virulence. *J Med Chem* 2013;**56**:6761–74.

Zender M, Witzgall F, Drees SL *et al.* Dissecting the Multiple Roles of PqsE in *Pseudomonas aeruginosa* Virulence by Discovery of Small Tool Compounds. *ACS Chem Biol* 2016;**11**:1755–63.

Zhang YF, Han K, Chandler CE *et al.* Probing the sRNA regulatory landscape of P. aeruginosa: post-transcriptional control of determinants of pathogenicity and antibiotic susceptibility. *Mol Microbiol* 2017;**106**:919–37.

Zhu T, Cao S, Su PC *et al.* Hit identification and optimization in virtual screening: Practical recommendations based on a critical literature analysis. *J Med Chem* 2013;**56**:6560–72.

Zulianello L, Canard C, Köhler T *et al.* Rhamnolipids are virulence factors that promote early infiltration of primary human airway epithelia by *Pseudomonas aeruginosa*. *Infect Immun* 2006;**74**:3134–47.